SYMPOSIUM

EUROPEAN CENTRE ON PREVENTION
AND FORECASTING OF EARTHQUAKES
ATHENS, GREECE

EARTHQUAKE PLANNING
AND PROTECTION ORGANIZATION
ATHENS, GREECE

Seismicity of the Carpatho-Balcan Region

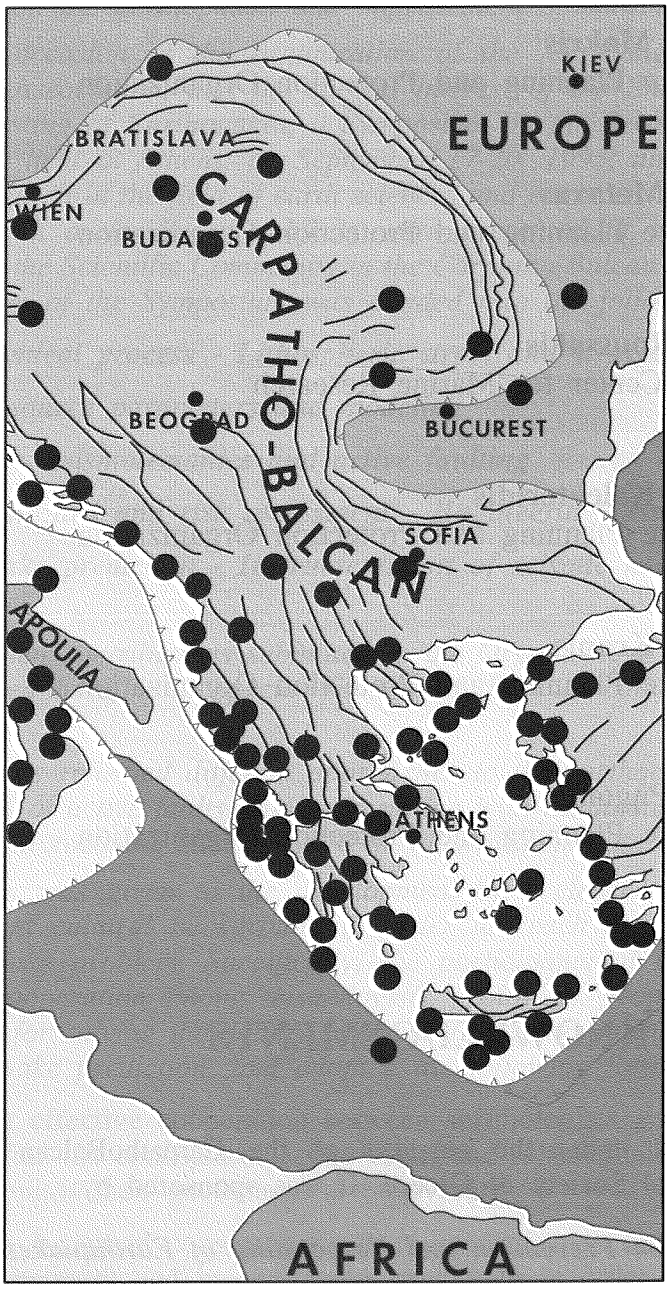

Proceedings

SEPTEMBER 17-20
1995
ATHENS, GREECE

ATHENS, 1996

XV Congress
of the Carpatho-Balcan

ORGANIZING COMMITTEE

President	**Prof. D. Papanikolaou** University of Athens
Secretary	**Dr. J. Papoulia** National Center for Marine Research
Treasurer	**Mrs Ch. Makris** Earthquake Planning and Protection Organization
Member	**Dr. Ch. Metaxas** Earthquake Planning and Protection Organization
Member	**Mr. G. Roussakis** National Center for Marine Research
Member	**Mr. Ch. Kalenteridis** Earthquake Planning and Protection Organization
Member	**Mr. Ch. Kranis** Earthquake Planning and Protection Organization
Member	**Mrs V. Pagoni** Earthquake Planning and Protection Organization

ACKNOWLEDGEMENTS

The Symposium was held under the auspices of the CarpathoBalcan Geological Association and the Geological Society of Greece. It was sponsored by:

— ***The European Center on Prevention and Forecasting of Earthquakes***

— ***The Earthquake Planning and Protection Organization***

FOREWORD

In many countries today, the subject of earthquake protection focuses public attention, because of the catastrophic earthquakes that have occurred in recent years, causing significant loss of life and properties. The Carpatho-Balcan and adjacent areas are certainly among those with the highest seismic risk, having experienced many severe earthquakes in the past, like that of Bucharest (1977), Friuli (1976), Irpinia (1980), Thessaloniki (1978), Alkyonides (1981), Kalamata (1986) and others. The opinion generally accepted today on preventing and mitigating the consequences of these events, is that research should concentrate on the deep scientific knowledge of the earthquake process, as well as on the development and improvement of networks of seismic monitoring.

On the occasion of the organization of the XV Congress of the Carpatho-Balcan Geological Association, and the special interest of the European Center for Prevention and Forecasting of Earthquakes, a Symposium on the Seismicity of the Carpatho-Balcan Region was held in Athens, on September 17-20, 1995, aiming at providing the present state of research in the field of earth sciences and engineering applied to seismic problems. 35 papers on a variety of subjects were presented at the Symposium, reflecting the response of the Scientific Community in the Carpatho-Balcan and other European countries. The program of the Symposium was divided into the following topics:

Geodynamical process - Lithospheric stress and structure

Seismic source parameters and modeling

Seismicity, seismotectonics and active faulting

Seismic hazard and risk assessment - Engineering seismology

Earthquake prediction - Instrumentation of seismic networks and earthquake catalogues

The written contributions submitted to the Organizing Committee after the Symposium are published here, in a Special Edition of the Publications of the Geological Society of Greece.

The papers reflected different approaches to the earthquake problem, focusing mainly on the study of active faults, their correlation with earthquake activity and the importance of detailed microzoning studies based on all available data and multidisciplinary methods.

Emphasis was given to the development of a closer cooperation among specialists with different cultural background in order to reach practical operational solutions to the earthquake problem. Specifically, the participants of the Symposium, recommended that close cooperation among seismologists, geologists, geophysists and other geoscientists is essential for solving the actual problems related to earthquake hazard, risk assessment and earthquake prediction, and adopted the following Resolutions.

— An effective cooperation between seismologists and geologists in order to refine the concepts of active faults and seismogenic structures and to better monitor their geodynamical behaviour.

— An increased cooperation among specialists in earthquake hazard and risk assessment and in earthquake prediction in order to improve significantly the corpus of available data, both in quantity and quality (earthquake

catalogues, instrumental and historical: palaeoseismicity data; deformation data) for seismic zonation purposes, in low seismicity areas as well, based on all available data.

— Development of channels to make data easily accessible to any potential user in favouring competitive, yet concerted interpretation.

— Survey of marine zones, presently poorly monitored, to improve the knowledge on their seismotectonic behaviour, since these areas cover a significant portion of the territory.

— With particular consideration to the crucial problem of earthquake prediction and its social impact, the participants in the Symposium observed that significant improvement has been achieved recently in the long and medium term prediction and this kind of approach has offered an important tool to the authorities to develop aseismic codes to minimize human losses and economic consequences. However, further efforts should be devoted to short term earthquake prediction, since this field is still at the stage of basic research and should be submitted to standard evaluation practices in use in scientific matters.

We believe that the organization of the Symposium fulfilled its goals in terms of presenting the state-of-the-art of research in the field of seismicity and seismic hazard evaluation in the Carpatho-Balcan region, giving as well the directions and identifying the priorities addressed towards practical solutions that are most important in the earthquake problem.

We would like to thank all participants for their interesting contributions and valuable assistance, and we do hope that this initiative will be a chance to strengthening the links and developing a closer cooperation among geoscientists in the Carpatho-Balcan and other European countries.

Prof. Dimitris Papanikolaou **Dr. Joanna Papoulia**

CONTENTS

GEODYNAMICAL PROCESS - LITHOSPHERIC STRESS AND STRUCTURE

SEISMIC SOURCE PARAMETERS AND MODELING

SEISMICITY, SEISMOTECTONICS AND ACTIVE FAULTING

SEISMIC HAZARD AND RISK ASSESSMENT-ENGINEERING SEISMOLOGY

EARTHQUAKE PREDICTION - INSTRUMENTATION OF SEISMIC NETWORKS AND EARTHQUAKE CATALOGUES

GEODYNAMICAL PROCESS - LITHOSPHERIC STRESS AND STRUCTURE

SEISMOTECTONIC PATTERN OF THE CONTACT ZONE BETWEEN THE WEST CARPATHIANS AND THE BOHEMIAN MASSIF

Vladimír Schenk, Zdenka Schenková

Institute of Rock Structure and Mechanics, Academy of Science, 18209 Praha 8 - Liben, Czech Republic e-mail: schenk@lorien.site.cas.cz

Abstract

In some areas a definition of contact zones between two main European geological units, the Hercynides and the Alpides, is still open. The contact zone between the West Carpathians (the Alpides) and the Bohemian Massif (the Hercynides) is one of such cases. In view of the fact that the West Carpathians have thrust to a considerale distance by nappes over the submerged Epivariscan complexes, the existence of the thrust nature of the contact zone between the West Carpathians and the Bohemian Massif and its extension below the Carpathian units is studied in this paper. The obtained results indicate that the Epivariscan structures are bound to continue in the Carpathian basement towards SE up to a distance of 120-130 km from the outcropping thrust plane between the Bohemian Massif and the West Carpathians. For the Revúca fault system, the origin of which in the West Carpathians is assumed to be genetically connected with the main tectonic Epivariscan directions in basements, it is found that dextral motions acting on its upper Carpathian blocks compensate the sinistral motions going on in its basement.

Geological Structure and Tectonic Pattern

The boundary between two fundamental units of Europe, the Hercynides and the Alpides, on the territory of former Czechoslovakia is located in the contact zone between the West Carpathians and the Bohemian Massif.

The Bohemian Massif is the easternmost part of an old resistant elongated zone located in the centre of Europe. From the Massif the zone goes westwards over the Harz (Germany) and the Vogessen to plateau Centrale (France). The zone played an important role in the geological development in this part of Europe in Mesozoic and Tertiary periods. During the creation of the West Carpathians, the motion of the Alpine-Himalayan units towards north and west in Central Europe was well protected by the Bohemian Massif. Therefore, the West Carpathians had a significant effect on the geodynamic development of the eastern parts of the Epivariscan platform, namely of the Bohemian Massif. The eastern marginal units of the Bohemian Massif were covered with Carpathian formations. It is evident that such mobile interactions of two geologically different systems (platform and orogene structures) are bound to give rise to earthquakes. In our case it concerns the seismicity pattern of eastern Moravia and western Slovakia.

Contact Zone between the West Carpathians and the Bohemian Massif

In the contact zone between the West Carpathians and the Bohemian Massif, in accordance with the opinions of Fusán et al. (1979, 1981) and of Balatka et al. (1983), the following

Special Publications of the Geological Society of Greece, No 6.

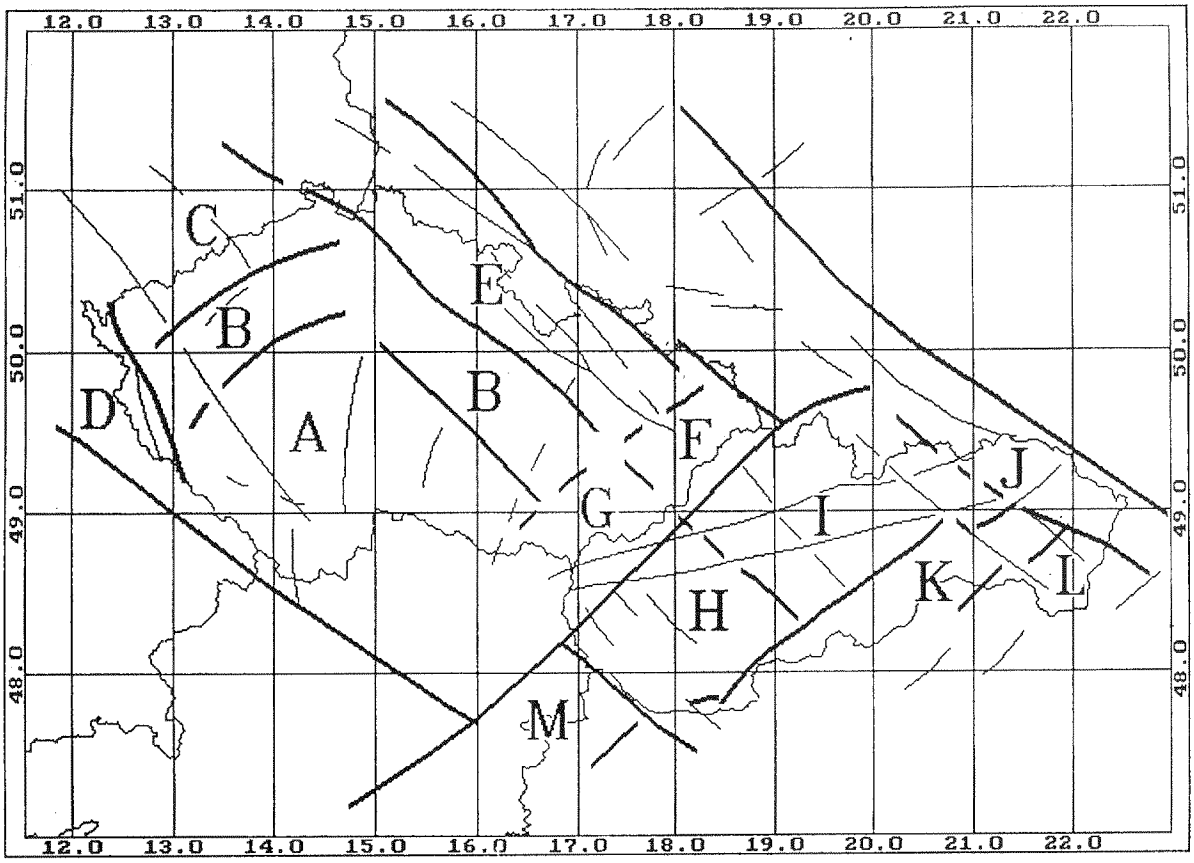

Fig. 1. Seismotectonic block pattern of former Czechoslovakia: thick lines - block boundary; thin lines - other fault lines; blocks: A-Vltava-Dyje, B-Elbe-Svratka, C-Krusné hory Mts., D-Cesky les Mts. and Smrciny Mts., E-Krkonoše Mts. - Jeseníky Mts., F-Slovakia - Silesia, G-Moravia - Slovakia, H-Danube, I-Fatra - Tatra Mts., J-Beskydy Mts. - Bukovina, K-Southern Slovakia, L-Eastern Slovakia and M-Sopron.

Neoid structural-tectonic blocks (Fig. 1) Slovakia-Silesia (F), Moravia-Slovakia (G), Sopron (M), Danube (H), Fatra-Tatra Mts. (I), Beskydy Mts-Bukovina (J) and fault zones (Fig. 2) Revúca (8), Prerov-Štiavnica (9), Hron (12), Myjava-sub-Tatra (13), Verona-Semmering-Váh (g), Murán (j), respectively, were distinguished (Schenk et al., 1986).

Geologically, the contract zone is formed by the Penipieninian lineament, tracing the Inner Klippen Belt. This is a deep-seated boundary which is interpreted by some geologists as a subduction zone along which the European Platform was subducted below the region formed by the Inner Carpathians. In this way, the Klippen Zone is understood as a boundary between the inner (blocks H, I, K and L) and outer (blocks G, F and J) parts of the Carpathian arc. The Outer Carpathians are mainly formed by nappes of the outer flysch thrust to a considerable distance over the submerged old fundament, on which also the complexes of the Carpathian foredeep sedimented (Dudek, 1981).

On the outside of the Peripieninian lineament there is another deep - seated fault zone, the Pericarpathian lineament (Sikora, 1976), which continues to the SW in the Lednice zone; the zone is situated close to the western boundary of block G (Fig. 1, dashed line). Between these two lineaments there is a region of the main gravity minima (Ibermajer, 1981) in the Carpathian arc, the area where the Earth's crust is the thickest and the accumulation of flysch nappes the largest. From the viewpoint of our topic it is important that, in 1981 its basement was still assigned to the European Platform, but the basement south of the Peripieninian lineament (Fig. 1, blocks H) was assumed to be formed by the Inner Carpathians of the Slovak Massif only (Dudek, 1981).

In the next part of our paper it will be shown that a continuation of the European Platform

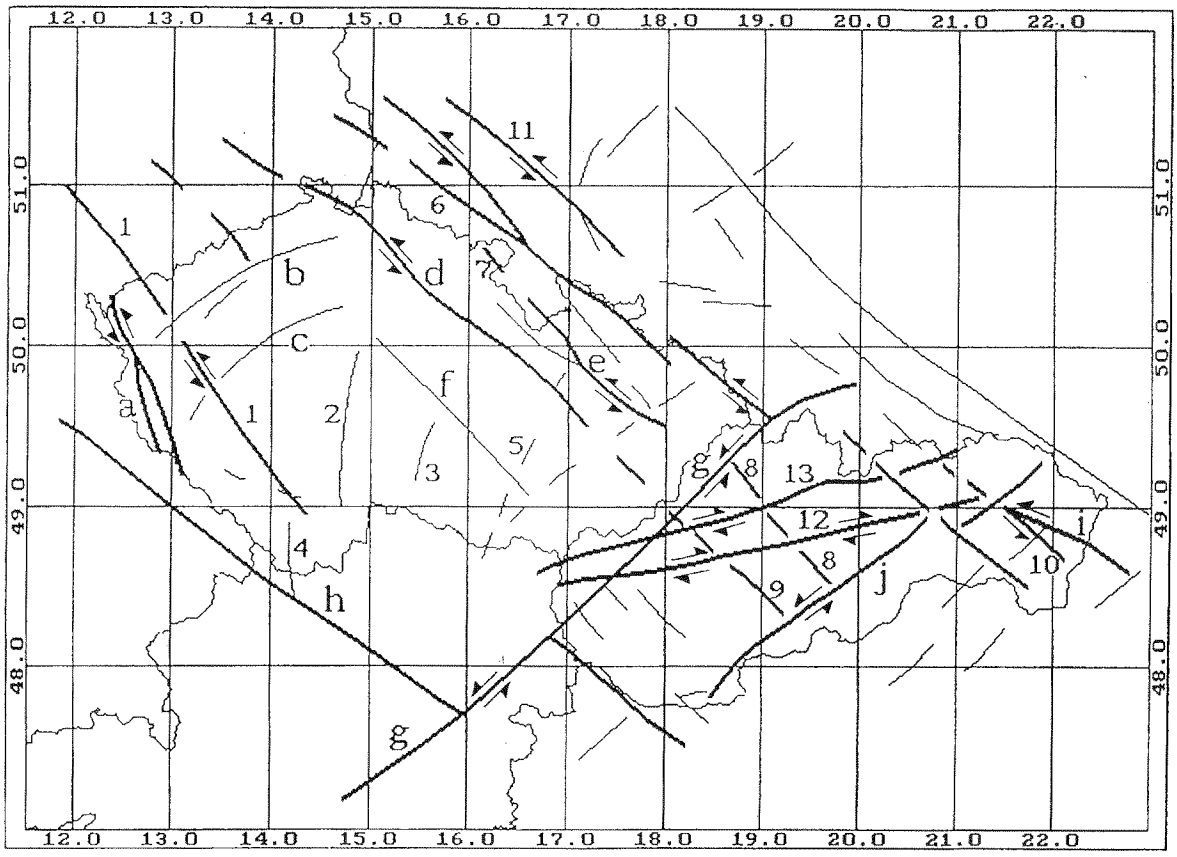

Fig. 2. Seismotectonic fault zones and boundaries of former Czechoslovakia: thick lines - main striking boundaries; thin lines - other striking boundaries; arrows - assumed horizontal displacement; fault zones in the Bohemian Massif: 1-Jachmov, 2-Blanice, 3-Pribyslav, 4-Rudolec trough, 5-Boskovice, 6-Intrasudetic, 7-Hronov - Porici, a-Cheb-Domazlice trench, b-Zatec - Litomerice, c-Klatovy - Zavist, d-Luzice - Jílovic, e-Kysperk - Zábreh, f-Podebrady - Zelezné hory Mts., and fault zones in the West Carpathians: 8-Revúca, 9-Prerov - Štiavnica, 10-Toplany - Mocarany, 11-Odra, 12-Hron, 13-Myjava - sub - Tatra, g-Verona - Semmering - Váh, h-Danube, i-Pareciany, j-Murán.

below the Inner Carpathians has to go up to town Rimavská Sobota. i.e. more than 100 km southeastwards of the Váh fault (g) (Fig. 2) and therefore, it is highly probable that the basement of this part of the Inner Carpathians has to belong to the European Platform units, too. In block H one can also observe faults of NW-SE directions, the origin of which could be explained by a copy effect of basement Epivariscan structures penetrating towards the surface.

Earthquakes and Their Relation to the Geological Structure of a Broader Area of the Contact Zone

The best known seismic activity of the West Carpathians is associated with the Peripieninian lineament zone which appears as a tectonic continuation of the Verona - Semmering lineament (g) crossing the region of the East Alps to the NE (Fig. 2). As assumption of a transcurrent fault existing between the east Alps and the West Carpathians (Unrung, 1984) which could explain the difference of Tertiary kinematics and tectogenesis of both mountain ranges, together with the conclusion of Biely (1975), made us designate this boundary as the Váh fault (g). On the basis of the results of remote sensing and geophysical data this fault can be regarded as transcurrent.

In the West Carpathians, the earthquake occurrence (Schenková, 1993) can be confined to three major structural - geological directions of (Fig. 2):

— thransverse faults (NW-SE) reflecting most

probably the Epivariscan platform structures underlying the West Carpathians,
— Carpathian faults (SW-NE) related to the origin of sliding surfaces between the main blocks, and
— shear and "gravity" thrust planes, along which the blocks move in the eastward direction (Pospíšil et al., 1986).

The recent seismic activity of the fault zones that separate the individual structural geological blocks of the Bohemian Massif and the West Carpathians from one another was studied by an inter-geoscientific analysis and correlation of available data on earthquake occurrences, neotectonics, geomorphology, photolineations, geophysical fields and recent crustal movements (Pospíšil et al., 1985, 1989, 1992; Schenk et al., 1982, 1986, 1989; Schenková et al., 1995). Regional schemes of both geological systems have been worked out (Schenk et al., 1982, 1986; Pospíšil et al., 1989, 1992) as well as seismotectonic analyses and seismotectonic models of a few mobile zones (Schenk et al. 1989, Schenková et al., 1995). The seismotectonic model of the West Carpathians (Schenk et al., 1986) exhibits a much higher degree of dynamics in the sub-Recent to Recent period than presumed so far.

If we consider that, on the one hand, the Sopron block (M) shifted considerably towards NE, which is documented by the course of the Danube fault zone (h) as well as by gravimetric data obtained in this region and that, on the other hand, the relatively immobile Tornquist - Teisseyre line which forms the western boundary of the Russian Platform did not make a continuation of these movements possible, then we can assume that due to a compression, a mutual shift of transverse fault zones took place towards NE (Fig. 2) and brought then closer. The presence of longitudinally extensive tectonic zones running WSW-ENE, Hron (12) and Myjava-sub-Tatra (13) zones (Pospíšil et al., 1986), seems to be a significant geodynamical element in this evolution. Along these tectonic zones, a superposition of blocks (shortening of lengths) as well as the dextral motion of the blocks situated to the north, may have taken place towards the east (Fig. 2).

This idea could be confirmed by the seismoactive segments of the transverse tectonic lines in the West Carpathians (Pospíšil et al., 1986). Their northern tips do not coincide with the position of the Klippen Zone (in the past regarded as a continuation of the Peripieninian lineament to the east), but with the [shear] transcurrent zones running WSW-ENE. The bending of the gravity and conductivity anomalies known from the Fatra-Tatra Mts. block (1) (Ibrmajer, 1981; Praus et al., 1981) corroborate this assumption.

What concerns geodynamics, relative sinistral movements take place along the Víh fault zone (g) even at present. The SE blocks move towards NE and, on the contrary, the NW blocks towards SW. This tendencies of the Sorpon block (M) towards the north or NE and by more frequent occurrences of earthquake foci in the NE direction. The NW-SE elongated shape of macroseismic isoline closures of strong West Carpathian earthquakes (e.g. Central Slovakia earthquake 1443, Komárno earthquake 1756, Zilina earthquake 1858) indicates an existence of a relatively shallow basement of the Carpathian units, the structural orientations of which must follow the NW-SE directions. From the regional geological viewpoint, these structures have to belong to the Epivariscan units only. It follows from the Fatra - Tatra Mts. block (I) could be understood as a continuation of the Podebrady - Zelezné hory Mts. zone (f). Analogously, a continuation of the Luzice-Jílovice (d) and the Kyšpert-Zábreh (e) fault zones could correspond to the intensive earthquake activity of the Revúca zone (8) and possibly the Odra fault zone (11) may continue into the Toplany-Mocarany fault zone (10).

This idea was also supported by results of the application of expert system GEO-1.2 for an evaluation of the maximum possible earthquakes of the non-Alpine part of the Central European territoy with the Bohemian Massif in its centre (Schenk et al., 1991, Fig. 3). The seismogenic character of the earthquake zones located in the broad vicinity of the contact between the Bohemian Massif and the West Carpathians can be explained with their help. In principle, system GEO-1.2 analyses geodata of an investigated area with respect to expert estimates, synthetizes the prognostic model respect to expert estimates, synthetizes the prognostic model (Schenk et al., 1994) and checks the results obtained. In the mentioned application, the earthquake catalogue, maps of Bouguer anomalies, the MOHO discontinuity, topographic relief of the Earth's surface and heat flow data

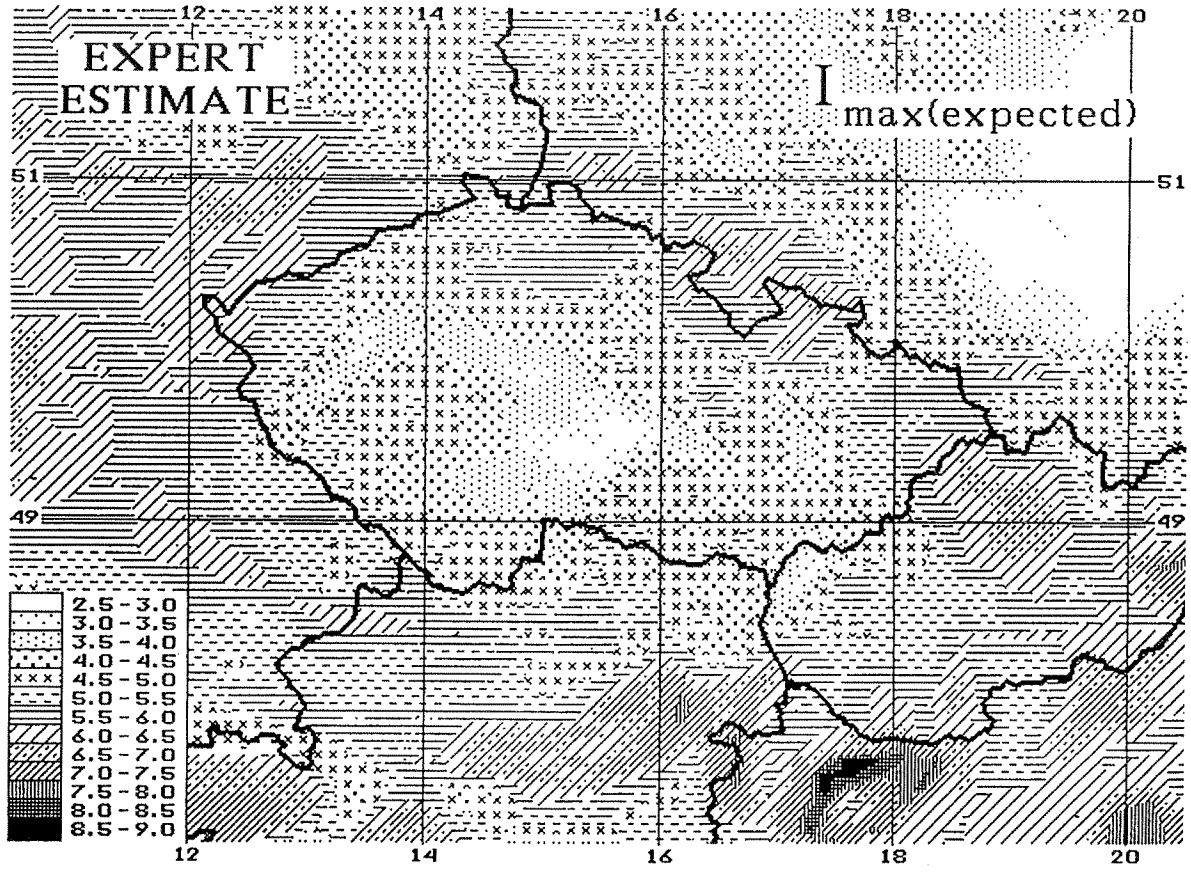

Fig. 3. Prognostic field of maximum earthquakes $I_{o(max)}$.

were used. The greatest contribution to the prognostic field of $I_{o(max)}$ was made by the MOHO discontinuity.

When the prognostic functions obtained for the non-Alpine area (Schenk et al., 1991) were applied to the West Carpathian arc in order to assess the maximum expected earthquake $I_{o(max)}$ field located in the broad vicinity of the contact zone with the Bohemian Massif, two seismically active focal zones ($I_{max.obs}$ = 7.5-8° MSK) with a different seismogenetic character were revealed. The Zilina focal zone was identified as an active zone with $I_{o(max)}$ = 6.5-7.5° MSK while for the other focal zone, the Little Carpathians $I_{o(max)}$ corresponds only to 6° MSK. This fact leads us to a conclusion that the seismogenesis of the Zilina focal zone has to be directly connected with non-Carpathian tectonic structures, i.e. with the Epivariscan European Platform units underlying the younger orogenic West Carpathian units. On the other hand, the earthquake activity of the Little Carpathians has to be linked mainly with the Carpathian tectonic elements. Such an interpretation is supported by focal depths of large earthquakes in these two zones. In the former, it is 20-25 km and in the latter, about 10 km.

All available geo-nomic data and materials on the West Carpathians were utilized in the last version of the seismotectonic map (Pospíšil et al., 1992). Its part corresponding to the broad area of our interest (Fig. 4) gives a simplifying view of the tectonic processes having taken place in the period from the Sarmatian until the Quaternary. The predominantly transcurrent character of seismotectonic systems corresponds to the NW-SE compression of the Epivariscan part of Europe (Müller et al., 1992).

The distribution of earthquake epicentres in Central Slovakia (Fig. 4) shows a linear pattern in the SE direction far behind the Zilina focal zone. this pattern displays a good azimuthal coincidence with the main Sudetic structural directions, which run through the Krkonoše-Jeseníky Mts. block (E), submerge below the Carpathians and continue in the SE direction (Fig. 2) to the Zilina focal zone up to town Rimavská Sobota (Schenk, 1984). It can be

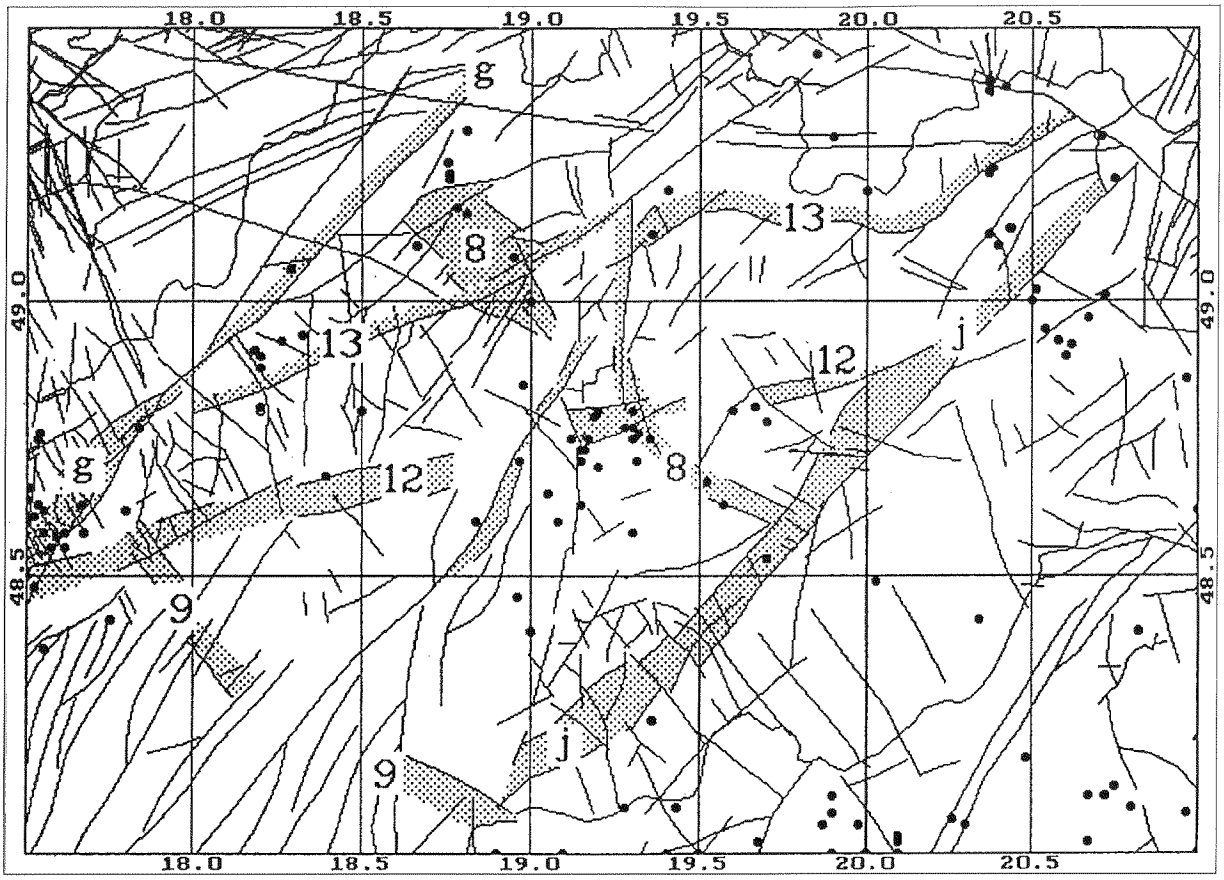

Fig. 4. Seismotectonic map of the broader area of the contact zone between the West Carpathians and the Bohemian Massif: point - earthquake epicentres, lines - faults, dotted belts - see Fig. 2.

concluded that the Epivariscan structures must continue in the Carpathian basement 120-130 km towards to SE from the outcropping thrust plane of the contact between the European Platform and the West Carpathians.

Applications of the Moody-Hill Model of Wrench Tectonics

In order to explain movements of West Carpathian blocks near the Zilina focal area, where a coexistence of two mobile trends is expected (Variscan and Alpine-Carpathian ones), Anderson's (1951) and Moody and Hill's (1956) theories on wrench-fault tectonics were applied to the Revúca fault system (8) (Fig. 5; Schenk et al., 1989), which belongs to one of the young Carpathian structures. The term wrench fault is synonymous with the terms strike-slip fault and transcurrent fault.

Anderson (1951) outlined that the planes of actual shear do not coincide with the planes of maximum shear stress, but lie closer to the axis of maximum compressive stress and far from the angle of shear. Moody and Hill (1956) extended the works on faulting by developing the hypothesis that folds, thrust faults and wrench faults could be generated as a result of the movement along a large wrench fault. This model can be applied if the dominant motion of one block relative to the other is horizontal and the fault planes are essentially vertical. Since these conditions correspond to the Revúca fault system (8), it can be assumed that the mobility of the system will reflect recent mobile trends which were affected by the latest Alpine orogenesis.

For the Revúca fault system (Fig. 5) the following features were studied: the geological development of the system during the Late Tertiary and Quaternary, geological evidences of horizontal and vertical movements of structural blocks, recent crustal movements, remote sensing

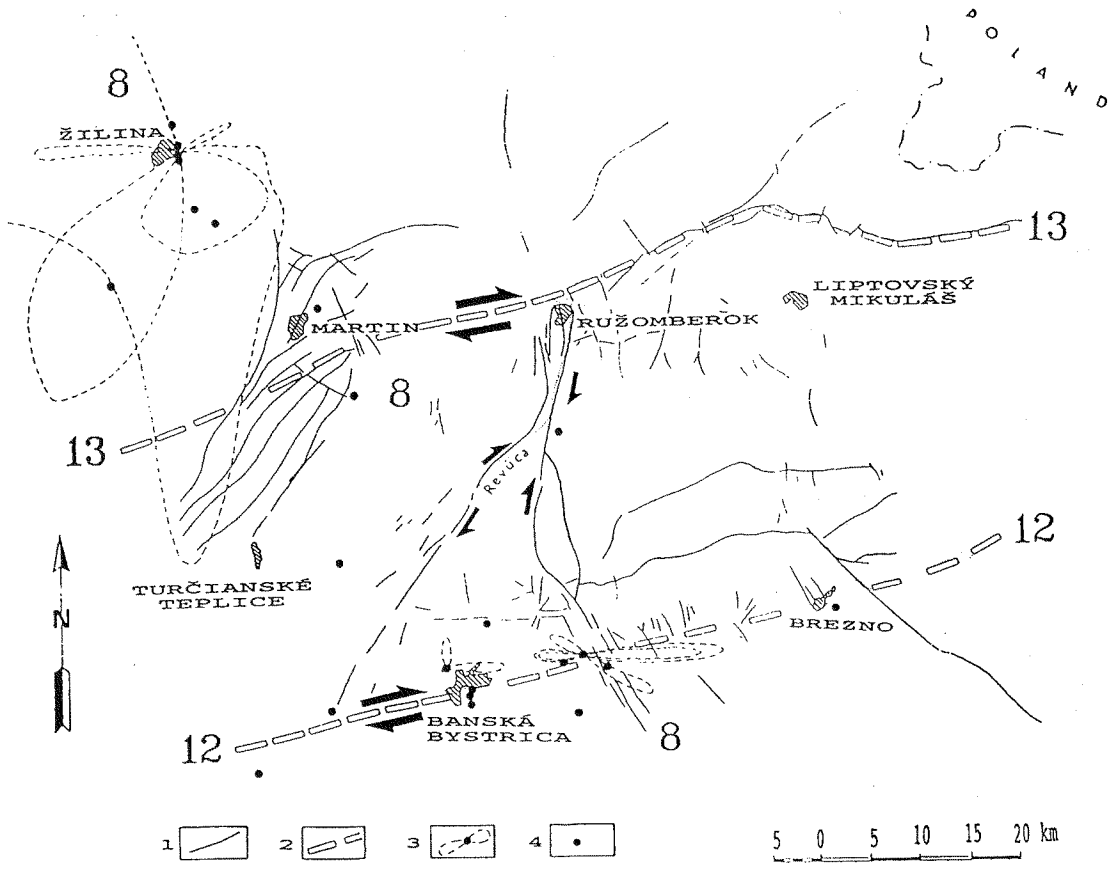

Fig. 5. Dynamics of the Revúca fault system: 1-faults, 2-wrench fault of the 1st order, 3-direction of the 1st order seismic energy attenuation, 4-earthquake epicentres.

data (lineaments determined from satellite images), earthquake activity, gravity and magnetic anomalies, etc. In order to obtain information on the dependence of seismic energy attenuation in the broader vicinity of earthquake foci and its relationship to the geological structure, available macroseismic fields (Procházková and Kárník, 1978) were analyzed (Schenk et al., 1989). The asymmetry of macroseismic fields of earthquakes discloses the directions of lower seismic energy attenuations around earthquake epicentres (Fig. 5). These directions coincide with main structural directions of the area.

The Revúca fault system is a dextral strike-slip fault (Bujnovsky 1979) accompanied by a system of secondary faults oriented perpendicularly to the main displacement direction. The whole fault system ((8) in Figs. 4 and 5) is located between two major tectonic elements, the Myjava-sub-Tatra (13) and the Hron (12) transcurrent tectonic zones on which horizontal dextral displacements are considered.

The earthquake occorrences in this area (Fig. 5) can be associated with weakened points of the Hron (12) and Myjava-sub-Tatra (13) zones, especially where the Revúca fault system (8) crosses them. The lack of instrumental seismic records has not allowed fault plane solutions for any events in this region to be determined. Nevertheless, the above mentioned analysis (Schenk et al., 1989) of available isoseismal maps allows the directions of decreased seismic energy in the northern and southern parts of the area, near towns Zilina and Banská Bystrica, to be establish (Fig. 5). E-W or actually ENE-WSW local structural direction has proved to prevail in the Hron river valley. Their coincidence with the direction of the Hron transcurrent tectonic zone (12) is fairly good.

Utilizing the results of gravity and magnetic measurements (Obernauer, 1980) and the correlation of seismological data with lineations determined from satellite images (Pospísil et al., 1985), we can include in the dextral transcurrent system also its broader surroundings. A paleogeographic analysis revealed the uplift of the

Low Tatra region (southern part of the studied area) with respect to its surroundings until the Pliocene Age (Klínec et al., 1985). In the last period, this uplift accelerated as a consequence of the horizontal movements of the Carpathian blocks along the faults of ENE-WSW directions (Janku et al., 1984, Pospísil et al., 1985).

Dextral motions along the Revúca fault system (8) seem to reflect a mobile activity of Epivariscan blocks of the European Platform creating the basement of the West Carpathians. As mentioned above, the mobility of the Epivariscan blocks has the sinistral character (Schenk et al., 1986). If it is assumed that the origin of the Revúca fault system is genetically connected with the main tectonic directions in basement (a probale copy effect to upper geological blocks is expected), then the dextral motion trends acting on the upper Carpathian blocks of the Revúca system compensate the sinistral motions going on in the basement.

This hypothesis is also supported by the existence of directions of lower seismic energy attenuation from earthquake epicentres in the Zilina focal area and from events within an area, where the Revúca fault system (8) crosses the Hron tectonic zone (12) (Fig. 5). We believe that earthquake motions occurring in thesee directions should act in accordance with the basement Epivariscan structures, i.e. they should most probably have sinistral character. On the other hand, the motion mechanisms of shallow foci situated near the crossing of the RevúLca (8) and the Hron tectonic systems (12), tectonic transcurrent zones. The described hypothesis could be proved by instrumental monitoring of earthquakes, which allows a determination of their fault plane solutions.

Conclusions

It is evident that the Epivariscan basement (an eastward continuation of the Bohemian Massif below the West Carpathians) can be identified in the SE direction up to a distance of 120-130 km from the NW rim contact of the West Carpathians. A detailed analysis of the movement of one of the inner West Carpathian tectonic systems, the Revúca fault system, the origin of which is assumed to be connected with the tectonic directions in the Epivariscan basement, shows that dextral movements acting on upper Carpathian blocks of the Revúca system compensate the long-term sinistral movements going on in its basement.

References

Anderson, E.M., 1951. The dynamics of faulting. Oliver and Boyd, Edinburgh, 206 pp.

Balatka, B., Róth, Z., Sládek, J., Zeman, A., 1983. The Bohemian Massif: discussion on its delineation and tectonic division (in Czech). Vestn. Ústr. Úst. Geol., 58, 369-376.

Biely, A., 1975. Note to the term "Peripieninian lineament" (in Slovak). Geol. Práce spr., GÚDŠ, Bratislava, 63, 205-209.

Bujnovsky, A., 1979. Geological profile and structure elements of nappes in the NW part of the Low Tatra and Revúca fault zone. Tectonic profils through the West Carpathians, Mahel, M. (Ed.). Geolog. Inst. Dionyza Štúra, Bratislava, 85-89.

Dudek, A., 1981. The principal features of the geological structure of Czechoslovakia with regard to adjacent regions. In "Geophysical syntheses in Czechoslovakia", Zátopek, A. (Ed.). Veda, Bratislava, 19-25.

Fusán, O., Ibrmajer, J., Kvitkovic, J., Plancár, J., 1981. Block dynamics of the West Carpathians. In "Geophysical syntheses in Czechoslovakia", Zátopek, A. (Ed.). Veda, Bratislava, 153-158.

Ibrmajer, J., 1981. Geological interpretation of gravity maps of Czechoslovakia. In "Geophysical syntheses in Czechoslovakia", Zátopek, A. (Ed.). Veda, Bratislava, 135-148.

Janju, J., Pospísil, L., Vass, D., 1984. Contribution of remote sensing to knowledge of the Western Carpathian structure (in Slovak). Mineralia Slovaca, Spišská Nová Ves, 16, 121-137.

Klinec, A., Pospíšil, L., Vass, D., 1984. Contribution of remote sensing to knowledge of the Western Carpathian structure (in Slovak). Mineralia Slovaca, 16, 121-137.

Moody, J.D., Hill, M.J., 1956. Wrench-fault tectonics. Geol. Soc. Am. Bull. 67, 1207-1246.

Müller, B., Zoback, M.L., Fuchs, K., Martin, L., Gregensen, S., Pavoni, N., Stephanson, O., Ljungren, Ch., 1992, Regional pattern of

tectonic stress in Europe. J. Geoph. Res., B8, 97, 11, 783-11, 803.

Obernauer, D., 1980. Geophysical research of the western part of the Slovenské Rudohorie Mts. and the eastern part of the Low Tatra (in Slovak). Faculty of Natural Science, Bratislava, PhD thesis, 115 pp.

Pospísil, L., Schenk, V., Schenková, Z., 1985. Relation between seismoactive zones and remote sensing data in the West Carpathians. Proc. 3rd Intern. Symposium on Analysis of Seismicity and Seismic Risk, Geoph. Inst. Czechosl. Acad. Sci. Praha, 256-263.

Pospísil, L., Nemcok, J., Graniczny, M., Doktór, S., 1986. Contribution of remote sensing data to the identification of the strike-slip faults in the West Carpathians. Mineral. Slov., Spišská Nová Ves, 18, 5, 385-402.

Pospísil, L., Schenk, V., Schenková, Z., 1989. Seismotectonic map of the West Carpathians - version 1989. Proc. 4th Intern. Symp. on Analysis of Seismicity and on seismic Risk, Geoph. Inst. Czechosl. Acad. Sci., Praha, 494-503.

Pospísil, L., Schenk, V., Schenková, Z., 1992. Seismotectonic map of the Western Carpathians - version 1990. Proc. 22nd General Assembly of the European Seismological Commission, 1, Barcelona, 475-480.

Praus, O., Pecová, J., Petr, V., Hvozdara, M., Cerv, V., Pek, J., Laštovicková, M., 1981. Electromagnetic induction and electrical conductivity of the Earth's body. In "Geophysical syntheses in Czechoslovakia", Zátopek, A. (Ed.). Veda, Bratislava, 297-315.

Procházková, D., Kárník, V. (Eds.), 1978. Atlas of isoseismal maps for Central and Eastern Europe. Geophy. Inst., Czechosl. Acad. Sci., Prague.

Schenk, V., 1984. Earthquake Occurrence and Main Tectonic Directions in the Bohemian Massif (in Czech). In "Vyzkum hlubinné geologické stavby Ceskoslovenska", Loucná n/Des., 97-101.

Schenk, V., Kárník, V., Schenková, Z., 1982. Seismotectonic scheme of Central and Eastern Europe. Stud. geoph. et geod. 26, 132-144.

Schenk, V., Schenková, Z., Pospísil, L., Zeman, A., 1986. Seismotectonic model of the upper part of the Earth's crust of Czechoslovakia. Studia geoph. et geod. 30, 321-330.

Schenk, V., Schenková, Z., Pospísik, L., 1989. Fault systeem dynamics and seismic activity - two examples from the Bohemian Massif and the Western Carpathians. Geoph. Trans. 35, 101-116.

Schenk, V., Gitis, V.G., Schenková, Z., Mantlík, F., Kottnauer, P., Yurkov, E.F., Shchukin, Yu. K., 1991. Maximum earthquake prediction in Central Europe given by the GEO 1.2 expert system. Proc. 4th Intern. Conference on Seismic Zonation, Stanford, Earthq. Eng. Res. Institute, 3, 83-91.

Schenk, V., Schenková, Z., Gitis, V.G., 1994. Features of Geonomic Prognostic Functions for the Maximum Possible Earthquake, Natural Hazards 10, 171-180.

Schenková, Z., 1993. Earthquake Catalogue for the Czechoslovakia, Geophysical Inst., Acad. Sci. of the Czech Republic, Prague, unpublished.

Schenková, Z., Schenk, V., Pospíšil, L., Kottnauer, P., 1995. Seismogeological pattern of a transition area between the Eastern Alps and the Western Carpathians. Tectonophysics 248, 235-245.

Sikora W.J., 1976. On lineaments found in the Carpathians. Rocz. Pol. Tow. Geol. 46, 3.

Unrung, L., 1984. Geodynamic evolution of the Carpathians. Rocz. Pol., Tow. Geol., Kraków, 52, 1/4, 39-66.

EARTHQUAKES VERSUS TECTONIC MOVEMENTS

Dana Procházková

State Office for Nuclear Safety, Praha, Czech Republic

Abstract

The present paper contains the regional geological characheristics of Central Europe, the chronological model of neotectonic movements with specification of neotectonic regional units and their present movements, the earthquake characteristics and the speciication of seismogenic movements.

It was found that the genesis of the focal regions with occurrence of the strongest earthquakes is connected with several movement trends in last 5 Ma. Six more of less tectonically separate regional units were revealed. The epicenters of earthquakes with the intensity equal and greater that 5° MSK-64 concentrate along the boundary lines of these neotectonic units.

Introduction

We are not able to stop the earthquake origin, we have not been able yet to predict earthquake origin successfully. We are only able to mitigate the earthquake's effects. To do it we must respect the regularities and the principles of their origin in our life and in siting and operating technological objects. From this point of view we study the relation "earthquakes vs. tectonic movements in Central Europe".

Geology and tectonics of Central Europe

From the geological point of view, the study area, Fig. 1, is essentially formed by the Hercynides and Alpides. It belongs to the collision zone between the continental block of Africa and the continental block of Euroasia; Euroasia represents a relative stable block and Africa has been moving to the North at an almost steady rate of about 25 mm per year over the last 200 Ma (Roth, 1987). The fundamental role of a tangencial stress transferred from the African Continent to the Alpides and their European foreland has been evidenced in Central Europe by a small scale tectonic analysis of the platform cover Cenozoic structures (Bergerat, 1987).

The tectonic history of present-day Central Europe (Fig. 2) has been controlled from the Late Palaeozoic times by permanently continuing collision of two converging lithospheric plates - the African and Euroasian (e.g. Ziegler, 1982, 1984). In the period of Alpine movements (since about 100 Ma ago) the African lithospheric plate

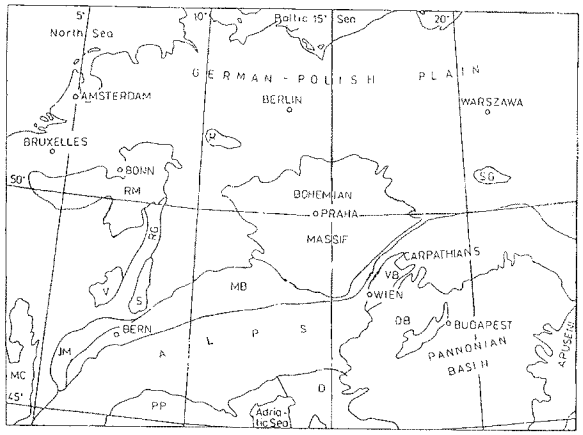

Fig. 1. The territory described and its principal orographic and geological units.
Abbreviations: D - Dinarides, DB - Danube Basin, H - Harz Mts, JM - Jura Mts, MB - Molasse Basin, MC - Massif Central, PP - Po Plain, RG - Rhine Graben, RM - Rhenish Massif, S - Schwarzwald Mts, SG - Holy Cross Mts, V - Vosges Mts.

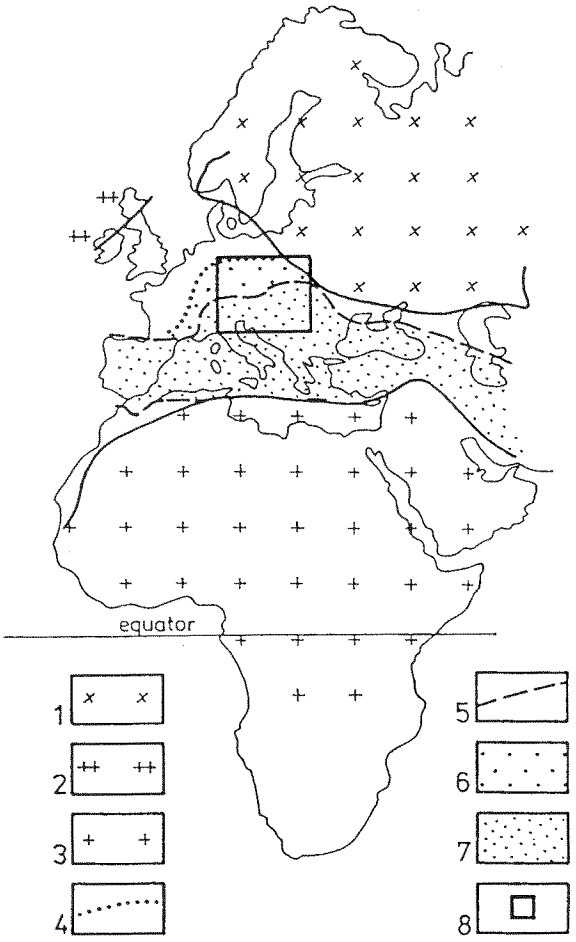

Fig. 2. Variscan - Alpine collision belt separating the African and Fennosarmatian Shields. **Explanation:** 1 - Fonnosarmatia, 2 - Eria, 3 - African Shield, 4 - northern border of strong Saxonian (i.e. Alpine) platform fracturing, 5 - boundary of the Alpides within the collision belt, 6 - zone of intense Saxonian fracturing within the collision belt, 7 - Alpides, 8 - the territory under consideration.

shifted the African continent as its part to the N, i.e. against the Euroasia, which was relatively stable as to its situation to the rotation axis of the Earth (Krs, 1982). Since the Devonian - Lower Corboniferous times these two domains moving towards each other with a steady velocity of about 25 mm per year continued (Roth, 1987). From the beginning of the collision the continental lithosphere of Africa has transmitted the subhorizontally oriented stress of the African lithospheric plate to the lithosphere of the developing Euroasian contitent (e.g. Bergerat, 1987).

In the about 1.500 km wide collision zone (Procházková and Roth, 1993) deformations, material changes and mutual movements of the thus formed blocks and microcontinental fragments occurred. The Mediterranean collision zone, of course, markedly extends beyond the limits of Central Europe not only in the N and S but also in the W and E direction. In the N and NE it is delimited against the old core of Europe (Fennosarmatia) by the Tornquist lineament (solid line in Fig. 2 in NE part) and in the S, by the Sahara (Agadir) line in norhtern Africa (solid line in Fig. 2).

Two belts can be distringuished within the Variscan - Alpine Mediterranean collision zone according to the predominant tectonic styles of the Alpine deformation:

— the prevailingly "Alpine-type" belt of Alpides,

— the "Germano-type" belt of epi-platform (epi-Palaeozoic) tables only broken up during the Alpine movements.

In Central Europe (Fig. 1) it is the wide belt of the Alpides (the Alps and Carpathians) in the S, forming the inner belt of the present-day form of the Mediterranean collision zone. The structure of the Alpides is in central Europe partly covered with Late Tertiary deposits of the inner Alpine basins (Pannonian Basin, Vienna Basin and others). The northern boundary of the Alpides in Central Europe is generally defined by the momentary overthrust line of the Alpide edifice upon the epi-Variscan table of their foreland.

In the northern foreland of the Alps - Carpathians in Central Europe there is the epi-Palaeozoic platform disrupted by the Alpine (Saxonian) block tectonics. In the NE it extends to the Tornquist lineament. It includes (as its southern margin) also the Tertiary foredeep of the Alps and of the Carpathians.

The development trends of neotectonic movements (especially in the last 5-10 Ma) are pictured in Fig. 3, details are in Table 1 (the synthesis of data is described in paper (Procházková and Roth, 1993)). In essence the movement trends represent a continuation of the Post - Early Sarmatian and partly Post - Dacian movements.

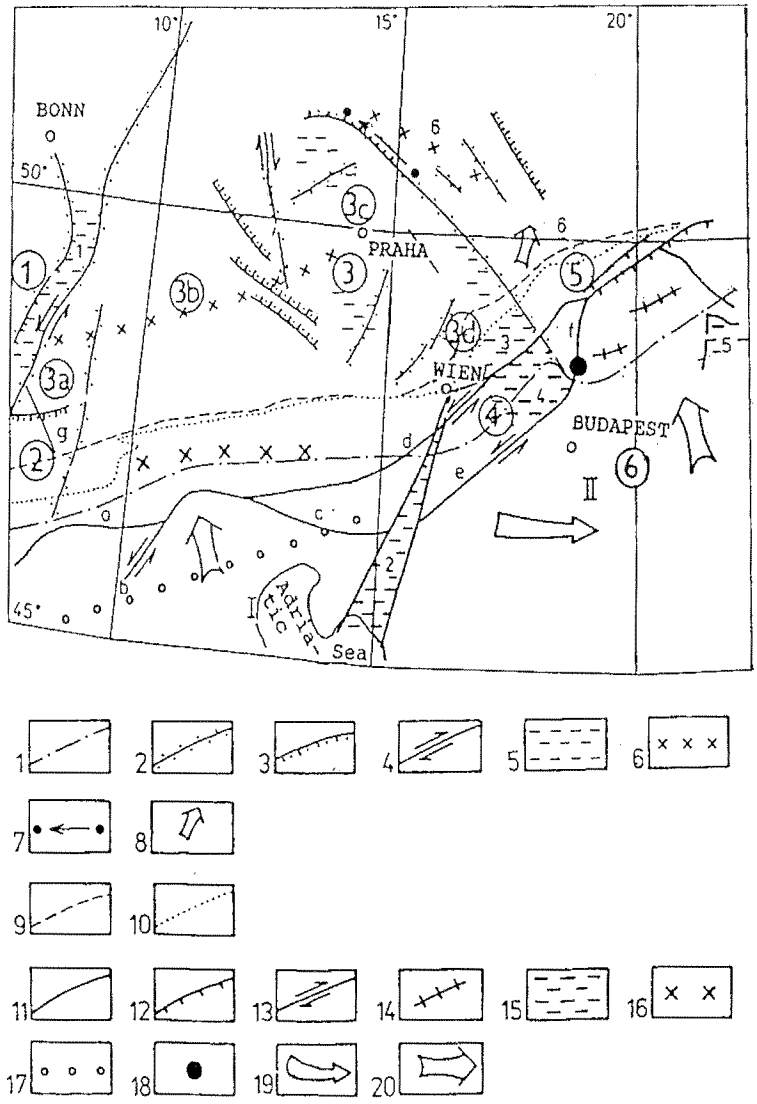

Fig. 3. Recent movement tendencies of the Earth s crust in Central Europe.
Explanations: Epi - Paleozoic Platform (1-8):
1 - S margin of the platform concealed below the northward overthrust Alpine chain, 2 - steep fractures, 3 - upthrusts, 4 - strike - slip, 5 - extension areas, 6 - linear doming of the platform, 7 - approximate center of the sinistral twist of the Sudetian - Maleník block under the attack of the Carpathians, 8 - sense of the sinistral twist of the Sudetian - Maleník block (Krs 1982).
Alpides (i.e. the Alps and the Carpathians, 9-20):
9 - frontal boundary of the Alpides (margin of the paraautochthone platform cover), 10 - frontal margin of the geosynclinal Alpine structure, 11 - steeo fractures, 12 - principal Cenozoic upthrusts, 13 - strike - slip, 14 - recent longitudinal roll - over faults separating the West Carpathian core - mountains (Grecula, Roth, 1978), 15 - extension areas, 16 - doming axis, 17 - down - warping axis, 18 - center of the recent sinistral twisting of the Pannonian - Carpathian block, 19 - direction of the recent excentric sinistral twisting of the Pannonian - Carpathian block, 20 - sites and directions of the principal stress of the Alpides in Central Europe.
Diphers: I - the Cenozoic megablock of the Alps, II - the Cenozoic megablock of the Dinarides - Carpathians; 1 - Rhine Graben, 2 - Vienna Kvarnerski Bay fault zone, 3 - Vienna Basin, 4 - Danube Basin, 5 - Trans - Carpathian Basin, 6 - Sudetian - Malenák block;
circled 1, 2, ..., 6 - independent neotectonic units.
Letters: a - Insubric - Drava line, b - Judicaria line c - Gailtal line, d - Mur - Mürz - Leitha - Zilina line, e - Raab line, f - Revuca line, g - Basel - Lùzern line.

Neotectonic Units of Central Europe

During the latest tectogenic developement up to 10 Ma ago the following more of less independent tectonic regional units developed in Central Europe (see Fig. 3, from W to E):

1. The Burgundy - Vosges region, the Rhone and Rhine grabens.

2. The region of the Dauphin folds and the Jura Mts.

3. The Central European neotectonic region including four subregions:

a- The Schwarzwald.

b- The region of the German - Bohemian triangle.

c- The region of the Central European mountain ranges.

d- The Brunovistulicum.

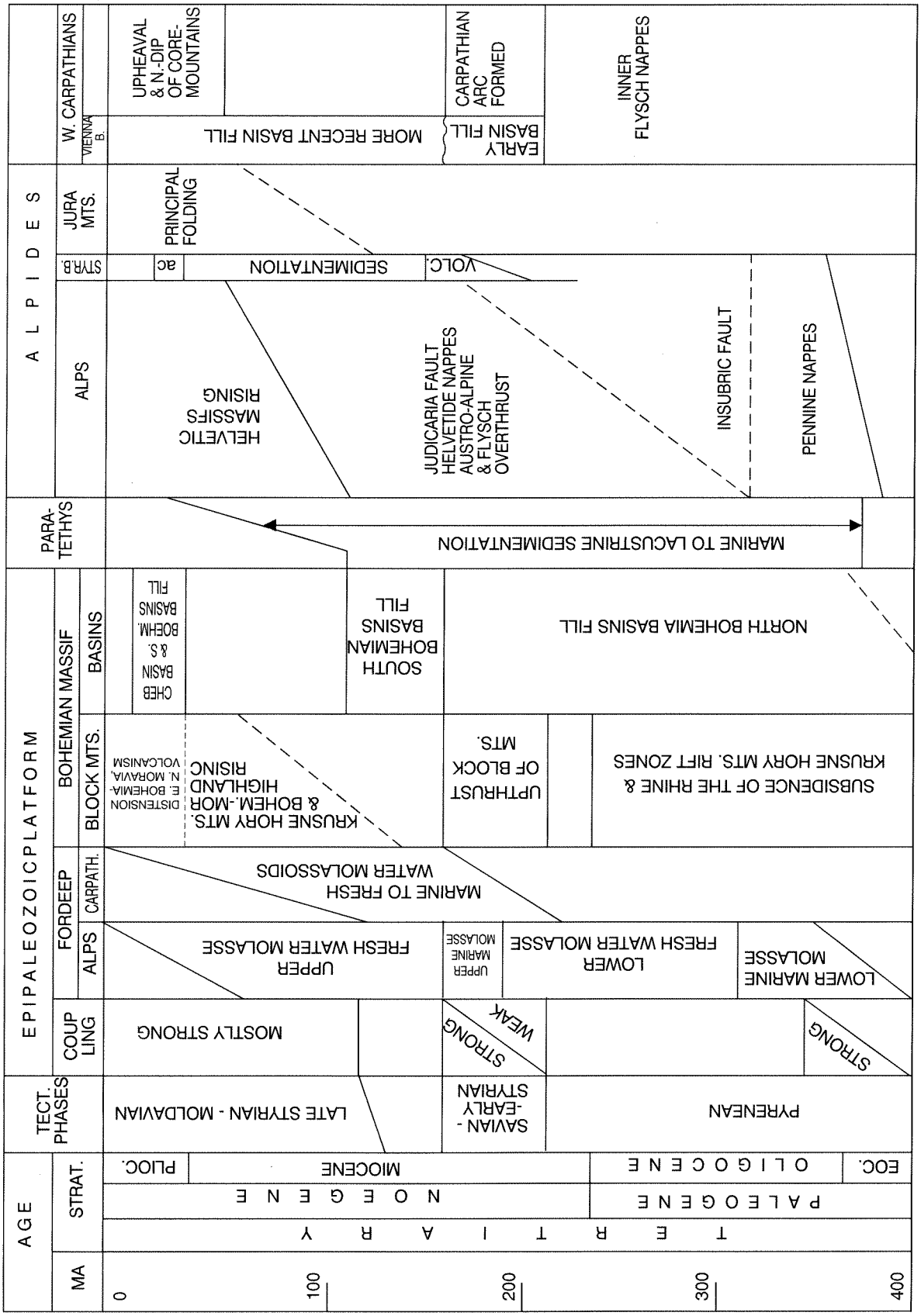
AGE
MA
STRAT.
TECT. PHASES
EPIPALEOZOICPLATFORM
COUP LING
FORDEEP
ALPS
CARPATH.
BOHEMIAN MASSIF
BLOCK MTS.
BASINS
PARA-TETHYS
ALPIDES
ALPS
STYR.B.
JURA MTS.
W. CARPATHIANS
VIENNA B.
0
100
200
300
400
TERTIARY
NEOGENE
PALEOGENE
PLIOC.
MIOCENE
OLIGOCENE
EOC.
LATE STYRIAN - MOLDAVIAN
SAVIAN - -EARLY STYRIAN
PYRENEAN
MOSTLY STRONG
STRONG
WEAK
STRONG
UPPER FRESH WATER MOLASSE
UPPER MARINE MOLASSE
LOWER FRESH WATER MOLASSE
LOWER MARINE MOLASSE
MARINE TO FRESH WATER MOLASSOIDS
KRUSNE HORY MTS. & BOHEM.-MOR HIGHLAND RISING
DISTENSION E. BOHEMIA-N. MORAVIA-VOLCANISM
UPTHRUST OF BLOCK MTS.
SUBSIDENCE OF THE RHINE & KRUSNE HORY MTS. RIFT ZONES
CHEB BASIN & S. BOEHM. BASINS FILL
SOUTH BOHEMIAN BASINS FILL
NORTH BOHEMIA BASINS FILL
MARINE TO LACUSTRINE SEDIMENTATION
HELVETIC MASSIFS RISING
JUDICARIA FAULT HELVETIDE NAPPES AUSTRO-ALPINE & FLYSCH OVERTHRUST
INSUBRIC FAULT
PENNINE NAPPES
ac
SEDIMENTATION
VOLC.
PRINCIPAL FOLDING
UPHEAVAL & N.-DIP OF CORE-MOUNTAINS
MORE RECENT BASIN FILL
EARLY BASIN FILL
CARPATHIAN ARC FORMED
INNER FLYSCH NAPPES

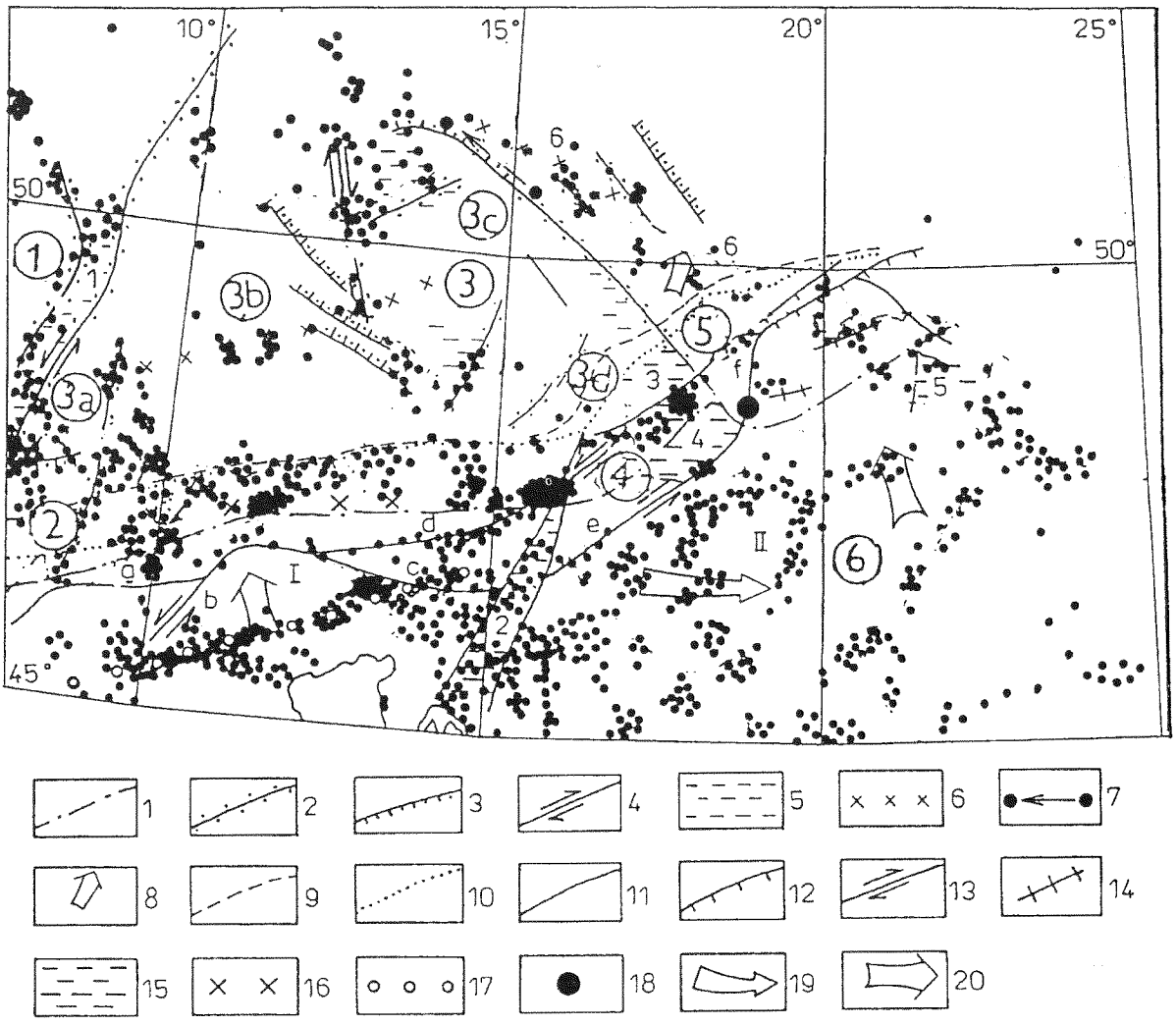

Fig. 4. Regional tectonic framework with marking recent tectonic tendencies (Fig. 3) and earthquake epicentres with intensities $I_0 \geq 5^o$ MSK-64 of the last thousand years.

4. The region of the Danube and SW Pannonian Basins.

5. The region of active nappe structure of the Flysh West Carpathians.

6. The Central Alpine - Carpathian neotectonic region.

Present Earthquake Pattern in Central Europe

Earthquakes originate by a sudden release of mechanical energy in the solid Earth's body. They are one of the manifestations of tectonic processes which constantly take place in the Earth.

The specific feature of the region under study is low seismic activity on its greater part, which means that the study has to involve also analyses of historical earthquakes since instrumental data only include a short time interval, the last 50-80 years. The distribution of epicenters, Fig. 4. It only covers epicenters of stronger shocks with epicentral intensity $I_0 \geq 5^o$ MSK-64 in the last thousand years (Procházková, 1984) represent the combinations of individual clusters of foci sharing the same characteristics of the seismic regime. The analysis of the quantitative earthquake characteristics (Procházkovaá, 1984, 1993) shows that even in a single focal region, earthquakes differ in size, mechanisms, focal depth and source dimension. The results can be summarized as follows:

— The maximum earthquake size in the region considered reached to 10^{o} MSK-64 (e.g. Villach 1348, Friuli 1976). Earthquake foci occur in the upper part of the Earth's crust (mostly h ≤ 10 km). In the southern part of the study area, the seismoactive layer (i.e. the layer with foci) is thicker (25-30 km) than in the northern and central parts.
— Even in one focal region there appear different focal mechanisms (e.g. the strongest shocks in Western Bohemia - December 21, 1985 and January 20, 1986, in Semmering region - April 15, 1984 and May 24, 1984, in Friuli - May 6, 1976 and September 15, 1976). The great difference in prevailing focal mechanisms are observed in Friuli - Villach region (Anderson and Jackson, 1987) where the shocks testify to an almost north - south subhorizontal compression and in the Mur - Mürz - Leitha region (Gangl, 1975, Procházková and Drimmel, 1989) where thw shocks clearly point to a prevailing sinistral displacement in the subvertical zone. In Western Alps the fault - plane solutions document NW-SE dilatation of the region (Pavoni, 1991).
— In none of focal regions distinguished the same types of earthquake activity have repeating regularly; in one region there are observed active periods and gaps in long-term and short-term time scales, earthquakes with low and high stress drop (see e.g. the strongest shocks in Friuli of May 6, 1976 and September 15, 1976), distinct time-space models of earthquake occurrence and even the existence of space - and - time tendencies in earthquake occurrence.

The existence of a great variety of seismicity in space and time documents not only the differences in focal processes but also the differences in the stress fields in the region considered that are caused by the changes of running tectonic processes.

Recent Seismogenic Movements in Central Europe

The great variety of earthquake occurence in time and space reflects the complexity of the geodynamic model of the region under study. A comparison of the regional geologically recent changes in the orientation and relative size of the principal stresses in the crust, geologically, geomorphologically established young movements of the Earth's surface, geodetically established recent movements with historical and recent seismicity (Fig. 4) leads to the following conclusions on the genesis of the focal regions in which stronger earthquakes occur:

— In the stydy area, earthquake epicenters often concentrate into the regions along lines, where principal movements take place at the present time, i.e. on the boundaries of the relative independent tectonic units limited in the foregoing paragraph.
— Foci of stronger earthquakes do not originate only in the dynamic system consisting of the Alpides (the Alps and Carpathians), but also in the revived platform forefield of the Alpides (epi-Hercynian Platform).
— Foci of stronger earthquakes originate in the platform (Fig. 4) only where it is evidently coupled with the Alpides, i.e. in a belt about 300 km wide, where movement in last 5-10 Ma as well as pronounced historical and recent seismicity are observed.
— The present day dominant stress (component σ_1), without which stronger shocks cannot originate in the platform, is the subhorizontal, approximately meridional stress (Bergerat 1987, Ziegler 1987) transferred by the Alpides from Africa, influenced probably by the lasting shift of the Carpathians to the NNE. As a rule, foci of these shocks lie in the brittle lithosphere, i.e. at depths of 3-20 km (predominantly 5-8 km), mostly on the pre-existing (Hercynian and older) disturbance zones, if their orientation is close to the regional greatest present shear stresses. The strongest shocks in the region of the Eastern Alps and the Western Carpathians occur in the space, where transversal vertical shear fault (with vertical σ_2) passes horizontally into longitudinal shear faults (with subhorizontal σ_2 - e.g. Friuli - Mur - Mürz - Leitha, Zilina, Komárno). Foci of stronger shocks in the Alpine - activated platform concentrated into the zones of strike - slips (e.g. Rhine graven) and into regions where bending (horizontal - as the Sudetian - Maleník block bent (in Trutnov area) under the stress of the displaced Carpathians at its eastern submerged end). In Central Europe, vertical as the Vosges - Schwarzwald dome

and its E extension, the neotectonic structure influence the transfer of the "African" stress inside the Alpides as well as from the Alpides to the platform very expressivel (Fig. 4).

— Stronger shocks do not occur in the fields of purely subsidence tectonics, i.e. unless the subsidence tectonics is accompanied by active strike - slips. From seismogenic point of view, there is a great difference e.g. between the subsidence tectonics of the aseismic Vienna Basin (E-W stretching outside the region of the Alpine stress transfer, i.e. NW of the strike - slip zone Mur - Mürz - Leitha, Zilina, Komárno). Foci of stronger shocks in the Alpine - activated platform concentrated into the zones of strike - slips (e.g. Rhine graben) and into regions where bending (horizontal - as the Sudetian - Maleník block bent (in Trutnov area) under the stress of the displaced Carpathians at its eastern submerged end). In Central Europe, vertical as the Vosges - Schwarzwald dome and its E extension, the neotectonic structure influence the transfer of the [African] stress inside the Alpides as well as from the Alpides to the platform very expressively (Fig. 4).

— Stronger shocks do not occur in the fields of purely subsidence tectonics, i.e. unless the subsidence tectonics is accompanied by active strike - slips. From seismogenic point of view, there is a great difference e.g. between the subsidence tectonics of the aseismic Vienna Basin (E-W stretching outside the region of the Alpine stress transfer, i.e. NW of the strike - slip zone Mur - Mürz - Leitha - Zilina), and between the subsidence tectonics of the Danube Basin, which is bounded as well in NW as in SE by seismogenic zones (Procházková and Roth 1993).

— The prevailing sinistral movements on seismogenic faults lead to a hypothesis on the existing vortex of the astenosphere (Fig. 3), at the Carpathians - Alps platform. Its product would be majority of movements in our study area.

— Seismo-tectonic units that were revealed by the analysis of seismic regimes of partial focal regions (Procházková 1984, 1993) belong always to only one of the regional neotectonic units.

Conclusion

The synthesis of data on the dynamic movements in Central Europe in the last 40 Ma made it possible to device a general idea of the dynamic development of the area and a chronological model of neotectonic movements in the area under investigation. It shows that endogenic neotectonic movements have a considerable time and regional stability. From this we can suppose they will go on (continuously or intermittently) also in the near future (measured by human history). If they manifested themselves as seismogenic in the past, we may presume that their future character will hardly change in the natural way. If we know them as aseismic movements, much depends on the length of the time interval the respective region has been historically observed; there are always historical limitations to seismological safety. The development of the lithosphere in the geological time scale documents the possibility of essential changes of the tectonic régime; at the same time it also documents its great stability judged by the standards of human history.

A total six tectonic regional units that act more or less independently in Central Europe have been identified. Only some parts of the boundaries of these relative independent regional tectonic units are seismically active. The predominant zone owing to earthquake occurrence is the zone Mur - Mürz - Leitha - Zilina rising as a consequence of the Late Styrian - Moldavian renewal of stress of the Alps (ca 5 Ma ago) and being noted for sinistral - strike - slip.

References

Anderson H. and Jackson J., 1987. Active Tectonics of the Adriatic Region. Geophys. J.R. Astr. Soc., 91, 937-983.

Bergerat F., 1987. Stress Fields in the European Platform at the Time of Africa - Eurasia Collision. Tectonics, 6, 99-132.

Gangl G., 1975. Seismotectonic Investigations of the Western Part of the Inneralpine Pannonian Basin (Eastern Alps and Dinarides). In: Proceed. XIV. th Gen. Ass. ESC, Berlin, 409-431.

Kárník V., Procházková D., Schenk V., Schen-

ková Z., Broucek I., 1988. Seismic Zoning Map - Version 1987. Studia geoph. et geod., 32, 144-150.

Krs M., 1982. Implication of Statistical Evaluation of Phanerozoic Paleomagnetic Data (Eurasia, Africa). Rozpravy Cs. Akad. Ved, 92, 86 p.

Pavoni N., 1991. Seismotektonik. ETH Erdwissenschaften Heute. Zürich, 16p.

Procházková D., 1984. Analyza zemetresení ve Strední Evropí (in Czech). Doctor s Thesis. Geoph. Inst. Czechosl. Acad. Sci., Praha, 386 p.

Procházková D., 1993. Earthquake Pattern in Central Europe. Acta Universitatis Carolinae - Mathematica et Physica. 34, 3-66.

Procházková D. and Drimmel J., 1989. Fault - Plane Solutions of the Three Strongest Earthquakes in the Semmering Region in 1984. Proc. ESC Sofia 1988, Sofia, 263-270.

Procházková D. and Roth Z., 1993. Complex Investigation of Earthquakes in Central Europe. In: Environmental Monitoring and Adjacent Problems. Czech Ecol. Inst. and Ministry of Environ., Praha, 287-349.

Roth Z., 1987. Kinematic Analysis of the Mutual Position of the Cretaceous Paleo magnetic Poles of the European epi-Variscan and African Platforms with Respect to the Alpine Movements in the Mediteranean Alpides. Mineral. Slov., 19, 193-202.

Ziegler P.A., 1982. Geological Atlas of Western and Central Europe. Shell, Int. Petrol M., Den Haag, 100 p.

Ziegler P.A., 1984. Caledonian and Hercynian Crustal Consolidation of Western and Central Europe - A Working Hypothesis. Geologie en Mijnbouw, 63. 93-108.

TECTONIC FACTORS FOR THE SEISMICITY OF SW BULGARIA

M.Matova, S.Shanov, G.Nikolov, K.Kurtev

Geological Institute, BAS, Sofia 1113, Bulgaria

Abstract

The main seismically active structures and the regional and local stress localization in SW Bulgaria have been established on the basis of field geological studies, remote sensing researches, geophysical investigations and advanced procedures of the geostatistics and the boundary elements method. The recent mobility of some seismic active deep levels in the Earth crust could be considered as an indication about the presence of superimposed allochtones in the studied region.

Southwest Bulgaria is the most seismically active territory in the country and it is the subject of the present seismic tectonic study. The tectonic blocks presented here have been developed in an extensional setting during the Neotectonic stage. Initially (during the middle and upper Miocene) the dominating trend was ENE-WSW. Asymmetric graben system, elongated 150-170 , confined from east by listric type faults (Zagorcev, 1969, 1992) is formed in this period. The normal fault and the strike slip movements along these faults continue during the whole Neotectonic stage with variable intensity. By the end of the Pliocene and during the Quaternary the dominant trend of extension changes from north to south. Grabens are formed perpendicular to the Struma system and more intensive normal fault movements occur along their confining faults during the Quaternary. The most active fault structures during the Quaternary are Kyustendil, Klisura, Gradevo, Krupnik, Podgorski, Predela, Gotse Delchev and Ognyanovo-Ilinden faults. Activities are also observed in the West-Rila, West-Pirin and Osenovo Ribnovo faults (Fig.1).

The analysis of the satellite images and the airphotos (Katzkov et al., 1985; Matova, Rizhikova 1980) indicates the presence of a number of lineaments trending NNW-SSE and NNE-SSW and transversal groups of lineaments trending NE- SW and almost E-W. (Fig.2). There are also circular structures, elongated and deformed, with axes 15 to 50km long. In the region of Kyustendil, Razlog, Simitly, to the south of the town of Dupnitsa there are intersections of satellite and airphoto lineaments and of circular structures.

The region is part of the Aegean seismic zone of the Mediterranean belt. Six earthquakes of magnitude $M \geq 7$ and several tens $M \geq 5$ are registered here (Shebalin et al., 1974) (Fig.2). The earthquakes of M are often localised to the south of Dupnitza whereas those of $M<5$ are in the region of Simitly, to the south of Razlog, and again to the south of Dupnitza. Subsided blocks as the Simitly graben, uplifted blocks as the Rila and Pirin horst are often involved in the seismic movements.

The hypocentres of the earthquakes of $M \geq 5$ and their deep distribution is presented graphically (Fig.3). The hypocentres of earthquakes of $M \geq 5$ identify five seismogenic layers, the upper four of which are probably an indication of superimposed allochthones. The first and second layers are often seimically mobile.

On part of the regional seismic profile Petrich-Nikopol (Dachev, 1988), in the situated in SW Bulgaria Petrich-Yakoruda sector, the epicentres of all earthquakes registered in an interval of 25km on either side of the profile are plotted on Figure 4. The Moho boundary is not a generator of seismic events. The Curie

Special Publications of the Geological Society of Greece, No 6.

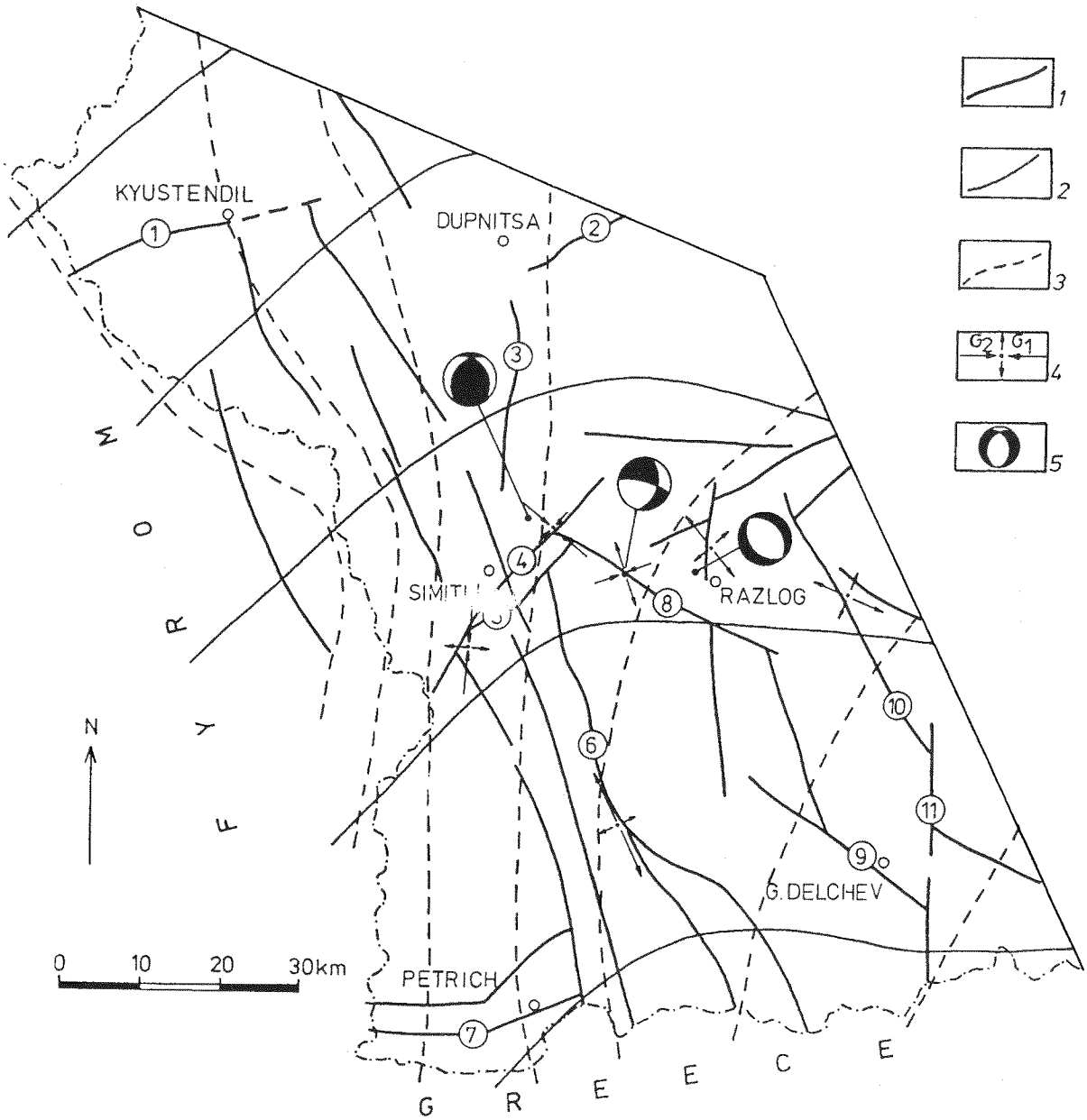

Fig. 1. Scheme of main regional and local geodynamic characteristics of the region: **1** - active faults: 1- Kyustendil fault; 2- Klisura fault; 3- West- Rila fault; 4- Gradevo Fault; 5- Krupnik fault; 6- West-Pirin fault; 7- Podgorski fault; 8- Predela fault; 9- Gotse Delchev fault; 10- Osenovo-Ribnovo fault; 11- Ognyanovo-Ilinden fault; **2** - regional trend of the maximum stress axis; **3** - regional trend of the minimum stress axis; **4** - recent local maximum and minimum principal horizontal deviatoric stresses; **5** - earthquake fault-plane solutions (upper hemisphere)

boundary (600° C), the zone of SiO_2 melting (below 30km depth), is represented by particular seismic activity. The layer above 18km thickness (Index B) is outlined as active (the allochthones according to Dachev, 1988), as its upper surface coincides with a layer of relatively lower velocity of seismic waves. The greatest number of earthquakes are concentrated in this layer. Its thickness varies from 2 to 8km and its top is about 8 to 10km below the earth's surface. It can be suggested that the earthquakes in the crust above this layer are related to sub vertical structures of the Struma - Krupnik fault type.

The reconstruction of the main tectonic strain

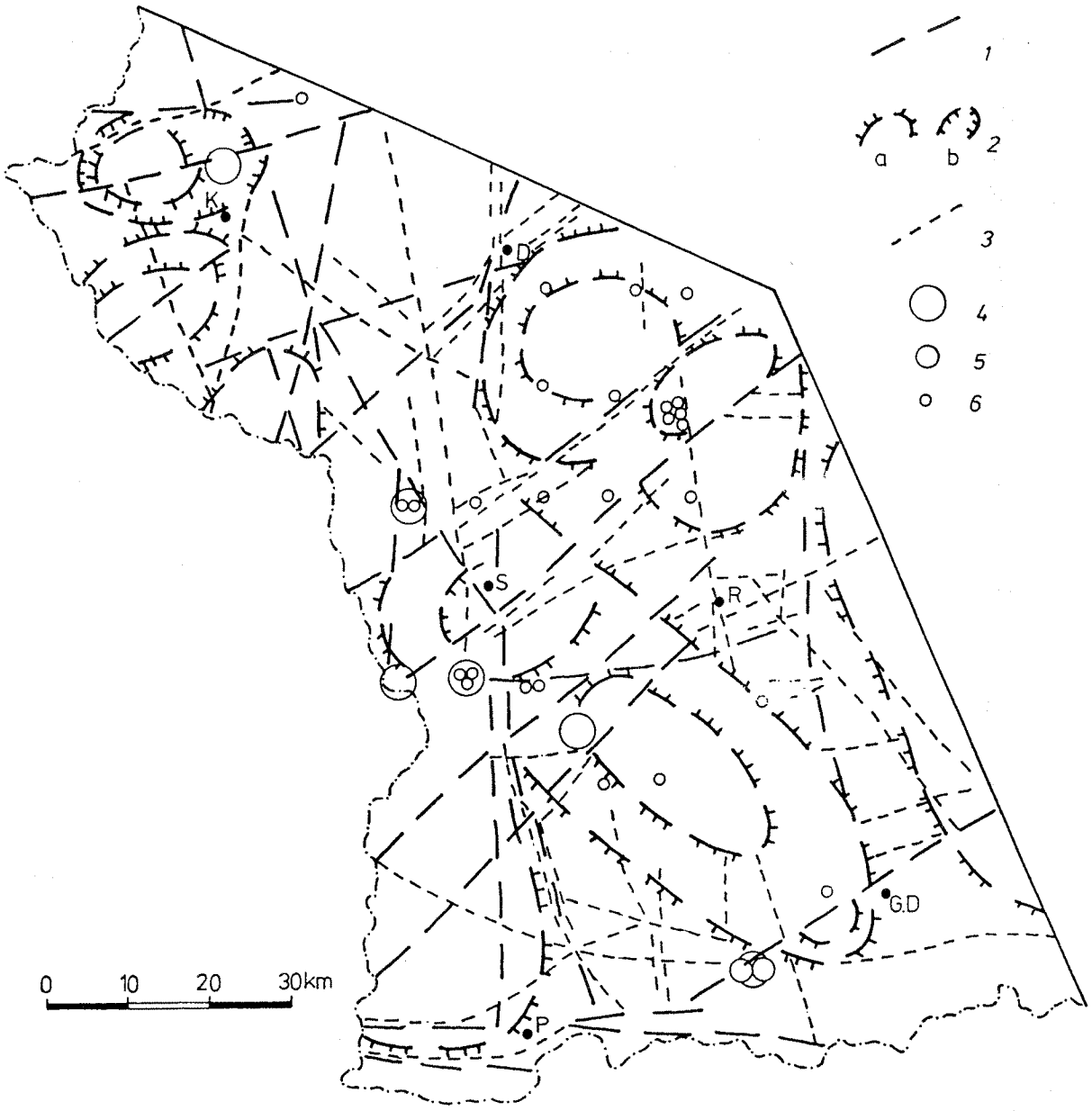

Fig. 2. Scheme of remote sensing structures and seismic events: **1** - spacephotolineament; **2** - circular structures: a- positive one, b- negative one; **3** - airphotolineament; **4-6** - epicentres of earthquakes with magnitude M ≥ 5: 4 - M ≥ 7; **5** - M=6-6.9; 6 - M=5-5.9

field is based on the analysis of 22 earthquakes (Georgiev, 1987; Shanov et al, 1992), the interpretation of the tectonic strain along tectonic fractures of the rocks at 16 points, processed by the methods of P.N. Nikolaev (1979) and by statistical analysis GEO-EAS programmes (Englund, Sparks, 1991). The contemporary tectonic field of the strain (Fig.1) is characterised by a general stress NE-SW and E-W in the zone of the Struma fault. The axis of the minimum tectonic stress is trending N-S in the western part of the territory whereas in the region of Gotse Delchev - Yakoruda towns it is NE-SW.

Based on the data for the contemporary active faults and the regional strain, 2D models using the boundary elements method of the local redistribution of the tectonic strain was accom-

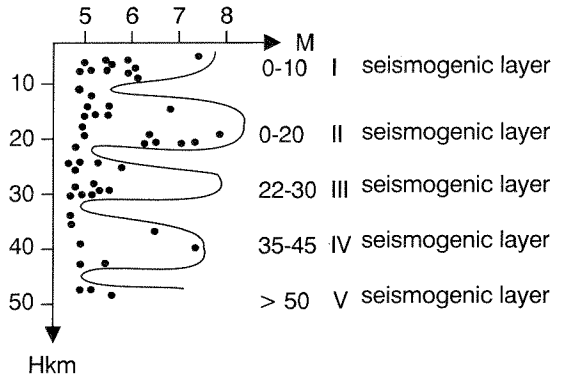

Fig. 3. Depth-magnitude distribution of the earthquakes with M35

plished. Figure 1 shows the tensor deviator in the greatest anomalies of σ1 and σ2 concentrations compared to the earthquakes of $M_s > 3$. Here the concentration of the strains changes relatively fast and depends on the geometry of the fault pattern. The interrelation between the Predela, Krupnik and Gradevo faults and the West- Pirin fault zone causes inverse fault movements. The local strain status is correlated very well with the earthquake mechanisms in the central part of Predela fault and the town of Razlog. The SW part of Gradevo fault is characterised by the presence of submeridional extension whereas the junction of Dospat fault and Osenovo-Ribnovo fault is an area where shear strains are concentrated. The shear strains are confined on the north by compression perpendicular to the zone.

Medium to large size blocks are often involved in seismic movements (Gocev, Matova, 1989). Some of the main blocks correspond to large size circular structures. In the blocks and in the concentric structures the epicentres of earthquake of M ≥ 5 usually lie on intersections of diagonal and orthogonal faults and are identified by local and regional strains. We assume that the occurrence of earthquakes of M ≥ 5 is possible in other sectors of the above mentioned structures or in similar structural conditions too

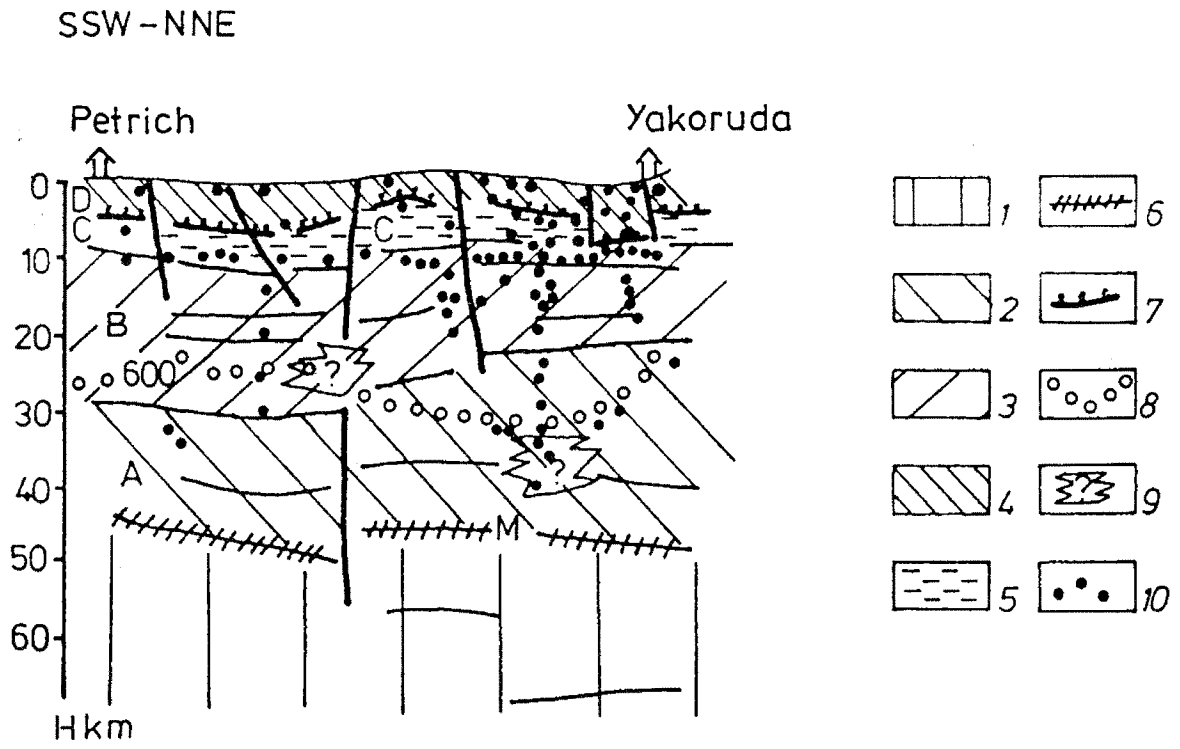

Fig. 4. Seismotectonic profile Petrich - Yakoruda (after Dachev, 1988, with additions): 1 - upper mantle; 2-5 - structural complex in the consolidated earth crust: 2 - complex A from the end of Baikalian stage (autochtone); 3 - complex B from the end of Paleozoic and the beginning of the Mesozoic (allochtone); 4 - complex C with sedimentary origin (autochtone); 5 - complex D of Alpine allochtones; 6 - Moho boundary; 7 - nappe surface; 8 - isotermic surface of Curie (600 C); 9 - probable magmatic foyer; 10 - hypocentres of earthquakes in 50 km large zone

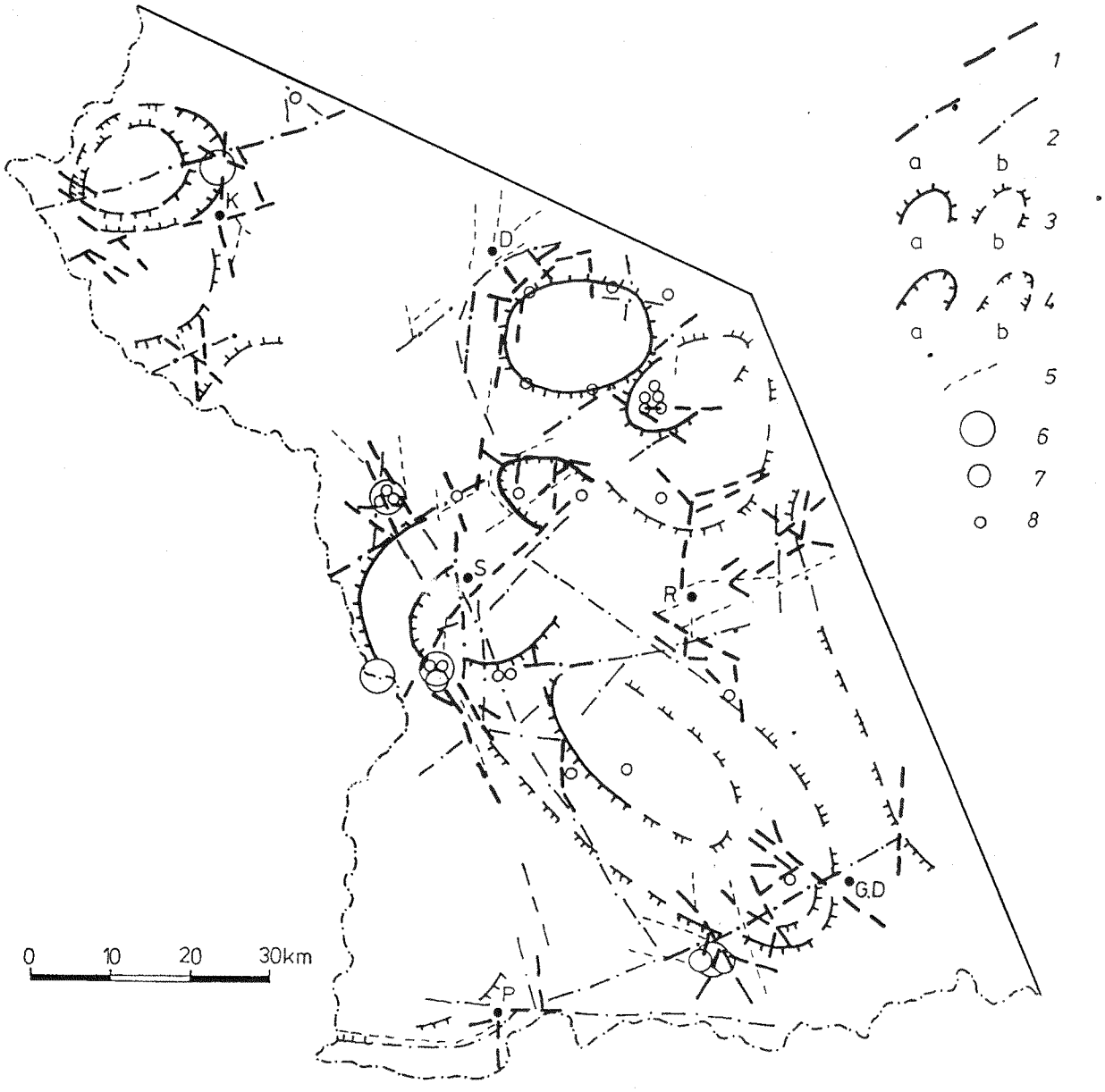

Fig. 5. Scheme of seismic active sector of structures and of probable active ones: **1** - active fault; **2** - sector of spacephotolineament: a- with seismic activity, b- with probable activity; **3** - sector of positive circular structure: .- with seismic activity, b- with probable activity; **4** - sector of negative circular structure: a- with seismic activity, b- with probable activity; **5** - sector of airphotolineament in seismic mobile territory; **6-8** - epicentres of earthquakes with magnitude M ≥ 5: **6** - M ≥ 7; **7** - M=6-6.9; **8** - M=5- 5.9

(west of Petrich, east of Gotse Delchev) (Fig.5).

In SW Bulgaria the seismic movements occur not only in the upper part of the earth's crust as in the larger part of Europe, but also in it's middle and lower part. The factors controlling the movements in the upper part of the earth's crust are probably the block structures, the faults, and the lineaments, on one hand, and specific geodynamic settings, on the other hand. The heterogeneous earth masses define the course of the seismic flow in the middle and lower part of the earth's crust.

References

Dachev, Ch. 1988. Structure of the Earth crust in Bulgaria. - Sofia, Technica, 334p. (in Bulgarian with English abstract)

Englund, E., A. Sparks. 1991. Geostatistical Enviromental Assessment Software. User's guide. Las Vegas.

Georgiev, T. 1987. Fault Plane Solutions Pressure and Tension Axes for some Earthquakes in South-western Bulgaria. - Bulg. Geophys. Journ., 13, 3, 102-107.

Gocev, P., M. Matova. 1989. Middle Mesta fault bundle and recent tectonic activity of part of the Rila-Rhodope region. - Geol. Rhodopica, 1, 139- 145.

Katzkov, N., D. Stoychev, N. Antova, A. Decheva, S. Yovchev, S. Kuleva, M. Spiridonova, Ts. Stoyanov, L. Filipov, L. Filipova. 1985. The cosmophototectonic map of Bulgaria. - Geol. Balc., 15, 1, 3-10.

Kurtev, K. 1993. Analysis of plane stress distribution around interacting faults by Displacement Discontinuity Method (DDM). - Compt. rend. Acad. Sci., 46, 4, 73-76.

Matova, M., S. Rizhikova. 1980. Tectonic and seismic peculiarities of SW Bulgaria. - Bulg. Geophys. Journ., 6, 3, 73-85. (in Russian, English abstract)

Nikolaev, P.N. 1977. Method of statistical analysis of joints and reconstruction of the tectonic stress fields. - J. of High Schools, Geology and Prospecting, 12, 103-115. (in Russian)

Shanov S., E. Spassov, T. Georgiev. 1992. Evidence for the existence of a paleosubduction zone beneath the Rhodope massif (Central Balkans). - Tectonophysics, 206, 307-314.

Shebalin, N., V. Karnik, D. Hadzievski. 1974. Cataloge of earthquakes in Balkan region. - Skopie, UNESCO, 366p.

Zagorcev, I. 1969. The Struma deep fault during the late Alpin Orogenic stage. - Acta Geol. Sci. Hung., 13, 437-441.

Zagorcev, I. 1992. Neotectonic development of the Struma (Kraistid) Lineament, southwest Bulgaria and Northern Greece. - Geological Magazine, 129, 2, 197-222.

SEISMIC CHARACTER OF YUGOSLAVIAN CARPATHO-BALKANIDES

Duško Sunaric[1], Slobodan Nedeljkovic,[2] Miodrag Popovic[3]

[1] *Faculty of Mining and Geology Djušina 7, 110000 Belgarde Yogoslavia*
[2] *Seismological Survey of Serbia Park Tašmajdan PO BOX 351, 11000 Belgade Yogoslavia*
[3] *Geoin-Internacional Šumatovacka 126, 11000 Belgrade Yugoslavia*

Abstract

An analysis of strong earthquakes in the Carpatho-Balkanides of Yugoslavia indicated the overestimate of this region's seismicity, because the influence of the geological engineering properties of rocks were not included in the estimates. The seismic geological engineering hazard has been neglected as argumented in this paper. This region of the Carpatho-Balkanides is characterized by earthquakes of low magnitudes, less than 4 on Richter scale, small hypocentral depth, and a small area bounded by central isoseismal line. Compared with the adjoining Carpatho-Balkanide regions, the seismicity of this region is much lower.

Introduction

The Yugoslavian part of the Carpatho-Balkanides, eastern Serbia, is characterized by both geological and seismological specific characters, which will be described in this contribution for the purpose of correlation with and argumented discussion of other parts of the same province.

To avoid possible misinterpretation, the meanings of some terms used in this paper will be explained. "Seismicity" means the united "seismotectonic and earthquake engineering hazard". "Earthquake engineering hazard" is a reflection of the focal earthquake effect, and the "earthquake engineering hazard" the effect of local engineering ground properties (dynamic resistance of rock mass, ground water, operation of exogeodynamic processes etc.) on megaseismic field. This definition of "seismicity" is applied to eastern Serbia, which almost entirely forms a part of the Carpatho-Balkan system. Our investigation was aimed at the assessment of partial seismic hazards in relation to their overall contribution to the seismic danger and their interrelation.

Seismicity of the southeastern part of the Carpetho-Balkanides is influenced by autochthonous earthquakes, but also the influence of strong earthquakes with epicentres in adjoining regions is not negligible. These regions of influence are primarily Vrancea, Romania; Rila, Bulgaria; and Pomoravlje, central Serbia.

Seismic character of the Carpatho-Balkanides in Serbia

On the basis of the available historical and instrumental records, general characters of earthquakes in the study area are the following:

- Earthquakes with autochthonous epicentres are mostly of intensities 3 to 5 degrees on MCS

Special Publications of the Geological Society of Greece, No 6.

seismic scale. There were several earthquakes of 6 degrees, one of 7 and one of 8 degrees on MCS scale. It should be mentioned that 8 degree earthquake spread only about 10 km from the epicentre; earthquakes of other intensities had similar extents (J. Mihajlovic 1933) (This was the reason why the isoseismal lines of these earthquakes could not be mapped. It indicates the occurrences in the study area of earthquakes with small focal depths and low magnitudes. The most frequent magnitudes of the registered earthquakes in the region have not exceeded 4 degrees on Richter scale, the commonest being between 3 and 3,5 degrees.

- Effects of strong earthquakes with epicentres beyond this region's boundaries are significant, and are even of higher intensities (Dimitrovgrad 9, Pirot and Negotin 8 on MCS scale). This fact was observed when preparing the seismic maps, and added to the seismicity of some local areas, which will be considered in the following paragraphs.

- Collected mega - and micro-seismic data for autochthonous and major allochthonous earthquakes were interpreted for preparation of the seismic maps shown in Figs. 1-4.

Figure 1 shows the region by its seismicity defined in the map of maximum intensities that occurred from 361 to 1950 on the territory of Yogoslavia (J. Mihajlovic and R. Nedeljkovic, 1950). Local seismicity of Pirot and Dimitrovgrad on the map is affected by earthquakes with epicentres in Rila area (earthquake, 1904) and local seismicity of Negotin by strong earthquakes in Vrancea, Romania. Local seismicities of other towns are infuenced by earthquakes with autochthonous epicentres. This map was the base map for design of structures in seismically active areas (1963 regulations were valid unitil 1973).

In the Seismological institute of Serbia, a map of seismic zoning of Serbia was prepared (author M. Vukacinovic) in 1973; the study area is shown in Fig. 2. The seismic degree on the map refers to the period of 100-150 years and a fictitous ("mean ground") clay sand flat with water table 4 m. below the surface. This map, after the regulaions on building in seismically active areas, replaced the former map. It was valid unitil 1981, when the Provisional Seismic Map of Yugoslavia was prepared (Community of Seismology of Yugoslavia, fig. 3). This map was based on the maximum intesities of earthquake events from 361 to 1980.

For amendment of regulations concerning the building in seismically active areas, a new seismic map was prepared in 1981, which consists of six oleates for different time intervals: 50, 100, 200, 500, 1.000 and 10.000 years. Seismic intensity on these maps is of 63% occurrence probability. Figure 4 shows the map oleate for 1.000 year the study area.

The main seismic intensity on the maps varies (3 to 9 degrees on MCS scale), though no major earthquake occurred in the area in the period 1950-1981. For a change in seismic intensity no factual arguments were available; it resulted from a different approach to the interpretation of mega- and micro-seismic data. It should be mentioned, however, that geological engineering properties were not considered when collecting and interpreting the data. This means that all the mentioned seismic maps are basically the maps of seismotectonic hazard, with the earthquake engineering hazard completely neglected. It does not seem a justified approach, as seismotectonic derofmations (faults of Saint Andreas type of california, in D. Sunaric and S. Nedeljkovic 1990) have not been registered by any earthquake on the territory of Yugoslavia. The effect of geological engineering properties of ground on defining the epicentral areas and earthquake elements is by no means negligible.

For argumentation of this conclusion, or the assessment of earthquake engineering hazard, a general engineering geological map is in Fig. 5.

The importance of geological engineering properties of ground for preparation of isoseismal contour maps, which are normally base maps for a universal seismic mapping, will be presented on the case example of 1977 earthquake in Kru / evac (D. Sunaric, S. Nedelkokovic and O. Paunkovic 1995):

- In the area of isoseismal line MCS 6, 26% communities;

- In the area of isoseismal line MCS 5, damages characteristic of this degree were registered in 30% of communities.

Analysed geological engineering properties of ground, quality of buildings and their damages indicated the damage mainly caused by low dynamic properties of the ground, shallow water table, or operation of exogenic geodynamic processes (sliding, flowage, etc.). Hence, the determined earthquake intensity of MCS 7 was incorrect for the unconsidered geological engi-

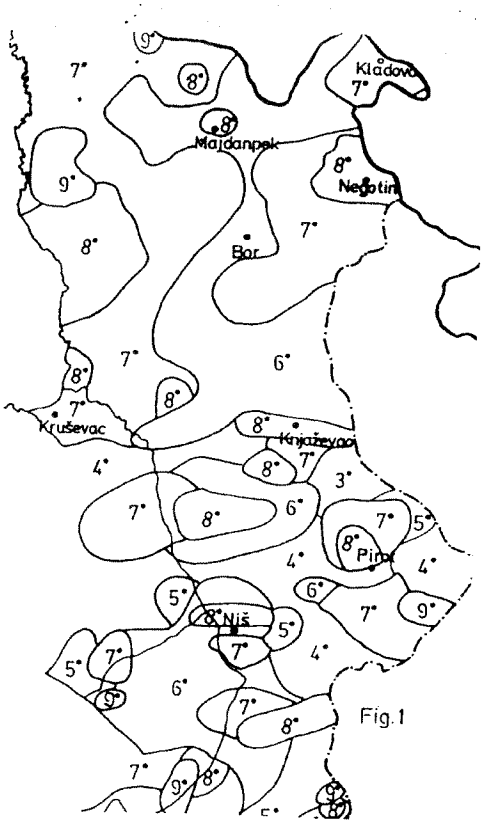

Fig. 1

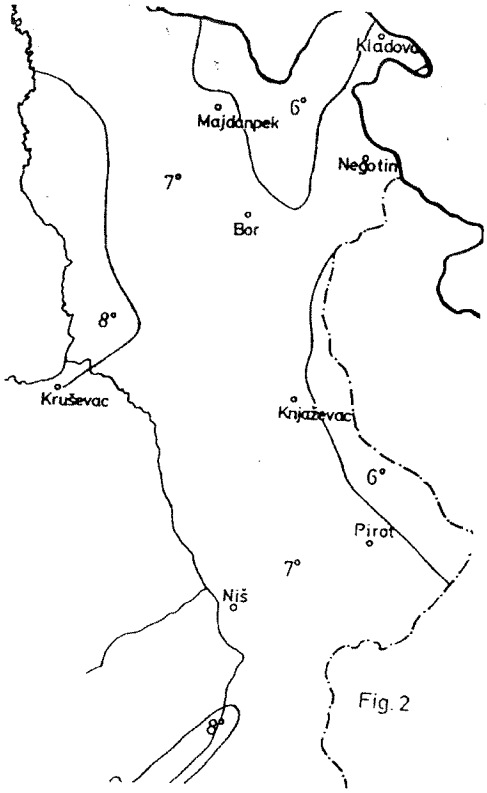

Fig. 2

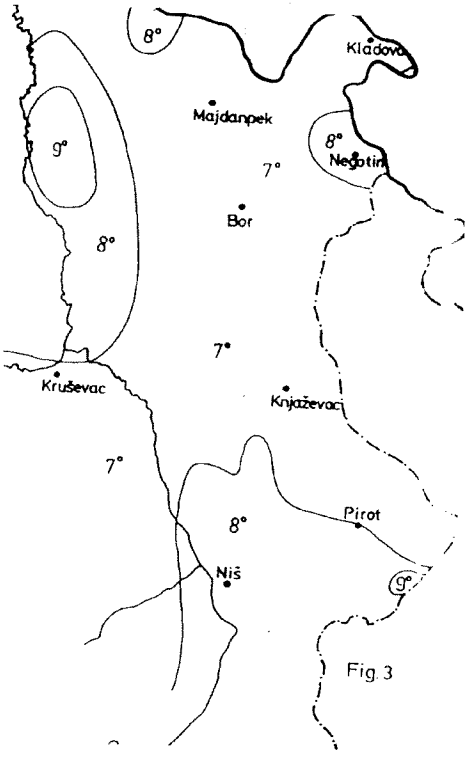

Fig. 3

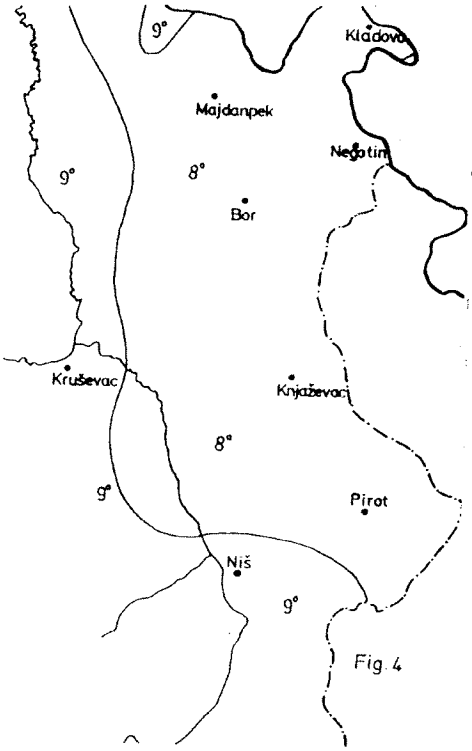

Fig. 4

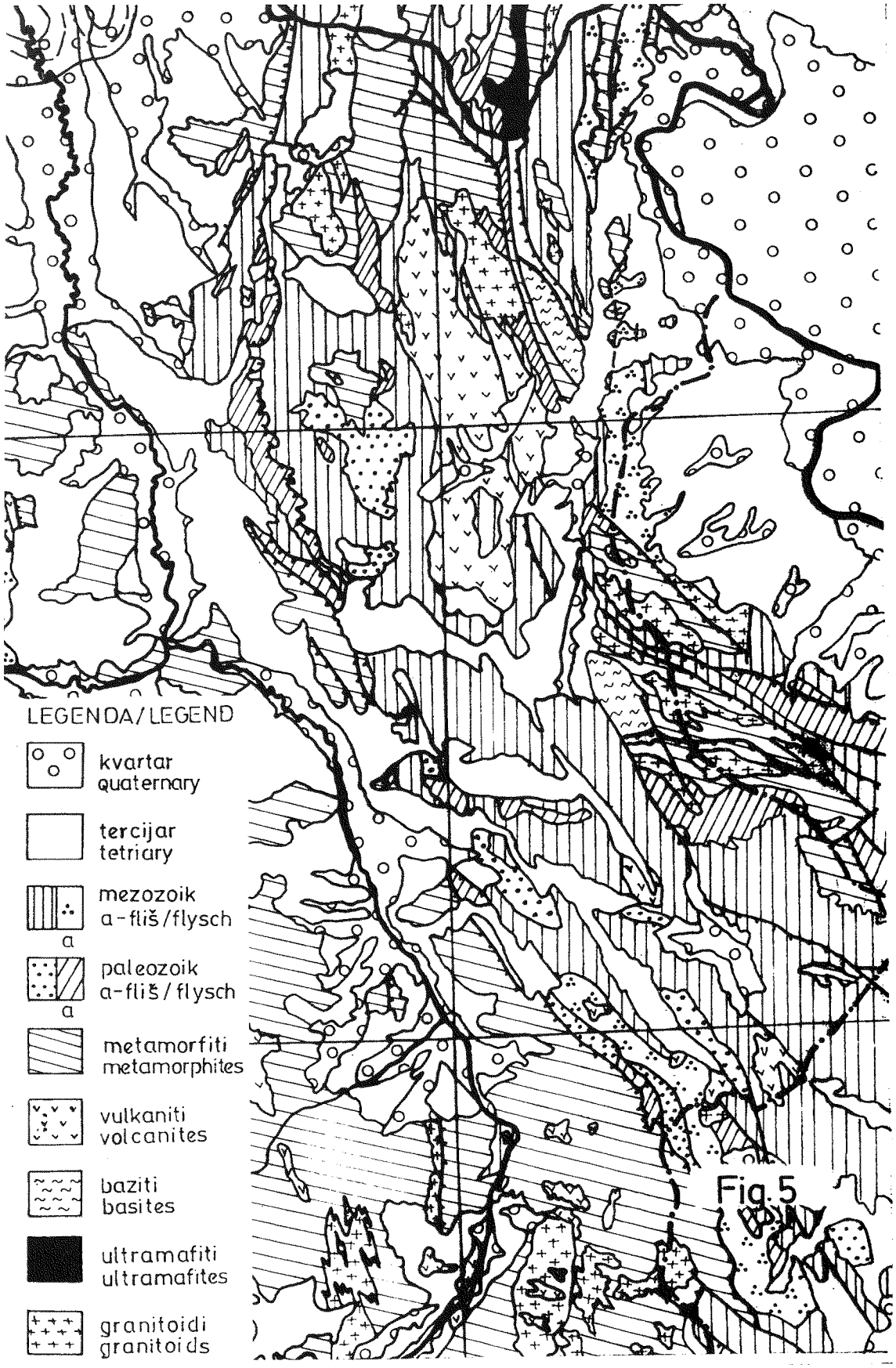
LEGENDA/LEGEND
kvartar
quaternary
tercijar
tetriary
mezozoik
a-fliš/flysch
a
paleozoik
a-fliš/flysch
a
metamorfiti
metamorphites
vulkaniti
volcanites
baziti
basites
ultramafiti
ultramafites
granitoidi
granitoids

Fig.5

neering properties of ground. This intensity should be corrected by reducing it at least by one degree on MCS scale. Similar inaccuracies were noted in other isoseismal contour maps of Yugoslavia. Consequently, the basic degree of earthquake intensity for the Yugoslavian territory of the Carpatho-Balkanides is increased, a result of insufficient consideration of geological engineering properties of ground in collecting and interpreting megaseismic data, or the geoengineering component in the seismic hazard of an area. The lower intensities of earthquake events in this region, compared to the rest of Yugoslavia, should be related inter alia to the relatively better geological engineering properties (primarily higher dynamic resistanse of rocks to the depth of the erected structures' influence) (Fig. 5). Increased intesities are associated with communities situated in alluvial plains, where water table is shallow or where landslides and other land instabilities are common.

Concusion

In our present knowledge, the Carpatho-Balkanides area of eastern Serbia is not characterized by earthquakes of high magnitudes. The average background magnitude is estimated at about 3,5 to maximum 4 degrees on Richter scale. Focal depths are small, and earthquake effects limited to small areas.

The seismicity of the Carpathians in eastern Serbia, in respect of possible magnitudes, is reduced; the seismicity of the Balkan tectonic unit is negligible compared with the eastern Balkan region.

In opinion of S. Nedeljkovic, the seismicity of eastern Serbia indicates the Carpathians and the Balkan as two separate structural units, each characterized by specific seismic regime. The two units should be considered separately.

The analyses of the earthquake engineering hazard have shown that earthquake hazard of the study region is overestimated and that it should be revised for eastern Serbia, consistent with the presented arguments.

References

Sunalic, D. and Nedelkovic, S. 1990: Reinterpretation of historic data of Destructive earthquake and seismodeformations of land on the territory of Yugoslavia. 8th EE JSSMFF, Vol. 1 (pp. 67-71), Tokyo.

Sunaric, D. and Nedelkovic, S. 1994: Analiza karata izoseista nekih naših zemljotresa sa aspekta egzogeodinamickih pojava, Zbornik rad. RGF, sv. 32 Beograd.

Mihajlovic, J. 1933: Timocka trusna oblast. Spomenica timocke kraine, Beograd fondovski materijali seismološkog Zavoda.

TYPE OF FAULTING AND SEISMIC DEFORMATION IN THE HELLENIC ARC

Basil C. Papazachos and Anastasia A. Kiratzi

Geophysical Laboratory, University of Thessaloniki GR-54006, GREECE

Abstract

A detailed study of the active deformation along the Hellenic arc is presented. The deformation attributed to earthquake activity with shallow focal depths <40 km and with depths in the range 40-100 km, is examined separately. The shallow seismicity produces crustal shortening along the convex (outer) part of the Hellenic arc of about 1.1. cm/yr in a mean direction N31°E. The direction of this shortening is changing from a nearly N-S trend along the southern coast of Peloponese to a ENE-WSW trend along the eastern coast of Crete up to Rodos. The shortening rate is larger at the western part of the hellenic arc. The area that is rapidly deforming is the upper surface of the Wadati - Benioff zone. The subducting slab is in a state of down-dip extension which occurs along the dip of the Wadati - Benioff zone at a rate of about 0.9 cm/yr, while a fast shortening, at a rate of about 1.8 cm/yr, occurs parallel to the general trend of the Hellenic arc.

Introduction

The Aegean sea lies on the most active part of the Africa - Eurasia collision zone. The eastern Mediterranean lithosphere, which is the front part of the (Papazachos and Comninakis, 1969). This subduction results in high shallow seismicity (magnitudes up to M_S=8.3) with low-angle thrust faults along the Hellenic arc and in intermediate depth seismicity which forms a well defined Benioff zone in southern Aegean (Papazachos and Comninakis, 1969; 1971; McKenzie 1978; LePichon and Angelier, 1979; Papazachos, 1990). The seismic activity is intense along the Hellenic arc and extents up to depths of 180 km (Comninakis dipping down to about 80-100 km and then its dip angle steepens down to 180 km (Papazachos, 1990; Hatzfeld and Martin, 1992). Plate motion models predict the overall motion between Africa and Eurasia to amount to about 1.0 cm/yr convergence at Crete island (Chase 1978; DeMets et al., 1990). The study of the deformation pattern along this area is very important, since the occurrence of a large (M~8.3) shallow or intermediate depth earthquake will have a tremendous impact to all the southern Aegean area (the islands of Crete, Rodos, are densely populated and high buildings have been constructed) and even to the coastal cities of the eastern Mediterranean.

The style of deformation along the Hellenic arc has attracted the attention of many researchers but the results are sometimes very controversial, regarding the deforming velocities. Along the convex side of the Hellenic arc values from 3 to 30 mm/yr have been calculated (Jachson and McKenzie, 1988 a, b; Papazachos et al., 1992; Kiratzi and Papazachos, 1995; Papazachos and Kiratzi, 1995), while Tselentis et al. (1988) have estimated a velocity of 11 mm/yr along the western part of the arc.

In this paper, we attempt to see how the earthquake source mechanisms may constrain the strain rate and hence the rates of motion along the Hellenic arc and within the subducting slab. We first examine the upper 10 km of the seismogenic layer where the shallow seismicity is confined and in the following we examine the gently dipping part of the subducting slab

Special Publications of the Geological Society of Greece, No 6.

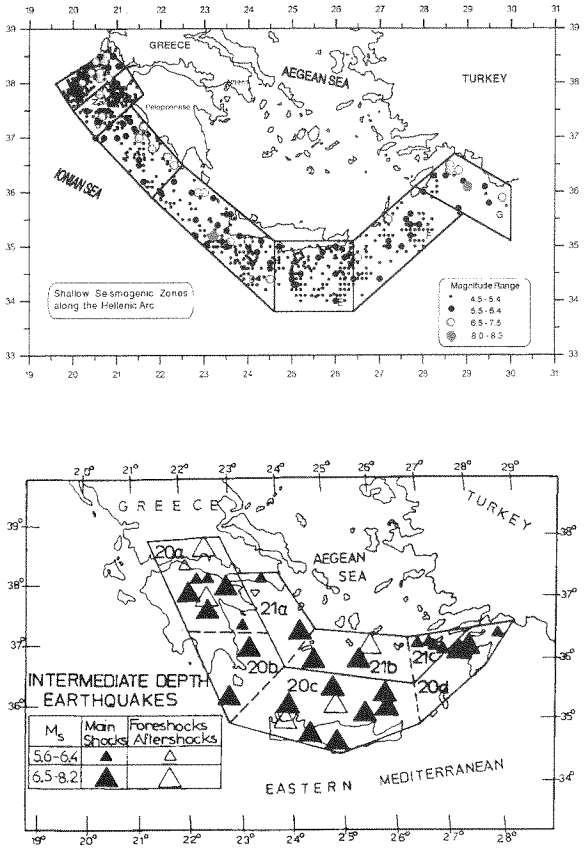

Fig.1(a) The 6 shallow and (b) the 4 intermediate depth (40 km ≤ h ≤ 100 km) seismogenic source volumes and the relative seismicity of the Hellenic arc for the last four centuries (Papazachos and Papaioannou, 1993).

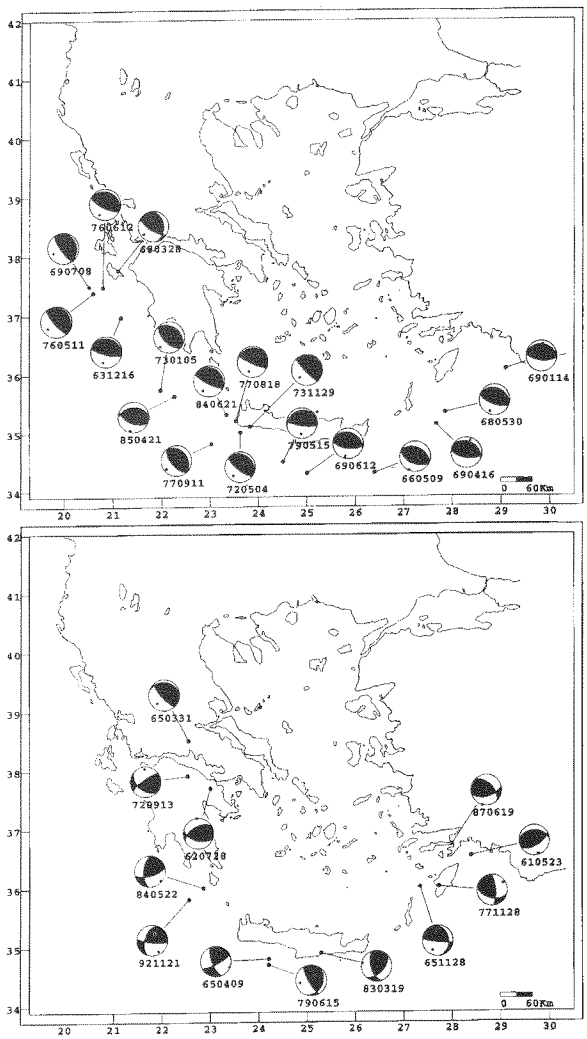

Fig. 2. Focal mechanisms used in the analysis for the shallow seismicity (a) and for the intermediate depth seismicity (b).

which is defined by the seismicity in the depth range of 400 to about 100 km. It is believed that in this depth range coupling occurs between the subducted oceanic lithospheric slab and the overriding Aegean lithosphere (Papazachos, 1990), and we thought the contribution of these intermediate depth events to the deformation of the Hellenic arc should be also considered.

Method of analysis, seismogenic sources and focal mechanisms used

The method of analysis followed here is the one proposed by Papazachos and Kiratzi (1992) which is based on the formulation of Kostrov (1974), Jackson and McKenzie (1988a) and Molnar (1979). Briefly, in order to get the components of the strain rate tensor, $_{ij}$, we sum the moment tensors obtained from the fault (1979) and then we divide by the volume, V, of each source. The seismogenic volume, V, is considered to be a parallelepiped prism with length, l_1, width, l_2, and depth extend, l_3. The value of l_3=10 km was used for the thickness of the seismogenic layer for the shallow seismicity and l_3=30 km was used in the case of the subducted part of the lithosphere (Kiratzi and Papazachos, 1995).

Figure (1a) shows the 6 seismogenic sources that are defined by the distribution of the shallow seismicity along the arc (Papazachos, 1995), while figure (1b) shows the 4 seismogenic sources defind by the distribution of the intermediate depth seismicity along the arc (Papa-

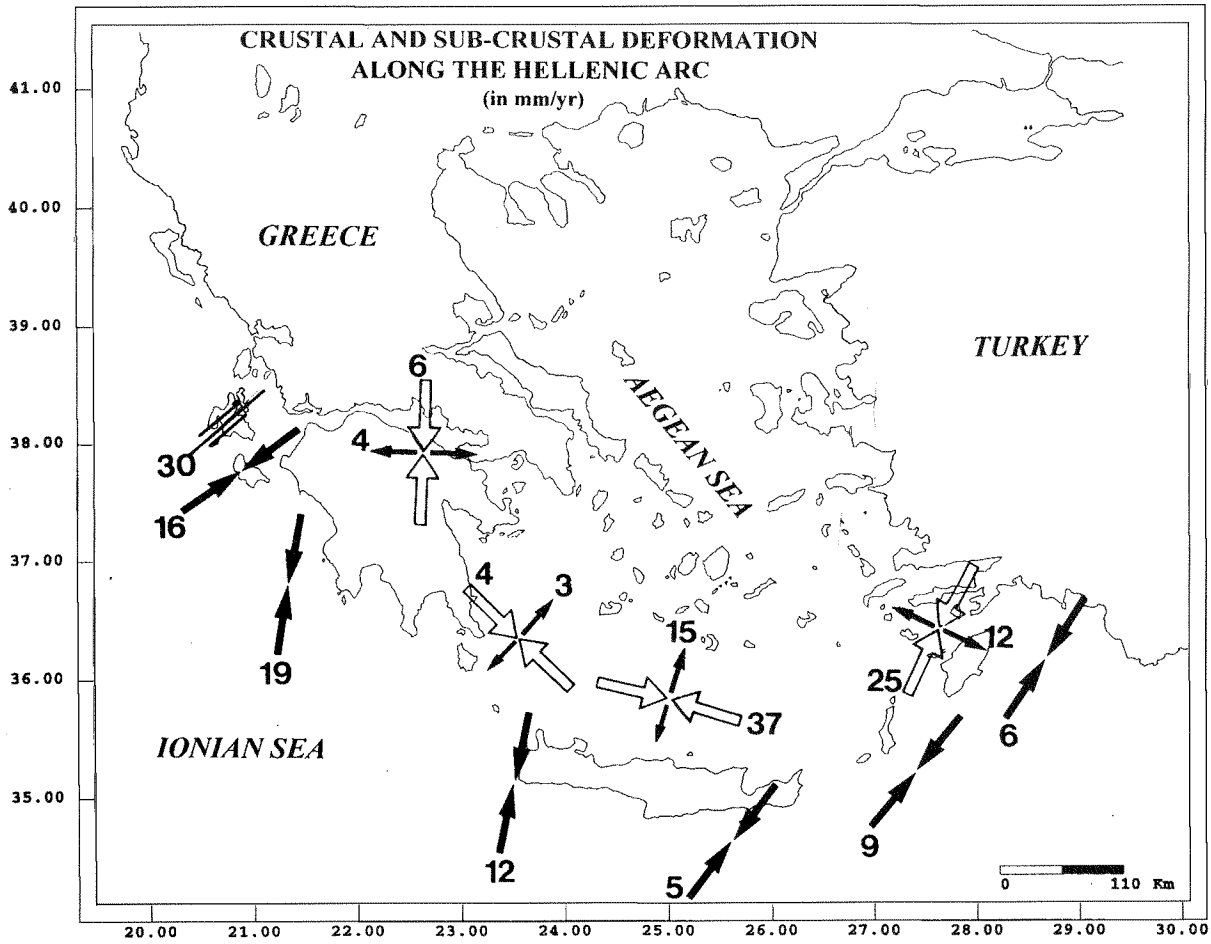

Fig. 3. Distribution of the deformation velocities (in mm/yr) for a) the shallow seismogenic sources and b) the intermediate depth seismogenic sources. Converging arrows indicate compressional velocity while diverging arrows indicate extensional velocity.

zachos and Papaioannou, 1993). Figure (2a) shows the focal mechanisms of the shallow (h<40 km) earthquakes along the Hellenic arc, with surface wave magnitude $M_S \geq 5.5$ which have occured in the studied area during the period 1963-1986. Figure (2b) shows the focal mechanisms of the intermediate depth events (h=40-100 km) within the shallow dipping part of the subducted slab of the period 1961-1992.

Strain rates and deformation velocities

Table 1 gives the parameters of the *typical* focal mechanisms of the earthquakes for each seismogenic source, shallow and intermediate depth, corresponding to the average P and T axes of the summed moment tensor.

In Table 2 the eigensystem of the velocity tensor, **V**, for the 6 shallow and the 4 intermediate depth seismogenic sources is presented, respectively. The results are graphically illustrated in figure (3) and are discussed in the following.

The compessional deformation is taking place at an average horizontal velocity of 1.1 ± 0.5 cm/yr in a mean direction at N31°E ± 17° for the whole Hellenic Arc. The average vertical crustal thickening is occuring at a rate of 1.1 ± 0.5 mm/yr.

The subducting slab, at the depths of 40-100 km, is in a state of down-dip tension that occurs normal to the strike of the Hellenic arc, at a mean rate o 0.9 cm/yr. At the eastern part of the Hellenic arc the dip of the vector of the maximum extension (~44°) is considerably larger than the mean dip of the shallow distribution. The most significant component of the deformation is the compression that occurs parallel

to the strike of the arc in all four seismogenic volumes at a rate of about 1.8 cm/yr. This compression takes place at a shallow angle, within the subducting lithosphere. The component of seismic extension could be easily attributed to slab pull-forces acting on the subducting lithosphere but the component of the compression is more difficult to be explained.

Table 1. Typical fault plane solutions for the seismogenic sources of the Hellenic arc

Source	**Fault p1.1**	**Fault p1.2**	**Null-axis**			**P-axis**			**T-axis**		
Name	str/dip/rake	str/dip/rake	λ	Az^o	Pl^o	λ	Az^o	Pl^o	λ	Az^o	Pl^o
SHALLOW SEISMICITY ALONG THE HELLENIC ARC											
CEPHALONIA	45/61/ 173	138/84/ 30	0.01	150	60	-0.97	269	15	0.96	6	25
WEST PART	312/19/ 96	126/71/ 88	-0.04	127	2	-0.91	218	26	0.95	33	64
EAST PART	290/27/ 97	102/63/ 86	-0.01	104	3	-0.95	195	18	0.96	4	72
INTERMEDIATE DEPTH SEISMICITY ALONG THE HELLENIC ARC											
20a	248/51/ 43	124/58/132	-0.17	99	-35	-0.74	6	-4	0.91	90	55
20b	190/52/ 23	85/72/140	-0.03	65	-46	-0.96	141	12	0.99	41	41
20c	48/51/150	158/67/ 43	-0.06	1	-42	-0.88	100	-10	0.94	20	46
20d	323/44/138	86/62/ 54	-0.17	105	31	-0.70	21	-10	0.87	127	-56

Table 2. Eigensystem of the velocity tensor, **U**, given in cm/yr, for the 10 seismogenic sources. (ξ/δ^o are the azimuth and the plunge of the associated eigenvector). Positive and negative values of **U** indicate tension and compression, respectively.

A. SHALLOW SEISMICITY						
Source	U_1	ξ_1/δ_1	U_2	ξ_2/δ_2	U_3	ξ_3/δ_3
A	-0.76	210/14	-.06	120/ 2	.18	22/76
B	-1.62	236/10	-.03	141/26	.23	346/62
C	-1.89	189/ 8	-.00	182/21	.24	79/67
D	-1.19	190/13	-.26	283/ 9	.25	46/74
E	-0.49	218/10	.01	335/19	.08	155/68
F	-0.90	220/ 5	-.03	129/16	.06	327/74
G	-0.63	211/16	-.11	120/ 5	.19	14/73
B. INTERMEDIATE DEPTH SEISMICITY						
20a	-0.63	185/ 6	0.39	94 /9	-.02	319/79
20b	-0.40	312/ 9	0.28	42 /3	.00	149/81
20c	-3.66	286/15	1.45	20/12	-.02	147/70
20d	-2.46	210/13	1.21	313/44	-.23	107/43

References

Chase, P. (1978). Plate Kimenatics: the Americas, east Africa and the rest of the world. Earth and Planet. Sci. Lett., 37, 355-368.

Comninakis, P. and Papazachos, B. (1980). Space and time distribution of the intermediate focal depth earthquakes in the Hellenic arc. Tectonophysics, 70, 135-147.

DeMets, C., Gordon, R., Argus, D. and Stein, S. (1990). Current plate motions. Geophys. J. Int., 101, 425-478.

Hatzfeld, D. and Martin, C. (1992). Intermediate depth seismicity in the Aegean defined by teleseismic data. Earth and Planet. Sci. Lett., 113, 267-275.

Jackson, J. and McKenzie, D. (1988a). The relationship between plate motions and seismic moment tensors, and the rates of active deformation in the Mediterranean and Middle East. Geophysical Journal Int., 93. 45-73.

Jackson, J. and McKenzie, D. (1988b). Rates of active deformation in the Aegean Sea and surrounding regions. Basin Res., 1, 121-128.

Kiratzi, A. and Papazachos, C. (1995). Active crustal deformation from the Azores triple junction to Middle East. Tectonophysics, 243, 1-24.

Kostrov, V. (1974). Seismic moment and energy of earthquakes, and seismic flow of rock. Izv. Acad. Sci. USSR Phys. Solid Earth, 1, 23-44.

LePichon, X. and Angelier, J. (1979). The Hellenic arc and trench system: a key to the neotectonic evolution of the eastern Mediterranean area. Tectonophysics, 60, 1-42.

Mckenzie, D. (1978). Active tectonics of the Alpine-Himalayan belt: the Aegean Sea and surrounding regions. Geophys. J.R. astr. Soc., 55, 217-254.

Molnar, P. (1979) Earthquake reccurrence intervals and plate tectonics. Bull. Seism. Soc. Am., 69, 115-133.

Papazachos, B. (1990). Seismicity of the Aegean and surrounding area. Tectonophysics, 178, 287-308.

Papazachos, B. (1995). Personal communication.

Papazachos, B. and Comninakis, P. (1969). Geophysical features of the Greek island arc and eastern Mediterranean ridge. C.R. Seances de la Conference Reunie a Madrid 16, 74-75.

Papazachos, B. and Comninakis, P. (1971). Geophysical and tectonic features of the Aegean arc. J. Geophys. Res., 76, 8517-8533.

Papazachos, B. and Papaioannou, C. (1993). Long-term earthquake prediction in the Aegean area based on a time and magnitude predictable model. Pageoph, 140, 593-612.

Papazachos, C. and Kiratzi, A. (1992). A formulation for reliable estimation of active crustal deformation and its application to central Greece. Geophys. J. Int., 111, 424-432.

Papazachos, C. and Kiratzi, A. (1995). A detailed study of the active crustal deformation in the Aegean and surrounding area. Tectonophysics, (in press).

Papazachos, C., Kiratzi, A. and Papazachos, B. (1992). Rates of active crustal deformation in the Aegean and the surrounding area. J. of Geodynamics, 16, 147-179.

Tymaz, T., Jackson, J. and Westaway, R. (1990). Earthquake mechamisms in the Hellenic Trench near Crete. Geophys. J. Int., 102, 695-731.

Tselentis, G., Stavrakakis, G., Makropoulos, K., Latousakis, J. and Drakopoulos, J. (1988). Seismic moments of earthquakes at the western Hellenic arc and their application to the seismic hazard of the area. Tectonophysics, 148, 73-82.

A TRAVERSE OF THE MARGIN OF THE IONIAN BASIN TO THE HELLENIDES: A COINCIDENT SEISMIC SURVEY AND EARTHQUAKE LOCATION TEST

M. Sachpazi[1], A. Hirn[2], M. Loucoyannakis[3], and THE STREAMERS Group

[1] *Seismological Institute. National Observatory. Athens, Greece*
[2] *Dpt Sismologie, UA 195 CNRS, Institute de Physique du Clobe, 4 pl Jussieu, 75252-Paris 05, France*
[3] *DEP-EKY, Public Petroleum Corporation, Athens, Greece*

Abstract

Most intense seismic activity occurs in Western Greece with a large variation of mechanisms on a traverse through the Ionian islands: strike-slip, thrust or normal faulting. This calls for strain concentration at specific places in different regimes, relating to a structural heterogeneity at depth varying along the traverse. Neither the location of seismic activity nor the structural image at crustal depth have yet been obtained with the resolution necessary to correlate them. The STREAMERS line of 30 fold multichannel reflection seismics with a large industrial 7200 c. i. array of 36 airguns provides state of the art penetration and resolution imaging of the structural variation, complemented by wide-angle data. It images the Ionian thrust on the pre-Apulian platform and intracrustal reflectors, some of which are likely of tectonic rather than lithological origin. A deeper crustal or Moho reflector is mainly evidenced by wide angle recording.

To resolve the seismically active structures among those imaged, we also deployed temporarily an earthquake recording array in this specific local region. First, its geometry was directed to constrain well epicenters along the reflection traverse, by placing seismographs on the islands on each side. Second, the use of three-component seismometers to add reliable shear wave data was aimed at giving a strong constraint on the estimation of depth. Well-constrained hypocenters then locate near to a well defined reflector in a domain where it steepens its eastward dip and is overlain by reflectors with contrary dips. This may correspond to the frontal deformation of the western Hellenides on to the Ionian plate. The subduction is however complicated here by an active transform fault, the Kefallinia fault, which connects it to a collision plate boundary further north.

I - Regional context: geology and seismicity

The Ionian islands are located at the northwestern part of the Hellenic Arc (Fig. 1). The evolution of this region has been studied by many authors (Brooks et al., 1988, Kahle et al., 1993, Hatzfeld et al., 1990, Underhill, 1989). In this area, intense active deformation occurs which is expressed by widely different earthquake mechanisms. South of the Islands, the Hellenic arc trench system is thought to have absorbed convergence, by subduction Ionian basin crust since the early Pliocene. North of

Special Publications of the Geological Society of Greece, No 6.

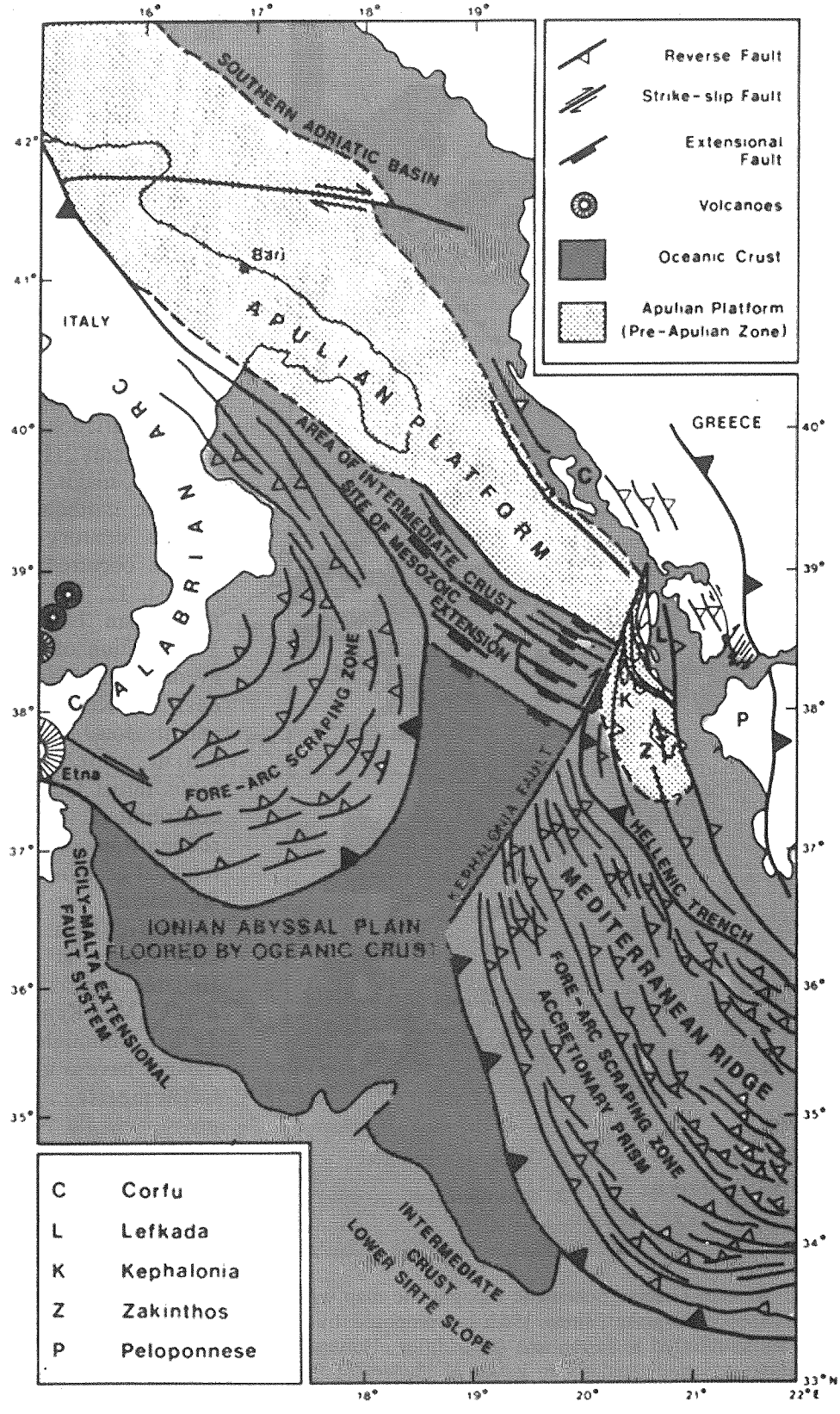

Fig. 1: Regional geological context of Western Greece as adapted from Underhill (1989).

the islands another type of deformation dominates, that of a continental collision due to the convergence of the Adriatic lithosphere with Northern Greece. These two systems are connected by a right lateral NNE - SSW transform fault west of Kefallinia (e.g. Le Pichon et Angelier, 1981). In the northern part of the Ionian Islands the Ionian thrust (IT) has formed since the middle Miocene the converging boundary of the Hellenides on the Apulian foreland. In the middle and southern Islands the position of this deformation front has been debated by many authors (Brooks and Ferentinos, 1984, Underhill, 1988, Stiros et al., 1994) and can be rediscussed with deep information from our new seismic data (Hirn et al., 1996). Here the convergence at the IT has been replaced since early Pliocene by convergence further West, of the pre-Apulian over

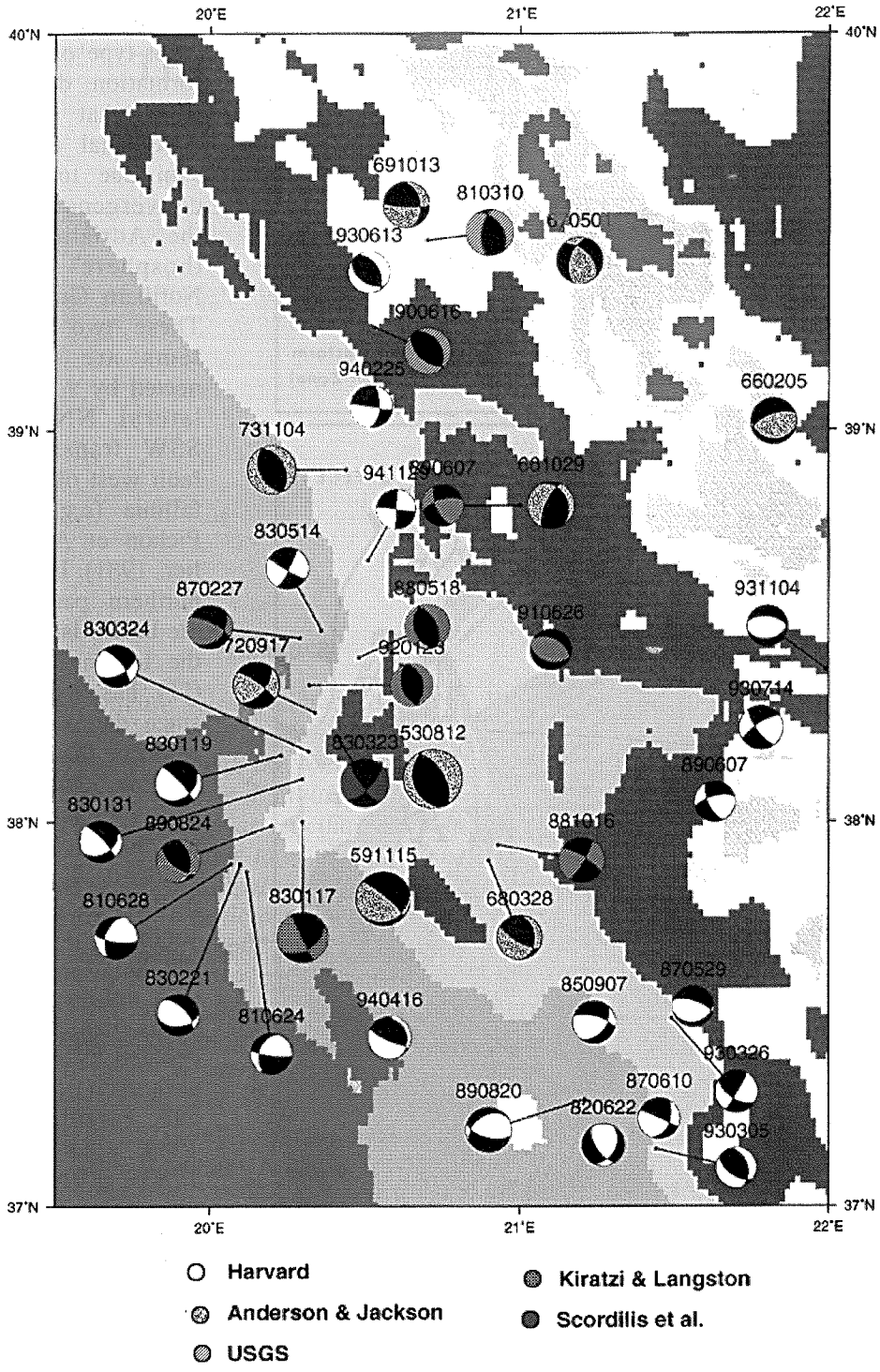

Fig. 2: Ionian Islands and Western Greece. Schematic topographic map with focal mechanism solutions of earthquakes since 1953, as proposed by diverse authors and agencies as referred to in the text (in addition, Harvard stands for the CMT solutions reported regularly in issues of Physics of the Earth and Planetary Interiors and USGS for the solutions in the Preliminary Determination of Epicenters distributed by this agency.

the oceanic crust of the Ionian basin.

This deformation causes the high level of seismicity of the Ionian islands, the highest in the whole of the Aegean and the surrounding area. The seismic activity has different character depending in which part of the Ionian it is located and exhibits a large spatial variation of mechanisms (Fig. 2). The major destructive earthquake of the century in Greece occurred on August, 12, 1953 in the Ionian Islands. The location of this event at the southeast of Kefallinia and its focal mechanism which exhibits thrust faulting contributted to the recognition of the regional geodynamic framework by the identification of convergence at the Hellenic arc as far north (Mc Kenzie, 1972), although it did not have a clear bathymetric expression as far NW, south of Kefallinia.

The seismicity changes character offshore west of Kefallinia. A series of earthquakes of 1983 right at the southwestern tip of Kefallinia have been diversely interpreted, opening the debate on the exist-

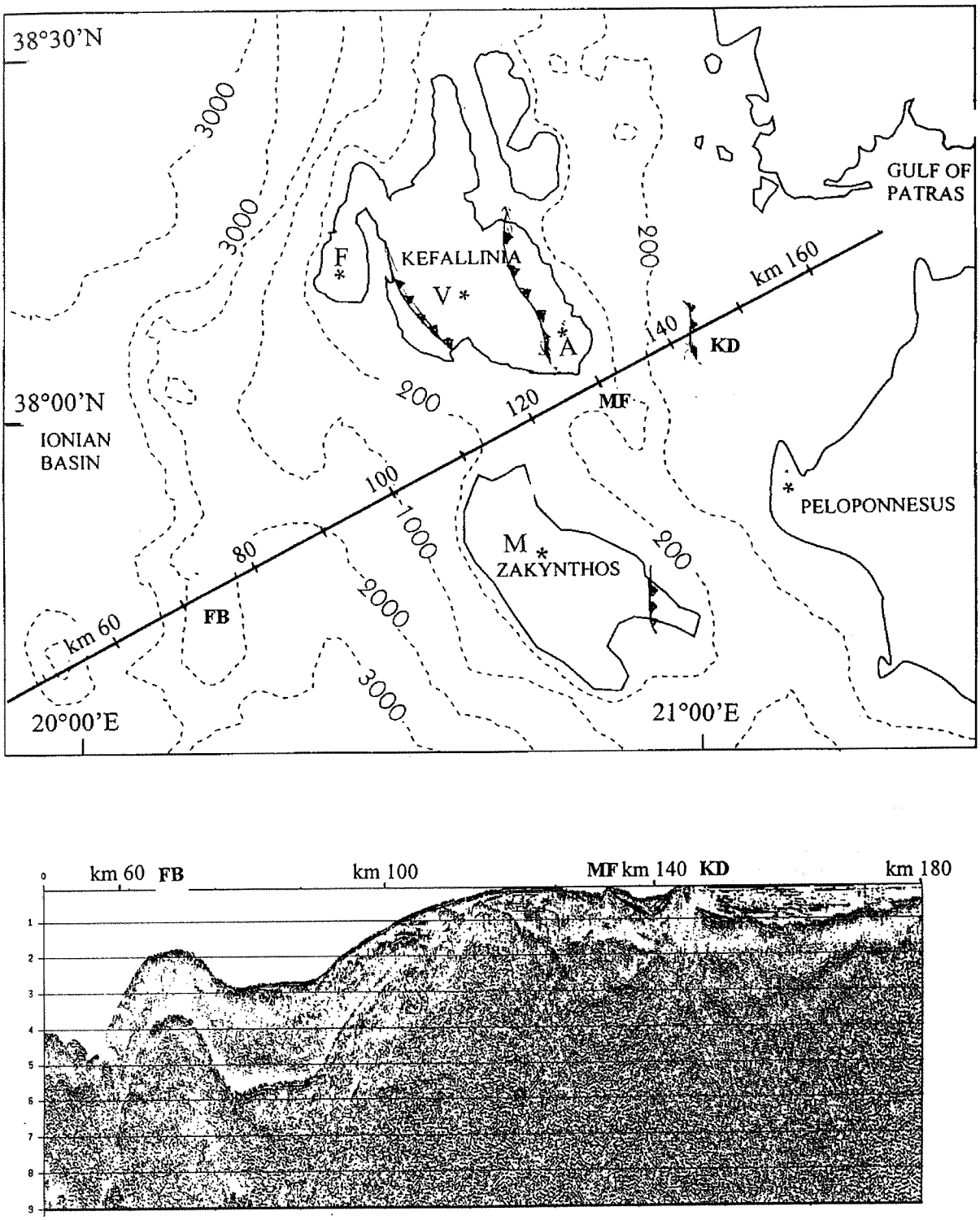

Fig. 3: Top schematic map and bathymetry of the Central Ionian islands of western Greece. Superimposed STREAMERS line ION-07 with distance identification. KD Kefallinia Diapir, MF Mounta Fault, ZA Zakynthos anticline, FB Frontal Bulge. V, F, M, A are the three-component seismographs. Bottom normal incidence stack section. Tuned array, 7118 cu. in. (about 120 litres), 4.5 km long, 180 channels streamer, 30-fold coverage stack. Coherence-weighting and trace decimation for scale compression. Distances and main features as on top.

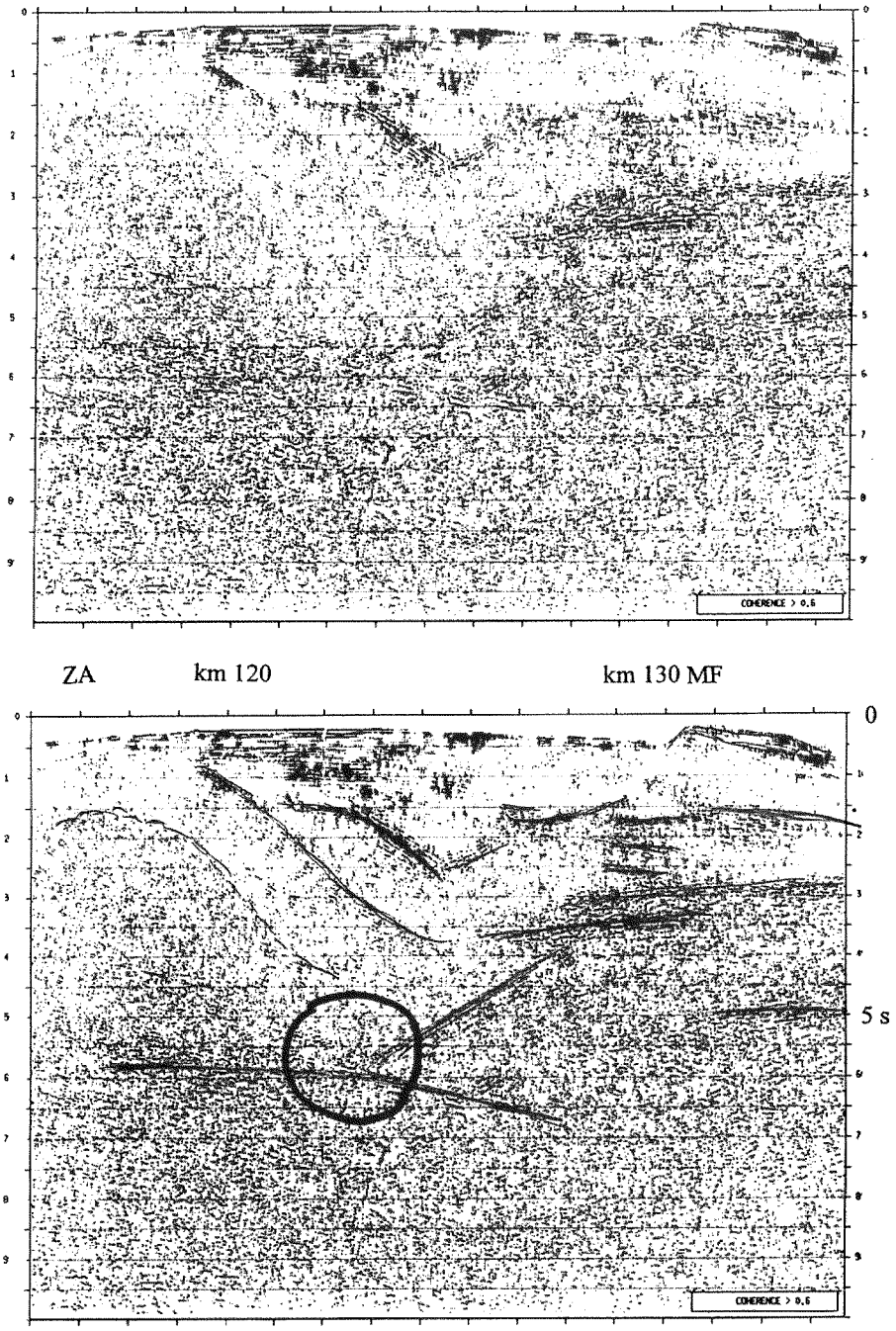

Fig. 4: **a)** Stacked section of ION 7 to the West of the Mounta fault (MF) and Zakynthos anticline (ZA) Compoensation for varying water depth by replacing water by 3 km s^{-1} sediments corrects the dip of deep reflectors.
b) The same with interpretation of a deep reflector at 5 s TWT flat of slightly dipping from west eastwards to beneath ZA where is possibly continues with a stronger dip. Circle represents source region of earthquakes well-located by a temporary array. Such activity in the vicinity of a change in dip of this seismic interface makes it a candidate for the western Hellenides overriding the Ionian crust along it (from Sachpazi et al., submitted).

ence or dominance of strike-slip motion in the Ionian islands themselves to the east of the transform fault. From the different focal mechanisms of the mainshock of January 17 and its major aftershocks of March 23, CMT solutions of pure strike-slip (NEIS bulletin) or pure thrust (Dziewonski et al., 1983) have been proposed. Based on first arrival polarities, Scordilis et al., (1985) report pure strike-slip for both events, whereas Anderson and Jackson (1987) report pure thrust for the first one and pure strike-slip for the seocond one. Liakopoulou et al. (1991) using the relative amplitude method on long period three-component GDSN stations, propose a vertical fault-plane with a quasi-vertical dip-slip motion and only a small strike-slip component. By interchanging their auxiliary plane and fault plane with respect to their choice, the

mechanism could as well be NE-SW right-lateral strike-slip on a flatly SE dipping fault. Kiratzi and Langston (1991) modeling P and S waveforms at WWSSN stations, determine right-lateral strike-slip on a SE dipping fault with a small thrust component. Their modeling indicates a focal depth of 8 km. This focal parameter cannot be checked independently, e.g. from the hypocenter location from arrival times since the nearest stations are not spaced densely enough with respect to the small depth.

The interpretation of focal solutions depends crucially on the locations of hypocenter being well-constrained, since the geological framework in which to view them varies strongly in space. To contribute to unravelling the seismotectonics of this region we took a double approach: investigate structure at depth since this is where earthquakes occur, not on superficial faults. and locate accurately earthquakes with a temporary local array.

II. - Deep structure from exploration seismics

Seismic exploration profiling adopted to larger penetration from oil exploration allows to resolve deep structure. Identifying subsurface elements which are presently active may be attempted on the basis of also recording seismicity with the adequate accuracy. Probing with a high quality specific local seismological array may allow to locate precisely earthquakes on some of the structural features, identifying them to be active. A grid of seismic profiles then may allow to map this feature. Such a geometrical description is a base needed for both understanding the geodynamics and quantifying the sources in view of realistic seismic hazard assessment.

In the frame of the STREAMERS survey of the CEC DGXII JOULE programme, a vertical incidence reflection seismic line with coincident wide-angle recording has been acquired running from SW through the channel between Kefallinia and Zakynthos into the Gulf of Patras (Fig. 3). We employed the largest source capacity and length of multichannel recording streamer available up to now in adaptation to deep crustal penetration of industrial oil exploration methods. GECO's vessel BIN HAI 511 operated a 4.5 km long, 180 channels streamer and a 36 guns, total 7200 cu. in. (120 litres) tuned airgun array shot at a high rate to achieve a 30 fold CMP coverage.

The detailed structural interpretation may be found in Hirn et al. (1996) and is only grossly summarized hereafter. The point which will be taken up in the second section of discussion with respect to earthquakes, is that of the existence of a relatively flat very clear and strong relfector around 5.5 s TWT, which in the figure of the seismic section compensated for the water layer variation appears to dip slightly eastwards from the marine part to the Ionian islands where at km 120 it changes to a stronger dip (Fig. 4).

Beneath the Neogene stratification and the disruptions of the surface of the Mesozoic carbonate platform which may be related to the Ionian thrust, or to active tectonics when they correlate with topography of recent sediments at sea-bottom other structures are well detected. Such other, deeper structures may correspond either to lithological contrasts, or tectonic elements, and in this case they may be ancient or active. To clarify the section we may migrate it. This is only effective in restoring the true geometry of reflectors if energy is not from out the plane, i.e. the section is a dip line, an assumption on which we have no control and will need additional profiles to check it. The energy at depth beneath the disrupted surface of mesozoic carbonates, in particular the very steep and strong one between MF and IT is not erased by migration but concentrates instead into a slightly westward dipping interface at 3.5 s TWT, approximately at 7 km depth beneath MF. A further interface beneath it has a very strong westward dip of 30° down to 5.5 s TWT or 13 km depth.

The upper of those strong interfaces joins to the west as if it might connect with the deepest part of the IT, which dips with an opposite and stronger slope of 40° from 1 to 3.8 s TWT. The deeper one dips steeply westward down to over 5.5 s TWT in direction on an other major interface. The upper 12 km of the crustal structure hence possess a strongly structured image. Dips of sedimentary reflectors in the uppermost 3 km can be locally strong. However it is difficult to imagine that reflections with strong dips down to 12 km are due to lithological bedding. They might well be attributed to tectonic contacts. Such strongly dipping rather li-

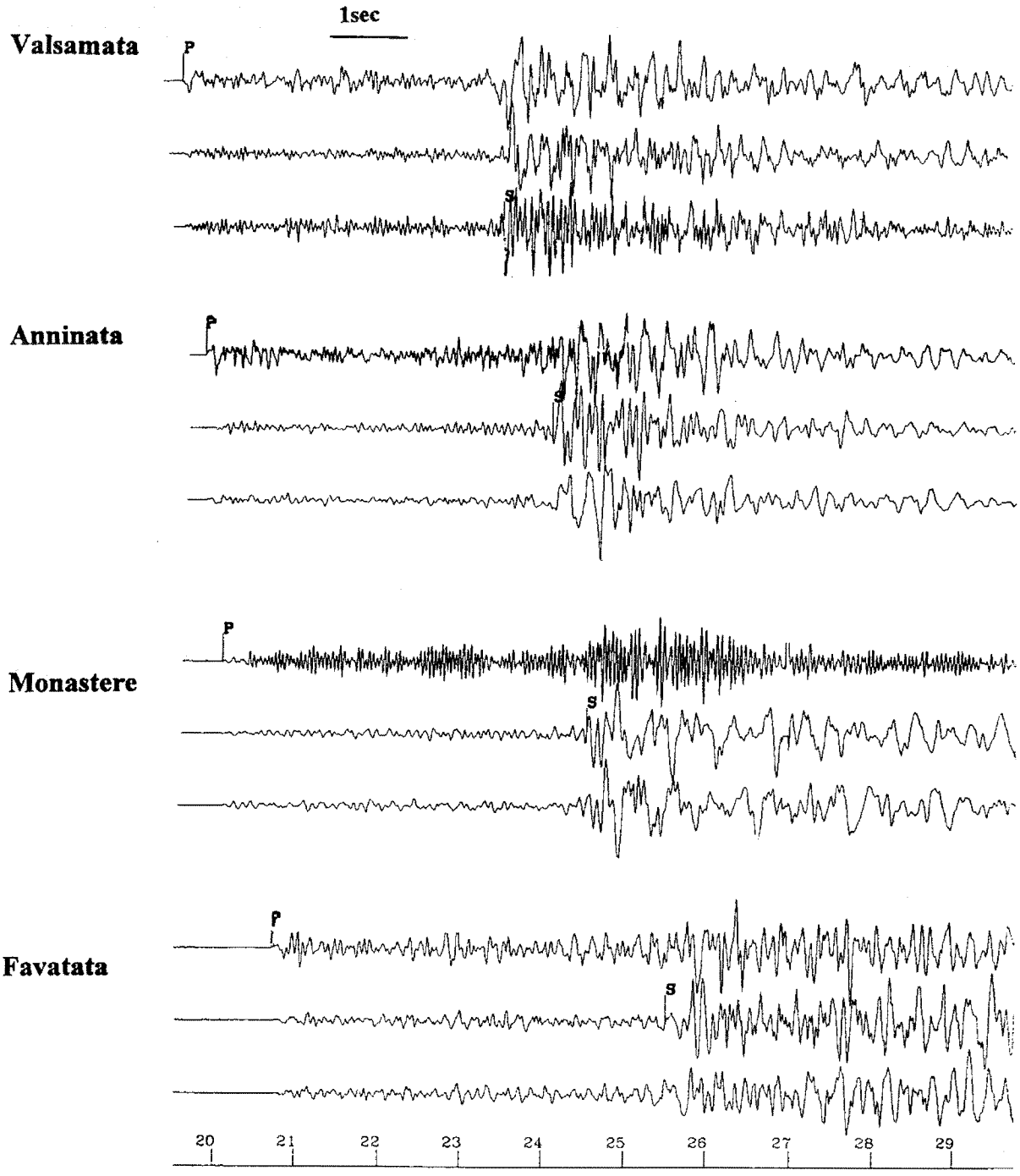

Fig. 5: Three-component seismograms with P and S arrivals, of the 4 stations nearest to a focus situated near the STREAMERS line ION-7, near km 110-120 (Fig. 3). Discussion in text.

near tectonic reflections althrough not demonstrably continuous with shallower ones like the Mounta Fault would then be good candidates for expression of present activation or reactivation.

III. - Earthquake detection and location with a temporary array

The permanent seismological array monitors regional seismicity with stations spaced about

60 km apart. Temporary deployements have been denser but with single component analogue paper recording seismographs and only either on Kefallinia or on Zakynthos at a time. To try and identify which one of these structures seismically imaged at depth have earthquake activity, we focused and earthquake recording experiment around the seismic line.

We deployed an array of 6 three-component digital seismographs, three on Kefallinia, two on Zakynthos, one near Killini and near Missolonghi on either side of the western gulf of Patras. Meteorological disturbances, a signal-triggered mode of operation with long intervals between maintenance tours, and repeated destruction of equipment limited data retrieval. Among the large number of earthquakes recorded in a three months period, several tens of events are located less than 20 km from the STREAMERS line. To reach high resolution on hypocenters where we have high resolution on structure, we restrict here the discussion to those of them well located by at least four stations on islands on both sides to be within 5 km of the line. An example of such three-component seismograms data st is shown in Fig. 5.

Since P waves arrive almost simultaneously at the four stations, the epicenter is well constrained geometrically between them irrespective of the velocity model. Since the event is between our stations, the minimum epicentral distance is 25 km, which for regional networks is considered a rather good situation for depth control, the more so with P and S waves. The hypocentral depth then derives readily from the interval time between P and S. For a fixed Poisson's ratio, the computed depth is a function of the average model velocity from the syrface. Hypocenters of the 10 best recorded earthquakes which occured in two sequences separated in time, cluster in space, but the value of average depth varies largely in dependance of model velocity. With a model of a half-space it varies from 10 to 15, 20 km for half-space velocities of 5.0, 5.5, 6.0 km/s space under a thin low velocity sedimentary cover.

The true velocity in the medium may here be approached independently through the velocity analysis performed during processing for the normal incidence reflection stacking. The very clear flat reflector described around 5-6 s TWT between km 95 and 120 allows to recover good quality velocity estimates. Five velocity analyses give consistently 5.2 km/s for the velocity between the base of Plio-quaternary sediments and that interface around 13 km. The highest point reached in the time section by the strong reflector is near Zakynthos under 300 m of water; the corresponding minimum two way time in the solid earth is 5.3 s.

From these analyses, the near-surface velocity is as low as 2.5 km/s but this is for Plioquaternary sediments at the sea bottom. However earthquake recording stations are offset the line on limestone. Stations ZAK and KEF in a similar situation during the STREAMERS line recorded first arrivals with higher, 3.7 km/s velocity beneath the Plio-quaternary on the normal incidence line. Using 3.7 km/s velocity under the stations and average 5.2 km/s beneath 2 km hypocenter of our well recorded earthquakes then is constrained to fit exactly with the depth of the strong flat reflector at 13 km depth near km 120, where it steepens and is overlain by contrary dipping reflections in the overburden.

Hence assuming this deep flat reflector exists 3 km north of the Streamers line, we document it, or the steeply opposite-dipping reflectors just on top of it, to be an active tectonic feature by identifying earthquakes to occur on it. This suggests that seismic activity can be associated with patterns of crustal heterogeneities of the structure as these appear in seismics and they can then be attributed to active deformation.

IV - Perspective

For the case presented here, seismic imaging provides structures which are candidates for the seismically active fault. If it is the flat reflector, this may also indicate a deep boundary marking the Ionian and pre Apulian thrusting on the subdected Ionian crust. Alternatively it may be the steeply opposite-dipping reflectors.

Characterization of the exact type of motion to decide between these possibilities will have to await for observation with an array distributed over a broader range of azimuths allowing to constrain focal mechanisms, i.e. including ocean bottom seismometers. We deployed such an on-shore-offshore seismicity array on the area in September 1995 which results will be the subject of future publication. On the other hand, ident-

ification of structures the activity of which provokes the other earthquakes we detected with the test array for seismicity at larger distance of the STREAMERS line, east of Kefallinia and east of it and of Zakynthos will have to await further lines of deep penetration high resolution exploration seismics.

Understanding of the geodynamical evolution depends on the description of where and how the earth's surface deforms or parts of it move with respect to the neighbouring and underlying medium. At an other time scale seismic hazard assessment and prediction of eartquake effect also depend strongly on deformation and its geometry, i.e. on the knowledge of the location and dimensions of faults, the nature of then motion and the rheology of adjacent material In a 3D deforming region like the Ionian-Preapulian frons the importance of blind faults and depth discordant motion is likely. Assessing them is out of reach of surface observation and modeling and needs in-situ imaging of structures and high-resolution onshore-offshore seismicity.

References

Anderson, H. & Jackson, J., Active tectonics of the Adriatic region, Geophys. J.R. Astr. Soc., 91, 937-983, 1987.

Brooks, M., Clews, J.E., Melis, N.S. & Underhill, J.R., Structural development of Neogene basins in Western Greece, Basin Research, 1, 129-138, 1988.

Brooks, M. & Ferentinos, G., Tectonics and sedimentation in the Gulf of Corinth and the Zakynthos and Kefallinia channels, western Greece, Tectonophysics, 101, 25-54, 1984.

Dziewonski et al. Centroid-moment tensors, PEPI, 1983.

Hatzfeld, D., Besnard, M., Makropoulos, K., Voulgaris, N., Koustouna, V., Hatzidimitriou, P., Panagiotopoulos, D., Karakaisis, G., Deschamps, A. & Lyon-Caen, H., Subcrustal microearthquake seismicity and fault plane solutions beneath the Hellenic Arc, J. Geophys. Res., 98, 9861-9870, 1993.

Hirn, A., Sachpazi, M., Siliqi, R., Mc Bride, J., Marnelis, F., Cernobori, L. & the STREAMERS - PROFILES GROUP, A traverse of the Ionian Islands fron with coincident normal incidence and wide-angle seismics. Tectonoph., in the press 1996.

Kahle, H.-G., Müller, M.V., Mueller, S., Veis, G., The Kephalonia transform fault and the rotation of the Apulian platform: evidence from satelite geodesy, Geophys. Res. Let., 20; 651-654, 1993.

Kiratzi, A.A. & Langston, C.A., Moment tensor inversion of the 1983 January 17 Kefallinia event of Ionian islands (Greece), Geophys. J. Int., 105, 529-535, 1991.

Le Pichon, X. & Angelier, J., The Aegean Sea, Philos Trans. R. Soc. London, A, 300, 357-372, 1981.

Liakopoulou, F., Pearce, R. G. & Main, I.G., Source mechanisms of recent earthquakes in the Hellenic arc from broadband data, Tectonoph., 200, 233-248, 1991.

McKenzie, D.P., Active tectonics of the Mediterranean region, Geophys. J.R. Astr. Soc., 30, 109-185, 1972.

Scordilis, E.M., Karakaisis, G.F., Karakostas, B.C., Panagiotopoulos, D.G. & Papazachos, B.C., Evidence for transform faulting in the Ionian Sea: the Cephalonia Island earthquake sequence of 1983, pageoph, 123, 387-397, 1985.

Stiros, S.C., Pirazzoli, P.A., Laborel, J. & Laborel-Deguen, F., The 1953 earthquake in Cephalonia (Western Hellenic Arc): coastal uplift and halotectonic faulting, Gehophys. J. Int., 117, 834-849, 1994.

Underhill, J.R., Triassic evaporites and Plio-Quaternary diapirism in western Greece, J. Geol. Soc., London, 145, 269-282, 1988.

Underhill, J.R., Late Cenozoic deformation of the Hellenide foreland, western Greece, Geol. Soc. Am. Bull., 101, 613-634, 1989.

SEISMIC SOURCE PARAMETERS AND MODELING

SEISMIC SOURCE MOMENT MEASUREMENTS FROM WAVEFORM INVERSION

J.Šileny[1], P.Campus[2] and G.F.Panza[2,3]

1 Geophysical Institute, Czech. Acad. Sci., Bocni II/1401, 14131 Praha 4, Czech Rep.
2 Universita di Trieste, Istituto di Geodesia e Geofisica, Via dellUniversita 7, 34123 Trieste, Italy
3 International Centre for Theoretical Physics, Strada Costiera 11, 34100 Trieste, Italy

Abstract

The method inverts either full waveforms or individual seismic phases and returns the mechanism and time history of a point source. As a by-product it allows to use amplitudes for relocalization of the event and in a simplistic way to optimize the structural model as well. This is accomplished by minimization of residual norm during modelling of the data in a phase space comprising both hypocentral coordinates and structural interpolation parameter. The unconstrained moment tensor is inverted in the initial step of the procedure, i.e. no a priori constraint of a double- couple mechanism is imposed, and the source mechanism is allowed to change with time. Thus, each moment tensor component has its own time history and, therefore, backslip is allowed. In the subsequent step of the method the independent moment tensor rate functions are processed to search for their correlated part and for six multipliers, the product of which models the moment tensor rate functions well. The correlated part is looked for supposing a positivity constraint which guarantees discarding of backslips, and results in a physical source time function. The multipliers represent the six moment tensor components describing constant in time average mechanism of the source. This method is a useful tool to study seismic sources in volcanic and geothermal areas, where seismicity can be caused not only by dislocations. Once the six moment tensor components are retrieved the source is decomposed into a volumetric part (V), representing an explosive or implosive component, and into a deviatoric part, containing both the double couple (DC) and the compensated linear vector dipole (CLVD) components. Both the depth of the source and the structural model representing the area in which the event occurred are permitted to vary within an "a priori" chosen range. If necessary, different structural model pairs can be used for each source-receiver path. The method includes an error analysis consisting of transformation of the data noise variance into confidence regions for volumetric, DC and CLVD parts of the retrieved moment tensor and for its principal axes (T, N and P) as well.

Introduction

Determination of mechanisms of weak events is of a prime interest while monitoring local seismicity, because they reflect stress pattern acting in the area under study and may help to map even its small scale tectonic structure. Using analog records the only applicable method is an analysis of first motions or, at most, first amplitudes picked up from the observed seismograms. These methods, excerpting only little information from the seismic record, are often dominating the processing of digital data as well. However, digital instrumentation allows more advanced processing aimed at earthquake source parameters retrieval than the classical

Special Publications of the Geological Society of Greece, No 6.

methods of first arrivals analysis. Provided that structural model of the region under study is available, synthetic seismograms generated by various types of source can be constructed and compared with observed records in a suitable inversion scheme.

Methods for point source mechanism retrieval with simultaneous determination of the source time function for teleseismic events have been developed, e.g., by Langston(1981), Sipkin(1982), Nábelek(1984); some of these approaches allow to determine the source depth as well. Sophisticated source retrieval methods exist for the inversion of near-source strong motion recordings (Anderson, 1991). These approaches make use of near-source data recorded by dense accelerometer arrays and provide most of recent information about seismic sources.

There is a gap between the teleseismic and near-source approaches which is not tackled satisfactorily. For regional and local earthquakes the seismic network is usually not dense enough and the knowledge of the medium is not detailed enough to allow to reconstruct a finite source model like in near-source studies. In comparison with teleseismic records, seismograms of regional and local events contain much higher frequencies which make the application of teleseismic approaches dubious (Koch, 1991a,b). The use of higher frequencies requires the use of more detailed models of inhomogeneous media for which the synthetic seismograms, specifically Green functions, should be computed.

This requirement was followed by Šileny and Panza(1992) and Šileny et al.(1992), who used the method of modal summation to compute Green functions in a vertically inhomogeneous medium with very fine structure. To improve their results, they used dynamic relocalization of the depth of the event, i.e. they used amplitudes to relocate the depth of the events determined from the kinematics. They also introduced a simple structural optimization, which allowed them to find a model of the structure, which fits best the observed data.

Recently, the method was generalized by Šileny and Pšencik (1995) for 3-D laterally varying layered isotropic structures by using ray Green functions for solving the forward problem.

Method

The method designed to retrieve the moment tensor of a point source together with the source time function by waveform inversion (Šileny et al., 1992; Šileny and Pšencik, 1995) consists of two successive steps: (i) determination of the moment tensor rate functions (MTRFs) describing, in general, a source with varying mechanism, and (ii) factorization of the MTRFs, i.e. looking for their correlated part specifying the time function of a source with a constant mechanism.

(i) Retrieval of moment tensor rate functions

The determination of the MTRFs requires the knowledge of the Green functions, i.e. the information on the structural model of the medium and the location of the hypocentre. Supposing that the Green functions are known we determine the MTRFs by means of a modification of the method originated by Sipkin (1982). The method starts with the commonly used equation relating the k-component of seismic displacement uk(t) with moment tensor time functions $M_{ij}(t)$

$$u_k(t) = M_{ij}(t) * G_{ki,j}(t), \qquad (1)$$

see, e.g., Aki and Richards (1980). The equation (1) is written for a point source approximation in a simplified notation: $u_k(t)$ is seismic displacement in the point of observation **r** (i.e. in the location of a particular station), $M_{ij}(t)$ is a time-dependent moment tensor in the hypocentral point **x** and $G_{ki,j}(t)$ is j-th spatial derivative of Green function $G_{ki}(\mathbf{r},\mathbf{x},t)$. We limit our approach to the far-field approximation, in which the Green function operates on time derivative of moment tensor only. Thus eq.(1) is transformed into

$$u_k(t) = \dot{M}_{ij} * g_{ki,j}(t), \qquad (2)$$

where g_{ki} is the far-field part of G_{ki}. From now on we are going to call the functions $g_{ki,j}(t)$ the Green functions. The $\dot{M}_{ij}(t)$are moment tensor rate functions (MTRFs). A suitable renaming $\dot{M}_{ij}(t) \rightarrow F_m$, $g_{kij} \rightarrow \Phi_m$ converts (2) into

$$u_k(t) = \sum_{m=1}^{6} F_m(t) \times \Phi_{km} \quad (3)$$

The parametrization of MTRFs by means of time-delayed overlapping triangles $T_{\Delta\tau}(t)$ of half-width $\Delta\tau$ (Nábelek, 1984) and suitable ordering of their weights yields

$$u_k(t) = \sum_{p=1}^{6N_t} w_p A_{kp}(t) \quad (4)$$

where N_t is number of parametrization triangles, $A_{kp}(t)$ is their convolution with Green functions and **w** is a vector containing the weights to be determined

$$w = (F_{11},...,F_{16},F_{21},...,F_{26},...,F_{Nt,1},..., F_{Nt,6}) \quad (5)$$

Equation (4) written for all the time points to be inverted forms a linear system **Aw=d** for Nt variables. Sipkin (1982) showed that the corresponding normal equations possess a block-Toeplitz symmetry allowing to use fast recursive schemes to solve the system. Koch (1991) demonstrated that inversion of high-frequency local waveforms requires damping of the normal equations, thus, the system to be solved reads

$$(A^TA+\upsilon^2I)\ w = A^Td \quad (6)$$

It should be pointed out that the step just described is a linear procedure, and thanks to high symmetry of the normal equation matrix it can be solved very quickly. If we are sure about the model of the medium and the location of the hypocentre, i.e. if we are able to construct credible Green functions, the MTRFs obtained in this step are the solution of the problem. However, in reality this is usually not the case: uncertainty in picking the arrival times together with uncertainty in the model of the medium itself lead to mislocation errors, and the model of the medium currently used can be only more or less accurate approximation of the real structure in the region under study. This situation is attacked by the method iteratively: we construct Green functions at individual gridpoints of a model space formed by hypocentral coordinates and a structural parameter and in a floating point of this model space we determine the Green functions by interpolation of the functions at the neighbouring gridpoints. In the version of the inversion method coupled with multimode summation method of constructing the Green functions (Panza, 1985; Panza and Suhadolc, 1987; Florsh et al., 1991) a grid along the depth only is assumed from the set of three hypocentral coordinates: the Green functions are computed initially for (1) a set of values of the source depth lying between two extremes, chosen on the basis of the uncertainty of the hypocentral location based on P and S-wave arrivals; (2) two structural models representing reasonable, preferably extreme, models for the region under study that will be denoted in the following with A and B. The different values of the source depth are indicated by means of different values of a variable X, while the parameter Y ($0 \le Y \le 1$) represents the different structural models: when Y=0, the structure used to compute the base functions is A, when Y=1 the considered structure is B. Intermediate values of Y define structural models which are more similar to A if Y<0.5, more similar to B if Y>.5. For each (X,Y) pair the Green functions are determined by weighted linear interpolation of the functions in the neighbouring nodes. At each floating point (X,Y) of the 2-D model space the MTRFs are determined by the modified Sipkin's method, the synthetic seismograms are calculated and compared with the observed ones. The comparison is performed in the L_2-norm of their residual

$$N_s = \left\{ \sum_{k=1}^{N} \sum_{i=1}^{3} \int_0^T \left[u_i^k(t)|^{obs} - u_i^k(t) \right]^2 dt \right\}^{\frac{1}{2}} \quad (7)$$

Here N is number of 3-component stations yielding the data, $u_i^k(t)|obs$ is the i-th component of observed seismogram recorded by the k-th station, uik(t) is the corresponding synthetic seismogram. Due to the dependence of the Green functions on the hypocentre location X and the structural parameter Y the norm N_s has to be considered as a function of X and Y, $N_s = N_s(X,Y)$. In the course of iterations the minimum N_s^{min} is searched and and the MTRFs obtained at this point are considered as a solution of the first step of the method.

(ii) Moment tensor rate function factorization

The MTRFs obtained in the step (i) are, in general, independent time functions describing a mechanism varying in time. A constant mechanism which is supposed to take place in the foci of especially weak events is deduced from the independent MTRFs by factoring them into a product of the corresponding component of the average moment tensor M_{ij} and the source time function describing the rupture history: $\dot{M}_{ij}(t) \rightarrow M_{ij}\dot{m}(t)$.

The factorization is an additional inverse problem: we use the MTRFs obtained in the step (i) as data and stream to fit them by specifying the average moment tensor and the source time function. This is accomplished by minimizing the normalized residual sum

$$N_r = \left\{ \sum_{i=1}^{3} \sum_{j=i}^{3} \int_0^T \left[\dot{M}_{ij}(t) - M_{ij}\dot{m}(t) \right]^2 dt \right\}^{\frac{1}{2}} \times$$

$$\times \left\{ \sum_{i=1}^{3} \sum_{j=i}^{3} \int_0^T \left[\dot{M}_{ij}(t) \right]^2 dt \right\}^{\frac{1}{2}} \qquad (8)$$

with respect to M_{ij} and $\dot{m}(t) \geq 0$ (T is the duration of the rupture process). If there is a physical reason to expect a change of the mechanism during the rupture process, the interval (0,T) can be divided into a few subintervals (T_{k+1}, T_k) and the norm (8) related to each of them. Then, in each individual subinterval a different average mechanism M_{ij}^k and the corresponding source time function $m^k(t)$ are allowed and the criterion of their determination is minimization of the sum of the norms N_r^k for all the subintervals covering the rupture process (0, T).

The fact should be stressed that the step (i) of the method yields an unconstrained solution, i.e., in general, the mechanism is variable with time and, in particular, backslips are possible. The six functions obtained in this step concern exclusively the source only in the case the following suppositions are satisfied: the Green functions are modelled exactly (i.e., we are sure about the model of the medium) and the source satisfies the point approximation. Strictly speaking, only in this case we are entitled to call the recovered functions the moment tensor rate functions (MTRFs). Obviously none of these presumptions is valid completely in reality. Then, the output of the step (i) is no longer a set of MTRFs in a physical sense but remains an useful tool for obtaining the final solution, i.e. the average moment tensor and the source time function, by preparing the input data for the subsequent step (ii), namely factorization. By determining these "pseudo MTRFs" we exclude the influence of the current structural model from the problem, because we deconvolve the Green functions corresponding to the current model from the input seismograms.

The principal advantage of this approach is a simplification of the problem: the problem of fitting the input seismograms is converted into the problem of matching the pseudo-MTRFs. The former data set can be rather large depending on the number of stations, number of components taken into account, and the sampling rate of the records. The latter one can be easier to handle, because there are always six traces only and their sampling rate can be controlled by means of their parametrization, i.e. the number of points to be fitted can be substantially lower than in the former case. Of course, this simplification of the problem can be paid by possible biasing of the solution due to accepting the above mentioned suppositions: good correspondence of the model to the real medium, exact construction of the Green functions in the model adopted, and acceptability of the point source approximation. The consequence of the unmodelled effects is a departure from correlation of the pseudo-MTRFs. Their subsequent factorization is believed to suppress these biases because it looks for their correlated part only. All the uncorrelated components of the pseudo-MTRFs are discarded, which is supposed to remove from the solution the unmodelled effects of the structure complexity and source finitness, or, at least, to constrain their effect on the solution.

Additional feature of the factorization step ensuring the physical sense of the solution is the positivity constraint imposed on the source time function: $\dot{m}(t) \geq 0$. Due to the unmodelled effects listed the pseudo-MTRFs themselves may be unphysical because they may comprise backslips along the fault plane. The positivity constraint guarantees a physical sense of the source time function, because it allows only forward

slips.

Of course, the effectivity of this algorithm has the limit: it cannot help if the above listed suppositions are violated too severely. However, in this case it can at least diagnose such a situation - the factorization simply does not find enough correlation in the pseudo-MTRFs.

Error analysis

For an estimate of errors imposed on the moment tensor rate functions by presence of random noise in the input seismograms the general theory of inverse problems developed by Tarantola (1987) was applied. He showed that for Gaussian shape of a priori data probability and probability of forward modelling and in the case of linear forward problem **g(m)=Gm** the a posteriori marginal density $\sigma_M(m)$ is Gaussian, too:

$$\sigma_M(m) \sim \exp\left[-\tfrac{1}{2}(m - \langle m\rangle)^T C_M^{-1}(m - \langle m\rangle)\right] \quad (9)$$

where

$$\langle m\rangle = (G^T C_D^{-1} G + C_M^{-1})^{-1} (G^T C_D^{-1} d_0 + C_M^{-1} m_0 \quad (10)$$

$$C_M' = (G^T C_D^{-1} G + C_m^{-1})^{-1} \quad (11)$$

Here **m** is the vector of model parameters, $\mathbf{m}_0$ a priori information on the model, **G** forward modelling operator, $C_D=C_d+C_T$, C_d is the data covariance, C_T covariance of the forward modelling and C_M covariance of a priori model information. Eq.(10) specifies the maximum likelihood vector of model parameters and (11) its a posteriori covariance matrix.

Applying this approach to our problem, the a priori data uncerntainty is originated by noise superimposed on the seismic records, while the modelization uncerntainty is caused by the use of improper Green functions for the construction of synthetic seismograms, due to mislocation of the hypocentre and/or imperfect knowledge of the structural model. The core of the inversion step is eq.(6) which coincides, in fact, with (10) provided that a priori model information m_0 = 0, and the damping constant corresponds to its inverse variance multiplied by the data variance: $\upsilon^2 = \sigma_d^2/\sigma_{M0}^2$. It should be pointed out that to compare (6) and (10) we have to set $C_d = \sigma_d^2 I$, $C_M = \sigma_{M0}^2 I$, i.e. all the data items must have the same variance σd and similarly the distribution of all the a priori estimates of the model parameters must be described by the same value of σ_{M0}.

Eq.(11) provides us with a posteriori variances of the MTRFs which are used in the factorization step (ii) for an estimate of the covariance matrix of the moment tensor M_{ij} and of the error bars of the source time function . Having the variances $\sigma_{ij}(t)$ of the MTRFs at hand, we can replace (8) by the weighted residual sum

$$N_f = \sum_{i=1}^{3}\sum_{j=i}^{3}\int_0^T \frac{1}{\sigma_{ij}^2(t)}\left[\dot{M}_{ij}(t) - M_{ij}\dot{m}(t)\right]^2 dt \quad (12)$$

In turn, N_f may be considered as a x^2 function of 6 degrees and 1 degree of freedom and by observing its increase in the vicinity of the resultant Mij and $\dot{m}(t)$ respectively, to map the confidence regions in an a priori selected probability level. Then, following Riedesel and Jordan (1989), by using first perturbation theory we can transform the covariance matrix of M_{ij} into confidence regions for its eigenvalues and eigenvectors (Šíleny et al., 1995).

Acknowledgments

The research has been carried out in the framework of the activities planned by the Central European Initiative Commitee for Earth Sciences, partially supported by the NATO Linkage grant ENVIR.LG 931206, EEC contract EPOCH-CT91-0042, ENV-CT94-0491, COPERNICUS contract CIPA-CT94-0238, Grant No.312104 of the Grant Agency of the Czech Academy of Sciences, and is a contribution to the ILP project 3DMET.

References

Aki, K. & Richards, P.G., 1980. Quantitative Seismology, Freeman, San Francisco.

Anderson, J.G., 1991. Strong motion seismology, Rev. of Geophysics, Suppl., 700- 720.

Florsh, N., Faeh, D., Suhadolc, P. and G. F. Panza, G. F (1991). Complete synthetic seis-

mograms for high-frequency multimode SH waves. (Udias and Buforn eds., El Escorial Workshop Proceedings), *Pageoph,* **136,** 529-560.

Koch, K., 1991a. Moment tensor inversion of local earthquake data - I. Investigation of the method and its numerical stability with model calculations, Geophys. J. Int., 106, 305-319.

Koch, K., 1991b. Moment tensor inversion of local earthquake data - II. Application to aftershocks of the May 1980 Mammoth Lakes earthquakes , Geophys. J. Int., 106, 321-332.

Langston, C.A., 1981. Source inversion of seismic waveforms: the Koyna, India earthquakes of 13 September 1967, Bull. seism. Soc. Am., 71, 1-24.

Nábelek, J.L., 1984. Determination of earthquake source parameters from inversion of body waves, PhD thesis, MIT.

Panza, G.F., 1985. Synthetic seismograms: the Rayleigh waves model summation, J. Geophys., 58,125-145.

Panza, G. F. and Suhadolc, P., 1987. Complete strong motion synthetics. In: *B. A. Bolt (ed.) Seismic Strong Motion Synthetics, Computational Techniques 4,* Academic Press, Orlando, 153-204.

Riedesel, M.A. & Jordan, T.H., 1989. Display and assessment of seismic moment tensors, Bull. seism. Soc. Am., 79, 85-100.

Šíleny, J. & Panza, G.F., 1991. Inversion of seismograms to determine simultaneously the moment tensor components and source time function for a point source buried in a horizontally layered medium, Studia geoph. geod., 35, 166-183.

Šíleny, J., Panza, G.F. & Campus, P., 1992. Waveform inversion for point source moment tensor retrieval with variable hypocentral depth and structural model, Geophys. J. Int., 109, 259-274.

Šíleny, J. & Pšencik, I., 1995. Mechanisms of local earthquakes in 3-D inhomogeneous media determined by waveform inversion, Geophys. J. Int., in press.

Sipkin, S.A., 1982. Estimation of earthquake source parameters by the inversion of waveform data: synthetic waveforms, Phys. Earth planet. Inter., 30, 242-259.

Tarantola, A., 1987. Inverse Problem Theory. Methods for data fitting and model parameter estimation, Elsevier, Amsterdam.

SIZE DETERMINATION OF WEAK VRANCEA (ROMANIA) EARTHQUAKES

M. Radulian[1], L. Ardeleanu[1], P. Campus[2], J. Sileny[3], G. F. Panza[4]

[1] *National Institute for Earth Physics, Bucharest, Romania*
[2] *Istituto di Geodesia e Geofisica, Universita' degli Studi, Trieste, Italy*
[3] *Geophysical Institute, Czech Academy of Sciences, Prague, Czech Republic*
[4] *Istituto di Geodesia e Geofisica, Universita' degli Studi, and International Center for Theoretical Physics, Trieste, Italy*

Keywords: source mechanism, Vrancea region, moment tensor, waveform inversion, modal summation.

Abstract

The inversion of high-frequency seismograms allowed us to retrieve the source size of two weak Vrancea earthquakes, one occurred in the crust, the other in the lithospheric part of the mantle. The source is described by the full moment tensor, allowing for both deviatoric and volumetric components.

The few P wave polarities available are not sufficient for the determination of a reliable source mechanism by using standard methods, while the used inversion allows us to retrieve source mechanisms and sizes that are stable with respect to different boundary conditions and in good agreement with the observed polarities.

Introduction

The method developed by Sileny and Panza (1991) and Sileny et al. (1992) allows us the inversion of short period seismograms of small earthquakes, recorded by local networks, in order to simultaneously determine the seismic moment tensor and the sourcetime function. It has been successfully applied to volcanic and orogenic areas (e.g., Panza et al., 1993), using data collected by local networks, and it has been extended by Radulian et al. (1995) to data collected by regional networks. They considered the digital Romanian telemetered network and showed that the waveform inversion is probably the only viable procedure to get reliable fault plane solutions of weak events.

Seismotectonics

The Vrancea region is situated at the major bend of the Eastern Carpathian Arc (Fig. 1). There the seismicity is concentrated in two, somehow distinct, seismogenic zones: crustal (h < 40 km) and subcrustal (h > 60 km). This particular seismic activity is correlated with the presence of a complex junction, characterized by a continent - continent collision, which is now in its final stage of evolution, among the East European plate and Intra-Alpine, Moesian and Black Sea subplates.

Several models are formulated for the seismotectonics of this region. Some of them propose a double subduction with a paleosubduction of the East European plate beneath the Intra-Alpine subplate from NE to SW and a still active subduction, from SE to NW, of the Black Sea subplate beneath the Intra-Alpine subplate.

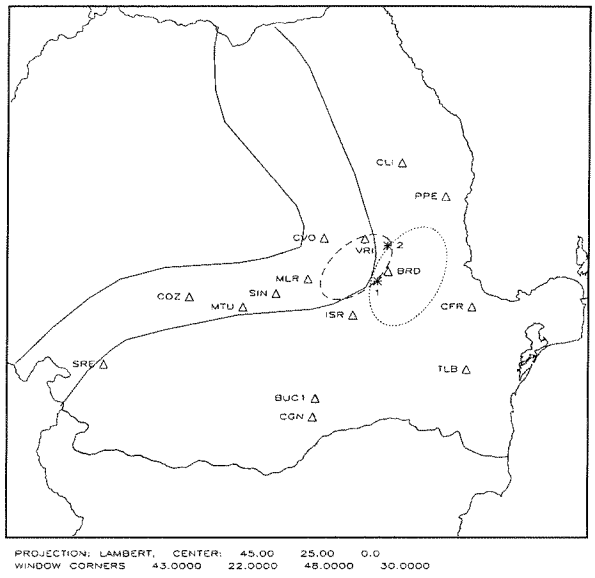

Fig. 1. Vrancea area and the Romanian telemetered network. Seismic stations are represented by triangles and epicentres by stars. The Carpathian mountain chain is indicated by the two continuous lines, while the epicentral areas of Vrancea crustal and subcrustal earthquakes are identified by dotted and dashed lines, respectively.

The south-eastern extremity of the subducted European plate is supposed to be detached at present from the rest of the plate (Fuchs et al., 1978; Oncescu, 1984). Another variant is a simple paleosubduction from SE to NW of the Black Sea subplate beneath Inter-Alpine subplate, with its extremity decoupled below a depth of 60 km (Constantinescu and Enescu, 1984). The nearly vertical distribution of hypocentres in the subcrustal domain is in good agreement with the hypotheses of the relict character of the subduction process and the gravitational sinking of a decoupled slab in the asthenosphere.

Data and Inversion Method

The Vrancea seismic activity is monitored at present by a local network of 15 stations (Fig. 1). The network consists of vertical S13 seismometers with 1 s natural free period and a flat response to velocity between 1 and 10 Hz. The high cut-off frequency is 12.5 Hz. The digital system samples the waveforms with the rate of 50 samples/sec.

The locations of the two weak events analysed have been computed by a HYPO algorithm and are given in Table 1. Event 1 occurred in the Ramnicu Sarat region; event 2 is localised in the north-eastern upper edge of the lithospheric slab.

The inversion method used is fully described by Sileny and Panza (1991) and Sileny et al. (1992). The source is described by the full moment tensor, having both volumetric (V) component and deviatoric part, separated into double couple (DC) and compensated linear vector dipole (CLVD) components.

Results

The input structural models used in the inversion are given by Radulian et al. (1995).

The available high-frequency waveforms (vertical component) recorded by the Romanian local network with a high signal/noise ratio, a low-pass Gaussian filter with the high cut-off frequency at 1 Hz, re-sampled with a step of 0.488 s, aligned to the origin time, and truncated by means of a Hanning window. To limit our analysis to the most energetic part of the observed signal only S-wave and surface-wave trains are considered in the inversion.

The Green's functions are computed, in correspondence of the epicentral determination and origin time, given by HYPO program, by using the multimode method (Panza, 1985). Since the method of inversion allows for variation of the hypocenter, we allow the depth to vary in the ranges from 14 to 24 km for the shallow event, and from 56 to 64 km for the deep event, centred around the initial depths determined with HYPO.

Table 1. Earthquakes studied

N	Date	h: m: s	Lat (^{o}N)	Lon (^{o}E)	Deth (km)	M_L
1.	June 23, 1982	17:51:36.41	45.461	26.883	19	3.3
2.	April 3, 1986	01:18:40.86	45.800	27.030	60	3.3

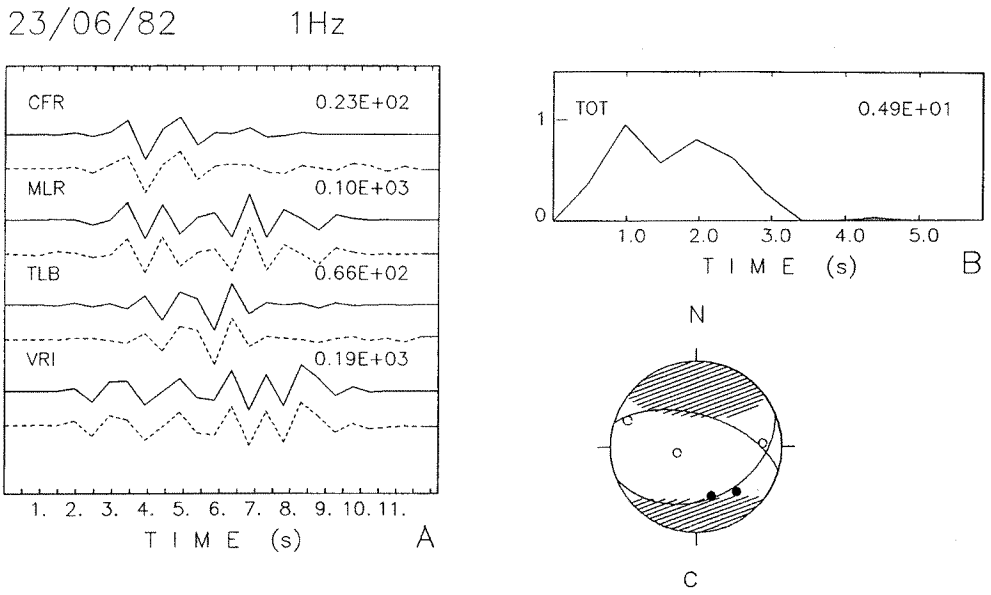

Fig. 2. Inversion of event 1 for 1 Hz cut-off frequency. A: recorded (solid lines) and synthetic seismograms (dashed lines). B: normalized joint source time function (scaling factor is indicated in the upper right conrer). C: average focal mechanism associated with the joint source time function.

The result of the inversion for the crustal earthquake is presented in Fig. 2. The observed seismograms together with the corresponding synthetic signals are depicted in Fig. 2A. As we could expect for a tectonic event, the V component is negligible (2.5% of the total), and the joint source time function of the total moment, plotted in Fig. 2B, practically corresponds to a deviatoric process, with 65.2% of DC and 32.3% CLVD.

The total source duration is about 3 s, suggesting a complex event. The limited frequency

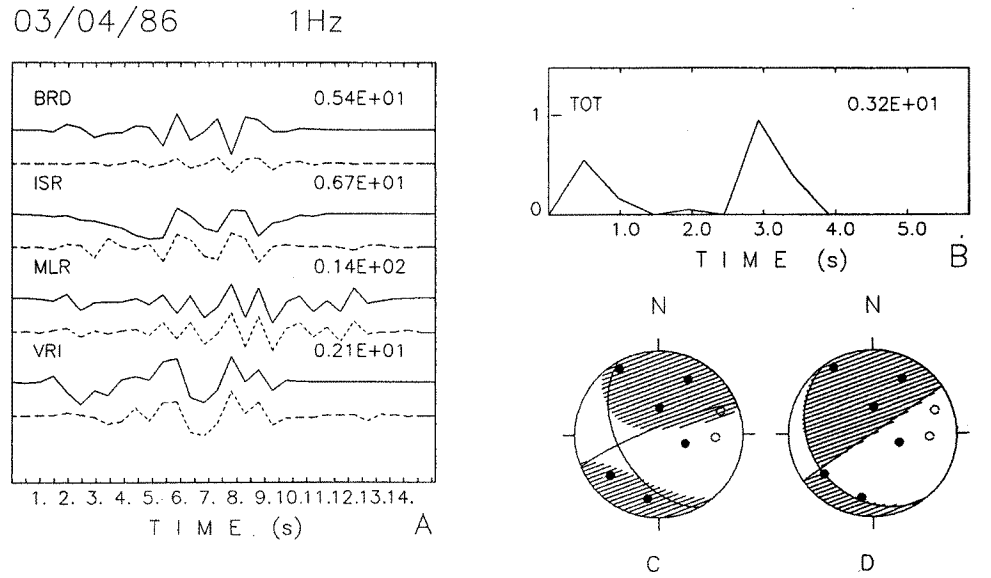

Fig. 3. Inversion of event 2 for 1 Hz cut-off frequency. A: recorded (solid lines) and synthetic seismograms (dashed lines). B: normalized joint source time function (scaling factor is indicated in the upper right corner). C: focal mechanism associated with the first large peak of the total moment tensor. D: focal mechanism associated with the second large peak of the total moment tensor.

bandwidth does not allow us to set off possible subevents. The existence of complex rupture processes seems not to be a characteristic proper of large events only, and it is reported for several small earthquakes by Kikuchi and Ishida (1993). The hypocentral depth determined by the inversion is 15 km, i.e. 4 km shallower than the depth determined with HYPO.

The average mechanism represented in Fig. 2C indicates a dominant normal faulting, and is in good agreement with the distribution of the few available P-wave polarities. The N-S extension and the tendency of the compressive axis to be vertical are the most common results for the fault plane solutions of the earthquakes occurred in the crustal outer part of the Carpathian Arc Bend (Oncescu, 1987).

The inversion of the records of event, 2, filtered at 1 Hz, is presented in Fig. 3. The V component of the moment tensor is small (3.9%), the DC is 63.0%, and the CLVD is 33.1% of the total moment.

The source time function for the total moment tensor is presented in Fig. 3B. Two subevents can be detected, one centred at 0.5 s from the beginning of the rupture process, with a duration of about 1 s, and the other centred at 3.0 s, with a duration of about 1.5 s. The two pulses are separated by a time interval of about 1.5 s, when fault is locked. The retrieved hypocentral depth is 64 km.

The fault plane solutions for the two peaks of the total moment tensor (Fig. 3c and 3D) indicate normal faulting with a large strike-slip contribution at the beginning of the faulting process. The P axis is oriented NW-SE in agreement with the general trend of the stress field in the Vrancea region (compression caused by the Black Sea subplate movement from SE to NW).

The source parameters, including the size, obtained for the two earthquakes analysed are summarized in Table 2. Stability tests indicate that in all cases the general trends of the focal mechanisms (normal faulting for both crustal and subcrustal event) are preserved. The distribution of compressions and dilatations associated to the deviatoric tensor is generally quite stable, while the orientation of the best fault planes, consistent with the deviatoric tensor, is more unstable, but in general, it fits well the few available polarities. In the source time function, although it presents a great variety in its detailed features, the complex character of the energy release is always present, with a good stability in the total duration.

Discussion and Conclusions

To obtain the focal mechanism, simple methods, as that one using the P-wave polarities, may be used only for cases when very local and dense networks or arrays are available. For the weak Vrancea events (M_0 about 10^{14} N m) it is impossible to find sufficient polarities to make an accurate determination of the focal mechanism and size. The inversion scheme used here offers a robust solution, even if the structural models considered in this paper are a simple one-dimensional approximation of the real structure.

The general features described in the literature about the focal mechanism of the Vrancea subcrustal earthquakes (e.g., Oncescu and Trifu, 1986) are: (1) the quasi-horizontality of the P axes and the contraction in the SE-NW direction; (2) the quasi-verticality of the T axes and the vertical extension. The first feature, which is present in our solution, can be explained by the movement of the Black Sea subplate from SE to NW. The second feature is attributed to the gravitationally sinking of the old slab into the mantle and does not fit our solution. If confirmed by the further investigations presently in

Table 2. Seismic source parameters obtained from the inversion

N	Depth	M_0	strike	dip	rake	strike	dip	rake	
	(km)	(N m)		Plane 1			Plane 2		
1.	15	90×10^{13}	68^o	37^o	58^o	286^o	59^o	112^o	
2.	64	13×10^{13}	248^o	83^o	221^o	151^o	49^o	350^o	Subevent 1
	64	25×10^{13}	144^o	26^o	218^o	236^o	89^o	244^o	Subevent 2

progress, we can offer two explanations for this discrepancy: (1) the upper part of the slab (60 < h < 80 km) is the less studied since there the seismic activity is significantly lower than in the deeper part; moderate or large events (M > 5.0) are very rare and have not yet been recorded by the regional Romanian digital network; (2) it is the part of the slab where the detachment from the crust took place and it is likely that here the stress field is more complex relative to the deeper part of the slab (Tavera, 1991).

For the crustal earthquakes a greater diversity in nodal plane orientantions is observed. The axis of the maximum compression tends to be vertical and equal in magnitude with the intermediate stress axis, indicating a pure bi-axial stress state (Oncencu, 1987). Our solutions is in fairly good agreement with this general result.

The V component of the moment tensor is small, less than 5% of the total moment. The rather large CLVD component (around 32%) could be due to some inadequancies present in the structural model or to the not completely satisfactory approximation of the seismic source by means of a point source.

Trifu and Radulian (1989) showed that there is a significant interdependence between small and large earthquakes in Vrancea region. The inversion method described offers the possibility to gather a statistically significant set of information from small events, since it requires no more than 4 stations to get a reliable solution of the focal mechanism, even if the joint source time function may be sometimes unstable. Therefore it provides a powerful tool in exploring and understanding the processes taking place in the Vrancea focal region, since it does not require to wait for a rare large earthquake to occur, but it can exploit immediately the very frequent small events, recorded by the Romanian regional digital network.

Acknowlegments

M.R. and L.A. are thankfull to Prof. D. Enescu for his support to this research.

The research has been carried out in the framework of the activities planned by the Central European Initiative Commitee for Earth Sciences, partially supported by the NATO Linkage grants ENVIR.LG 931206, and SA. 12-5-02 (CN. SUPPL 940880) 453, the EEC contract EPOCH-CT91-0042, ENV-CT94-0491, COPERNICUS CIPA-CT94-0238, Grant No. 312104 of the Grant Agency of the Czech Academy of Sciences, and is a contribution to the ILP project 3DMET.

Special thanks go to ENEA for allowing us to use of the IBM 3090E of the Computer Centre ENEA INFO BOL.

References

Constantinescu L., and Enescu C., 1984. A tentative approach to possibly explaining the occurrence of the Vrancea earthquakes. Rev. Roum. Geol., Geogr., Geophys., 28: 19-32.

Fuchs K., Bonjer K.P., Bock G., Radu C., Enescu D., Jianu D., Nourescu A., Merkler G., Moldoveanu T., and Tudorache G., 1978. The Romanian earthquake of March 4, 1977. II. Aftershoks and migration of seismic activity. Tectonophysics, 53: 225-247.

Kikuchi M., and Ishida M., 1993. Source retrieval for deep local earthquakes with broadband records. Bull. Seism. Soc. Am., 83: 1855-1870.

Oncescu M.C., 1984. Deep structure of the Vrancea region, Romania, inferred from simultaneous inversion for hypocenters and 3-D velocity structure. Ann. Geophys., 2: 23-28.

Oncescu M.C., 1987. On the stress tensor in Vrancea region. J. Geophys., 62: 62-25.

Oncescu M.C., and Trifu C.I., 1986. Depth variation of moment tensor principal axes in Vrancea (Romania) seismic region. Ann. Geophys., 5B: 149-154.

Panza G.F., 1985. Synthetic seismograms: the Rayleigh waves modal summation. J. Geophys., 58: 125-145.

Panza G.F., Sileny J., Campus P., Nicolich R., and Ranieri G., 1993. Point source moment tensor retrieval in volcanic, geothermal and orogenic areas by complete waveform inversion. Journal of Applied Geophysics, 30: 89-118.

Radulian M., Andeleanu L., Campus P., Sileny J., and Panza G.F., 1995. Waveform of weak Vrancea (Romania) earthquakes. Tectonophysics (submitted).

Sileny J. and Panza G.F., 1991. Inversion of seismograms to determine simultaneously the moment tensor components and source time function for a point source burried in a horizontally layered medium. Studia Geoph. Geod., 35: 166-183.

Sileny J., Panza G.F., and Campus P., 1992. Waveform inversion for point source moment tensor retrieval with variable hypocentral depth and structural model. Geophys. J. Int., 109: 259-274.

Tavera J., 1991. Etude des mecanismes focaux de pros seismes et seismicite dans la region de Vrancea-Roumanie. Raport de stage de recherche, Institute de Physique du Globe, Universite de Paris, 7: 53pp.

Trifu C.I., and Radulian M., 1989. Asperity distribution and percolation as fundamentals of earthquake cycle. Phys. Earth Planet. Interiors. 58: 277-288.

PARTIAL DERIVATIVES OF SYNTHETIC SEISMOGRAMS OF P-SV WAVES WITH RESPECT OF THE STRUCTURAL PARAMETERS

L. Urban[1], F. Vaccari[2]

[1] *Department of Geophysics, Charles University, Prague, The Czech Republic*
[2] *CNR-GNDT, c/o University of Trieste, Institute of Geodesy and Geophysics, Trieste, Italy*

Keywords: synthetic seismograms, partial derivatives, eigenfunctions, structural parameters, inversion, modal summation.

Abstract

Analytical formulas for partial derivatives of eigenfunctions of synthetic seismograms of P-SV waves with respect to the structural parameters are given in this paper. Computations are based on the method of multimode dispersion computations (Knopoff's method).

Introduction

Direct numerical modelling of the Earth's interior by analysing geophysical data is based on achieving a good fit between observations and the corresponding theoretically computed values. Agreement can be achieved by making trial changes of the structural parameters, and checking how the perturbation modifies the computed values. These changes of the structural parameters can be made manually in an empirical way or by use of an inversion technique. After a change of some structural parameter a new direct computation of the theoretical values is necessary. To avoid this, which is quite time-consuming, it is useful to calculate the partial derivatives of the theoretical formula with respect to structural parameters. These partial derivatives can be computed in two ways, numerically, which is again time-consuming, or analytically. The theoretical formula under our investigation is a synthetic seismogram of P-SV Rayleigh waves. Our computations are based on modern and the most efficient methods of multimode dispersion computations (Panza, 1985).

The development of a linear inverse theory for the multimode case, for synthetic seismograms under our investigation, requires highly efficient computation of the partial derivatives of phase and group velocities, eigenfunctions and energy integral for Rayleigh-wave modes, with respect to the structural parameters. The first part - method of computing the partial derivatives of phase and group velocities with respect to the P- and S-wave velocity (α and β) and the pensity (ρ) was already published by Urban at al. (1993). The dispersion computations are based on Knopoff's method (Knopoff, 1984; Schwab, 1970; Schwab and Knopoff, 1972).

Derivatives of Eigenfunctions

At present the computations of displacement-depth and stress-depth functions-eigenfunctions for Rayleigh-wave modes with respect to the above mentioned structural parameters is under our investigation. For the evaluation of eigenfunctions we use an algorithm described in Schwab at al. (1984).

In this paper we will use the notation of Schwab (1970). Then, the evaluation of partial

derivatives for the eigenfunctions u (z), w σ(z), (z), and τ(z) is reduced to the determination of partial derivatives for layer constants A_m, B_m, C_m, D_m for the layers above the homogeneous half-space, and the constants A_n and D_n for this deepest structural unit.

In the first part we calculate the derivatives of the elements of the (1 x 6) matrix, appearing in the basic interface-matrix multiplication of Knopoff's method (Schwab and Knopoff, 1972):

$$[U^{(m+1)}, iV^{(m+1)}, W^{(m+1)}, R^{(m+1)}, iS^{(m+1)}, -U^{(m+1)}]$$

where U^i, V^i, W^i, R^i, S^i are i-th elements in the fast form of Knopoff's method for Rayleight-wave computation.

If we denote $\gamma^1 = 2\beta_1^2/c^2$, where β_1 is S-wave velocity in the upper layer, and c is phase velocity, then the elements for the first interface are

$$U_0 = -\gamma_1(\gamma_1 - 1),\ V_0 = 0,\ W_0 = (\gamma_1 - 1)^2,\ R_0 = \gamma_1^2,$$

and $S_0 = 0$ (in the case of continental structure).

Then the derivatives with respect to the β_1 velocity are:

$$\frac{\partial}{\partial\beta_i} U_0 = -2\gamma_1\gamma'_1 + \gamma'_1,\ \frac{\partial}{\partial\beta_i} V_0 = 0,$$

$$\frac{\partial}{\partial\beta_i} W_0 = 2(\gamma_1 - 1)\gamma'_1,\ \frac{\partial}{\partial\beta_i} R_0 = 2\gamma_1\gamma'_1,\ \frac{\partial}{\partial\beta_i} S_0 = 0$$

where $\gamma'_1 = -\frac{4\beta_1\beta'_1}{c^3}c'$ when $i \neq 1$,

and $\gamma'_1 = -\frac{4\beta_1\beta'_1}{c^2} - \frac{4\beta_1^2}{c_3}c'$ when $i = 1$.

Here c′ denote the derivative $\partial c/\partial\beta_i$. This value is computed by the method described in Urban et al. (1993). Next step consists in evaluation of derivatives for quantities ε and ζ which are given in Urban et al. (Table 1, 1933) and Schwab (Table 2, 1970). The most important quantity is ε_1 which is, for m-th layer $\varepsilon_1^{(m)} = 2(\beta_m^2 - \varepsilon_0^{(m)}\beta_{m+1}^2)$.

The derivative with respect to the β velocity is

$$\frac{\partial}{\partial\beta_i}\varepsilon_1^{(m)} = 2\left(\beta_m^2 - \varepsilon_0^{(m)}\beta_{m+1}^2\right)\left(-\frac{2}{c_3}c'\right)$$

(for $i \neq m,\ i \neq m+1$),

$$= \frac{4\beta_m\beta'_m}{c_3} + 2\left(\beta_m^2 - \varepsilon_0^{(m)}\beta_{m+1}^2\right)\left(-\frac{2}{c^3}c'\right)$$

(for $i \neq m$) and

$$= -\varepsilon_0^{(m)}\frac{4\beta_{m+1}\beta'_{m+1}}{c_2} + 2\left(\beta_m^2 - \varepsilon_0^{(m)}\beta_{m+1}^2\right)\left(-\frac{2}{c_3}c'\right)$$

(for $i = m + 1$).

The quantities ζ are:

$$\zeta_1 = \cos P_m, \qquad \zeta_2 = \cos Q_m,$$
$$\zeta_3 = r_{\alpha m}\sin P_m, \qquad \zeta_4 = (1/r_{\alpha m})\sin P_m,$$
$$\zeta_5 = r_{\beta m}\sin Q_m, \qquad \zeta_6 = (1/r_{\beta m})\sin Q_m,$$

where $P_m = d_m \cdot \omega_c/c \cdot r_{\alpha m}$ and $Q_m = d_m \cdot \omega_c/c \cdot r_{\beta m}$ respectively. d_m - thickness of m-th layer,

$$r_{\alpha m} = \sqrt{-\left(1 - \frac{c^2}{\alpha_m^2}\right)} \text{ and } r_{\beta m} = \sqrt{-\left(1 - \frac{c^2}{\beta_m^2}\right)}.$$

Then the derivatives of P_m and Q_m are

$$\frac{\partial}{\partial\beta_i} P_m = -d_m\frac{\omega_c}{c}c' \cdot r_{\alpha m} + d_m\frac{\omega_c c'}{\alpha_m^2}\frac{1}{r_{\alpha m}}$$

$$\frac{\partial}{\partial\beta_i} Q_m = -d_m\frac{\omega_c}{c}c' \cdot r_{\beta m} + d_m\frac{\omega_c c'}{\beta_m^2}\frac{1}{r_{\beta m}} \text{ (for } i \neq m),$$

$$= -d_m\frac{\omega_c}{c^2}c' \cdot r_{\beta m} + d_m\frac{\omega_c(c'\beta_m - c\beta_m')}{\beta_m^3}\frac{1}{r_{\beta m}}$$

(for $i = m$),

and the derivatives of quantities ζ become

$$\frac{\partial}{\partial\beta_i}\zeta_1 = -\frac{\partial}{\partial\beta_i}P_m\sin P_m,\ \frac{\partial}{\partial\beta_i}\zeta_2 = -\frac{\partial}{\partial\beta_i}Q_m\sin Q_m,$$

$$\frac{\partial}{\partial\beta_i}\zeta_3 = \frac{cc'}{\alpha_m^2}\frac{1}{r_{\alpha m}}\sin P_m + r_{\alpha m}\frac{\partial}{\partial\beta_i}P_m\cos P_m,$$

$$\frac{\partial}{\partial\beta_i}\zeta_4 = \left(r_{\alpha m}\frac{\partial}{\partial\beta_i}P_m\cos P_m - \frac{cc'}{\alpha_m^2}\frac{1}{r_{\alpha m}}\sin P_m\right)\frac{1}{r_{\alpha m}^2},$$

$$\frac{\partial}{\partial\beta_i}\zeta_5 = \frac{cc'}{\beta_m^2}\frac{1}{r_{\beta m}}\sin Q_m + r_{\beta m}\frac{\partial}{\partial\beta_i}Q_m\cos Q_m$$

(for $i \neq m$)

$$= \frac{c(c'\beta_m - c\beta'_m)}{\beta_m^3} \frac{1}{r_{\beta m}^2} \sin Q_m + r_{\beta m} \frac{\partial}{\partial \beta_i} Q_m \cos Q_m$$

(for i = m),

$$\frac{\partial}{\partial \beta_i} \zeta_6 = \left(r_{\beta m} \frac{\partial}{\partial \beta_i} Q_m \cos Q_m - \frac{cc'}{\beta_m^2} \frac{1}{r_{\beta m}} \sin Q_m \right) \frac{1}{r_{\beta m}^2}$$

(for i ≠ m),

$$= \left(r_{\beta m} \frac{\partial}{\partial \beta_i} Q_m \cos Q_m - \frac{c(c'\beta_m - c\beta_m')}{\beta_m^3} \frac{1}{r_{\beta m}} \sin Q_m \right) \frac{1}{r_{\beta m}}$$

(for i = m),

This allows to express the derivatives of the interface-matrix elements $\frac{\partial}{\partial \beta_i} U^{(m)}$, $\frac{\partial}{\partial \beta_i} V^{(m)}$, $\frac{\partial}{\partial \beta_i} W^{(m)}$, $\frac{\partial}{\partial \beta_i} R^{(m)}$, and $\frac{\partial}{\partial \beta_i} S^{(m)}$, for all intefaces down to the half-space.

After that the computation of derivatives of layer constants A_{n-1}, B_{n-1}, C_{n-1}, D_{n-1} uses scheme described in Schwab et al. (1984, eqs. 25-42):

computing the right hand quantities for an application of Cramer's rule

$$A_{n-1} = \frac{A_{n-1}\Delta_{n-1}}{\Delta_{n-1}} \qquad r_{\alpha n-1}B_{n-1} = \frac{r_{\alpha n-1}B_{n-1}\Delta_{n-1}}{\Delta_{n-1}},$$

$$r_{\beta n-1}C_{n-1} = \frac{r_{\beta n-1}C_{n-1}\Delta_{n-1}}{\Delta_{n-1}} \qquad D_{n-1} = \frac{D_{n-1}\Delta_{n-1}}{\Delta_{n-1}}$$

and evaluating of the vector of inhomogeneities ψ:

$$\psi_1^{(n)} = A_n + r_{\beta n}, \qquad \psi_2^{(n)} = r_{\alpha n}A_n - 1.$$

Then the scheme continues in a loop over all layers with the only change in the definitions of the two elements of the vector of inhomogeneities: for m < n

$$\psi_1^{(m)} = A_m + r_{\beta m}C_m, \qquad \psi_2^{(m)} = r_{\alpha m}B_m - D_m.$$

It is not necessary to display here all formulas for derivatives of these quantities. The formulas are rather long, but containing only simple algorithmic manipulations.

Conclusions

The most important point in the described procedure is that not only quantities with β_i have non zero derivatives with respect to β_i velocity, but also all quantities where the phase velocity occurs. To the contrast to the computations of partial derivatives of phase and group velocities here we cannot find groups or sequences of the derivatives of layer or interface quantities which could be, as a definition, put to the zero. Then, we cannot use this "feature" or "property" for the shortening of the time of compulation and, instead of it, other possibilities should be tested. The most efficient way consists in saving already computed quantities and thus avoiding repeated computations. In comparison with the procedure where the partial derivatives have been obtained numerically, the method described here is almost 100 times faster. Also it should be pointed out that this method is accurate and none additional evaluations or judgements should be taken into account in contrast to the numerical computations.

Acknowledgements

Authors highly appreciate fruitful discussions with G.F. Panza and P. Suhadolc.

The research has been carried out in the framework of the activities planned by the Central European Initiative Committee for Earth Sciences, partially supported by the NATO Linkage grants ENVIR.LG 931206, and SA. 12-5-02 (CN. SUPPL 940880) 453, the EEC contract COPERNICUS CIPA-CT94-0238 and CNR grant 94.01.703.PF54.

References

Panza G.F., 1985. Synthetic seismograms: the Rayleigh waves modal summation. J. Geophys., 58: 125-145.

Urban L., Cichowicz A., Vaccari F., 1993. Computation of analytical partial derivatives of phase and group velocities for Rayleigh waves with respect to structural parameters. Studia geoph. et geod., 37: 14-36.

Knopoff L., 1964. A matrix method for elastic wave problem. Bull. Seism. Soc. Am., 54: 431-438.

Schwab F.A., Knopoff L., 1972. Fast surface wave and free mode computations. In.: B. A. Bolt (Ed.): Methods in computational physics. Vol. 11, Academic Press, New York.

Schwab F.A., Nakanishi K., Cuscito M., Panza G.F., Liang G., Frez J., 1984. Surface wave computations and the synthesis of theoretical seismograms at high frequencies. Bull. Seism. Soc. Am., 74: 1555-1578.

RAYLEIGH WAVE GROUP AND PHASE VELOCITY MEASUREMENTS IN THE PANNONIAN BASIN

István Bondár[1], Zoltán Bus[1], Mladen Zivcic[2], Giovanni Costa[3], Anatoly Levshin[4]

[1] *Seismological Observatory, Hungarian Academy of Sciences*
Meredek u. 18, H-1112 Budapest, Hungary
fax: (36-1) 185-2672
e-mail: istvan @ sunsas.seismology.hu, @ sas.seismology.hy

[2] *Geophysical Survey of Slovenia*
Pot na Golovec 25., 61000 Ljubljana, Slovenia
fax: (386-61) 140-5370
e-mail: mladen.zivcic@uni-lj.si

[3] *Dipartimento di Scienze della Terra, University of Trieste*
Via Eduardo Weiss 1-4, 34127 Trieste, Italy
fax: (39-40) 575-519
e-mail: costa@geosun0.univ.trieste.it

[4] *Department of Physics, University of Colorado*
Campus Box 583, Boulder CO80309-0583, USA
fax: (1-303) 492-7935
e-mail: levshin@jspc.colorado.edu

Abstract

Up to now, dispersion analysis of surface waves across the Pannonian basin and the adjacent zones has been based on analog data recorded at small number of long-period stations. The growing number of digital stations in the area, equipped with broadband seismometers, makes it possible to investigate the Pannonian Basin structure from high quality records.

To extract the fundamental-mode Rayleigh wave from the seismograms and to determine group velocities, frequency-time analysis is employed. Whenever it was possible, the two-stations method was applied to measure interstation phase velocities.

The group and phase velocities are inverted by two different inversion schemes, the genetic algorithm (GA) and the hedgehog (HG) method. The comparison of the results shows that within the resolving power of the data set both methods give similar solutions.

The experiments with the two inversion methods show that when the parameter search space is relatively small (10^2-10^4 distinct models with 3-5 variable parameters) the hedgehog method requires much less CPU time (both method were run on a Sun workstation) than the GA. However, it requires a good starting model, and in the lack of a priori knowledge on the underlying structure the HG should be executed several time in order to tune the parameters and find reliable solutions. In those cases when the parameter search space is much larger (10^9-10^{12} distinct models with 8-12 variable parameters) the Monte Carlo search becomes ineffective whilst the GA, because of its imbedded parallelism performs much better than the HG.

Some events from the adjacent regions are included in the inversion in order to investigate

the Pannonian Basin contact to the Eastern Alps, Dinarides and Balkan.

The results of inversion of the Rayleigh fundamental mode dispersion curves in the Pannonian Basin show a relatively thin crust with 28-33 km Moho depth. The S wave velocities in the lower crust are in the range of 3.6 and 3.9 km/s, whilst the S wave velocity in the lid is 4.2-4.3 km/s.

The average structure as revealed by the inversion of Rayleigh wave fundamental mode dispersion curves in the Dinarides Mountain chain shows thick (more than 15 km) upper crust with S wave velocities of up to 3.5 km/s. Lower crust velocity and thickness of the crust is less constrained but seem to be in the range of 3.6 to 3.8 km/s and 40 to 45 km. The results agree well with depths estimated from deep seismic sounding.

At the Eastern Alps-Pannonian Basin contact the structure seems rather complicated. The inversion results indicate a thicker crust with 47 km Moho depth where the S wave velocity increases from 3.4-3.6 km/s to 4.2-4.3 km/s.

Introduction

The present structural layout of the Pannonian basin can be considered as a result of complex kinematic and dynamic processes that took place since the Neogene, triggered by the continent-continent collision of the European and African plates (Horváth, 1988; Royden and Báldi, 1988, Royden, 1988, Sandulescu, 1988; Horváth, 1993). Consequently, the Pannonian basin can be described as an extensional back-arc basin developed by lithospheric stretching behind the collisional fold-thrust belts of the Carpathians and the Dinarides (Csató, 1993).

The crust is rather thick in the mountain ranges around the Pannonian basin, while the basin itself is characterized by thin crust, ranging from 22.5 km to 30 km, where the 30 km depth isoline encircles the whole basin (Horváth, 1993).

The earthquakes occurring in the Pannonian basin are mostly shallow crustal events with focal depths not greater than 20 km and their observed magnitudes rarely exceed ML=5.

This is very likely connected with the presence of a thinned lithosphere overlying hot mante material. Teleseismic P-wave travel time residual analysis (Babuska et al., 1987, 1990), magnetotelluric soundings (Praus et al, 1990) and electrical resistivity profiles (Ádám et al, 1982, 1989, 1990) suggest that the lithosphere under the Pannonian basin is thinner than 80 km.

One of the most powerful tool for determining the elastic properties of the lithosphere-asthenosphere system is represented by the measurements of the dispersion of surface waves. From the study of surface-wave dispersion it is possible to determine the distribution of S-wave velocity as a function of depth. From the combination of surface-wave analysis and deep seismic soundings regional maps have been constructed in the past 15 years showing the gross features of the lithosphere thickness and S-wave velocities under the Mediterranean and Western Europe (Panza et al, 1980; Suhadolc and Panza, 1989; Calcagnile and Panza, 1990; Panza and Suhadolc, 1990; Yanovskaya et al, 1990).

Up to now, dispersion analysis of surface waves across the Pannonian basin and the adjacent regions has been based on analogue data

Table I: Station location

Code	Latitude N	Longitude E	Name
GRA1	49.6919	11.2217	Grafenberg, Germany
GRB1	49.3913	11.6520	Grafenberg, Germany
GRB2	45.2712	11.6691	Grafenberg, Germany
GRC1	48.9962	11.5214	Grafenberg, Germany
LJU	46.0438	14.5272	Ljubljana, Slovenia
PSZ	47.9184	19.8945	Piszkéstetö, Hungary
TTE	45.646	13.779	Trieste, Italy

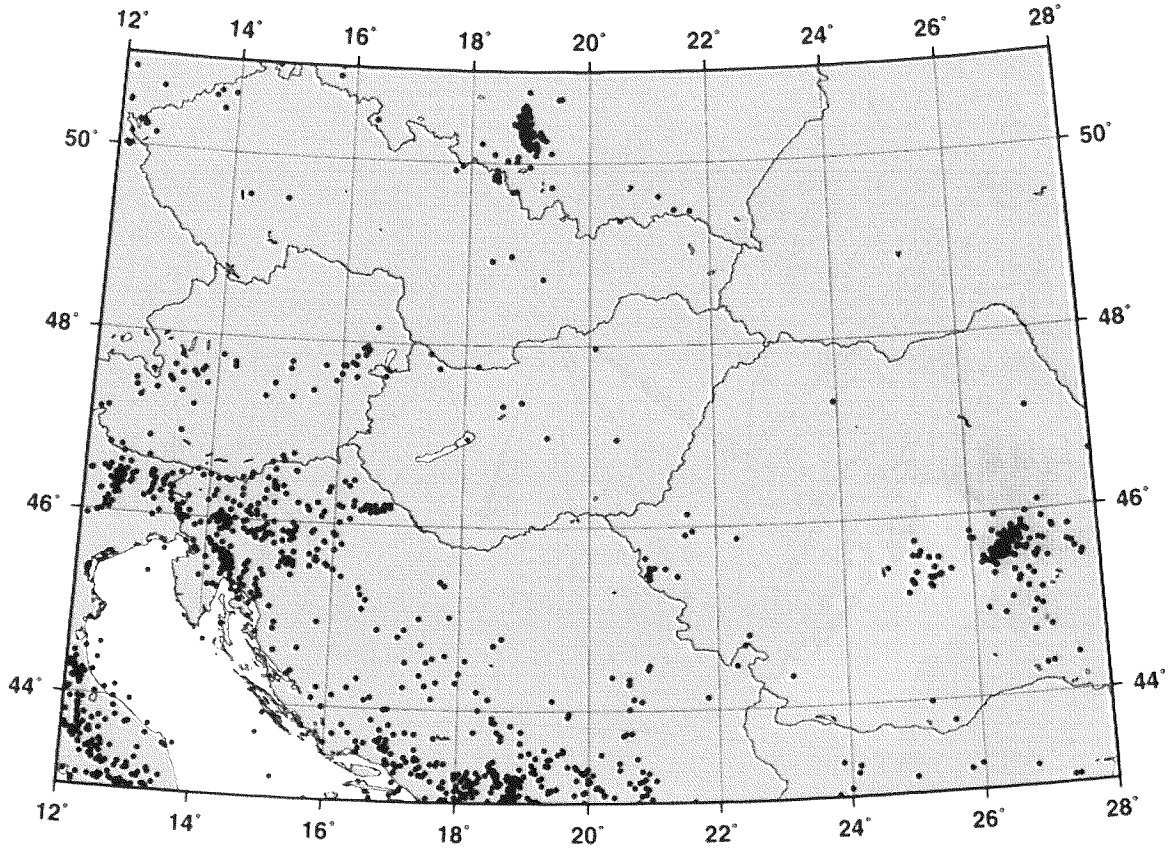

Fig. 1: Seismicity in the Pannonian basin and the adjacent regions, 1992-1995. The epicenters of the events are taken from the PDE monthly listings.

recorded at small number of long-period stations (Bisztricsány and Kiss, 1960; Gobarenko et al, 1987). The increasing number of digital stations allows to investigate the Pannonian basin structure from high-quality records.

Instruments and data

For the collection of local events in the Pannonian basin the data recorded at the stations PSZ, LJU, TTE, GRA1, GRB1, GRB2 and GRC1 have been used. Table I shows the codes and locations of these stations.

Two types of events were selected for analysis. The first includes earthquakes that occurred in the Pannonian basin and the adjacent regions, so that the wave paths to stations cross mainly the Pannonian basin and the surface waves were well recorded at least one of the stations. For these events the single-station method can be applied which provide us with epicenter-to-station group velocities.

Fig. 1 shows the seismicity of the area between 1992 and 1995. The epicenter coordinates and magnitudes were taken from the NEIC PDE lists. The station-event great circle paths of the selected events are shown in Fig. 2.

It can be seen that the paths concentrate around several azimuthal beams, thus, processing the events that lie around the same station-event azimuth and have similar epicentral distance allowed to determine not only the average Rayleigh group velocity dispersion curves but the error in the group velocity measurements, too.

The second type of events includes those teleseismic events that occurred near the great

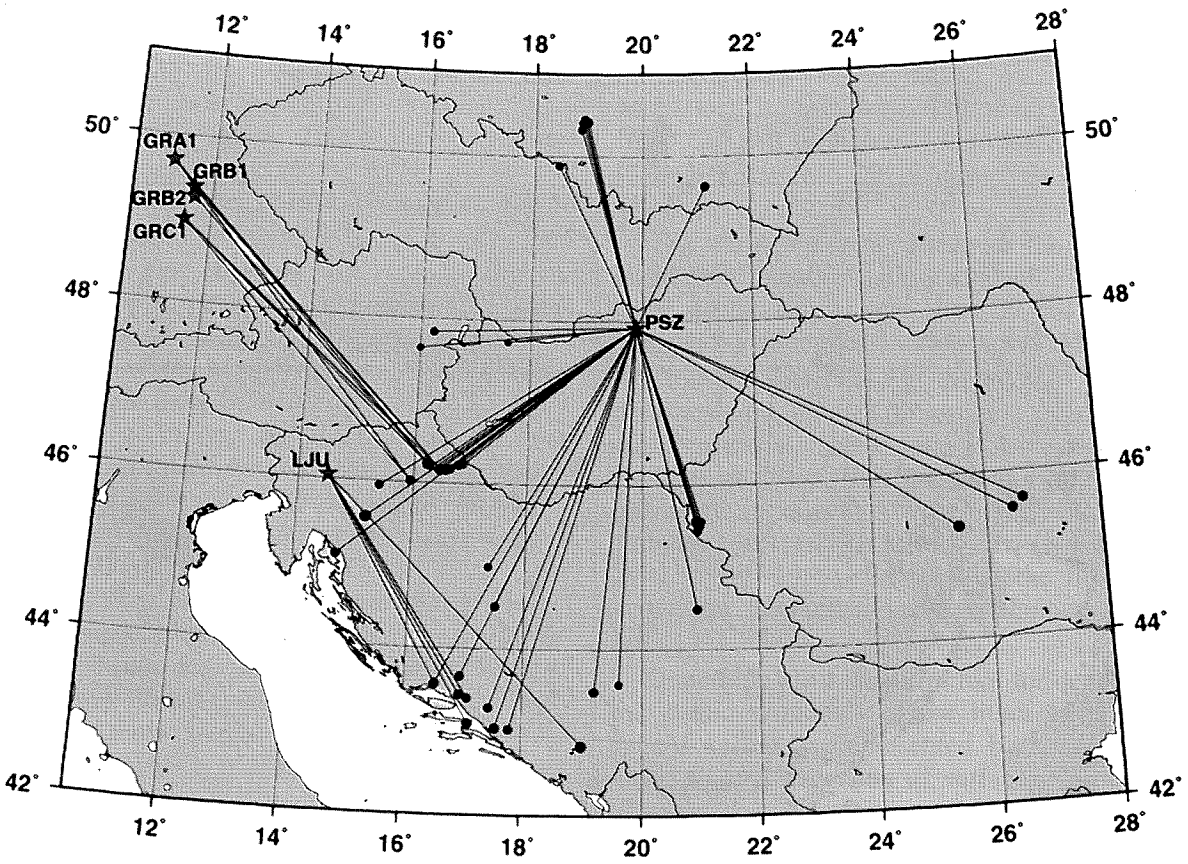

Fig. 2. Station-to-epicenter paths of the events selected for analysis.

Table II. Groups of events according to station to epicenter azimuth

#	Station	Azimuthal range	Mean epicentral distance	# of events
1	PSZ	25	212	1
2	PSZ	110-120	550	3
3	PSZ	160-170	300	7
4	PSZ	180-190	490	2
5	PSZ	195-215	510	7
6	PSZ	230-240	320	7
7	PSZ	230-240	450	3
8	PSZ	260-270	250	3
9	PSZ	340-350	280	6
10	LJU	130-150	380	5
11	GRF	130-140	500	3

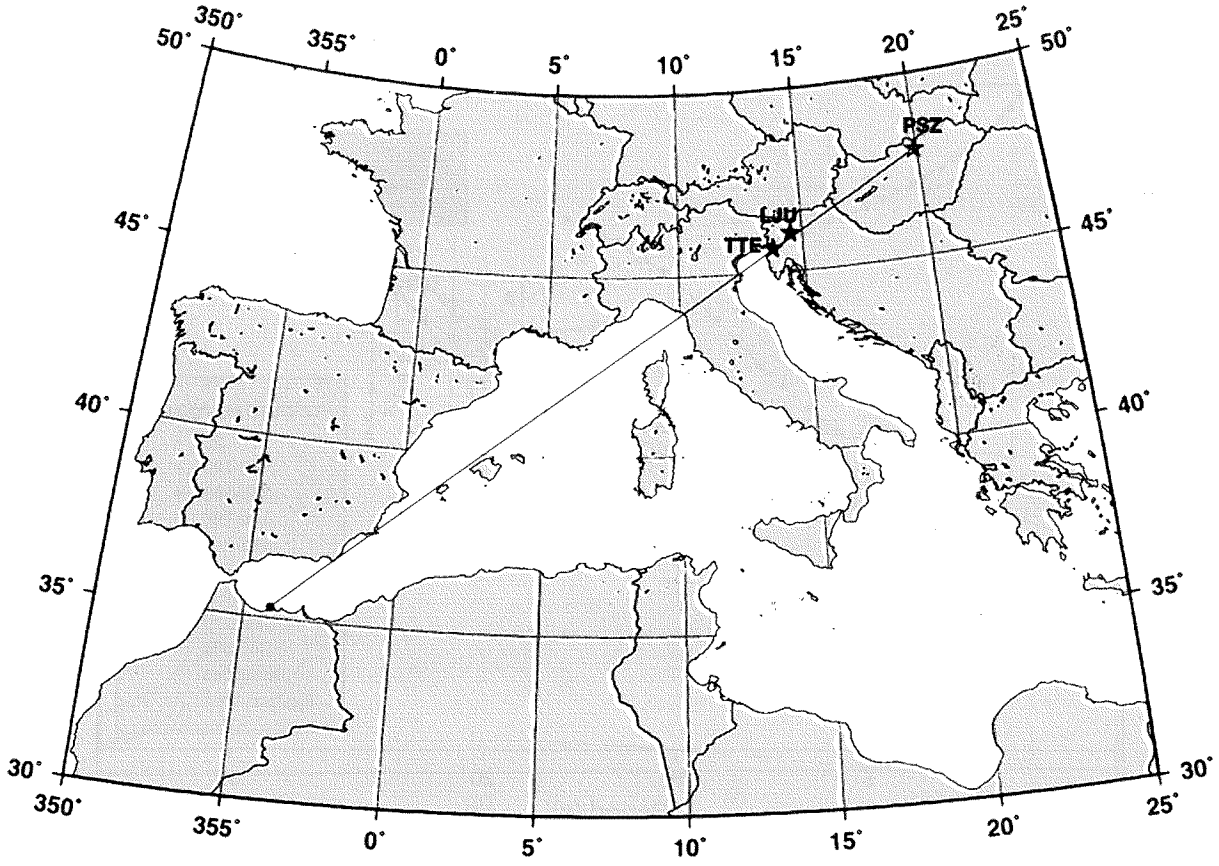

Fig. 3. Station-to-epicenter paths of the events selected for interstation measurements.

circle passing through any pair of the stations, and were strong enough that the surface waves were well recorded by both stations. The criterium of acceptance of an event was that the azimuths from the epicenter to each of the two stations should differ less than 5°. Events selected in this way would provide data for interstation measurements of phase velocities. Unfortunately, we have found only one event that were well recorded at both stations. However, this event lies on the great circle defined by PSZ, LJU and TTE, and all of the three stations recorded the event. Fig. 3 shows the great circle path to this event.

The data were processed by interactive frequency-time analysis (Levshin et al, 1972; Levshin et al, 1989; Levshin et al, 1992) using a set of narrow band Gaussian filters. With the FTAN processing of the records the Rayleigh group velocity dispersion curves were determined for each event path. The interstation phase velocity dispersion curves were also measured by the FTAN representation of the signals.

Results of dispersion measurements

As Fig. 2 shows the epicenter to station paths are concentrated along specific azimuths, which allowed us to render the events into several groups, in which the station-epicenter azimuths and epicentral distances are similar. In this way nine groups were defined for PSZ, one for LJU (Dinarides paths) and one for the Grafenberg (Eastern Alps paths) stations. The groups are listed in Table II.

In the course of processing the event with the best S/N ratio was selected from each group and processed by the FTAN. Then, using the measured group velocity curves of the selected [characteristic] events as a guideline, the rest of the events were processed. Thus, after FTAN processing the events belonging to the same

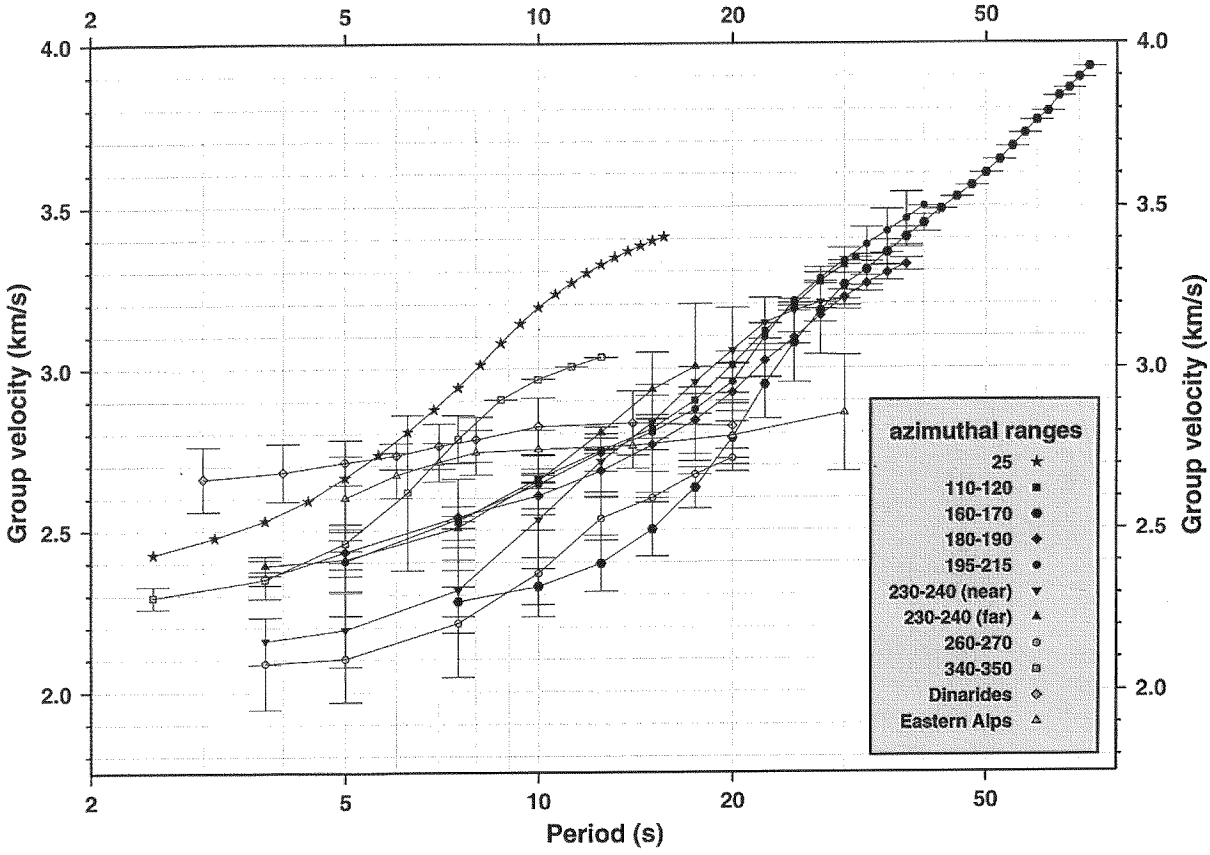

Fig. 4. Average Rayleigh fundamental mode group velocity curves for the groups of events recorded at PSZ, LJU and Grafenberg.

groups the average fundamental mode Rayleigh wave group velocity dispersion curves could be determined, together with the error in group velocity neasurements at each individual period.

Fig. 4 shows the average group velocity curves of the extracted Rayleight fundamental modes. The error bars depict the extermal group velocity values at the observed periods in the event groups, which is a more pessimistic estimation of the measurement error than the standard deviation. According to this, the typical scatter in group velocity readings moves between 0.05 and 0.12 km/s.

The average Rayleigh fundamental mode group velocity curves belonging to group 1 and 9 (azimuthal ranges 25 and 340-350, PSZ records) show much larger group velocities than the rest of the PSZ records. This can be attributed to the station to event paths which cross the Nothern Carpathians. The events in the Northern Carpathians are connected to mining activity and usually rather weak. The longest observed periods for these azimuthal beams were between 12 and 18 seconds which provides reasonable resolution only for the upper 10-15 km in the crust. Therefore we did not attempted to invert the dispersion curves belonging to these two groups.

The lowest group velocities were measured at the groups, 3, 6 and 8 (azimuthal ranges 160-170, 230-240 and 260-270 from PSZ) which consist of events with purely Pannonian paths. However, at larger periods they close to the dispersion curves observed at PSZ that belong to group 2 (azimuthal range 110-120, Vrancea) and groups 4, 5 and 7 (azimuthal ranges 180-190, 195-215 and 230-240, with sources in the Dinarides. The events in these groups have mixed station to event paths, i.e. Pannonian-Eastern Carpathians (Vrancea) or Pannonian-Dinarides.

The dispersion curves belonging to events

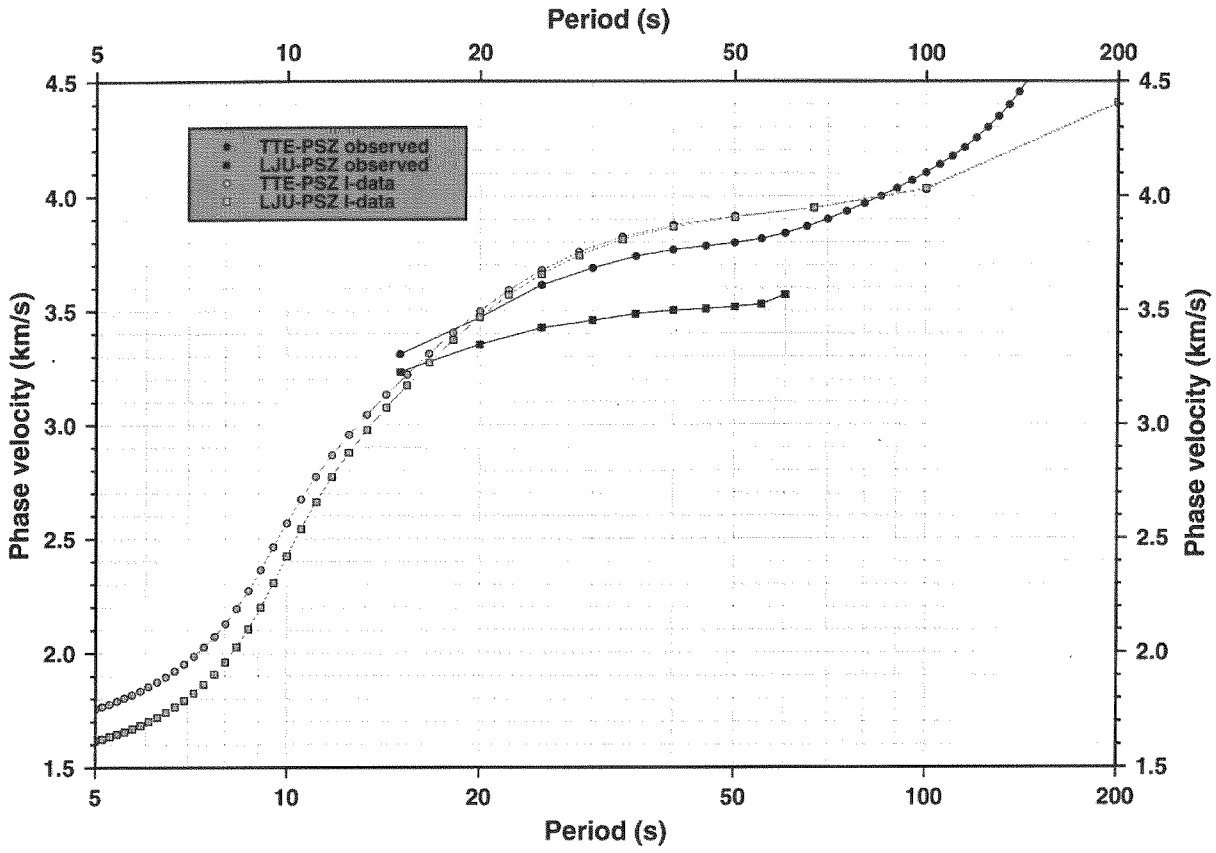

Fig. 5. Observed Rayleigh fundamental mode differential phase velocity curves between TTE-PSZ and LJU-PSZ compared to the predicted ones from the I-data set.

with purely Dinarides (LJU records) or Eastern Alps paths (Grafenberg records) show distinct features. At lower periods they are represented by large group velocities, but do not show much dispersion in the observed period range.

The differences in the group velocity curves belonging to the distinct groups of events indicate structural differences in the upper crust which could be resolved by the inversion of the observed dispersion curves.

For the interstation phase velocity measurements only one event has been found but it was recorded by three stations, PSZ, LJU and TTE. Fig. 5 shows the measured differential phase velocity curves and those of predicted by the I-data set - a 3D data set for the anelastic properties of the lithosphere - astenosphere system in Europe (Du and Michelini, 1995). The observed dispersion curves are in good agreement with the predicted ones. Only the LJU-PSZ differential phase velocities show larger deviations which can be attributed to measurement errors in phase velocity, therefore we excluded from the inversion procedure the ifferential phase velocities observed between LJU and PSZ.

Inversion

For the inversion of the measured dispersion curves of the Rayleigh fundamental modes two different inversion methods were applied, the hedgehog (Valyus, 1972; Keilis-Borok and Yanovskaya, 1967) and the genetic algorithm (Holland, 1975; Goldberg, 1989; Davis, 1990; Bondár, 1994; Lomax and Snieder, 1995) method. Both inversion schemes are able to

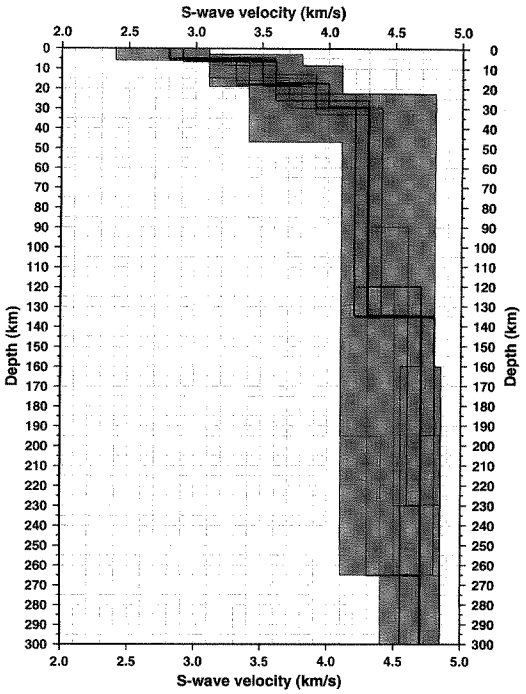

Fig. 6. 12-parameter GA inversion of Rayleigh differential phase velocities and fundamental mode group velocities along the TTE-PSZ path. The gray-shaded area indicates the parameter search space, the accepted models are drawn by solid lines.

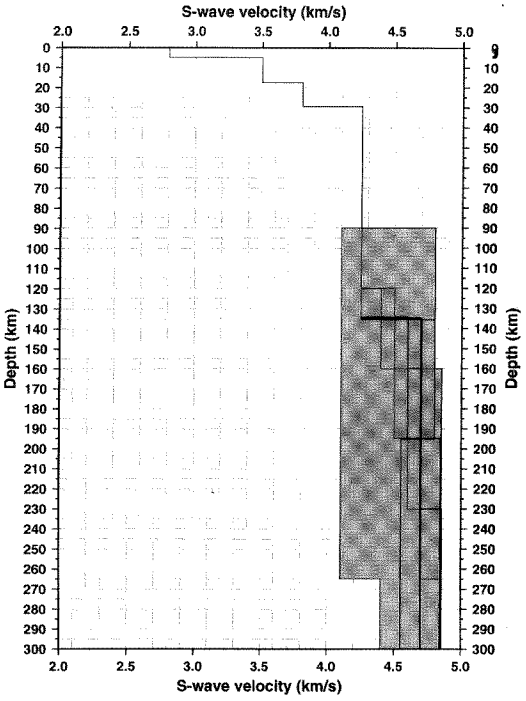

Fig. 7. 4-parameter GA inversion of Rayleigh differential phase velocities and fundamental mode group velocities along the TTE-PSZ path. The gray-shaded area indicates the parameter search space, the accepted models are drawn by solid lines.

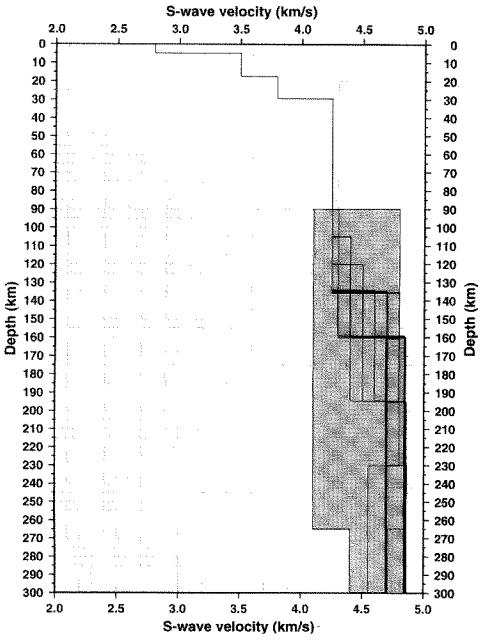

Fig. 8. 4-parameter HG inversion of Rayleigh differential phase velocities and fundamental mode group velocities along the TTE-PSZ path. The gray-shaded area indicates the parameter search search space, the accepted models are drawn by solid lines.

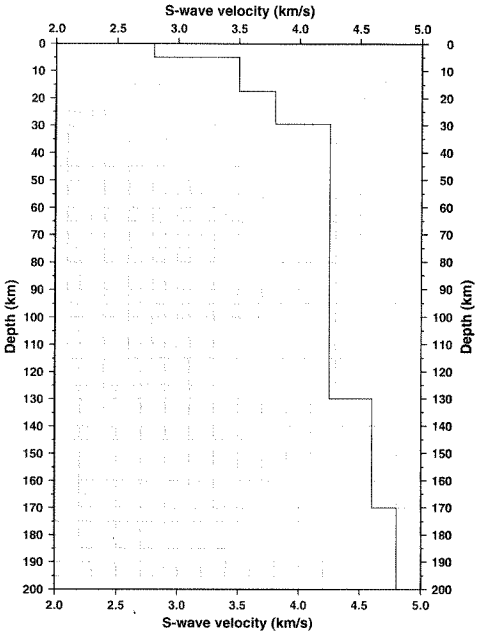

Fig. 9. Model for the Pannonian-Eastern Alps path, derived from the inversion of interstation phase velocity measurements between TTE and PSZ.

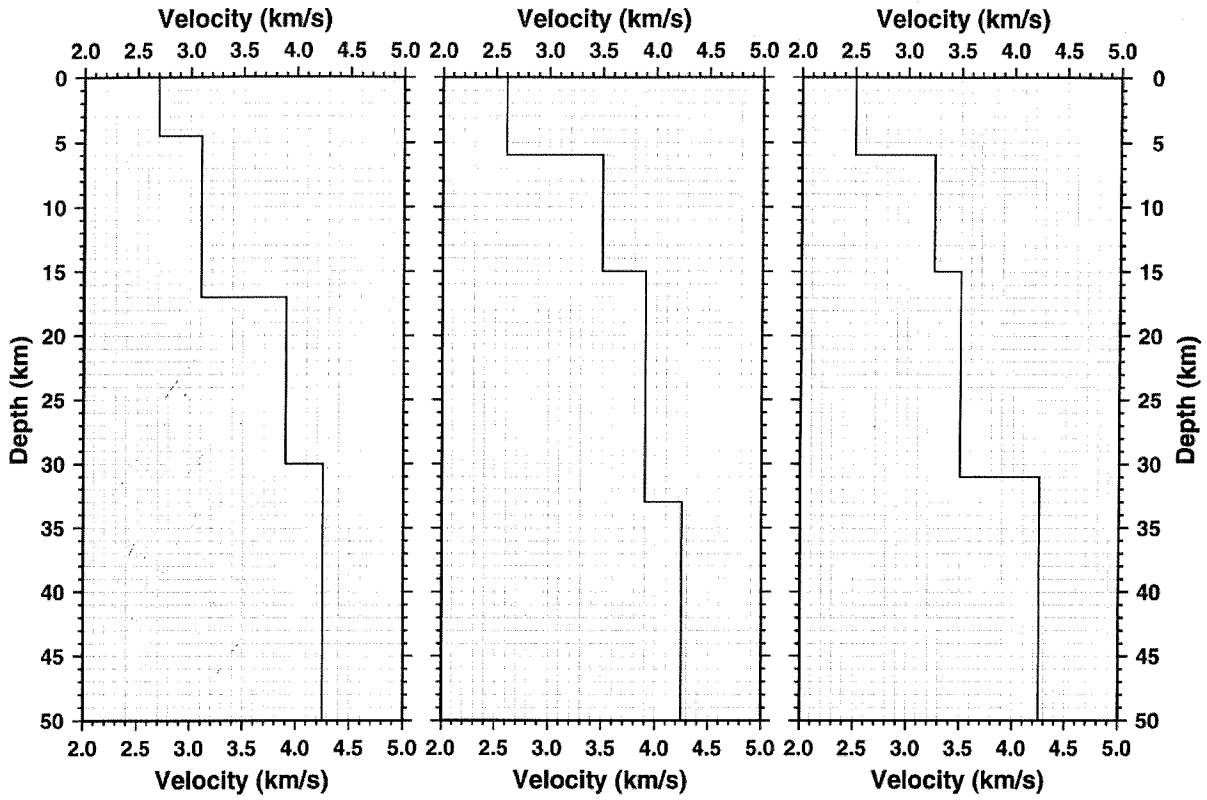

Fig. 10. Models for the pure Pannonian station to event paths.

explore large parameter space and get close to the optimum.

In the course of inversion the forward problem, i.e. to compute the Rayleigh phase and group velocities for a given structural model, has to be solved several times. For the forward problem computation the code developed by F. Schwab and G. F. Panza at the University of Trieste (Schwab and Knopoff, 1972, Schwab et al, 1984) was used.

The difference between the two inversion methods is the different philosophical approaches. The GA adopts itself to the inverse problem via the natural selection principle, requiring minimal assumptions and physical approximations, whilst the hedgehog method tries to find all the single-connected acceptable solutions within the measurement errors. Taking into consideration also the single-point errors of the observed data is an advantage of the HG method over the GA.

Both the hedgehog and the GA method are able to provide a number of acceptable solutions. Since the generation of new trial models requires practically negligible CPU time, the speed of the two methods depends on how many times the forward problem should be solved.

The performance of the inversion methods is illustrated on the inversion procedure for the interstation differential phase velocity measurements. In the inversion the single-station group velocity measurement along a Pannonian-Dinarides path that was close enough to the great circle path between TTE and PSZ was also involved. Thus, in the simultaneous inversion the group velocity dispersion curve constrained the upper crustal structure and the differential phase velocities provided information on the lower crust and the subcrustal region.

First we applied a 12-parameter GA inversion for a structure that consisted of three layers in the crust, a lid, channel and subchannel. In the model the layer boundaries, the S-wave velocities and the P-wave velocity of the sedimentary

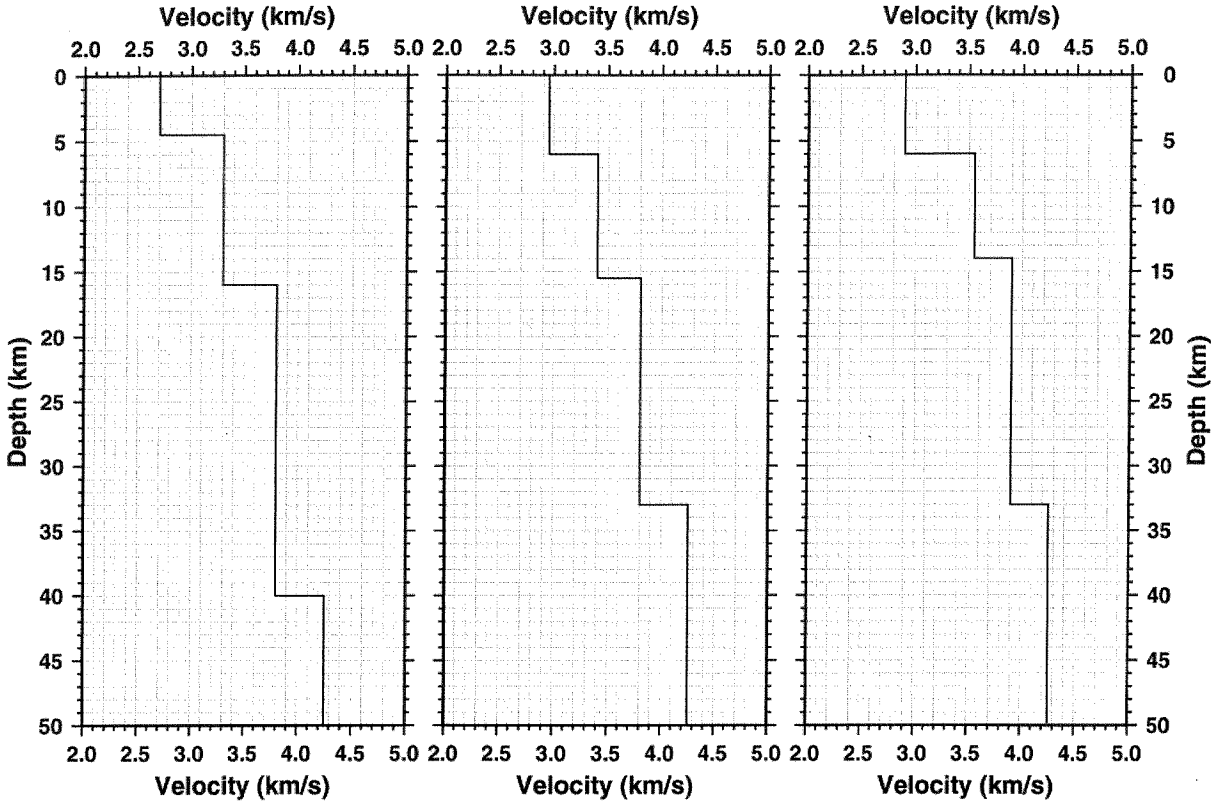

Fig. 11. Models for the Pannonian-Dinarides station to event paths.

layer were allowed to change. For the rest of the model the P-ware velocities were taken from the results of deep seismic soundings, refraction and wide-angle measurements (Meissner and Stegena, 1988; Posgay et al, 1981, 1990). Below 400 km depth the *iasp91* model (Kennett and Engdahl, 1991) was accepted. The resolution step fot the velocities were set to 0.1 km/s (except the subchannel where it was 0.15 km/s). As the resolving power of the data decreases with depth, different resolution steps were defined for the layer boundaries: 1 km for the bottom of the sedimentary layer, 1.5 km for the bottom of the upper crust, 3.5 km for the Moho discontinuity, 15 km for the bottom of the lid and 35 km for the bottom of the channel.

Fig. 6 shows the accepted models by the GA inversion. The gray-shaded area indicates the parameter search space that consited of $4.3 \cdot 10^9$ distinct models. The crustal structure and the lid are well resolved while the resolution below the lid is a bit poorer.

In order to achieve a better resolution for the structure below the lid we performed a 4-parameter inversion, where only the bottom of the lid, the S-wave velocity in the channel and in the subchannel as well as the channel-subchannel boundary were taken as variable parameters. The resolution steps were the same as in the previous experiment, defining a parameter search space of 512 models.

Fig. 7 shows the results of the 4-parameter GA inversion; Fig. 8 that of the HG inversion. The comparison of the figures shows that the two inversion methods gave practically the same results.

Discussion and conclusions

Since the earthquakes in the Pannonian basin are rather weak and the epicentral distances are relatively short, the longest observed periods

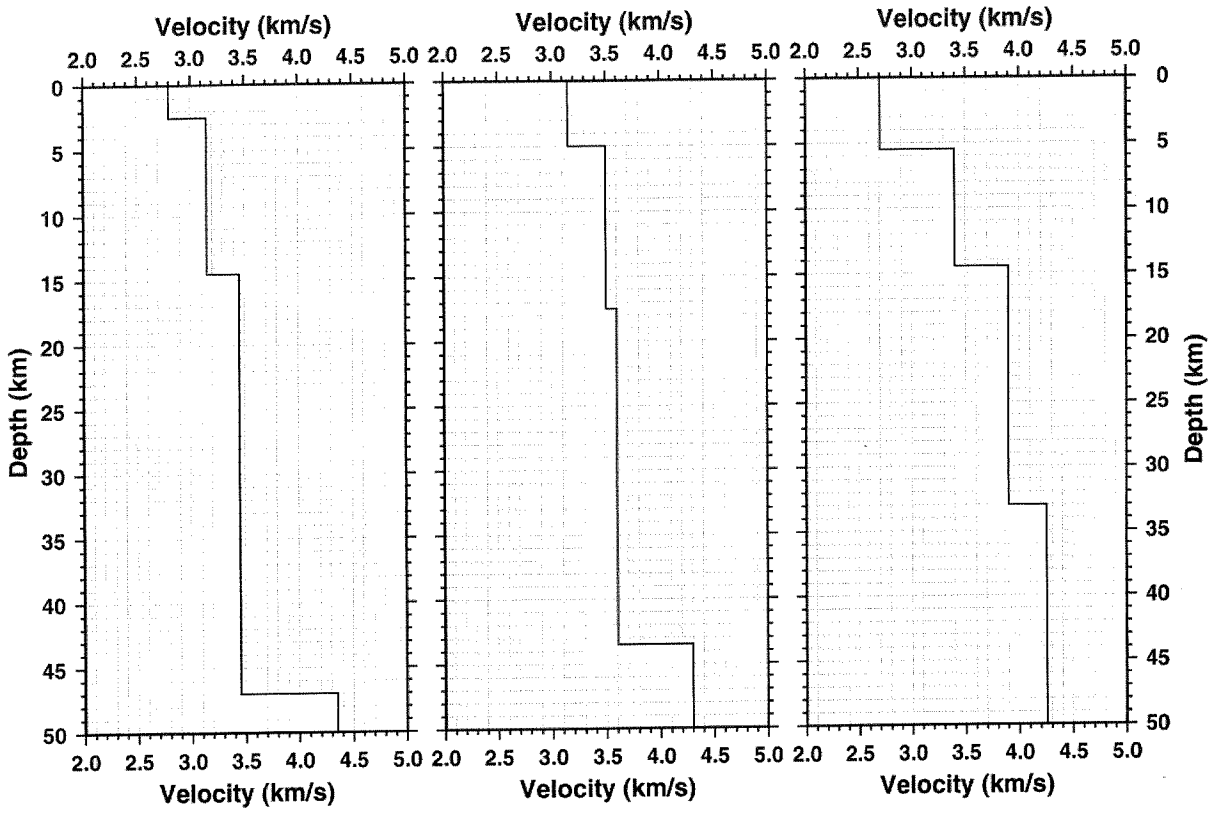

Fig. 12. Models for the Eastern Alps, Dinarides and Pannonian-Vrancea station to event paths.

rarely exceed 30 seconds. Therefore the resolving power of the single-station group velocity measurements is limited to the crust. The geometry of the epicenter to station paths was such that the events are clustered along specific azimuthal ranges and epicentral distances, which allowed the determination of the average Rayleigh fundamental mode group velocity dispersion curve for each groups, as well as the rms and single-point measurement errors.

The interstation measurement for the Strait of Gibraltar event between the stations TTE and PSZ provided reliable differential phase velocity observations up to 100 seconds, which was used to explore the lithospere-astenosphere system along the TTE-PSZ great circle path.

For the inversion of the observed dispersion curves two different inversion scheme were applied, the hedgehog and the genetic algorithm methods. Both methods have advantages and disadvantages when compared to the other. The GA optimizes only in rms sense, whilst the HG takes into account the single-point errors, too. The GA starts from a random initial set of models, thus it needs minimal *a priori* knowledge on the underlying structure, while the HG requires a good initial model to start with. The performance of the HG is superior to the GA when the parameter search space grows larger, whilst the GA can easily handle parameter search spaces containing 10^8-10^{12} distinct models.

Since the results provided by the two methods are rather similar, the decision on which inversion scheme is to be used should depend on the number of variable parameters, i.e. the size of the parameter search space. At few-parameter inversion scenarios the HG is recommended, while the GA should be applied when the number of parameters is larger than 5.

The inversion of dispersion curves provides an average model along the epicenter to station path, showing the gross features of the underlying structure. Fig. 9 shows the model for the

Pannonian-Eastern Alps path derived from the inversion of interstation measurements between TTE and PSZ. The result of inversion indicates some 5 km thick sedimentary layer with 2.8 km/s S-wave velocity; a relatively thin crust (30 km) with 2.8 km/s lower crustal velocity and with relatively slow, 4.2-4.3 km/s lid velocity. It is remakable that the inversion does not prove the existence of a low velocity layer, but an increase in velocity to 4.6 km/s instead. The thickness of the lithosphere is given by the inversion as 130 km.

For the single-station measurements the group velocity curves belonging to the different azimuthal groups were inverted separately. In the inversion of the dispersion curves we sought for a crustal structure consisting of three layers, namely a sedimentary layer, the upper and lower crust. For the subcrustal structure we accepted the results provided by the inversion of the interstation measurement and below 400 km the *iasp 91* model was applied. The observational data provided good constraints on the upper crust while the resolution of the Moho depth and lower crustal velocities were poorer.

Fig. 10 shows the resulting models from the inversion for the purely Pannonian station to event paths. The results indicate a rather thick, 4.5-6 km sedimentary layer with 2.5-2.7 km/s S-wave velocity, thêthickness of the upper crust is between 15 and 17 km with 3.1-3.5 km/s velocities. The resolution of the lower crust is poorer, it indicates 3.5 km/s velocity for the path crossing the Little Hungarian Plain, and 3.8-3.9 km/s velocities for the Southern and Southwestern Pannonian paths. The depth of the Moho discontinuity moves between 28 and 33 km.

Figs. 11-12 show the results of inversion for the Pannonian-Dinarides, Pannonian-Vrancea and purely Eastern Alps and Dinarides paths. For the mixed paths the upper crustal structure is similar to that of the purely Pannonian paths (4-6 km thick sediments with 2.7-2.9 km/s velocity, rather thick, 14-17 km upper crust, with 3.3-3.6 km/s velocities). The lower crustal structure indicates a deeper Moho between 33 and 40 km, with 3.8-3.9 km/s lower crustal velocity.

The results for the Eastern Alps paths show a much thinner, 2-3 km thick sedimentary layer with 2.8 km/s S-wave velocity. Also the upper crust is thinner, 14-15 km, with velocities between 3.1-3.2. On the other hand the crust is thicker, with 47 km Moho depth and 3.4-3.6 km/s lower crustal velocity.

The inversion of the purely Dinarides shows a 5 km thick sedimentary layer with 3.1-3.2 km/s velocity, a thick upper crust (some 17 km). Although the resolution is poorer in the lower crust, the results indicate a weak velocity contrast between the upper and lower crust, and a deeper Moho between 40-45 km.

Acknowledgements

The authors are grateful to Prof. Giuliano F. Panza for his encouragement and the inspirative discussions. This work has been done in the frame of CEC CIPA CT 94-0238 (Copernicus), OTKA T 014976 and the NATO ENVIR.LG 931206 project.

Referneces

Ádám, A., Vanyan, L.L., Varlamov, D.A., Yegorov, I.V. Shilovsky, A.P. and Shilovsky, P.P., 1982: Depth of crustal conductivity layer and astenosphere in the Pannonian basin determined by magnetotellurics, *Phys. Earth Planet. Inter.*, **28,** 251-260.

Ádám, A., Landy, K., and Nagy, Z., 1989: New evidence for the electric conductivity in the Earth's crust and upper mantle in the Pannonian basin as a "hotspot", *Tectonophysics,* **164,** 361-368.

Ádám, A., Nagy, Z., Nemesi, L. and Varga, G., 1990: Electrical conductivity anomalies along the Pannonian Geotraverse and their geothermal relation, *Acta Geod. Geophys. Mont. Hung.,* **25,** 291-307.

Babuska, V., Plomerovà, J. and Sileny, J., 1987: Structural model of the subcrustal lithosphere in Central Europe, In: *Composition, Structure and Evolution of the Lithosphere - Atenosphere System,* K. Fuchs and C. Froidevaux (editors), AGU Geodyn. Ser., 16, 239-251.

Babuska, V., Plomerovà, J. and Granet, M., 1990: The deep lithosphere in the Alps: a model inferred from Presiduals, *Tectonophysics,* **176,** 137-165.

Bisztricsány, E. and Kiss, Z., 1960: A computation of average crustal thickness from Love

wave dispersion, for an Eurasian wave path, *Annales Univ. Sci. Bud. R. Eötvös - Sectio Geologica,* **III,** 15-17.

Bondár, I., 1994: Hypocenter determination of local earthquakes using genetic algorithm, *Acta Geod. Geoph. Hung.,* **29,** (1-2), 39-56.

Calcagnile, G. and Panza, G.F., 1990: Crustal and upper mante structure of the Mediterranean area derived from surface-wave data, *Phys. Earth Planet. Inter.,* **60,** 163-168.

Csató, I., 1993: Neogene sequences in the Pannonian basin, Hungary, *Tectonophysics,* **226,** 377-400.

Davis, L. (ed.) 1990: *Genetic Algorithms and Simulated Annealing,* Research Notes in Artificial Intelligence, Pitman, London.

Du, Z.J. and Michelini, A., 1995: Database of 3-D structure beneath Europe and the Mediterranean Sea, *IUGG XXI General Assembly,* Boulder, Colorado, Abstracts, B394.

Gobarenko, V.S., Nikolova, S.B. and Yanovskaya, T.B., 1987: 2-D and 3-D velocity patterns in southeastern Europe, Asia Minor and the eastern Mediterranean from seismological data, *Geophys. J.R. Astr. Soc.,* **90,** 472-484.

Goldberg, D.E., 1989: *Genetic Algorithms in Search, Optimization and Machine Learning,* Addison-Wesley, Reading, MA.

Holland, J.H., 1975: *Adaptation in Natural and Artificial Systems, University of Michigan Press, Ann Arbor.*

Horváth, F., 1988: Neotectonic behavior of the Alpine-Mediterranean region, In: *The Pannonian Basin, a Study in Basin Evolution,* L.H. Royden and F. Horváth (editors), *Am. Assoc. Pet. Geol. Mem.,* **45,** 49-55.

Horváth, F., 1993: Towards a mechanical model for the formation of the Pannonian basin, *Tectonophysics,* **226,** 333-357.

Keilis-Borok, V.I. and Yanovskaya, T.B., 1967: Inverse problems of seismology, *Geophys. J. R. Astr. Soc.,* **13**, 223.

Kennett, B.L.N. and Engdahl, E.R., 1991: Travel times for global earthquake location and phase identification, *Geophys. J. Int.,* **105,** 429-466.

Levshin, A., Pisarenko, V. and Pogrebinsky, G., 1972: On a frequency time analysis of oscillations, *Ann. Geophys.,* **28,** 211-218.

Levshin, A.L., Yanovskaya, T.B., Lander, A.V., Bukchin, B.G., Barmin, M.P., Ratnikova, L.I. and Its, E.N., 1989: *Seismic Surface Waves in a Laterally Inhomogeneous Earth, V.I. Keilis-Borok (editor), Kluwer, Dordrecht.*

Levshin, A.L., Ratnikova, L.I. and Berger, J., 1992: Peculiarities of surface wave propagation across the Central Eurasia, *Bull. Seism. Soc. Am.,* **82,** 2464-2493.

Lomax, A. and Snieder, R., 1995: The contrast in upper mantle sheat-wave velocity between the East European Platform and Tectonic Europe obtained with genetic algorithm inversion of Rayleigh wave group dispersion, *Geophys. J. Int.* **123,** 169-182.

Meissner, R. and Stegena, L., 1988: Lithosphere and evolution of the Pannonian basin, In: *The Pannonian Basin, a Study in Basin Evolution,* L.H. Royden and F. Horváth (editors), *Am. Assoc. Pet. Geol. Mem.,* **45,** 147-152.

Panza, G.F., Mueller, St. and Calcagnile, G., 1980: The gross features of the lithosphere-astenosphere system in Europe from seismic surface waves and body waves, *Pure Appl. Geophys.,* **118,** 1209-1213.

Panza, G.F. and Suhadolc, P., 1990: The Mediterranean area: A challenge for plate tectonics, In: *Critical Aspects of the Plate Tectonics Theory,* Vol. I, 339-363.

Posgay, K., Albu, I., Petrovics, I. and Ráner, G., 1981: Character of the earth's crust and upper mantle on the basis of seismic reflection measurements in Hungary, *Earth Evol. Sci.,* **3-4,** 272-279.

Posgay, K., Hegedü, E. and Timár, Z., 1990: The identification of mantle reflections below Hungary from deep seismic profiling, *Tectonophysics,* **173,** 379-385.

Posgay, K., Albu, I., Hegedüs, E. and Timár, Z., 1990: Deep seismic investigations along the Pannonian Geotraverse, *Acta Geod. Geophys. Mont. Hung.,* **25,** 267-277.

Praus, O., Pecovà, J., Petr, V., Babuska, V. and Plomerovà, J., 1990: Magnetotelluric and seismological determination of lithosphere-astenosphere transition in Central Europe, *Phys. Earth Planet. Inter.,* **60,** 218-228.

Royden, L.H. and Báldi, T., 1988: Early Cenozoic tectonics and paleogeography of the Pannonian and surrounding regions. In: *The Pannonian Basin, a Study in Basin Evolution,* L.H. Royden and F. Horváth (editors), *Am. Assoc. Pet. Geol. Mem.,* **45,** 1-16.

Royden, L.H., 1988: Late Cenozoic tectonics of the Pannonian basin system, In: *The Pannonian Basin, a Study in Basin Evlution,*

L.H. Royden and F. Horváth (editors), *Am. Assoc. Pet. Geol. Mem.,* **45,** 27-48.

Sandulescu, M., 1988: Cenozoic tectonic history of the Carpathians, In: *The Pannonian Basin, a Study in Basin Evolution,* L.H. Royden and F. Horváth (editors), *Am. Assoc. Pet. Geol. Mem.,* **45,** 17-25.

Schwab, F., Nakanishi, K., Cuscito, M., Panza, G.F., Liang, G., and Frez, J. 1984: Surface-Wave Computations and the Synthesis of Theoretical Seismograms at high Frequency, *Bull. Seism. Soc. Am.,* **74,** 1555-1578.

Suhadolc, P. and Panza, G.F., 1989: Physical properties of the lithosphere-astenosphere system in Europe from geophysical data, In: *The Lithosphere in Italy, Advances in Earth Science Research,* A Boriani, M. Bonafede, G.B. Piccardo and G.B. Vai (editors), Acad. naz. Lincei, 15-44.

Valyus, V.P., 1972: Determining seismic profiles from a set of observations, In: *Computational Seismology,* V.I. Keilis-Borok, (editor), Consult. Bureau, New York.

Yanovskaya, T.B., Panza, G.F., Ditmar, P.G., Suhadolc, P. and Mueller, St., 1990: Structural heterogeneity and anisotropy based on 2D phase velocity patterns of Rayleigh waves in Western Europe, *Atti Acad. Naz. Lincei,* **1**, 127-135.

SITE EFFECTS ESTIMATION BASED ON SOURCE AND PATH MODELING OF MACROSEISMIC INTENSITIES IN THE AREA OF GREECE

By A.S. Savvaidis, C.B. Papazachos and P.M. Hatzidimitriou

Geophysical Laboratory, University of Thessaloniki, GR-45006, Greece.

Abstract

The macroseismic intensity of an earthquake in a specific site depends on three main factors: the properties of the source, the wave path from the source to the site, and the properties of the site. On the basis of a previous work, a modelling of the source and of the wave path was performed for 113 earthquake in Greece, using 20475 macroseismic intensities observed at 3967 sites. Based on this modeling, the theoretical intensities at these sites were computed and the difference between the theoretical and the observed intensity was considered to be a "site effect". Spatial clustering of positive residuals (amplification effect) are observed in some regions with dimensions of order of several tenths of kilometers as well as of negative residuals (diminish of intensities) in some other regions of similar dimensions. In many cases, however, sites with positive and negative residuals are very close, which indicates that site effects are phenomena of very local scale.

1. Introduction

"Site effects" are considered to be the influence of the local geological and geomorphological characteristics to the seismic motion at site. Four experimental methods are usually applied in order to estimate the site effect (Bard, 1992). By the first two, the ground motion characteristics are studied using weak or strong motion data. By the third method, microtremor data are employed and the last one is based on the macroseismic intensity data. Ground motion data have often been used for estimating site effect (Celebi et al., 987; Aki, 1988, 1993; Gazetas et al., 1990; Chavez-Garcia et al., 1990; Gariel et al., 1991; Theodoulidis, 1991; Hatzidimitriou, 1994;). In addition microtremor, data have been also correlated with the site conditions. This method has been widely used in Japan and to a less extent in USA and Europe (Aki, 1988; Lermo and Chavez-Garcia, 1994). However, macroseismic intensity data have not been widely used for the estimation of site effects. This is mainly due to difficulties in modelling the macroseismic field in order to estimate the theoretical intensity at a site and correct the observed intensity values (Evernden et al., 1973; De Rubeis et al., 1994; Tosi et al., 1995).

Macroseismic intensities in Greece have been used by various scientists mainly for attenuation studies or for magnitude estimation of historical earthquakes (Drakopoulos, 1978 a, b; Drakopoulos and Stamelou, 1986; Chandra, 1982; Papoulia, 1988). In order to estimate [site effects], Koyskoyna et al. (1988) used macroseismic data for two events and correlated macroseismic intensities with areas of deep alluvial fills, in comparison with the response of bedrock formations.

In the present study an attempt is made to determine site effects in the area of Greece using macroseismic intensity data. In order to remove the source and path effects, the data were initially processed by using a model that considers parameters which depend on the seis-

Special Publications of the Geological Society of Greece, No 6.

mic source (magnitude, focal depth, radiation patern) and on the wave path (epicentral distance, attenuation, geometrical spreading). Theoretical macroseismic intensities were calculated using this model and the difference between the observed and calculated was attribited to "site effects".

2. Data used

The macroseismic data used in the present study are the observed macroseismic intensities from 113 large shallow earthquakes with magnitude $M_s \geq 5.0$ that occurred in the area of Greece during the period 1950-1993.

The source of the data is the macroseismic intensity observations, in the MM scale, published in the Bulletins of the Seismological Institute of the National Observatory of Athens (BSINOA). Information on the earthquakes for which data have been used, such as origin time, latitude and longitude of the epicenter, focal depth and surface wave magnitude, M_s, were taken from the catalogue of Comninakis and Papazachos (1986) for the time period 1901-1985 and from the Annual Bulletins of the Geophysical Laboratory of the University of Thessaloniki for the period 1986-1993.

A data base has been created which originally was consisted of three data sets. The first one included the data as they were given in BSINOA (one data file for each earthquake with a header giving information on the date, origin, epicentral coordinates and M_s of the earthquake and a list of the macroseismic intensities, names of the villages and the county that each one belongs). The second file included the coordinates of the Greek villages (Ordinance Survey) and the third file included the boundaries of all the counties in Greece in latitude and logitude (kindly offered by the Hellenic Corporation of Local Authority and Developement). These three data sets were conbined to create a unified database of 113 files (on for each earthquake) with a total of 20475 macroseismic observations from 3967 sites. Figure 1 shows a map of the epicenters of the earthquakes for which data have been used in the present study.

3. Method Applied

For each site the difference between the observed macroseismic intensity and the theoretical one, calculated by a source and path modelling of the macroseismic field is considered as a "site effect".

The method applied here for modeling the macroseismic intensity field was developed by C. Papazachos (1992). According to this method, the observed macroseismic intensity, ***I***, depends on the source properties, the geometrical spreading, the anelastic attenuation and the properties of the site and is given by the relation

$$I = I_f + v\log\left(\sqrt{\Delta^2 + h^2}\right) + c\left(\sqrt{\Delta^2 + h^2}\right) + d \qquad (1)$$

where I_f is the intensity at the source which represents the "macroseismic size" of the earthquake, Δ is the epicentral distance, v is the geometrical spreading factor, c is the anelastic attenualtion coefficient and d is the site amplification factor. According to this method, two alternative models can be applied. The first is based on the hypothesis that seismic energy is isotropically radiated, therefore the isoseismals should have a circular shape (circular model). The second one is based on the hypothesis that the shape of short distance isoseismals is due to anisotropic radiation of seismic intensity at the source, while the shape of long distance isoseismals is due to anistropic radiation and attenuation. This model assumes that the isoseismal at intermediate distances from the epicenter has an elliptical shape, with axes $\alpha > \beta$ and ellipticity e, and therefore is hereafter re-

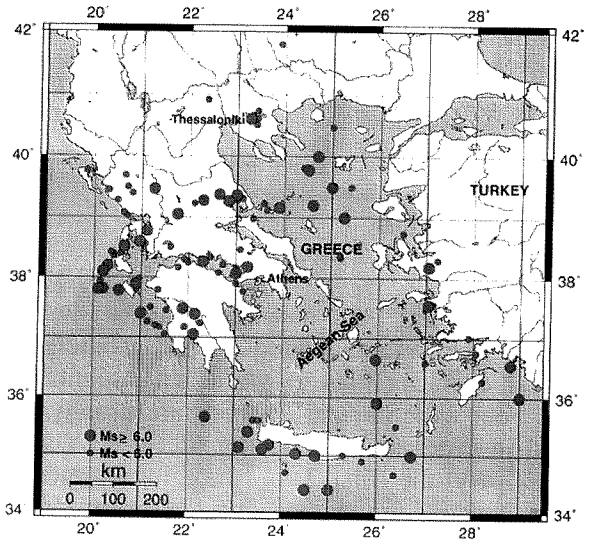

Fig. 1. Map of epicenters of the earthquakes for which data were used in the present study.

fered to as "elliptical model".

The circular model is described by the following relations:

$$I-I_0 = \nu\log\sqrt{1+\frac{\Delta^2}{h^2}} + c\left(\sqrt{\Delta^2+h^2}-h\right), \qquad \Delta<\Delta \tag{2}$$

$$I-I_0 = \nu\log\sqrt{\frac{h^2+\Delta^2}{h^2+\Delta_0^2}} + \nu\log\sqrt{1+\frac{\Delta_0^2}{h^2}} + c\left(\sqrt{\Delta^2+h^2}-h\right) \qquad \Delta>\Delta_0$$

where I_o is the epicentral intensity (Δ=0), ν is the geometrical spreading factor for S-waves, ν_L is the geometrical spreading factor for L_g -waves, h is the macroseismic focal depth, Δ_0 is the critical distance that L_g -waves overtake S-waves and c is the anelastic attenuation coeffient.

For the elliptical model these relations are modified for the anisotropic radiation pattern to

$$I-I_{0_{min}} = \nu\log\left(s^{1}\!/_{2}\sqrt{1+\frac{\Delta^2}{h^2}}\right) + c\left(\sqrt{\Delta^2+h^2}-h\right), \Delta<\Delta_0 \tag{3}$$

$$I-I_0 = \nu\log\sqrt{\frac{h^2+\Delta^2}{h^2+\Delta_0^2}} + \nu\log\left(s^{1}\!/_{2}\sqrt{1+\frac{\Delta^2}{h^2}}\right) + c\left(\sqrt{\Delta^2+h^2}-h\right), \qquad \Delta>\Delta_0$$

where the "sape" factor S, is given by the relation:

$$S = I - e^2\cos^2(\zeta-\phi) \qquad 0 \le S < 1 \tag{4}$$

ζ and ϕ are the azimuths from north of the major axis of the ellipse and the epicenter-site axis, and $I_{0_{min}}$ is the value of the intensity for the minor axis of the ellipse.

Papazachos (1992) applied these models in 13,008 intensity observations grouped in 4,228 values and he estimated the macroseismic focal depth, the geometrical spreading factor, the macroseismic size, I_β, the radiation pattern and the radiation pattern and the anelastic attenuation coefficient for each earthquake. The grouping of the intensity values was made in order to diminish observational errors and mainly site effects.

In the present study, there were used intensity observations without grouping the data and giving the same weight to each observation. Then, the above mentioned parameters were recalculated using both the circular and the elliptical model. For both models the values of Papazachos (1992) were accepted for the spreading factor (ν=-3.49, ν_L=-3.30) and the value of 100 km was given to the critical epicentral distance, Δ_0. Using the Levenberg - Marquadt method (Levenberg, 1994; Marquadt, 1963) the parameters I_o, h, for the circular model and $I_{0_{min}}$, e, ζ, c, for the elliptical model were initially calculated. As a starting value for the attenuation coefficient, the value of -0.003 was adopted (Papazachos, 1992).

For each earthquake, the direction of maximum intensity, ζ, (elliptical model) was accepted if the attenuation coefficient had a value within the range c = 0.0035 ± 2σ (with σ = 0.0016) which corresponds to reasonable Q_s values for this area (Hashida et al., 1988; Kovachev et al., 1991; Papazachos, 1992). For those earthquakes that ζ had a large error or was not acceptable using the above procedure, the mean value of ζ from the surrounding earthquakes was adopted.

For each earthquake, the parameters $I_{0_{min}}$ e, c, were recalculated by using the elliptical model, keeping a constant direction of maximum intensity, ζ, and using as a starting value for the attenuation coefficient c. As such the one

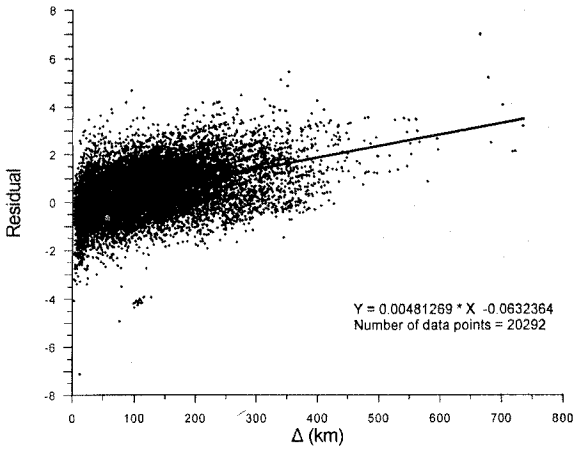

Fig. 2. Plot of the residual (I_{obs}-I_{cal}) for each site versus epicentral distance, Δ.

Table 1

Information of the site name, geographic coordinates, φ_0^0, λ_E^0, of the site, number of macroseismic observations for each site, n, average residual, RESave, and standard deviation, Sdev, for each site.

Site Name	Φ_N^0	λ_N^0	n	RESave	Sdev
KALANDRA	39.97	23.40	3	.41	.27
MILOS	36.73	24.42	3	2.24	.84
KONITSA	40.05	20.75	3	.23	1.03
RODOS	36.43	28.23	3	1.01	.80
SIGRION	39.20	25.85	4	-.62	.64
DRAMA	41.15	24.15	4	82	.93
KILKIS	40.98	22.88	4	-.03	.33
SAMOTHRAKI	40.47	25.53	4	-.46	.29
FERAI	40.88	26.17	4	.93	.39
PILION	38.75	23.58	4	.13	.80
PSARA	38.55	25.55	5	.60	.82
ALAXANDROUPOLIS	40.85	25.87	5	1.01	.70
NAXOS	37.10	25.37	5	1.01	.45
VLACHERNA	37.72	22.23	5	1.65	.87
NEON PETRITSION	41.28	23.30	5	-.62	.56
KEA	37.63	24.33	5	.34	.73
ASTYPALAIA	36.53	26.35	6	-1.23	.67
KAVALA	40.93	24.42	6	.24	.49
ALONNISOS	39.15	23.83	6	-.28	.43
SERVIA	40.18	22.00	6	.26	.62
KARPATHOS	35.50	27.22	6	.75	.65
TINOS	37.53	25.15	6	1.04	.84
MAVROTHALASSA	40.88	23.75	6	.97	1.09
VATHY	37.73	26.98	6	.10	.64
PAROS	37.08	25.15	7	.77	.50
ARGYRADES	39.43	19.97	7	.25	.83
DIDYMOTEICHON	41.35	26.48	7	1.04	.42
KYTHIRA	36.15	22.98	7	-.05	.49
ANDROS	37.83	24.93	7	.43	.79
SAPAI	41.02	25.70	8	.53	.71
MARGARITION	39.35	20.43	8	.31	.82
KALLONI	39.23	26.22	9	1.12	.82
ERMIONI	37.38	23.23	9	.08	.78
KALYMNOS	36.95	26.98	9	1.19	1.23
IOS	36.72	25.28	9	.95	1.27
XANTHI	41.13	24.88	9	.95	.68

Site Name	Φ_N^0	λ_N^0	n	RESave	Sdev
DROSOPIGI	39.77	21.18	9	.85	.82
KARPENISION	38.92	21.80	9	.16	1.04
MOUZAKION	37.78	21.55	10	.52	.66
TYMPAKION	35.07	24.77	10	.18	.68
KASTORIA	40.52	21.27	10	.70	.51
MYRINA	39.87	25.07	10	.23	.55
THASOS	40.77	24.70	10	.97	.75
METSOVON	39.77	21.18	11	.63	.54
FARSALA	39.28	22.38	11	-.22	.81
CHIOS	38.38	26.13	11	.31	.49
PATMOS	37.30	26.53	11	1.00	1.54
SERRAI	41.08	23.55	11	.77	.75
KARDAMYLA	38.53	26.08	12	.53	.57
GREVENA	40.08	21.42	12	1.02	.87
KAMENA VOURLA	38.77	22.77	12	.36	.61
FLORINA	40.78	21.40	12	.91	.80
THIRA	36.42	25.43	12	1.27	1.01
THESSALONIKI	40.63	22.93	12	.22	.55
RETHYMNON	35.37	24.48	12	.82	.45
SITEIA	35.20	26.10	12	.91	.95
KOMOTINI	41.12	25.40	12	.89	.65
IGOYMENITSA	39.50	20.27	13	.47	.76
PYRGOS	37.67	21.43	13	.76	.75
KOZANI	40.30	21.78	13	.35	.45
CHANIA	35.52	24.02	13	.69	.67
KOS	36.90	27.30	13	.70	1.39
AMFISSA	38.52	22.38	14	.51	.61
AIGION	38.25	22.07	14	.19	.79
IOANNINA	39.67	20.85	14	.87	.66
KARYSTOS	38.02	24.42	14	.76	.49
EDESSA	40.80	22.05	14	1.02	.71
POLYGYROS	40.37	23.43	14	.19	.51
KAPANDRITION	38.22	23.87	14	.45	.77
KYLLINI	37.93	21.13	15	.84	1.15
IERISSOS	40.38	23.87	15	.18	.48
GYTHEION	36.75	22.55	15	.40	.51
LEONIDION	37.17	22.85	16	.50	.85
PTOLEMAIS	40.52	1.67	16	1.28	.60
ISTIAIA	38.95	23.15	16	.57	.47
SKIATHOS	39.17	23.48	16	.00	.57

Site Name	Φ_N^0	λ_N^0	n	RESave	Sdev
ELASSON	39.88	22.18	16	.25	.59
VEROIA	40.52	20.22	17	.88	.87
LAGKADAS	40.75	23.07	17	.44	.86
LEVADEIA	38.43	22.87	17	.12	.81
KATERINI	40.27	22.50	17	.67	.82
AGIA	39.72	22.75	17	.47	.62
SKYROS	38.90	24.57	18	.36	.41
PYLOS	36.92	21.70	18	.20	.73
ZAKYNTHOS	37.78	20.88	18	.47	.50
ATHINAI	37.98	23.72	19	.64	.42
SKOPELOS	39.12	23.72	19	-.32	.74
AIGINA	37.75	23.43	19	.98	.86
CHALKIS	38.47	23.58	20	-.05	.52
KYMI	38.63	24.10	20	.92	.60
MESOLONGION	38.37	21.42	20	.69	.63
KERKYRA	39.62	19.92	20	.77	.70
KALAMATA	37.03	22.10	20	.58	.62
IRAKLEION	35.35	25.12	21	.86	.60
VOLOS	39.37	22.97	21	.41	.66
KORINTHOS	37.93	22.92	22	.52	.91
ARTA	39.15	22.98	22	.58	.53
FILIATRA	37.15	21.58	22	.42	.63
THIVAI	38.32	23.32	23	.81	.80
TRIKALA	39.55	21.78	23	1.05	.78
MEGALOPOLIS	37.42	22.12	25	.78	.60
ARGOSTOLION	38.17	20.48	25	.25	.95
LAMIA	38.90	22.43	26	.37	.78
XYLOKASTRON	38.07	22.63	26	.81	.70
KARDITSA	39.37	21.92	26	1.04	.64
ATALANTI	38.65	22.98	27	.55	.62
ITHAKI	38.37	20.72	27	.30	.76
TRIPOLIS	37.50	22.37	30	.53	.68
PATRAI	38.27	21.73	32	.85	.74
LARISA	39.63	22.42	32	.91	.59
LEFKAS	38.82	20.70	42	.51	.73
AGRINION	38.62	21.40	45	.88	.78

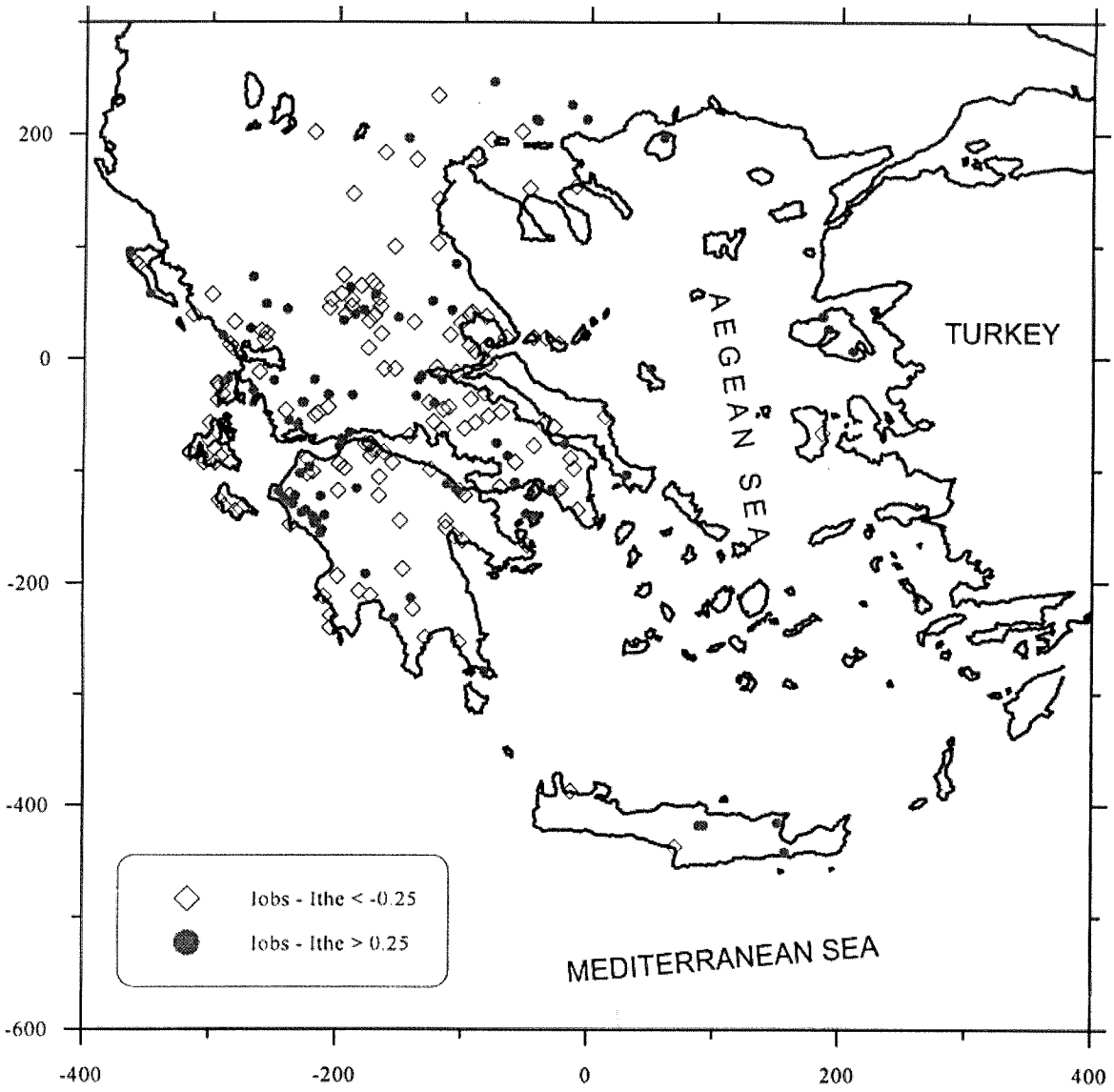

Fig. 3. Spatial distribution of the average residuals of sites with at least 10 macroseismic observations. Positive values correspond to amplication and negative to deamplification.

that was previously calculated if this was within the range c=-0.0035 ± 2σ were adopted, otherwise the mean value of c for the surrounding area was adopted. For ellipticity e, the values that were within 0.3 to 0.9 were accepted. For the earthquakes that e were outside this field, the mean values of e of the surrounding area were adopted. For h the values as estimated from the circular model were adopted and the values that were less then 20 km were accepted. For the earthquakes that h were greater than 20 km the mean values of h of the surrounding area was adopted.

Using the above values for ζ, c, e, h, $I_{0_{min}}$ and I_f the macroseismic intensity, I_{cal}, was calculated using the "elliptical" model (relations 3).

4. Results and Discussion

For each site, the difference I_{obs}-I_{cal} was calculated and was considered as a site effect. In figure 2 a plot of the residual, I_{obs}-I_{cal}, versus epicentral distance, Δ, is presented. As it can

be seen from this figure, there is a slight increase of I_{obs}-I_{cal} with the epicentral distance. The solid line in figure 2 is the least squares' fit to the data given by:

$$I_{obs}-I_{cal}=0.0048-0.063 \quad (6)$$

For each site, an average residual and the corresponding standard deviation were calculated, and this average was recalculated excluding this time the values that were not within ±2 standard deviation.

In Table 1, information is given on the average residuals calculated for 110 selected sites in the area of Greece. The name of the site is given in the first column, and its geographical coordinates are given in the second and the third column. The number of the macroseismic observations that were used for each site is given in the fourth column, the average residual is given in the fifth column and the standard deviation in the sixth column.

Figure 3 shows the spatial distribution of the average residuals for all sites with more than 10 macroseismic observations. As it can be seen from this map, there is some tendency of clustering of positive residuals (amplification) in some areas with dimensions of the order of tenths of kilometers (e.g. in northwestern Peloponnese, Lesbos island, etc.) and of negative residuals in other areas of similar dimensions (e.g. in Cephalonia island, in Zakynthos island etc.). There are, however, many cases where sites of positive and negative residuals are very close. For this reason, the best way to make a practical use of the calculated residuals is to take their values directly from Table 1.

5. Acknowledgments

The authors express their gratitude to the Ordinance Survey of Greece and to the Hellenic Corporation of Local Authority and Development of Greece for offering information on the geographical coordinates of sites used in the present paper. This work has been supported by the EC Projects EV5V-CT94-05013 (Climatology and Natural Hazards).

REFERENCES

Aki, K., 1988. Local site effects on strong ground motion. Proceedings of Earthquake Engineering & Soil Dynamics II GT Div/ASCE, Park City, Utah, June 27-30, 1988, 103-155.

Aki, K., 1993. Local site effects on weak and strong ground motion. "Techonophysics". 218, 93-111.

Bard, P.Y., 1992. Site effects: Basic physical phenomena and estimation methods for microzoning studies, "Lecture Notes", 20 pp.

Chandra, U., 1982. Attenuation of intensities with distance in Greece. "3rd Int. Conf. Earth. Microz." Seattle, 2, 541-552.

Chavez-Garcia, F.J., Pedotti G., Hatzfeld, D., and Bard, P.-Y. 1990. An experimental study of site effects near Thessaloniki (Northern Greece). "Bull. Seism. Soc. Am.", 80, 784-806.

Celebi, M., Prince, J., Dietel, C., Onate M., and Chavez, G., 1987. The culprit in Mexico city - Amplification of motions, "Earthquake Spectra", 3, No 2, 315-328.

Comninakis, P.E. and Papazachos, B.C. 1986. A catalogue of earthquakes in Greece and the surrounding area for the period 1901-1985, "Publ. of the Geophys. La., Univ. Thessal.", 1, 167 pp.

De Rubeis, V., Maramai, A., and Tertulliani, A., 1994. National borders earthquakes: an attempt at intensity maps unification. "Annali di Geofisica", 37, 77-91.

Drakopoulos, J.K., 1978a. Magnitude estimation as a funcrion of intensities for shallow shocks in the area of Greece. "Symposium on the Analysis of Seismicity and Seismic Risk, Liblice, Czechoslovakia, 17-22 June, 1977", 159-172.

Drakopoulos, J.K., 1978b. Attenuation of intensities with distances for shallow earthquakes in the area of Greece. "Bull. Geof. Teor. Appl.", 20, 235-250.

Drakopoulos, J.K., and Stamelou, I., 1986. Intensity - distance relations along max and min axis of a proposed elliptical isoseismal map in Western Greece. "8th Eur. Conf. Earthq. Eng., Lisbon", 3, 79-86.

Evernden, J.F., Hibbard, R.R., and Schneider, J.F., 1973. Interpretation of seismic intensity data. "Bull. Seism. Soc. Am.", 63, 399-422.

Gariel, J.C., Bard, P.Y., and Pitilakis, K., 1991. A theoretical investigation of source, path and site effects during the 1986 Kalamata earthquake (Greece). "Geoph. J. Int.", 104, 165-177.

Gazetas, G., Dakoulas, P., and Papageorgiou, A., 1990. Local - soil and source - mechanism effects in the 1986 Kalamata (Greece) earthquake. "Earth. Engin. and Struc. Dynamics.", 19, 431-456.

Hashida, T., Starakakis, G., and Shimazaki. K., 1988. Three-dimensional Seismic Attenuations Structure Beneath the Aegean Region and its Tectonic Implication. "Tectonophysics.", 145, 43-54.

Hatzidimitriou, P.M., 1994. Relative site amplification factors using the coda waves from local earthquakes for the seismological network of the Geophysical Laboratory of the University of Thessaloniki. "Proc. 2nd Cong. Hellenic Geophysical. Union, Florina, May, 1994", 1, 397-404.

Kouskouna, V., Makropoulos, K., Drakopoulos, J., and Burton, P., 1988. Effects of site geology on the attenuation of macroseismic intensity in Central Greece. "Geofizika", 5, 49-62.

Lermo, J., and Chavez-Garcia, F.J., 1994. Are microtremors useful in site response evaluation? "Bull. Seism. Soc. Am.", 84, 1350-1364.

Levenberg, K., 1944. A method for the solution of certain nonlinear problems in least-squares. "Quant. Appl. Math." 2, 164-168.

Marquadt, P.W., 1963. An algorithm for least-squares estimation of nonlinear parameters. "J. Soc. Ind. Appl. Math." 11, 431-441.

Papazachos, C.B., 1992. Anisotropic Radiation Modelling of Macroseismic Intensities for Estimation of the Attenuation Structure of the Upper Crust in Greece. "Pageoph", 138, 445-469.

Papazachos, C.B., and Kiratzi, A.A., 1995. A detailed study of the active crustal deformation in the Aegean and surrounding area. "Tectonophysics". In press.

Papoulia, L.E., 1988. Statistical and Seismotectonic models in seismic hazard estimations with parameter the seismic intensity. "Ph.D. Thesis., University of Athens", 266 pp.

Theodoulidis, N., 1991. A contribution to the study on strong ground motion in Greece (in Greek). "Ph.D. Thesis., University of Thessaloniki", 500 pp.

Tosi, P., De Rubeis, V., and Gasparini, C., 1995. An analytic method for seperating local from regional effects on macroseismic intensity. "Annali di Geofisica", 38, 55-65.

FOCAL PROPERTIES OF THE 13 MAY 1995 LARGE (M_S=6.6) EARTHQUAKE IN THE KOZANI AREA (NORTH GREECE)

B.C. Papazachos, D.G. Panagiotopoulos, E.M. Scordilis, G.F. Karakaisis, Ch.A. Papaioannou, B.G. Karacostas, E.E. Papadimitriou, A.A. Kiratzi, P.M. Hatzidimitriou, G.N. Leventakis, Ph.S. Voidomatis, K.I. Peftitselis, A. Savaidis and T.M. Tsapanos

Laboratory of Geophysics, University of Thessaloniki, Thessaloniki GR 54006, Greece

Abstract

Spatial distribution of seismic events associated with the mainshock of May 13, 1995 in the Kozani area and its fault plane solution indicate that this earthquake was generated by a normal fault, with a small dextral strike slip component (strike=240°, dip=31°, rake=-98°) which strikes in an ENE-WSW direction, dips to NNW and has a length, L=30 km and a width, w=15km. This kind of faulting resulted in a strong deformation of the hanging wall of the fault, indicated by field observations. The generation of the mainshock in the central and deepest part of the fault and the space-time distribution of aftershocks indicates a bilateral rupture propagation. The foci of all large earthquakes of the sequence (foreshocks, mainshock, aftershocks) are located along a line of the fault which connects the deepest part of the fault with its southwestern shallow part. Evidence is presented for a genetic relation between the water loading of the artificial lake Polifitou and the generation of this earthquake.

Introduction

On May 13, 1995, a very strong earthquake occurred in northwestern Greece (08h:47min:15sec, 40.16°N, 21.67°E, M_S=6.6, M_O=7.6*10^{25} dyn-cm) in a region (Kozani region) of low seismicity. The earthquake caused extended destruction in many villages and some damage in the two largest cities of the area Kozani, Grevena. However, no people were killed or seriously injured by this earthquake. Five relatively strong foreshocks (M_S=3.4-4.5) occurred some minutes before the mainshock and for this reason many people in the villages were out of their houses. The earthquake occurred on Saturday and the students were not in schools, several of which were destructed by the earthquake. The earthquake occurred at a time (11h 47min local time) when most of the people were out of their houses (in the fields, etc). The two cities (Kozani, Grevena) are out of the rupture zone of this earthquake and the houses are, generally, well constructed.

In the present paper, the focal properties of this earthquake are investigated on the basis of the space-time distribution of the shocks of this seismic sequence (foreshocks, mainshock, aftershocks), of a fault plane solution and of macroseismic observations. Furthermore, an attempt is made to examine any relation between the water loading of the artificial lake Polifitou, the southwestern part of which is in the rupture zone of this earthquake. The Polifitou dam was constructed in 1974 at the river Aliakmon, near

Special Publications of the Geological Society of Greece, No 6.

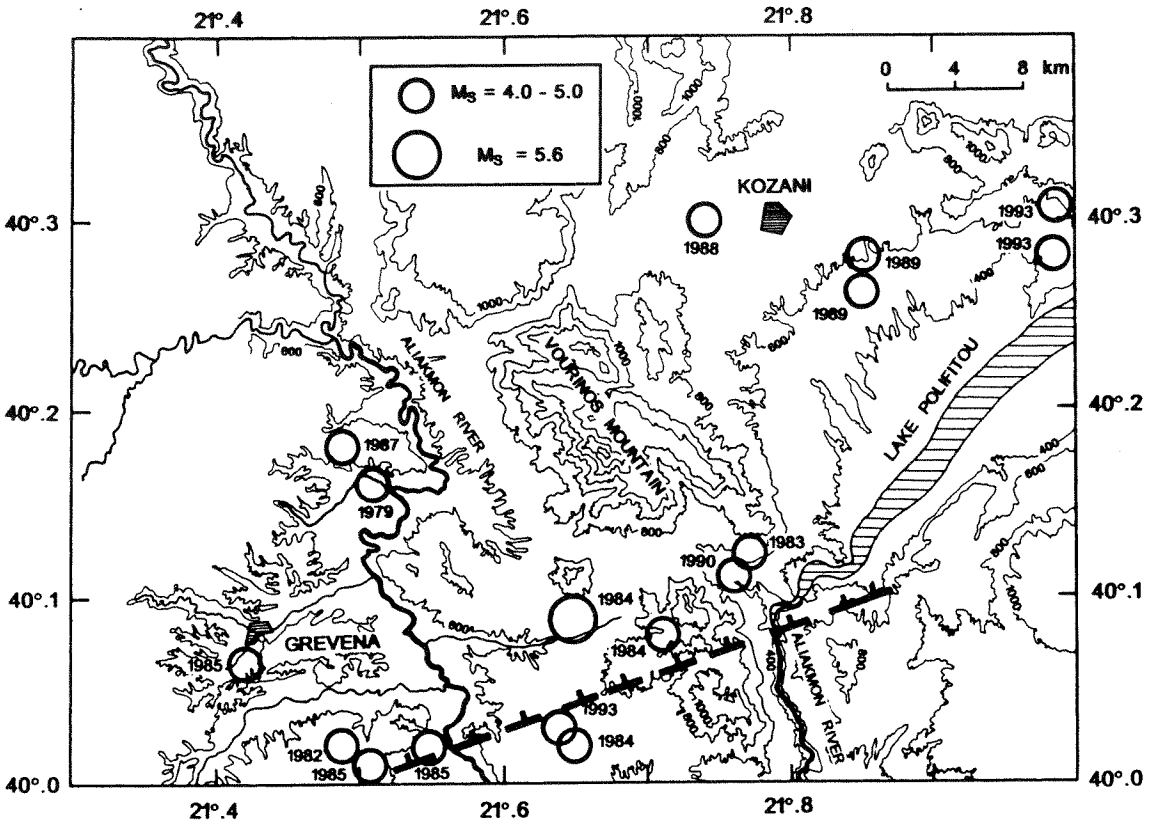

Fig. 1. Seismic activity in the Kozani area during the present century. The number close to each epicenter is the year of occurrence of the corresponding shock. The dashed line shows the inferred fault trace of the 13 May 1995 large earthquake.

the village Imera of the Kozani county. During the spring and summer time the water in the lake is in its highest level (~90 m from the bottom) as it was the case during the generation of this earthquake.

Seismicity of the Kozani Region

The area where this earthquake occurred (Kozani area) is of low seismicity (Papazachos, 1990; Hatzidimitriou et al., 1994). The only known historical earthquake (M~6.0), occurred in the broader area, on February 896 and destroyed the city of Veria, situated 45 km northwest of Kozani (Papazachos and Papazachou, 1989). It is probable, that this earthquake is also related to the northeast trending branch of the Aliakmon river but its epicenter cannot accurately be determined with the available macroseismic information. Some information exists for damage at some churces in Kozani in 1721 but there is no certainty that the cause of this damage is due to earthquakes. For this reason, the only reliable seismological data for this region (40.0°N-40.3° N, 21.4°E-22.0°E) are the instrumental ones. These data are complete for the following time periods and magnitudes: 1901-1995 for $M_S \geq 5.5$, 1911-1995 for $M_S \geq 5.0$, 1950-1995 for $M_S \geq 4.5$ and 1981-1995 for $M_S 4.0$. Information for the earthquakes of this complete sample of data is given in table (I). From this table it is indicated that no earthquake with $M_S \geq 5.0$ occurred between 1911 and 1983 in this area, which supports its low seismicity. The source of these data is the catalogue of Comninakis and Papazachos (1986) and the annual bulletins of the Geophysical Laboratory of the University of Thessaloniki.

Figure (1) shows the epicenters of this complete data sample. It is interesting to note that all these earthquakes occurred after the filling of the lake with water, that is, after 1974. This

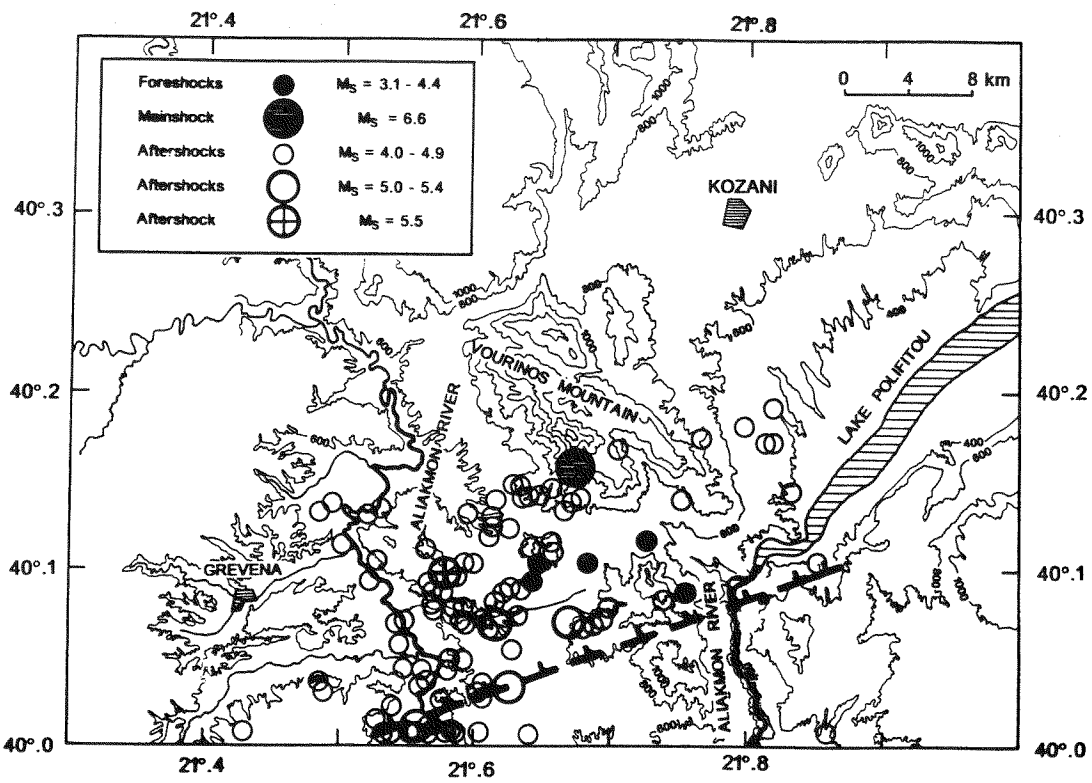

Fig. 2. Distribution of the epicenters of the strongest events ofthe seismic sequence associated with the 13 May 1995 mainshock (seismicity of the period 13 May - 31 August, 1995). The dashed line indicates the inferred fault trace and the dip direction of the fault, as this was defined by the distribution of aftershocks.

Table I. Information on the available complete instrumental data for the Kozani region

Date	Origin Time	$\phi^{o}N$	$\lambda^{o}E$	Depth (km)	Ms
1979, Oct. 14	150016.00	40.200	21.500	10.0	4.5
1982, Sep. 24	23455.72	20.020	21.490	4.0	4.3
1983, May 6	2505.94	40.117	21.768	10.0	4.0
1984, Apr. 4	172357.60	40.023	21.656	1.4	4.3
1984, Oct. 24	9531.49	40.080	21.710	4.3	4.2
1984, Oct. 25	143828.30	40.090	21.650	1.0	5.6
1985, Aug. 1	205411.40	39.940	21.507	0.1	4.0
1985, Aug. 1	205622.00	40.022	21.553	17.2	4.1
1985, Aug. 1	205719.50	40.077	21.416	4.8	4.3
1987, Feb. 19	224123.40	40.180	21.490	3.4	4.7
1988, Nov. 3	51643.00	40.300	21.740	9.3	4.2
1989, Feb. 19	15046.32	40.260	21.850	10.7	4.3
1989, Feb. 19	85231.96	40.280	21.850	4.0	4.0
1990, Apr. 21	162855.90	40.110	21.760	1.8	4.1
1993, Mar. 4	112823.60	40.030	21.640	8.8	4.0
1993, Oct. 18	141934.50	40.310	22.100	0.5	4.1
1993, Oct. 18	142922.50	40.280	22.060	1.3	4.1

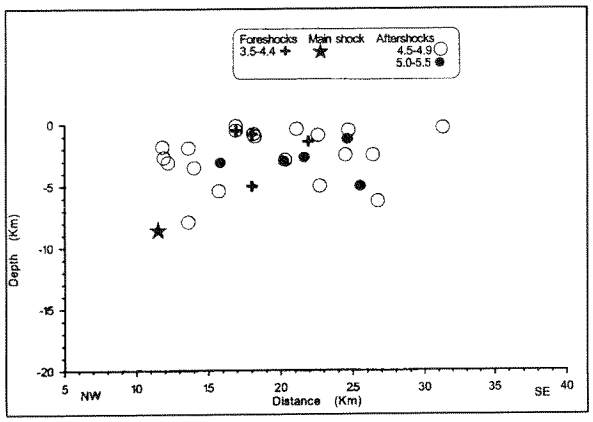

Fig. 3. Plot of the foci of shocks of the seismic sezuence associated with the 13 May 1995 mainshock onto a plane parallel to the dip direction of the fault.

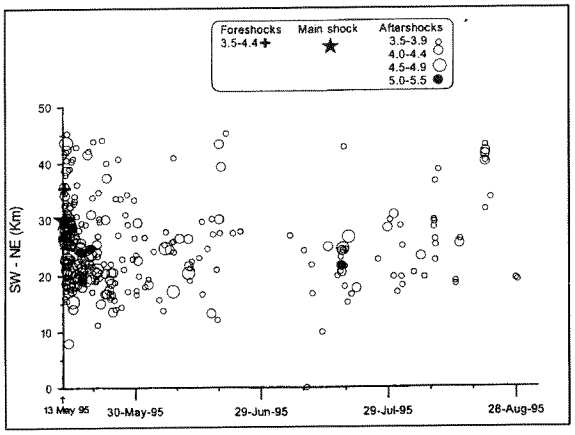

Fig. 4. Space-time plot of the foci of the earthquakes associatedwith the 13 May 1995 mainshock.

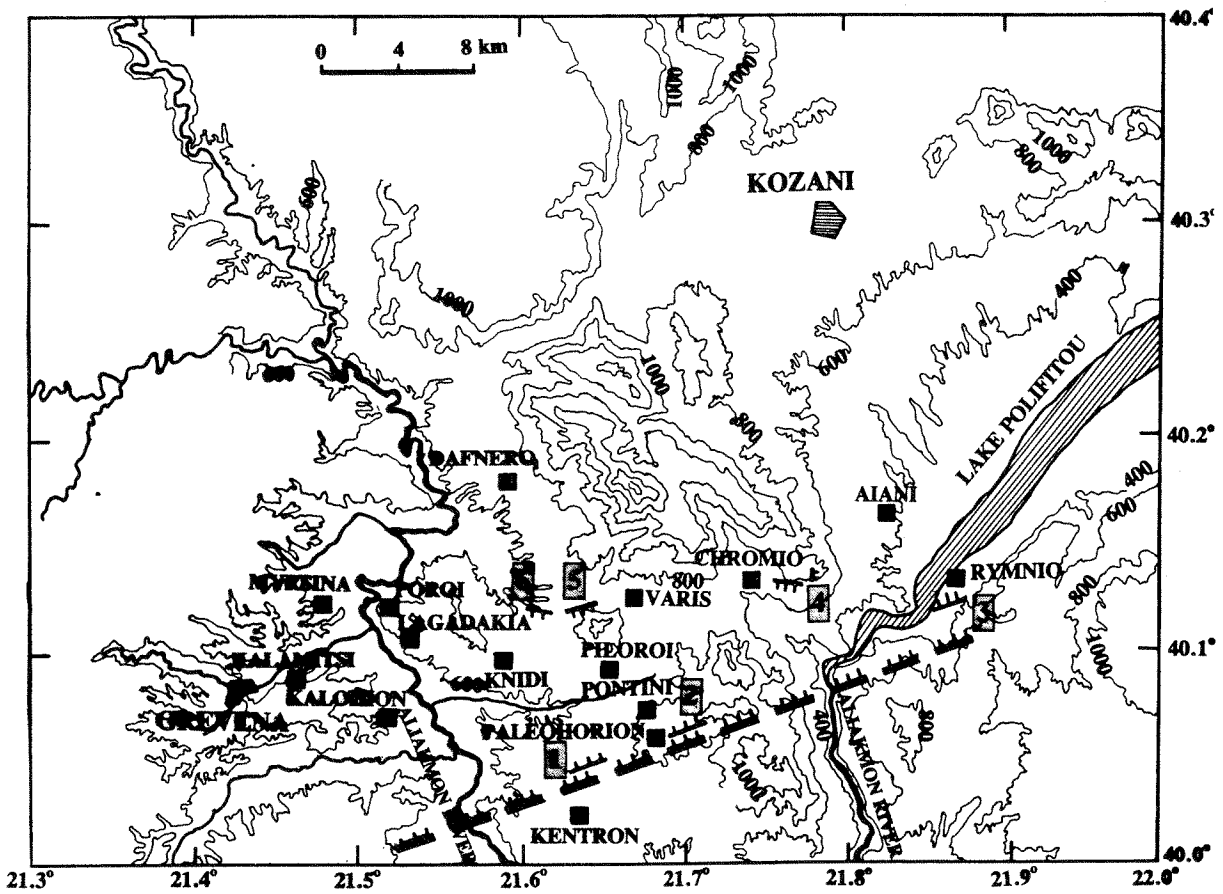

Fig. 5. Macroseismic effects of the 13 May 1995 earthquake. Black squares indicate sites with high macroseismic intensity (I8), small dashed lines show observed ground breaks, while the large dashed line shows the inferred fault trace associated with the 13 May 1995 mainshock.

Table II. Information on the focal parameters of the events of the sequence for the time period May 13 - August 31.1995

Date	Origin	Time	Lat N	Lon E	Depth (km)	Ms	No	GAP	DMIN	RMS	ERH	ERZ
950513	818	868	40.116	21.724	3.3	3.1	11	97	65.	0.2	1.0	1.6
950513	842	11.50	40.103	21.681	0.8	3.8	14	100	69.	0.5	2.0	2.7
950513	843	16.88	40.103	21.643	0.5	4.4	14	103	72.	0.4	1.7	2.1
950513	844	36.62	40.086	21.753	1.4	3.8	13	156	63.	0.4	2.1	2.9
950513	847	1.21	40.092	21.638	5.0	4.2	9	103	73.	0.4	1.9	3.3
950513	847	14.39	40.158	21.673	8.6	6.6	12	164	70.	0.2	1.9	2.2
950513	9 1	2.30	40.109	21.655	5.2	4.2	14	102	71.	0.3	1.0	1.3
950513	929	41.59	40.148	21.624	1.3	4.4	9	106	74.	0.5	1.8	3.0
950513	947	43.12	40.139	21.750	3.7	4.4	17	96	63.	0.4	1.5	1.6
950513	1011	59.22	40.082	21.738	5.7	4.3	12	96	64.	0.4	1.7	2.4
950513	1033	7.78	40.115	21.653	2.5	4.4	13	103	71.	0.5	1.8	2.2
950513	1058	35.86	40.103	21.591	2.5	4.4	17	107	77.	0.4	1.4	1.8
950513	1143	31.43	40.142	21.634	3.1	4.9	11	189	73.	0.3	2.2	1.9
950513	1416	31.19	40.141	21.644	5.5	4.1	11	104	72.	0.4	2.3	2.5
950513	1426	6.84	40.370	21.868	15.0	4.1	12	86	62.	0.4	2.9	4.2
950513	1754	55.84	40.001	21.804	7.0	4.3	17	90	60.	0.4	1.6	1.5
950513	18 6	1.52	40.138	21.668	7.9	4.8	15	102	70.	0.3	1.6	1.5
950513	19 0	51.15	40.103	21.852	5.0	4.6	14	153	54.	0.5	2.4	2.4
950513	1937	12.45	40.145	21.832	5.0	4.4	17	90	56.	0.5	1.7	1.8
950513	2353	43.45	40.024	21.574	1.5	4.3	17	106	79.	0.4	1.6	1.9
950513	2356	27.31	40.025	21.604	0.5	4.8	17	104	76.	0.4	1.5	2.0
950514	1 3	0.20	40.095	21.584	1.0	4.3	14	108	77.	0.5	1.8	2.3
950514	238	57.77	40.103	21.593	0.5	4.2	13	107	76.	0.5	1.8	2.6
950514	247	0.95	40.086	21.574	0.1	4.7	16	108	78.	0.5	2.0	1.5
950514	3 2	28.57	40.069	21.545	0.8	4.5	14	200	81.	0.4	1.9	1.8
950514	3 9	38.75	40.103	21.642	0.5	4.6	16	103	72.	0.3	1.3	1.5
950514	429	24.95	40.169	21.702	5.0	4.0	16	100	68.	0.3	1.3	1.5
950514	514	53.71	40.077	21.589	1.9	4.1	15	107	77.	0.5	1.7	2.1
950514	559	16.98	40.042	21.545	0.4	4.7	13	109	81.	0.3	1.4	2.0

Date	Origin	Time	Lat N	Lon E	Depth (km)	Ms	No	GAP	DMIN	RMS	ERH	ERZ
950514	627	8.73	39.986	21.424	5.2	4.4	12	116	89.	0.3	1.6	2.2
950514	835	11.07	40.131	21.516	1.5	4.3	12	114	73.	0.3	1.2	1.8
950514	945	41.63	40.154	21.680	4.0	4.4	15	101	69.	0.3	1.3	1.8
950514	1446	57.19	40.133	21.662	3.5	4.5	15	102	71.	0.3	1.4	1.6
950514	2131	12.77	40.073	21.629	3.6	4.2	14	104	73.	0.4	1.6	1.9
950515	024	19.16	40.134	21.526	4.5	4.2	13	114	73.	0.3	1.3	1.5
950515	120	16.15	40.104	21.524	4.6	4.3	13	113	76.	0.3	1.5	1.8
950515	413	56.86	40.068	21.669	2.7	5.1	20	87	70.	0.4	1.5	1.8
950515	642	27.77	40.077	21.582	0.5	4.0	15	93	30.	0.3	1.3	1.6
950515	817	0.01	40.113	21.498	1.8	4.5	15	115	75.	0.3	1.2	1.4
950515	9 1	52.77	40.086	21.566	0.5	4.1	16	109	79.	0.3	1.1	1.5
950515	919	44.73	40.132	21.480	8.3	4.4	14	118	73.	0.2	1.0	1.2
950515	17 5	42.76	40.068	21.541	2.5	4.4	14	110	81.	0.5	1.6	2.3
950515	2247	34.27	40.148	21.630	8.6	4.1	12	105	73.	0.2	1.0	1.1
950516	437	28.59	40.002	21.549	0.5	4.4	14	107	81.	0.4	1.6	1.9
950516	1757	51.40	40.068	21.590	0.5	4.4	19	106	77.	0.5	1.4	2.0
950516	2154	17.06	40.041	21.559	0.5	4.3	22	108	80.	0.4	1.1	1.4
950516	23 0	41.91	40.017	21.563	2.5	4.7	16	107	80.	0.5	1.9	2.1
950516	2357	27.96	40.086	21.618	1.0	4.9	19	105	74.	0.3	1.2	1.5
950517	354	53.89	40.088	21.632	0.5	4.3	16	104	73.	0.4	1.6	2.1
950517	414	25.69	40.067	21.614	3.0	5.3	14	105	75.	0.3	1.9	1.9
950517	448	35.14	40.089	21.623	0.5	4.4	17	104	74.	0.4	1.3	1.9
950517	945	7.70	40.007	21.558	5.0	5.0	14	107	80.	0.3	1.1	1.7
950517	10 7	38.57	40.022	21.587	0.4	4.0	17	105	78.	0.4	1.5	2.0
950517	1125	28.33	40.010	21.545	0.5	4.0	19	108	81.	0.4	1.3	1.8
950517	1128	38.15	40.034	21.604	2.1	4.0	14	104	76.	0.5	1.7	2.2
950517	1136	48.90	40.004	21.564	0.3	4.1	18	106	80.	0.5	1.6	2.1
950517	1538	0.45	40.041	21.578	1.3	4.1	14	107	78.	0.4	1.5	2.1
950517	2351	48.23	40.028	21.601	1.4	4.0	14	104	76.	0.3	1.0	1.2
950518	349	1.03	40.069	21.588	2.4	4.0	18	107	77.	0.4	1.4	1.8
950518	622	55.04	40.032	21.557	0.9	4.6	17	148	35.	0.4	1.5	1.8

Date	Origin	Time	Lat N	Lon E	Depth (km)	Ms	No	GAP	DMIN	RMS	ERH	ERZ
950518	1526	41.62	40.173	21.817	3.1	4.1	20	91	58.	0.4	1.2	1.3
950519	1 3	42.83	40.071	21.604	3.5	4.1	17	105	76.	0.6	1.8	2.4
950519	130	24.52	40.048	21.580	1.8	4.0	18	107	78.	0.4	1.4	1.6
950519	133	55.49	40.047	21.590	0.1	4.0	21	106	77.	0.4	1.2	1.5
950519	648	50.41	40.031	21.625	1.2	5.1	16	195	74.	0.4	2.1	1.9
950519	736	49.44	40.065	21.608	2.9	4.8	16	105	75.	0.3	1-0	1.5
950519	1229	53.14	40.077	21.696	0.5	4.0	19	99	68.	0.4	1.1	1.5
950519	13 7	48.37	39.998	21.563	4.9	4.1	17	106	80.	0.4	1.3	1.8
950520	20 9	31.78	40.004	21.578	1.4	4.3	18	105	79.	0.5	1.9	2.0
950520	2011	54.82	40.001	21.639	5.0	4.1	16	146	73.	0.5	1.8	2.0
950520	21 6	25.18	40.005	21.583	2.5	4.5	16	105	78.	0.5	1.7	2.1
950520	2119	35.51	40.080	21.612	0.5	4.1	14	105	75.	0.4	1.3	2.3
950520	2225	0.56	39.998	21.578	2.5	4.0	15	105	79.	0.4	1.4	1.7
950521	4 4	23.66	40.035	21.562	2.5	4.4	14	108	80.	0.4	1.5	2.0
950521	2038	27.29	40.137	21.490	0.2	4.2	18	117	72.0	0.4	1.4	1.7
950522	2021	34.43	40.091	21.563	0.5	4.4	21	109	79.	0.5	1.3	1.7
950522	2110	33.54	40.000	21.530	1.0	4.1	15	109	83.	0.3	1.2	1.5
950522	2230	41.13	40.067	21.686	2.5	4.2	20	99	69.	0.4	1.1	1.3
950523	437	40.24	40.092	21.518	0.5	4.2	19	113	78.	0.3	1.1	1.3
950523	551	58.87	40.175	21.764	4.7	4.1	19	95	62	0.3	1.1	1.2
950523	20 9	53.86	40.008	21.537	1.0	4.3	19	108	82.	0.4	1.4	1.7
950523	2059	51.11	39.997	21.561	1.0	4.2	18	106	80.	0.4	1.2	1.5
950524	522	43.94	40.078	21.566	3.3	4.0	18	109	79.	0.4	1.4	1.8
950524	624	9.02	39.995	21.554	0.5	4.4	17	107	81.	0.4	1.4	1.9
950524	7 0	3.01	40.012	21.525	0.3	4.3	126	110	83.0	0.3	1.4	1.6
950524	1445	22.56	40.028	21.486	3.2	4.0	19	113	84.	0.5	1.5	1.9
950524	1734											
950530	12 6	43.19	40.065	21.567	0.9	4.1	15	108	79.	0.4	1.6	2.1
950630	1430	2.65	40.005	21.602	0.7	4.4	22	90	36.	0.4	1.2	1.5
950602	747	15.72	40.056	21.542	0.5	4.0	21	110	81.	0.4	1.1	1.4
950606	435	59.26	40.139	21.612	2.7	4.8	24	106	23.	0.5	1.5	1.6

is the first evidence that the loading of the lake Polifitou with water facilitated aseismic motion which progressively triggered this recent seismic activity in an area which was almost aseismic for a very long time before. It is also of interest to note that the largest of these earthquakes (M_S=5.6) as well as other eight smaller shocks occurred close to the fault (dashed line in figure 1) where the May 1995 seismic sequence occurred. This indicates that parts of this fault or other smaller faults, which are close to this long fault, were activated during the period 1979-1993.

On the basis of the available complete data for the Kozani region, the parameters "a" and "b" of the Gutenberg - Richter relation were determined and found equal to:

a (for 1 year period) = 4.22 b=1.0 (1)

Using these values and assumming that the maximum magnitude of the earthauakes in this region is M_{max}=6.6, the seismic moment rate, m_o in this region is, according to a formula proposed by Molnar (1979),

$m_o=0.77*10^{24}$ (dyn cm/yr) (2)

Active Crustal deformation in the region

The active crustal deformation of the region determined as in the work of C. Papazachos and Kiratzi (1992), requires two sets of information. The first kind of information is the seismic moment rate and the spatial dimensions of the deformed region and the second kind of information is a typical fault plane solution for the region. The seismic moment rate has been already determined for the Kozani region (relation 2). The dimensions of the deformed volume, which strikes in N78°E, are:

length, I_1=89km; width, I_2=25km; (3)
thickness, I_3=10km

The fault plane solution determined by Harvard for the mainshock of 13 May 1995 has as follows:

NP1: strike=240°, dip=31°, rake=-98° (4)
NP2: strike-70°, dip=59°, rake=-85°

The parameters of the first nodal plane are in agreement with the spatial distribution of the foci of the seismic sequence as well as with the geomorphology of the area and the macroseismic effects of the earthquake. This solution shows that the seismogenic fault is a normal fault with a small dextral component, it strikes in an ENE direction (N60°E) and dips to the NNW at a low angle (31°). This solution is in good agreement with the typical fault plane solution expected for this region (C. Papazachos and Kiratzi, 1995).

On the basis of these data and the application of the above mentioned method the following values were determined for the eigenvector of the deformation velocity:

v(mm/yr)	Azimuth	Plunge
1.4	**148°**	**11°**
0.1	**240°**	**10°**
-0.6	**10°**	**75°**

which indicates that the main crustal deformation in the Kozani is an almost horizontal extension in a N32°W direction at a rate of 1.4 mm/yr. Such a direction and rate is expected for this region (C. Papazachos and Kiratzi, 1995).

Spatial distribution of the Seismic Sequence

Table (II) gives information on the five largest foreshocks, on the mainshock and on the aftershocks wwith $M_S \geq 4.0$ which occurred up to 31 August 1995. The four last columns give the number of observations used for the calculations and the errors in the origin time, epicenter and focal depth, respectively. These earthquakes are presented in Figure (2).

The mainshock was preceeded by foreshocks, five of which were strong (M=3.4-4.5). The first occurred 29 min before the mainshock and the last occurred 13 sec. before the mainshock. The first four had very shallow depth (h<3 km) and the two weaker foreshocks (M=3.4 and M=3.7), occurred at the eastern part of the area close to the artificial lake Polifitou (fig. 2). The last event that occurred 13 sec before the mainshock, had a greater focal depth (h=5 km), that is, its focus was closer to the focus of the mainshock

(h=9 km), under the mountain of Vourinos. A chain triggering was observed during the occurrence of the foreshocks that seems to have started from the east and then propagated towards the focus of the mainshock at the deeper part of the fault surface.

The aftershocks had initially (the first 11 hours) their foci at the central and eastern part of the fault. In the following, the epicenters of the aftershocks migrated towards west and the seismicity continued at very high levels for many days along a straight line that connects the focus of the mainshock with the southwestern shallow part of the fault (magnitudes reached a value of 5.5). The low seismicity that was observed at the eastern section of the fault, indicates that in this area, where the artificial lake is situated, there are not many barriers and therefore an aseismic movement is possible at this part of the fault. It is interesting to note that the two strongest foreshocks (M=4.2, M=4.5) have their foci along the same line of the fault, where the foci of the most and largest aftershocks are found. The rupture region, as this region is defined by the spatial distribution of aftershocks (fig. 2), has a N71°E trend and a length along this trend equal to 30km. This trend is in fairly good agreement with the fault strike (N60°E) difined by the fault plane solution.

Figure (3) shows the distribution of the foci of these shocks of the seismic sequence on a vertical section in a direction (N19°W) normal to the strike of the fault and it shows that the rupture zone dips to the NNW. The width of the rupture zone, along the dip, is w=15 km and its dip angle is equal to 30°, that is, almost equal to the dip angle determined by the fault plane solution.

Figure (4) shows a space-time plot of the events of the seismic sequence. It is observed that the seismic activity migrated towards west, after the first hours. It is also clearly seen that the easternmost part of the rupture zone, that lies near the artificial lake Polifitou, was the less active part of this zone during this sequence because a small number of weak aftershocks occurred there. In terms of the barrier model (Aki, 1982), it means that this is the only relatively large part of the fault plane which lacks important barriers and is reasonable to assume that this part of the fault plane slipped relatively smoothly during this physical procedure and the intrusion of the lake water in the fault area played an important role in this process. This motion (creep) can be attributed to a decrease of the friction in the fault due to an increase of the pore pressure caused by the water loading.

Macroseismic observations

Figure (5) shows some of the results of the field observations. The inferred, by the distribution of the aftershock epicenters, surface fault trace is also shown (thick dashed line). The villages where the macroseismic intensity, in the MKS scale, is equal to or larger that eight ($I \geq 8$) are shown by black squares. It is observed that all major macroseismic effects (high seismic intensities, ground ruptures) are observed on the surface of the hanging wall of the fault. Ground ruptures (1, 2, 3 in fig. 5) observed close to the inferred fault trace are also shown. These ruptures are probably due to the main fault or secondary faults which have the same properties (normal with a strike slip component). Such faults that strike parallel to the main fault are usually observed in the hanging wall of normal faults (Papazachos et al., 1983). Several ground ruptures have been also observed in other parts of the hanging wall which are due to the severe some times (4, 5 in fig. 5). It is of interest to note that at least one of the ground ruptures (5 in fig. 5) appeared some days before the mainshock (D. Kaliabakas, pers. com.,) which indicates that aseismic motion (creep) occurs also in this area. Further indication that the southwesternmost part of the lake Polifitou is in the hanging wall of normal faults (Papazachos et al., 1983). Several ground ruptures have been also observed in other parts of the hanging wall which are due to the severe deformation of this wall. Some of these may be due to smaller faults, antithetic to the main fault in some times (4, 5 in fig. 5). It is of interest to note that at least one of the ground ruptures (5 in fig. 5) appeared some days before the mainshock (D. Kaliabakas, pers. com.,) which indicates that aseismic motion (creep) occurs also in this area. Further indication that the southwesterenmost part of the lake Polifitou is in the hanging wall of the fault, gives the fact that macroseismic effects (see strong deformation in Aiani bridge). Such a result is expected by the model proposed

for the generation of this earthquake, because, according to this model, this hanging wall dropped by about half a meter during the generation of this earthquake.

Discussion

On the basis of the above mentioned observations, the following model can be proposed on the generation of this seismic sequence and its consequences. A tectonic horizontal extension, exerted in the crust of the Kozani region at a rate of about 1 mm/yr and in the N32°W direction, produced aseismic slip (creep) in the easternmost and shallow part of the rupture zone where the water loading of the artificial lake Polifitou acilitated this motion. This creep trigerred the generation of foreshocks in the shallow eastern and central part of the rupture zone. Then, a chain triggering occurred similar to the one observed in the artificial lake of Kremasta (Comninakis et al., 1968). That is, the very shallow foreshocks were triggered first by the creep motion in the lake and these foreshocks triggered the last strong foreshock and other smaller ones at a depth of about 5 km. Such an abrupt displacement (~1 cm) close to the focus of the mainshock and in the downdip direction of the fault trigerred the generation of the mainshock at a depth of about 9 km by breaking an important barrier beneath the Vourinos mountain. Further support of the idea that aseismic motion, which is facilitated by the water loading in the artificial lake Polifitou, triggerred this seismic sequence is the fact that considerable seismic activity (with magnitudes to 5.6) occured in this area only after the filling of the aftificial lake. Moreover, important ground ruptures (aseismic) were observed in the epicentral area before the generation of the mainshock of May 13, 1995.

From the focus of the mainshock, in the middle and lowest part of the fault, the rupture was propagated bilaterally and stopped at the two ends of the fault. This is a normal fault (with a small dextral strike slip component) which strikes in an EVE-WSW direction and dips to NNW. The length and the width of the fault are L=30 km, w=15 km which give a fault area S=450 km^2. The mean displacement at the fault is expected to be u=50cm (Papazachos and Papazachou, 1989). Such downward motion of the hanging wall of the fault in respect to the footwall resulted in severe deformation of the crustal material (ground ruptures, landslides, etc.) in the hanging wall. For this reason, the most important destructions are in the villages built on this hanging wall. The bilateral rupture propagation in the fault, during the mainshock, caused a stress redistribution in the rupture zone with a subsequent generation of aftershocks in the whole rupture zone. During the first eleven hours, the aftershock activity was concentrated in the eastern and central part of the rupture zone by the occurrence of relatively small aftershocks. After that, this activity takes place almost exclusively along a straight line that connects the focus of the mainshock with the southwestern shallow part of the fault, where it continued for many weeks by the occurrence of aftershocks with magnitudes up to 5.5 which caused additional damage. Very close to this line the foci of the largest foreshocks were also located (M=4.5, M=4.2).

References

Aki, K. (1982). Strong motion prediction mathematical modeling techniques. "Bull. Seism. Soc. Am.", 79, 29-41.

Comninakis, P.E., Drakopoulos, J., Moumoulidis, G. and Papazachos, B.C. (1968). Foreshock and aftershock sequences of the Kremasta earthquake and their relation to the waterloading of the Kremasta artificial lake. "Annali di Geofisica", XXI, 39-71.

Comninakis, P.E. and Papazachos, B.C. (1986). A catalogue of earthquakes in the Aegean and the surrounding area. "Publ. of the Geophys. Lab., Univ. Thessal.", 1, 167 pp.

Hatzidimitriou, P.M., Papazachos, B.C. and Karakaisis, G.F. (1994). Quantitative seismicity of the Aegean and surrounding area. "Proc. XXIV Gen. Ass. Europ. Seism. Comm., Athens, September, 1994", *in press.*

Molnar, P. (1979). Earthquake recurrence intervals and plate tectonics. "Bull. Seism. Soc. Am.", 69, 115-133.

Papazachos, B.C. (1990). Seismicity of the Aegean and surroundin area. "Tectonophysics", 178, 287-308.

Papazachos, B.C., Panagiotopoulos, D.G., Tsa-

panos, Th. M., Mountrakis, D. and Dimopoulos, G. (1983). A study of the 1980 summer seismic sequence in the Magnesia region of central Greece. "Geophys. J.R. astron. Soc.", 75, 155-168.

Papazachos, B.C. and Papazachou, C. (1989). The earthquakes of Greece. "Ziti Publ. Co., Thessaloniki", 356 pp.

Papazachos, C.B. and Kiratzi, A.A. (1992). A formulation for reliable estimation of active crustal deformation and its application to central Greece. "Geophys. J. Int.", 111. 424-432.

Papazachos, C.B. and Kiratzi, A.A. (1995). A detailed study of the active crustal deformation in the Aegean and surrounding area. "Tectonophysics" (in press).

SOURCE PARAMETERS OF THE ARNEA, KOZANI AND AIGION EARTHQUAKES BASED ON DIGITAL DATA

G.N. Stavrakakis and G. Chouliaras

Institute of Geodynamics, National Observatory of Athens, 11810 Athens, Greece

Abstract

In 1995, three moderate to large earthquakes occurred in three different seismic zones in Greece. The predominant stress field in those seismic areas is extensional. Digital data have been processed to determine the source parameters of these mainshocks, by using two spectral models proposed by Brune and Madariaga, respectively. The stress drop, seismic moment, source radius (fault lenghth) and the average displacement on the fault plane have been obtained and discussed.

Introduction

Source parameters of earthquakes have often been estimated using two characteristic spectral parameters, the corner frequency f_o and the long period constant level Ω_o (Hanks and Wyss, 1972; Thatcher, 1972; Wyss and Hanks, 1972; Kondorskaya et al., 1979; Kulhanek and Meyer, 1979; Kulhanek et al., 1983; Scherbaum and Stoll, 1983; Stavrakakis et al., 1989). Values of the source parameters inferred from seismic spectra are based either on Brune's model or on Madariaga's model. The former gives a lower stress drop than the latter (Modiano and Hatzfeld, 1982; Stavrakakis et al., 1989). The characteristic parameters f_o and Ω_o are, however, almost always obtained from spectra which are computed using a FFT routine.

Determination and interpretation of body-wave spectra

A general feature of all dislocation models (Keilis - Borok, 1959; Maruyama, 1963; Ben-Menahem and Harkrider, 1964; Burridge and Knopoff, 1964; Ben-Menahem et al., 1965; Aki, 1967) is that the long period spectral level is proportional to the seismic moment, M_o, and the corner frequency f_o is proportional to the reciprocal of the source dimension, r. Assuming a circular rupture model, the average displacement on the fault plane and the stress drop can be inferred from M_o and r. In addition the seismic energy radiated in P and S waves can also be obtained.

In case of a complete effective stress drop, the seismic moment is (Keilis-Borok, 1960):

$$M_o(S) = 4\pi\rho\beta^3 k\Omega_o(S)G(\Delta)_{/R\theta\phi}(S) \qquad (1)$$

where:

$M_o(S)$=seismic moment determined by the S wave spectrum
ρ=the crustal density
β=the shear-wave velocity
k=the free-surface coefficient
$\Omega_o(S)$=the long period spectra level of the S wave
G<Δ> the geometrical spreading factor
$R_{\theta\varphi}(S)$=the radiation pattern for the S wave
r(S)=the source dimension (Brune, 1970, 1971):

$$r(S) = 2.34\beta/2\pi f_o(S) \qquad (2)$$

Hanks and Wyss (1972) extended Bryne's model to P waves and proposed an analogous relationship for the seismic moment and source dimension:

$$M_o(P) = 4\pi\rho k\alpha^3\Omega_{o(P)G}(\Delta)_{/R\theta\phi(P)} \qquad (3)$$

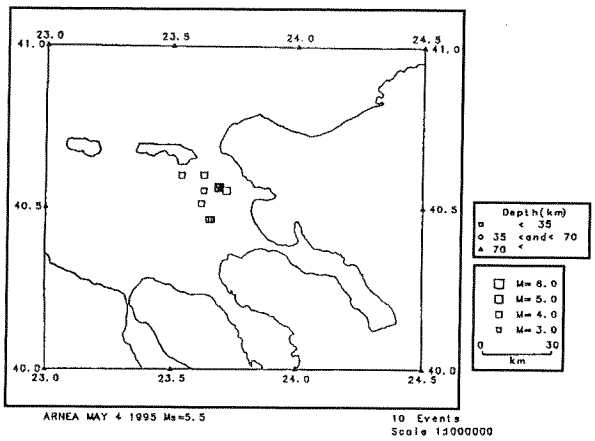

Fig. 1. Epicenters of the Arnea seismic sequence.

$$r(P)=2.34\alpha/2\pi f_o\ (P) \qquad (4)$$

where α is the *P* wave velocity.

On the other hand, Madariaga (1976) proposed for the source dimension the formula:

$$r(P)=0.32\beta/f_o(P) \qquad (5)$$

where the shear wave velocity β is taken to be equal to $\alpha/1.78$.

The main difference between the two models is that in the Madariaga model the slip increases linearly after rupture, so that the final slip is greater than that expected for a static solution. Consequently, the stress drop for a dynamic solution is larger than the effective stress considered by Brune. In the present analysis, Madariaga's model was chosen to calculate the source radius, because of the dynamic nature of the model. Assuming the ratio $f_o(P)/F_o(S)=1.5$, Brune's model computes a radius of about two times that calculated using the Madariaga model, but gives a stress drop that is about six times lower.

If we now look at symmetrical propagation, i.e. similar physical parameters near the source and beneath the stations employed, the geometrical factor $G(\Delta)$ is given by:

$$G(\Delta)=R\ \cos i_o\ \sin \Delta/\sin i_h \qquad (6)$$

where:
R=the earth's radius 6.372 km
i=the angle of incidence
Δ=the epicentral distance in degrees
Indices *h* and *0*=the source and receiving station, respectively.

The seismic moment and the radius of the rupture area provide an estimate of the stress drop (Brune, 1970):

$$\Delta\sigma=0.44\ M_o\ (P)\ /\ r^3(P) \qquad (7)$$

and the average displacement on the fault plane is given by:

$$<u>=M_o(p)/\pi\mu r^2(P) \qquad (8)$$

where μ is the rigidity.

(A) ARNEA (NORTHERN GREECE) EARTHQUAKE

On May 4, 1995 a moderate earthquake of M_s=5.5 took place in northern Greece, close to the town of Arnea in the peninsula of Chalkidiki. This event was preceeded by a low foreshock activity and followed by a moderate aftershock activity. **Figure 1** shows the epicenter distribution of the foreshock, main shock and the foreshocks. The significant events of this sequence have been recorded by the digital network of the Institute of Geodynamics. The wave forms of the mainshock are shown in **Fig. 2,** which were processed using the PITSA package (Scherbaum and Johnson, 1992). An example of the

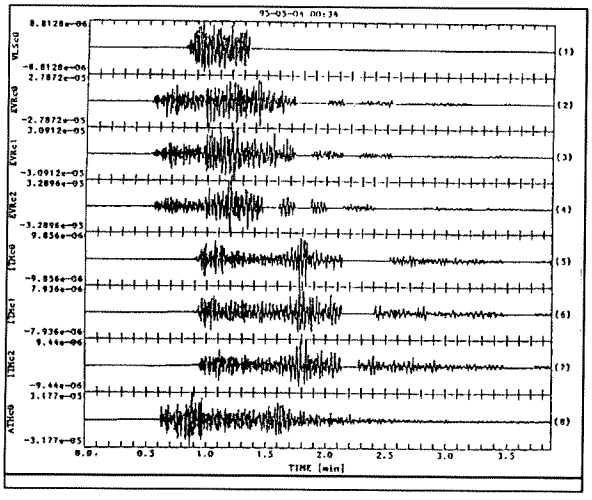

Fig. 2. Waveforms of the Arnea main shock.

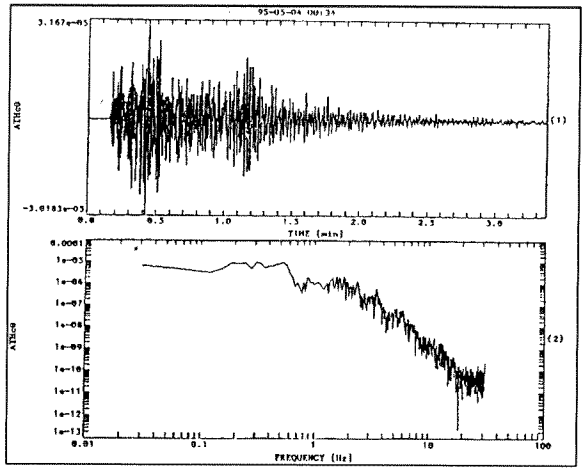

Fig. 3. Example of the fourier spectrum of the Arnea main shockfrom the Athens digital station.

obtained specta is shown in Fig. 3, for the *P*- and *S*- waves. For each seismological station relevant spectra have been obtained, and the spectral parameters, namely the corner frequency, f_c, and the constant spectral level, Ω_o, have also been determined.

Following the formulae mentioned above, the seismic moment and the fault radius have been computed for each station and then the average values or these parameters were obtained.

Using the P-wave spectra, an average corner frequency f_c=0.42 Hz and Ω_o=2.4 x 10^{-5} m/Hz are obtained. Based on these values, a seismic moment $\langle M_P^o \rangle = 9.3 \times 10^{22}$ dyne.cm. Using the S- wave spectra, a value of $\langle M_S^o \rangle = 3.0 \times 10^{24}$ dyne.cm is obtained. For the source radius, the following values were determined: r_B^P = 2.93 km, r_M^P = 2.51 km, r_B^S = 6.93 km, r_M^S = 2.16, where the indices *B* and *M* correspond to Brune and Madariaga models, respectively. Thus $\langle r_B \rangle$ = 4.9 km and $\langle r_M \rangle$ = 2.4 km. Using these values, the stress drop has also been determined, $\Delta\sigma_B$ = 6 bars and $\Delta\sigma_B$ = 47 bars, with an average seismic moment of $\langle M_o \rangle = 1.5 \times 10^{24}$ dyn.cm.

(B) KOZANI - GREVENA EARTHQUAKE OF MAY 13, 1995

On May 13, 1995 an unusual seismic activity started in the area close to the city of Kozani. The mainshock of M_S=6.6 was preceeded by

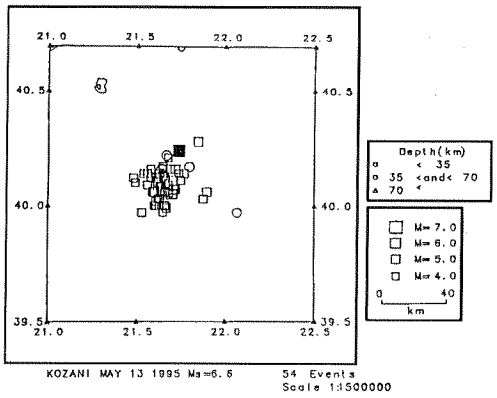

Fig. 4. Epicenters of the Kozani Seismic Sequence.

low foreshock activity and followed by a severe aftershock activity which lasted for more than six months. Figure 4 shows the epicenter distribution of the largest aftershocks as well as the fault plane solution determined by Harvard University. Figure 5 shows the digital waveforms used to determine the spectra of P-, and S-waves. Following the same procedure as described above, the following cource parameters have been obtained: $\langle M_o^P \rangle = 4.2 \times 10^{26}$ dyn.cm, $\langle rsu^P \rangle = 117$ with a $\langle f_c^P \rangle = 0.092$ Hz, $\langle M_o^S \rangle = 1.4 \times 10^{26}$ dyn.cm and $\langle r^S \rangle$ = 13.7 km with a $\langle f_c^S \rangle = 0.055$ Hz. Thus, the mean values of $\langle M_o \rangle = 2.8 \times 10^{26}$ dyne.cm, $\langle r \rangle$ = 12.7 km, $\langle \Delta\sigma \rangle$ = 60 bars and $\langle u \rangle$ = 108 cm were determined, where $\langle u \rangle$ the average displacement on the fault plane. Centroid moment solution gives $M_o = 4.79 \times 10^{25}$ dyne.cm.

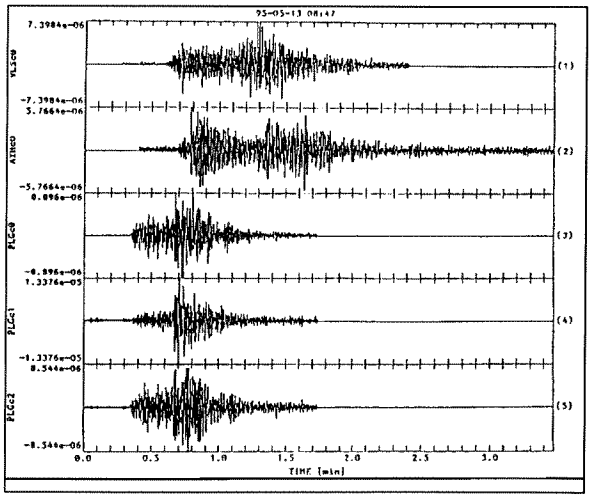

Fig. 5. Waveforms of the Kozani main shock.

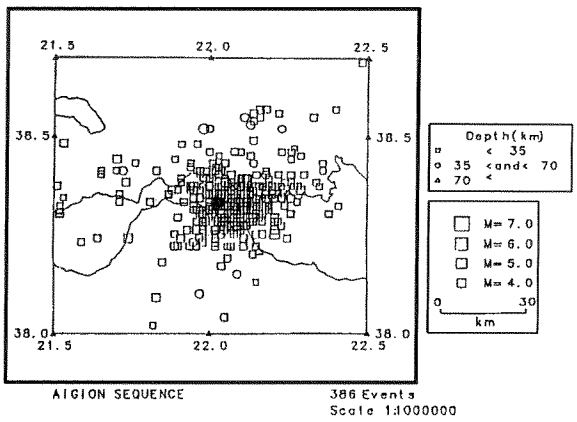

Fig. 6. Epicenters of the Aigio seismic sequence.

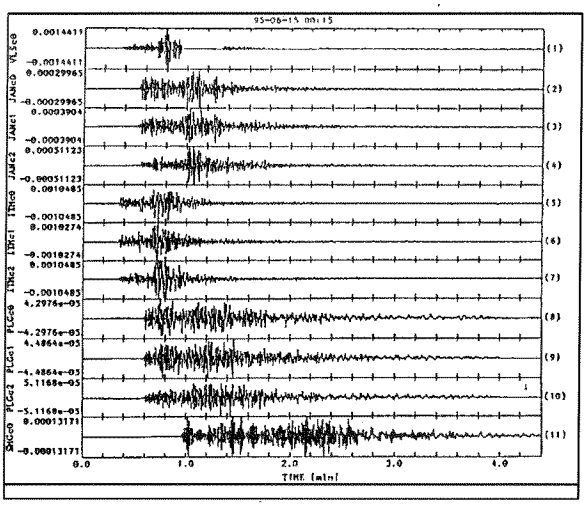

Fig. 7. Waveforms of the Aigio main shock.

(c) AIGION EARTHQUAKES OF JUNE 15, 1995

Figure 6 shows the epicenter distribution of the significant events of the Aigion earthquake sequence of June 15, 1995 as well as the fault plane solution of the mainshock, determined also by Harvard University. Figure 7 shows the digital waveforms used in the present analysis. By following the same procedure we obtained. $\langle M_o^P \rangle = 2.5 \times 10^{25}$ dyne.cm, $\langle r^P \rangle = 8.0$ km with a $\langle f_c^P \rangle = 0.136$ Hz, $\langle M_o^S \rangle = 4.6 \times 10^{25}$ dyne.cm, $\langle r^S \rangle = 5.4$ km with $\langle f_c^S \rangle = 0.138$ Hz. Thus, the mean values: $\langle M_o \rangle = 3.6 \times 10^{25}$ dyne. cm $\langle r \rangle = 6.7$ km $\Delta\sigma = 53$ bars and $\langle u \rangle = 85$ cm were determined. The centroid moment solution gives a seismic moment of $M_o = 5.7 \times 10^{25}$ dyne.cm.

Discussion - Conclusions

In the present study, digital data were processed to obtained the source parameters of the mainshocks of three characteristic earthquake sequences occurred in three different seismic zones in Greece.

It is worth emphasizing that in all cases the predominant stress field is extensional, thus the obtained source parameters correspond to the similar seismotectonic regime.

The spectra have been corrected by introducing a correction coefficient $R_{\theta\phi} = \sin 2f \cos^2\theta$, where f and θ the strike and dip of the fault plane. The obtain source parameters were computed by using two spectral models, namely that of Brune and that of Madariaga. The seismic monents are in a good agreement with the values obtained by centroid moment inversion. The stress drops computed on the basis of the Madariaga's model are higher than those obtained by Brune's model. An explanation is given by Stavrakakis et al. (1989) and by Stavrakakis et al. (1990). The fault dimensions accounting for the dip of the fault plane, however, the average displacents are higher than those observed.

References

Aki, K., 1967. Scaling low of seismic spectrum. J. Geophys. Res. 84, 6140-6148.

Ben-Menahem, A., 1961. Radiation of seismic surfece waves from finite moving sources. Bull. seism. Soc. Am. 51, 401-435.

Ben-Menahem A., and Harkrider D.G., 1964. Radiation patterns of seismic surface waves from buried dipolar point sources in a flat stratified earth. J. Geophys. Res. 69, 2605-2620.

Ben-Menahem A., Smith S.W. and Teng T.L., 1965. A procedure for source studies from spectrums of long period seismic waves. Bull. Seism. Soc. Am. 55, 203-235.

Brune, J.N., 1971. Tectonics stress and the spectra of seismic shear waves from earthquakes. J. Geophys. Res., 75, 4997-5009.

Brune, J.N., 1971. Correction. J. Geophys. Res., 76. 5002.

Burridge R.E., Lapwood R. and Knopoff L.,

1964. First motions from seismic sources near a free surface. Bull. Seismol. Soc. Am. 54, 1889-1913.

Hanks T.C. and Wyss M., 1972. The use of body wave spectra in the determination of seismic source parameters. Bull. Sism., S. A., 62, 561-589.

Keilis-Borok, V.I., 1959. On the estimation of the displacement in an earthquake source and of source dimensions. Ann. Geofis., 12, 205-214.

Kulhanek O., and Meyer K., 1979. Source parameters of the Volvi-Langadhas earthquake of June 20, 1978 deduced from body-wave spectra at stations Uppsala and Kiruna. Bull. Seism. Soc. Am. 68, 1289-1294.

Kulhanek O., VanEck J., John N., Meyer K. and Wahlstrom R., 1983. Spectra of the earthquake sequence February-March 1981 in south central Sweden. Tectonophysics 93: 337-350.

Madariaga R., 1976. Dynamics of an expanding circular fault. Bull. Seism. Soc. Am., 66, 636-666.

Modiano T., and Hatzfeld D., 1982. Experimental study of the spectral content for shallow earthquakes. Bull. Seism. Soc. Am., 72, 1739-1758.

Scherbaum F. and Stoll D.J., 1983. Source parameters and scaling laws of the 1978 Swabian Jura (Southwest Germany) aftershocks. Bull. Seismol. Soc. Am., 73 (5), 1321-1343.

Stavrakakis G.N., Drakopoulos J., Latoussakis J., Papanastassiou D. and Drakatos G., 1989. Spectral characteristics of the 1986 September 13 Kalamata (southern Greece) earthquake. Geophys. J. Int., 98, 149-157.

Stavrakakis G.N. and Blionas S.V., 1990. Source parameters of some large earthquakes in the Eastern Mediterranean Region based on the Iterative Maximum Entropy Technique. Pageoph. 132 (4) 579-697.

Thatcher W.R., 1972. Regional variations of seismic source parameters in the northern Baja California area. J. Geophys. Res. 77, 1549-1565.

Wyss M. and T.C. Hanks, 1972. The source parameters of the San Fernando Earthquake inferred from teleseismic body waves. Bull. Seism. Soc. Am. 62, 591-602.

THE 13 MAY 1995 WESTERN MACEDONIA (GREECE) EARTHQUAKE. PRELIMINARY RESULTS ON THE SEISMIC FAULT GEOMETRY AND KINEMATICS

Mountrakis D., Pavlides S., Zouros N., Chatzipetros A. and Kostopoulos D.

Department of Geology and Physical Geography, Aristotle University of Thessaloniki, GR - 54006, Thessaloniki, Greece.

Abstract

On Saturday, 13 May 1995, at 11:47 local time (8:47 GMT), a devastating earthquake (Lat.: 40.16° N, Long.: 21.67° E, M_s = 6.6, M_w = 6.4) occurred in western Macedonia (Kozani - Grevena area), continental Greece. The total meisoseismal area covers approximately 5,000 km^2.

A zone of about 50 km length and 10 - 15 km width has been affected by "faults", either reactivated neotectonic ones, or other surface ruptures and sympathetic faults. Surface fault traces directly associated with the main seismic fault were observe d in the unconsolidated sediments in the Rymnio village area (NE edge of the rupture zone), and in the villages of Palaeochori affecting ophiolites and recent sediments, Sarakina, Kentro and Nisi affecting molasse and recent sediments. The ground ruptures consist of open fissures (heaves 1 - 10 cm) with small displacement (1 - 15 cm) of normal slip (dip towards NW). This rupture zone trending N 75° coincides with the focal mechanism solution which suggested a fault striking N 70°, with a total length of 30 km. Thus the seismic fault is a segment of the Aliakmon river fault in between the villages of Rymnio, Palaeochori, Kentro and Nisi. The non - activated segment (Servia fault) is an impressive active normal fault affecting marbles and gneisses (ENE - WSW strike, dip towards the NW) with fresh fault scarps and Holocene scree. The latter have clearly been affected by previous tectonic events.

A series of subparallel antithetic ruptures with E - W strike, dipping towards the South, follows a second line (Chromio, Varis, Knidi) of about 10 km length that may extend up to the village Kalamitsi. Some of these ground ruptures are connected with a dextral strike-slip geological fault in Vourinos mountain, which has been found by geophysical research (I.G.M.E.).

The previously calculated Quaternary and active stresses in the area (Pavlides 1985, Pavlides and Mountrakis 1987) and the geometry of the active faults are in good agreement with the focal mechanism of the main shock.

Introduction

On Saturday, 13 May 1995, at 11:47 local time (8:47 GMT), a devastating earthquake (Lat.: 40.16° N, Long.: 21.67° E, M_s = 6.6, M_w = 6.4) occurred in western Macedonia (Kozani - Grevena area), Greece. The Structural Geology group of the University of Thessaloniki conducted research all over the affected area, in close collaboration with the Geophysical Laboratory of the University of Thessaloniki, in order to understand the seismic fault geometry and kinematics.

The greatest observed intensity (MM) was IX+. The meisoseismal area covers approximately 5,000 km^2. There was major destruction

Special Publications of the Geological Society of Greece, No 6.

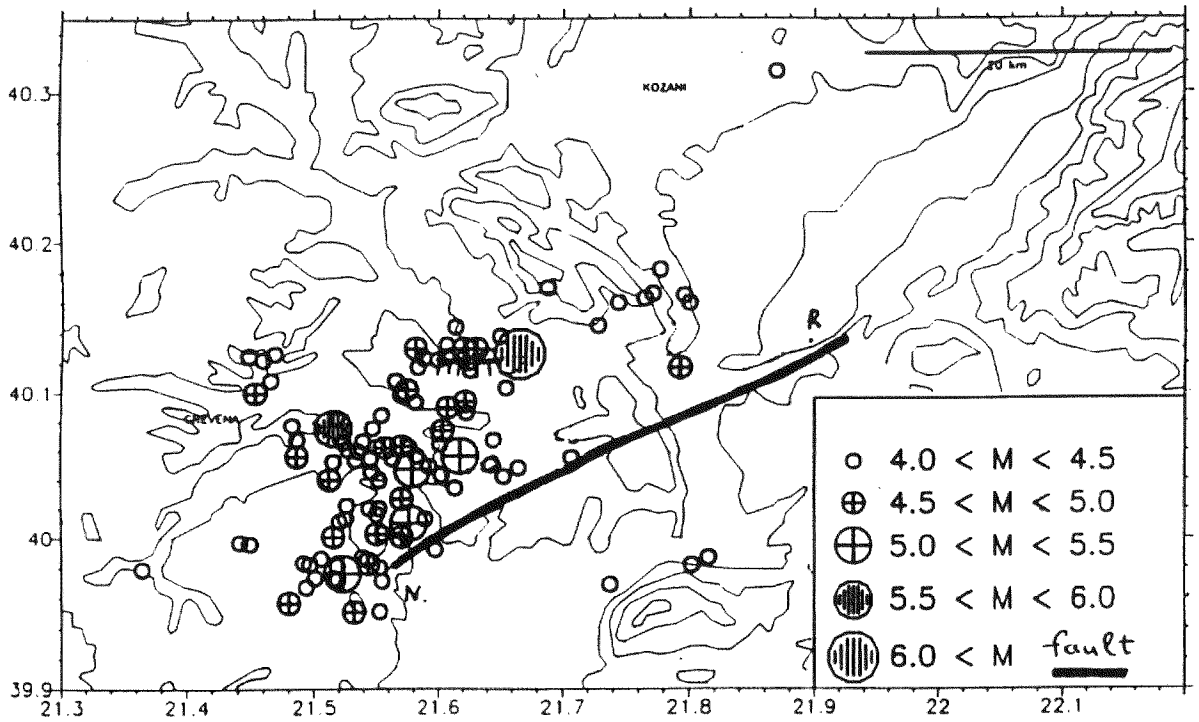

Fig. 1. Distribution of the epicentres of the strongest events of the seismic sequence associated with the 13 May 1995 main shock (M = 6.6). Seismicity of the period between 13 May and 31 August, 1995 (after *Papazachos et al. 1995*). Heavy line indica tes the geological fault which was reactivated during the earthquake in between the villages of Rymnio (R) and Nisi (N).

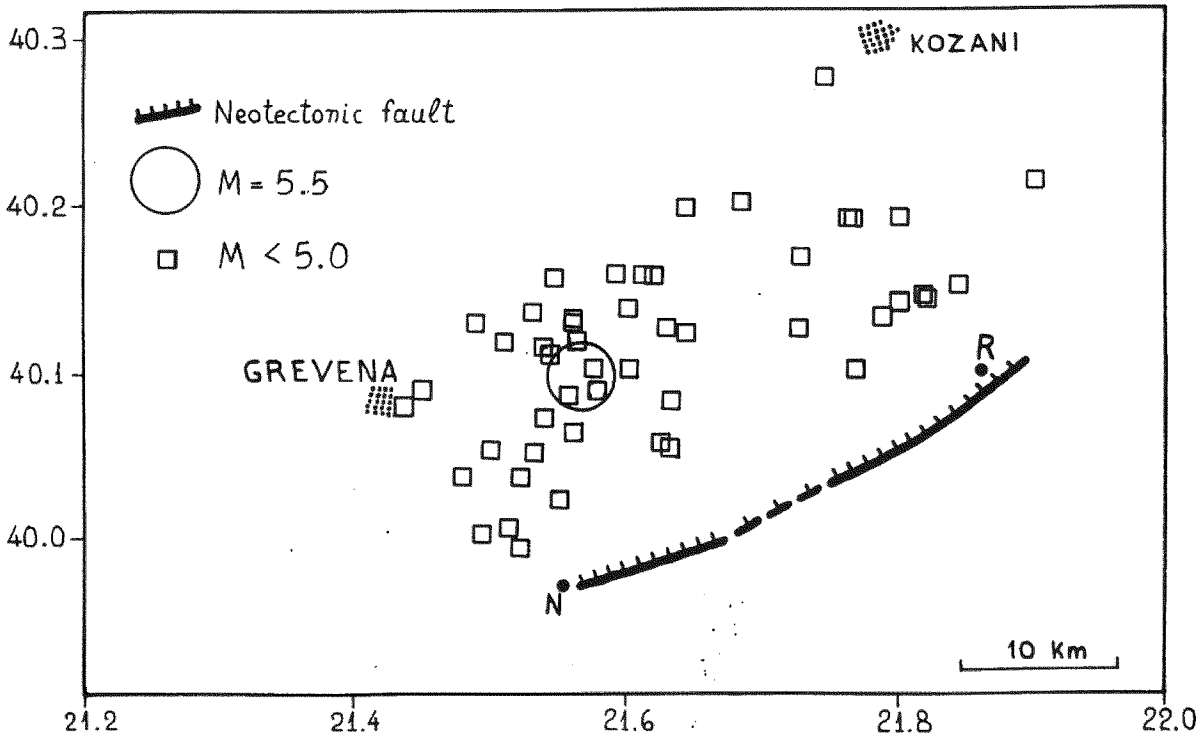

Fig. 2. Distribution of the epicentres of the seismic sequence associated with the 11 July 1995 aftershock M = 5.5. Seismicity of the period between 11 - 19 July (personal communication with V. Karakostas, Seismological Station, University of Thessal oniki). Heavy line indicates the geological fault (seismogenic) which is in good agreement with the distribution of the aftershocks.

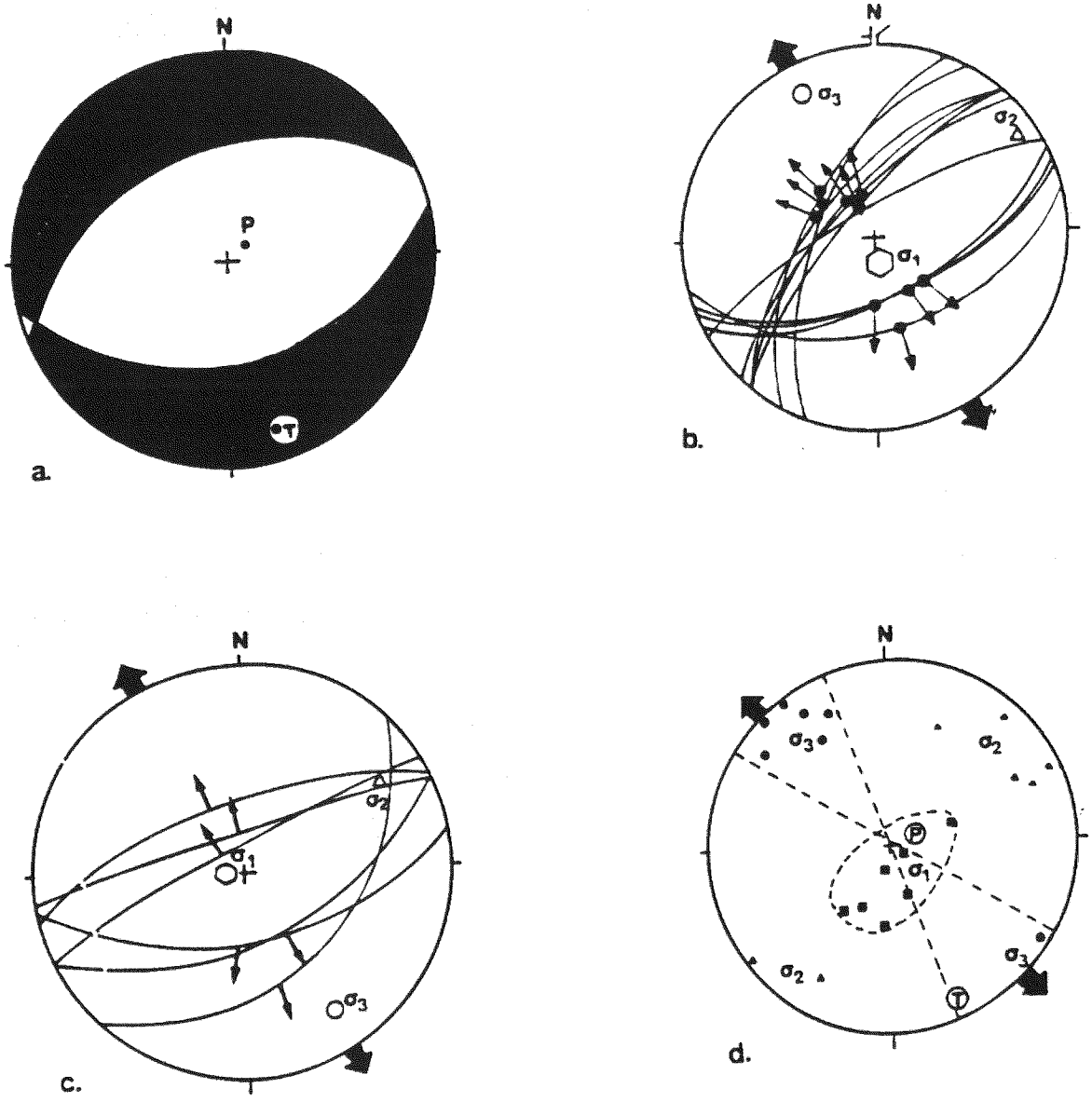

Fig. 3. **a.** Focal mechanism of the main shock provided by the solution of the Geological Society of Japan (P-axis: 60/82, T-axis: 157/1). **b.** Stress pattern (σ_3: NNW - SSE trending, (1: vertical) in western Macedonia as derived by palaeostress analysis of neotectonic striated faults *(Pavlides 1985)*. **c.** Stress pattern in the meisoseismal area as derived by the analysis of seismic fault data. **d.** P and T axis of the main shock in the areas of σ_1 and σ_3 previously calculated from neotectonic data.

in the road network, water drillings, and change in the water supply of some springs, mainly increase, after some days. Extensive rock falls and landslides were also observed all over the area.

The first seismological approach of the earthquake *(Papazachos et al. 1995)* gave a distribution of the 13 - 19 May seismic sequence epicentres aligned in an ENE - WSW direction *(fig. 1, 2)*. This distribution indicated a seismic fault (theoretical fault line) trending ENE - WSW, while a cross section with the distribution of the shock foci indicated a small dip (about 30°) of the seismogenic fault towards NW. Additionally the focal mechanism solutions determined by the Geological Society of Japan and Harvard University (automatic CMT inversion) suggested a normal fault trending 70° with the extensional *(T)* axis in the NNW direction *(fig. 3)*.

Thus, taking into account these seismological information we tried to find the seismic faults in the field and study their geometry and kinematics.

Geological and structural framework of the epicentral area

The earthquake area is situated in the western margin of the Pelagonian geotectonic zone to the Subpelagonian oceanic zone *(Brunn 1956, Mountrakis 1983, 1986).* Three main lithological groups can be distinguished in the region: the Pelagonian Alpine and pre-Alpine rocks, the sediments of the Meso - Hellenic Trough and the lacustrine - continental deposits of Plio - Quaternary age.

The Alpine - prealpine basement of the area consists of Pelagonian rocks (gneisses, amphibolites, mica schists, meta-granites and the Permotriassic meta-sediments) which are covered by the crystalline limestones of Triassic - Jurassic age. Subpelago nian ophiolites and deep sea sediments of Jurassic age, comprising the Vourinos ophiolitic complex, thrust over the Pelagonian carbonate rocks and are covered by the Cretaceous sediments *(Brunn, 1956, Mavrides et al. 1977, Mountrakis 1986).* The ophiolites in Grevena basin are overlain unconformably by the molassic sediments of the Meso - Hellenic Trough (Brunn 1956). These are the Tsotylion Formation mainly, of Burdigalian (Early - Middle Miocene) age, and the Pentalophos Formation of Aquitanian (Early Miocene) age.The major part of the epicentral area is covered by fluvial and lacustrine deposits, which overlie unconformably the molassic sediments and the Alpine basement *(Brunn 1956).* An age of Middle Pliocene - Middle Pleistocene is sugg ested for the Grevena basin *(Brunn 1956, Koufos et al. 1991).*

Kinematic analyses carried out in western Macedonia *(Mountrakis et al. 1992)* showed that several successive tectonic events took place during the neotectonic evolution. Two successive compressional tectonic events took place during Middle and Late M iocene. The first one with an ENE - WSW direction of compression, caused NNW - SSE trending reverse faults, imbrication within the ophiolites and important dextral strike-slip faults trending E - W to NE - SW. The second event, with a NNE - SSW direction of compression, produced conjugate reverse faults trending E - W and caused further imbrication of the ophiolites and the molassic sediments.

A large dextral strike-slip structure that was formed during the Miocene compressional deformation is the Chromion - Varis Valley fault *(fig. 4)* which affects the Vourinos ophiolitic complex, divides the northern from the southern Vourinos mountain, and forms the well known corridor. This structure has been detected by geophysical exploration (aeromagnetic research) carried out by the Institute of Geology and Mineral Exploration *(I.G.M.E.)* several years ago.

An extensional tectonism during Late Miocene - Pliocene followed the compressional deformation. This activated NNW - SSE trending normal faults and caused the formation of the Ptolemais - Kozani basin. A subsequent Early - Middle Pleistocene extensi onal deformation formed major normal faults trending NE - SW to ENE - WSW. This deformation is responsible for the Basin-and-Range type of morphology that was developed across these faults, and appear to be still active. This is indicated by numerous geological evidence, such as recent sediments affected by the youngest faults, geomorphological features, and very recent striations on some polished faults covered by unconsolidated recent alluvial fans *(Pavlides 1985, Pavlides and Mountrakis 1987).*

One of the main NE - SW trending faults in western Macedonia is the Aliakmon river valley fault (also known as the Servia fault), that forms the exit of the river to the Aegean Sea. This fault is also detected from satellite images as a long and con tinuous lineament *(fig. 4).*

Field observations on the seismic fault geometry and kinematics

Taking into account the geological structure of the area, as well as the available seismological instrumental data, we started the field work trying to locate the surface expression o f the seismogenic fault. Two possibilities were examined *(fig. 4):*

- The first was the well known Aliakmon

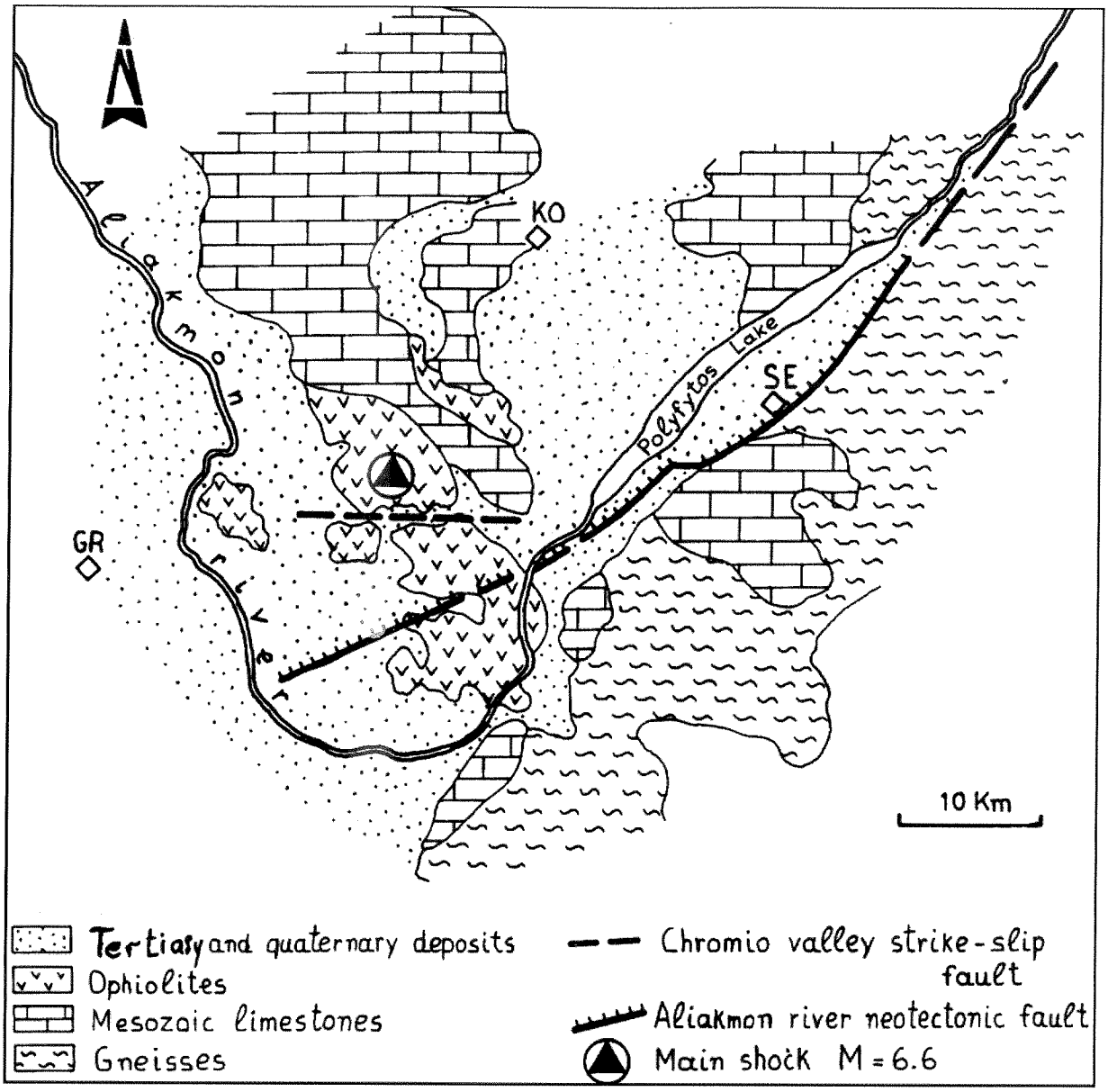

Fig. 4. Geological sketch map of the Kozani (KO) - Grevena (GR) area (western Macedonia, Greece) showing the Aliakmon river (double line) and Polyphytos Lake and the two main geological faults in the area: the Aliakmon neotectonic fault, a segment of which was the seismogenic fault, and the Chromio Valley strike-slip fault detected by geophysical research. Molasse type sediments and Plio-Pleistocene continental sediments are shown as undivided Tertiary and Quaternary deposits. The Alpine basemen t consists of Pelagonian gneisses, Mesozoic limestones and ophiolites.

river fault, which is a neotectonic normal fault with strike N 70° and dip to the NNW and a total length of more than 60 km. It affects the Trias sic - Jurassic crystalline limestones and the gneisses of the Pelagonian zone in the area of Servia town and Rymnio village, and extends westwards towards the villages of Palaeochori, Kentro and Nisi, affecting the molassic sediments of the Meso - Hellenic Trough and the Plio - Pleistocene continental sediments.

• The second was the Chromion - Varis Valley tectonic line, that is a dextral strike-slip fault of the basement located in the corridor of the Vourinos ophiolites with an E - W direction. It has been detected by geophysical research and can only be observed in a few quarries in the area, because it is completely covered by the Quaternary deposits which have not been

affected by that. However, small strike-slip faults of the same system cut all of the ophiolitic terrain and offset chrome ore bodies, particularly close to the covered main strike-slip fault.

All the instrumental data described above, that is the distribution of the epicentres along a NE - SW direction *(fig. 1, 2)* and the focal mechanism suggesting a normal fault trending 70° and dipping to the NW *(fig. 3)*, indicate that the fault which caused the earthquake is the Aliakmon fault. In addition there are certain geological and seismotectonic evidence for it:

• The distribution of the damages all over the meisoseismal area shows that they are very serious in the villages on the downthrown block, and particularly in those that are located along the NE - SW trending Aliakmon fault. It means that the villages which are located on the hangingwall of the fault have been affected by more intensive deformation than those located on the footwall.

• The Aliakmon fault shows a great similarity to several other normal faults trending NE - SW which have been investigated some years ago by the Laboratory of Geology at the University of Thessaloniki in the Ptolemais basin, which is located north of the Kozani area. All these faults have been recognized as neotectonic - active ones with very recent Holocene activity *(Pavlides 1985, Pavlides and Mountrakis 1987)*. The neotectonic faults have been created by the widespread extensional stress field with the principal axis (3 trending NNW - SSE *(fig. 3)*.

During the earthquake of 13 May many surface fractures were formed in the epicentral area, particularly along the Aliakmon fault in between the villages of Rymnio, Palaeochori, Sarakina, Kentro and Nisi. Surface fault traces that are believed to be directly associated with the main seismogenic fault were observed affecting the unconsolidated sediments in the area of the village of Rymnio (NE edge of the rupture zone). Liquefaction phenomena were observed along a wide zone more than 2 km in length at the southern shore of the Polyfytos artificial lake, near the village of Rymnio following approximately the strike of the main seismic fault *(fig. 5)*. Many sand and mud volcanoes were formed in the same area, showing orientation of their elongation axis N 45° to N 100°.

The most impressive surface ruptures however, were formed along the Palaeochori - Nisi part of the fault, and especially near the villages of Palaeochori, Sarakina, Kentro and Nisi, affecting ophiolites, molassic sediments, Plio-Pleistocene and recent deposits. The Palaeochori - Sarakina fault forms a very characteristic scarp within the molassic sediments and the Plio-Pleistocene deposits *(fig. 6)*. The total length of these fracture lines, consisting of surface ruptures, is about 15 km. The surface ruptures consist of open fissures (heaves 1 - 10 cm) with small displacement (1 - 15 cm) of normal slip (dip towards NW).

This tectonic line, consisting of surface ruptures and trending NE - SW (N 75°) coincides with the focal mechanism solution that suggested a fault striking N 70°. Thus, the seismogenic fault must be a segment of the Aliakmon river fault in between t he villages of Rymnio, Palaeochori, Sarakina, Kentro and Nisi.

The total length of the of the reactivated segment is about 30 km from Rymnio to Nisi villages. The Servia fault segment, that is the northeastern part of the Aliakmon fault, was not reactivated during the 13 May earthquake. However, it is an impr essive typical normal fault (ENE - WSW strike, dip 80° towards the NW) that affects crystalline limestones and gneisses in the southern part of the Kozani basin with very recent (Holocene) reactivation. The faulted Holocene scree of previous tectonic events confirm this recent reactivation *(fig. 7)*. This fault segment is characterized by very steep scarp slopes, fresh reactivated slickensides and new uneroded fault traces. These characteristics show that this segment is an active fault as well. It is separated from the segment of Rymnio - Palaeochori - Sarakina - Nisi, which was reactivated on 13 May, by a geometrical barrier which is a point where the fault traces form an angle between them *(fig. 5)*. This geometrical barrier can be considered as a seismic segment barrier as has also been shown by the distribution of the foreshock and aftershock sequence *(Papazachos et al. 1995)*.

Besides the ground ruptures along the main seismic fault of Aliakmon river (Rymnio - Palaeochori - Sarakina - Nisi), some other ground ruptures were formed in smaller antithetic normal faults trending NE - SW or E - W and dipping to the South. A series of antithetic surface fractures trending E - W and dipping to the South follows the aforementioned tectonic line of the Chromio - Varis Valley in the Vourinos ophiolitic corridor (the dextral strike-

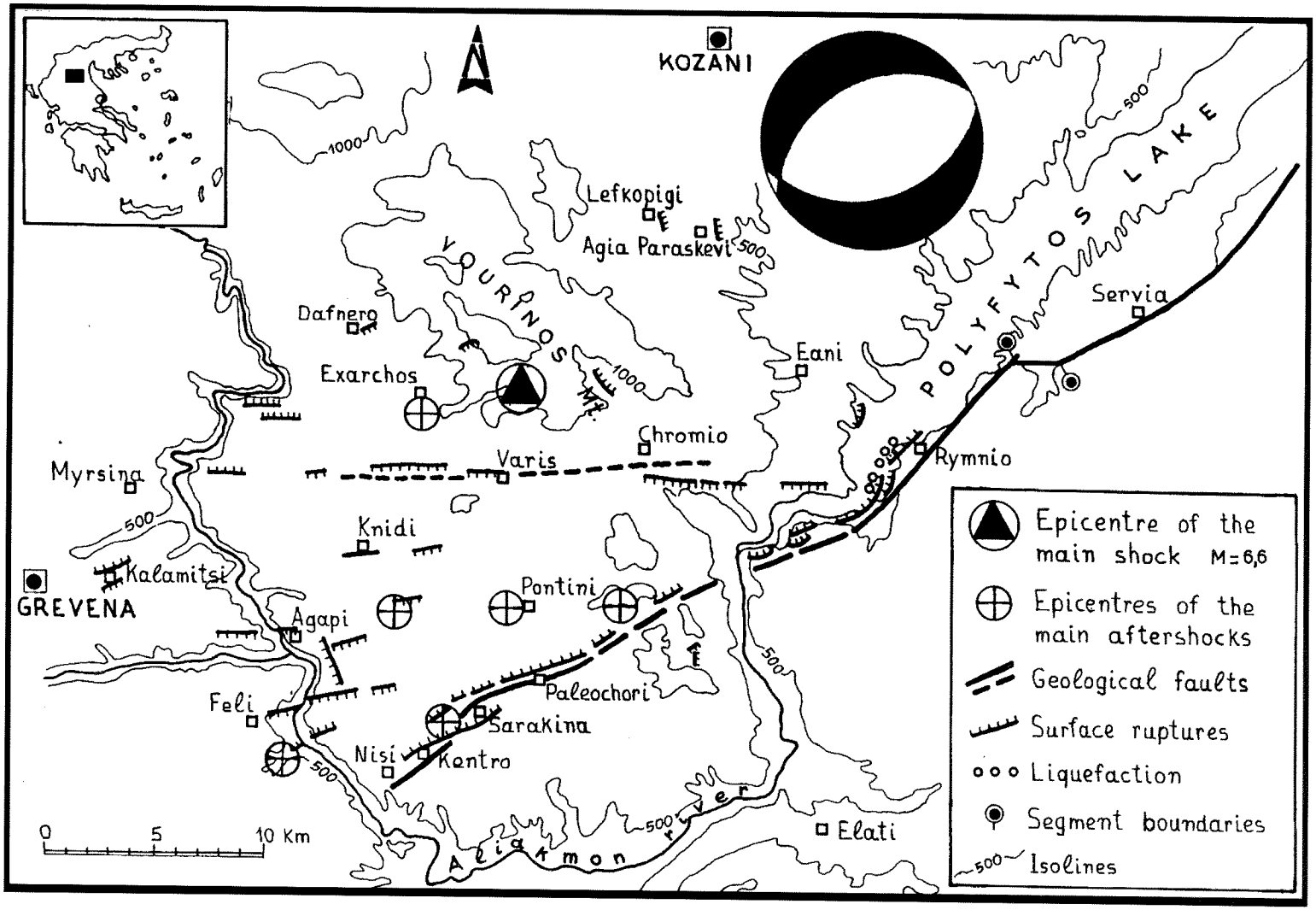

Fig. 5. Sketch map of the Kozani - Grevena meisoseismal area with the epicentres of the 13 May main shock and its main aftershocks, the main geological faults (the Aliakmon fault and the Chromio - Varis Valley strike-slip fault) and the recent ground ruptures. The liquefaction phenomena and the segment boundaries (geometrical barrier) between the Rymnio-Nisi segment and the Servia one (non-activated) are also shown. The sketch of the focal mechanism of the main shock was provided by the ERI auto matic CMT inversion of the Geological Society of Japan.

Fig. 6. Reactivation of the Rymnio - Palaeochori - Sarakina - Nisi fault affecting molassic and Plio-Pleistocene sediments. The picture shows the previous slickenside of the neotectonic fault on the molassic conglomerates near the village of Sarakin a and the downthrow of 15 cm which was produced during the 13 May 1995 earthquake.

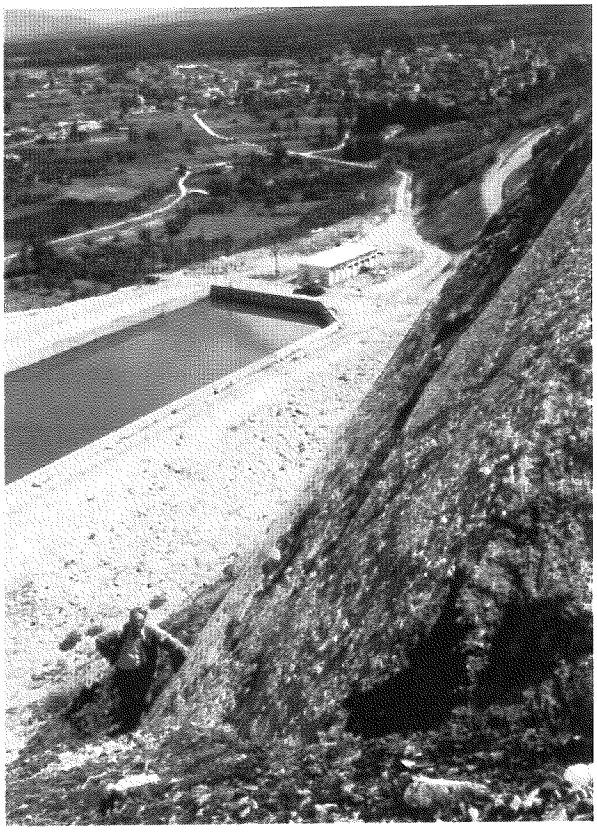

Fig. 7. The [Servia fault] segment of the Aliakmon river tevtonic line affecting in this location near Servia town Mesozoic limestones. The picture shows a very recent (Holocene) slickenside on red color scree material which has been produced during previous Quaternary reactivations of the fault, and covered the neotectonic slickenside on the Mesozoic limestones.

slip fault of the basement). The total length of this tectonic line is about 10 km, although it may extend westwards to the village of Kalamitsi where some very impressive ground ruptures were found, but without any observable connection with the fault traces of Chromio - Varis Valley.

Another very important antithetic fault was observed in the valley of Aliakmon river near the village of Felli. It is a neotectonic fault, trending ENE - WSW and dipping 80^{o} - 85^{o} to the SSE, with previous strike-slip activity which was reactivated as a normal antithetic fault during the May - June seismic sequence and produced displacement of about 15 cm and heaves 1 - 8 cm in the well consolidated molassic conglomerates.

Conclusions

The above mentioned geological and seismological data lead to the conclusion that the seismic fault which was activated and produced the earthquake of 13 May 1995 is a segment of the Aliakmon fault. The total length of this segment is about 30 km, starting from the geometrical barrier between Rymnio and Servia up to the villages of Palaeochori, Sarakina, Kentro and Nisi. This is an ENE - WSW trending normal fault dipping to the North and is the main seismogenic structure with high angle of dip at the surface and low angle at depth.

The strike-slip fault of Chromio - Varis cor-

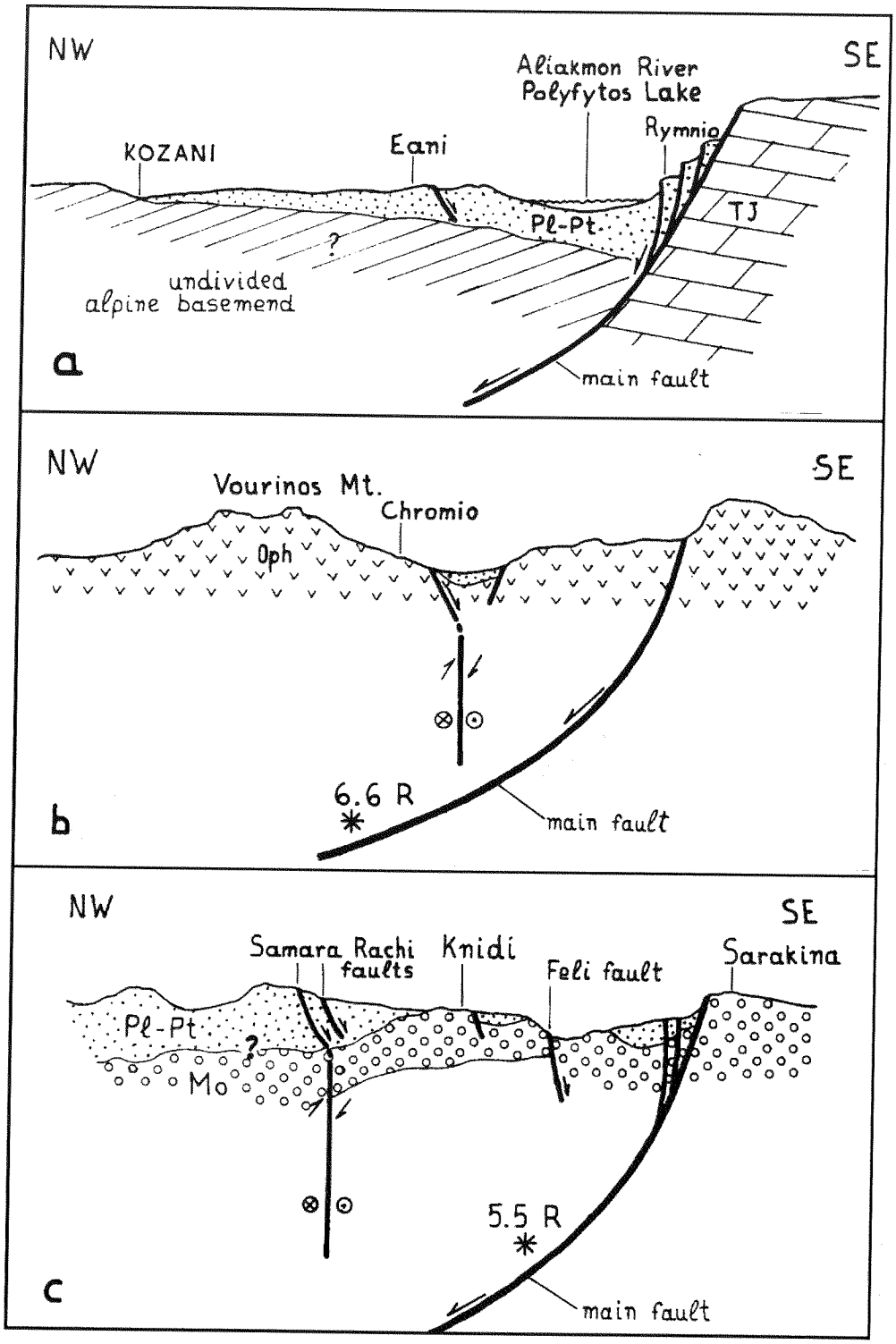

Fig. 8. Sketch of the possible geological model for the western Macedonia earthquake. Three simplified cross-sections through the epicentral area show the reactivation of the main neotectonic normal fault in between the v illages of Rymnio, Paleochori, Sarakina and Nisi, producing the main shock of 13 May (M = 6.6) and the aftershock of 11 July (M = 5.5). The dextral strike-slip fault of the Chromio - Varis Valley which has been detected by aeromagnetic research and w as reactivated as a series of small antithetic normal faults is also shown in cross sections b. and c. **Pl-Pt:** Plio-Quaternary continental deposits. **Mo:** molassic sediments. **oph:** ophiolitic rocks. **TJ:** Triassic - Jurassic limestones.

ridor at the basement was reactivated during the earthquake as a series of small normal antithetic faults trending E - W and dipping to the South and caused additional damages in the villages of Chromio, Varis and Knidi.

The epicentres of the aftershocks of the May - June sequence are distributed mainly on the hangingwall of the reactivated segment of the Aliakmon fault *(fig. 1, 2)* and they are associated with the surface faulting of the main fault and the antithetic faults.

A possible geological model for the geometry of the faults which were reactivated during the earthquake is shown with three simplified cross sections in *fig. 8.*

References

Brunn, J. H. (1956). Contribution à l' étude géologique de Pinde septentrional et de la Macèdoine occidentale., *Ann. Geol. Pays Hellen., 7, 1-358.*

Koufos G. D., Kostopoulos D. S. and Koliadimou K. K. (1991). Une nouveau gisement de mammifères dans le Villafranchien de Macèdoine occidentale (Grèce). *C. R. Acad. Sc. Paris, ser II, 313, 831-836.*

Mavrides, A., Skourtsis - Coroneou, V. and Tsaila - Monopolis, S. (1977). Contribution to the geology of the Subpelagonian zone (Vourinos area, West Macedonia). *In: VI Coll. Aegean region, I, 175-195.*

Mountrakis, D. (1983). Structural geology of the North Pelagonian zone s.l. and geotectonic evolution of the internal Hellenides. *Unpublished "Habilitation", University of Thessaloniki, Greece, 283pp (in Greek).*

Mountrakis, D. (1986). The Pelagonian zone in Greece: a polyphase deformed fragment of the Cimmerian continent and its role in the geotectonic evolution of East Mediterranean. *J. of Geology, 94, 335-347.*

Mountrakis, D., Kilias, A., and Zouros, N. (1992). Kinematic analysis and tertiary evolution of the Pindos-Vourinos ophiolites (Epirus-Western Macedonia, Greece)., *Bull. Geol. Soc. Greece (in press).*

Papazachos B.C., Panagiotopoulos D.G., Scordilis E.M., Karakaisis G.F., Papaioannou Ch. A., Karacostas B.G., Papadimitriou E.E., Kiratzi A.A., Hatzidimitriou P.M., Levendakis N., Voidomatis Ph. S., Peftitselis K. I., and Tsapanos T.M. (1995). Focal properties of the 13 May 1995 large (Ms= 6.6) earthquake in the Kozani area (north Greece). *Geophysical Laboratory, Aristotle University, Publ. No 4.*

Pavlides, S. (1985). Neotectonic evolution of the Florina-Vegoritis-Ptolemais basin (W. Macedonia, Greece). *Ph.D. Thesis, University of Thessaloniki, 265 pp (in Greek).*

Pavlides, S. and Mountrakis, D. (1987). Extensional tectonics of northwestern Macedonia, Greece, since the late Miocene. *J. Struct. Geol. 9, 4, 385-392.*

THE VIOLENT EARTHQUAKE OF THE MAY 13, 1995 AT KOZANI-GREVENA (NW GREECE)

D. Papanastasiou, G. Drakatos, I. Kalogeras, J. Papis, M. Kourouzidis and G. Stavrakakis

Institute of Geodynamics, National Observatory of Athens, 118 10 Athens, Greece

Abstract

At 08:47 GMT, on May 13, 1995, a strong earthquake of Ms=6.6 occurred in the north-west part of Greece and caused serious damages in the prefectures of Kozani and Gevena. The maximum observed macroseismic intensity was IX+ of the MM scale. The main shock was preceded by several foreshocks and followed by an intense aftershock activity.

Immediately after the main shock the Institute of Geodynamics of the National Observatory of Athens, (I.G), installed, in order to monitor the aftershock activity, a seismic network of nine (9) stations which operated for a period of 50 days. Thousands of aftershocks have been recorded. Their spatial distribution defines a zone o NNE-SWW trend, dipping to the NW. In the field a surface rupture of normal slip has been observeed following a NNE-SWW direction, for a length of 10 km.

The focal mechanism of the main shock as well as of some aftershocks recorded by the local network were determined showing also normal faulting.

Based on these observations, the temporal-spatial evolution of the earthquake sequence has been investigated.

Introduction

The area of Greece is part of the collision zone between the Eurasia and the African lithospheric plates. The majority of the earthquakes results from crustal extension and normal faulting and is not produced by slip along the plate contact which appears to be mostly aseismic (Jackson and McKenzie, 1988). The direction of extension is about north-south in the area of central and northern Greece.

The area of Kozani-Grevena (west Macedonia) has been considered as a region of low seismicity. The only known earthquake, during the historical period, that affected this region occurred in February 896 AD and destroyed the city of Veria located about 40 km NE of Kozani (Papazachos and Papazachou, 1989). During this century, 3 instrumentally recorded earthquakes (Makropoulos et al., 1989) eccurred close to the epicenter of the recent shock, those of 1922, Dec. 7 (40.01°N-21.51°E, Ms=5.5), 1943, Mar. 25 (40.41°N - 21.89°E, Ms=5.5) and 1984, Oct. 25 (40.11°N - 21,62°N - 21.63°E, MS=5.6).

The earthquake of May 13, 1995, occurred at 11:47 local time (08:47 GMT) on Saturday, so public offices and schools were closed. Some minutes before the main shock, some significant foreshocks preceded it and forced the inhabitants to evacuate and no human life was lost. On the contrary, the shock caused severe damages at the region south of the cities of Kozani and Grevena.

Immediately after the main shock, I.G. deployed a temporary seismic network of 9 stations - which operated for a period of 50 days - to monitor the aftershock activity. In this study the results of the spatial distribution and the focal mechanisms of the recorded aftershocks by the

Special Publications of the Geological Society of Greece, No 6.

portable network are presented. Moreover, tectonic observations collected in the field, results of the relocation and the focal mechanism of the main shock and macroseismic observations are given. Finally, a combination of seismological and tectonic observations has been made, in order to understand better the rupture process and the regional tectonics.

Geological and Tectonic Observations

The geology and the tectonics of the area of Kozani-Grevena has been studied by several researchers, among them, Brunn 1956, Pavlides and Mountrakis 1987, Johnes and Robertson 1991.

This area belongs to the Pelagonian geotectonic zone. The basement consists of Pre-Alpine and Alpine rocks like gneisses and schists and is covered by Triassic-Jurassic crystallized limestones, ophiolites, Cretaceous limestones and Tertiary flysch. These rocks are unconformably overlain by molassic sediments, conglomerates, sandstones, marls and silts of the Meso-Hellenic basin. The area is covered by lacustrine, fluvial and torrential deposits of Neogene age while over them Quaternary deposits of talus cones and extended fluvial terraces are present. These deposits show significant vertical and lateral variations.

Although this area has been characterized by low seismic activity, from neotectonic point of view is dominated by a NE-SE striking normal fault zone with a length of 80 km which bounds the southern bank of Aliaknom river as well as the southern shore of the Polyphyto artificial lake. The southern segment of this zone, the Servia fault, is trending N 60^{o} and dipping 60 towards the NW. This is the most prominent feature of the area and its front suggest that significant slip has occurred on this fault during the Holocene.

Immediately after the occurrence of the shock the epicentral area has been inspected for surface fault breaks. There was no any evidence of breaks around the major Servia fault, but a continuous break of 10 km length has been observed (Fig. 1) between the villages of Palaeokhori and Nision along a pre-existing N 70^{o}, striking NW dipping normal fault that cut the Miocene and younger sediments of the Meso-Hellenic basin. The break consisted of open fissures and small scarps with 2-4 cm of normal slip. On the northeastern extension of the same fault system a third segment about 5 km long may also ruptured in peridotic rocks.

The earthquake caused liquefaction at some places around the Polyphyto artificial lake and triggered small scale landslides, rock falls and slumps while many fissures of non tectonic origin were observed throughout the epicentral area.

Mainshock and foreshock on May 13, 1995

Mainshock and foreshock on May 13, 1995.

The mainshock occurred at 08:47 GMT and preceded by som significant foreshocks (3.5< magnitude <4.5) the latest of them occurred about 15 sec before the main event. Their routine locations given by I.G. have fixed depths as the solutions did not converge. In order to obtain more accurate locations and especially resolved focal depths, the main shock and the foreshocks have been relocated by including in the data set arrival times from nearby stations belonging to the network of the Public Power Corporation, located around the Polyphyto artificial lake, and by introducing revised stations corrections for the permanent network of I.G. The corrections were obtained by comparing the solutions of 54 well located aftershocks (M≥3.0) by the local temporary network and recorded also by the permanent network.

The obtained relocated position for the main shock (Fig. 1) is 40.11^{o}N - 21.67^{o}E, with a depth of 16 km. The minimum standard errors were 0.2 sec for RMS, 2 km and 2.5 km for horizontal direction (ERH) and the depth (ERZ) respectively. This solution is very close to that one given by Harvard University (40.08^{o}N - 21.68^{o}E, at a depth of 16 km). The solutions given by NEIC and by Geophysical Laboratory of the University of Thessaloniki are located about 6 km to the north from the relocated solution and with shallower depths (Fig. 1).

For the main shock, the record of a three-component strong motion instrument (SMA-1) operated at the town of Kozani shows a time difference of 4.4 sec between the S arrival and the triggering time (Lekidis and Theodoulidis,

1995). Assuming a mean P velocity, larger than 5.5. km/sec, and a V_p/V_S ratio of 1.78, this time difference implies that the hypocentre of the main shock should be located at a minimum distance of 31 km from the city of Kozani. So, the relocated hypocentre is in good agreement with this remark.

Recording and analysis of aftershocks

As mentioned above, a portable seismic network was deployed after the occurrence of the main shock. Before the noon of the next day, the whole network was in operation. This network consisted from 8 smoked paper instruments (Sprengnether MEQ. 800) equipped with 1 Hz vertical seismometers domplemented by the permanent station of I.G. in Kozani (Fig. 1).

The aftershock activity was continuously monitored for a period of 50 days, from May 14 through July 4. During the first week after the main shock, more than 1.000 events of Ml>1.5 were recorded per day.

No detailed information about the velocity structure of the area was available. Thus, in order to find a reliable velocity model, 74 well recorded aftershocks were selected, with more than six (6) P wave and two (2) S wave readings and with a magnitude of Ml≥3.0. This set would be a representative sample all the aftershocks both in location and depth. The events were relocated first at different half-space models and then at layered velocity models. Every time the standard errors (MRS, ERH, ERZ) were checked. The final chosen velocity model, yields a smaller RMS than any one of the tested models. The model consisted of 4 layers with upper bounds at 0 km, 10 km, 20 km and 40 km with P velocity of 5.5, 6.0, 6.5 and 8.0 km/sec respectively. For the velocity of S waves the ration of 1.78 was adopted.

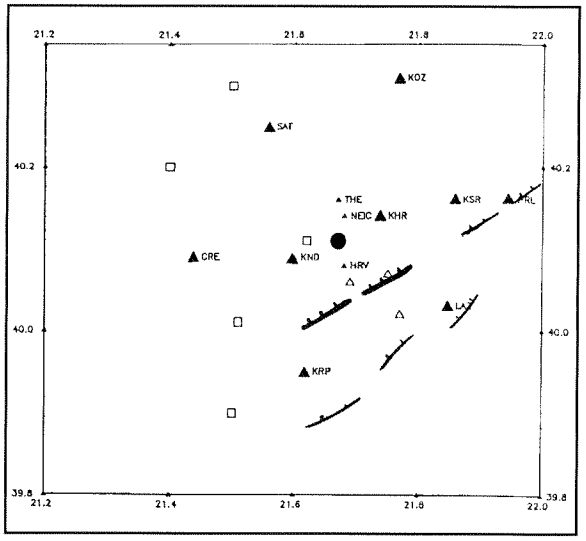

Fig. 1. Solid triangles with names show the local seismological network. Solid circle gives the relocated position of the main shock. Open triangles with names are the location of the main shock according to the named centre. Squares are the earthquakes occurred during this century. Triangles are the foreshocks. The location of the Servia fault zone (thin barbed line) and the observed surface breaks (thick barbed line) are also shown.

Aftershock distribution

The network provided a good coverage of the aftershock area and allowed for well resolved hypocentres and reliable individual focal mechanism determination. 800 events were selected and located on the basis of having at least five (5) P wave and one (1) S wave readings (Fig. 2).

The events were located by using the Hypo71 computer program (Lee and Lahr, 1975). In

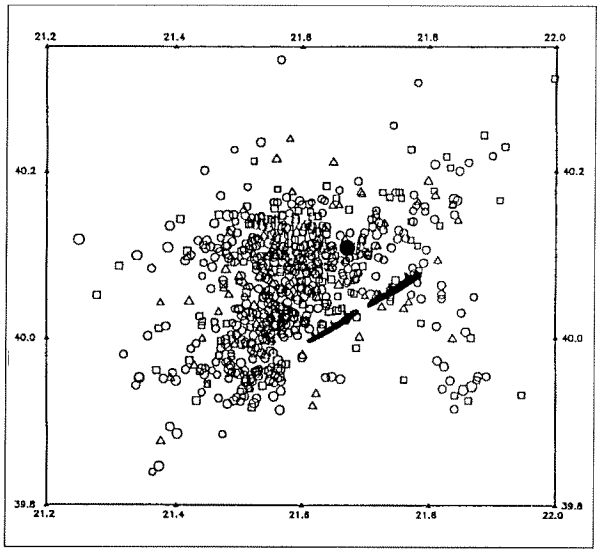

Fig. 2. Map view of the 800 located aftershocks. Heavey line is the observed surface rupture. Solid circle gives the location of the main shock.

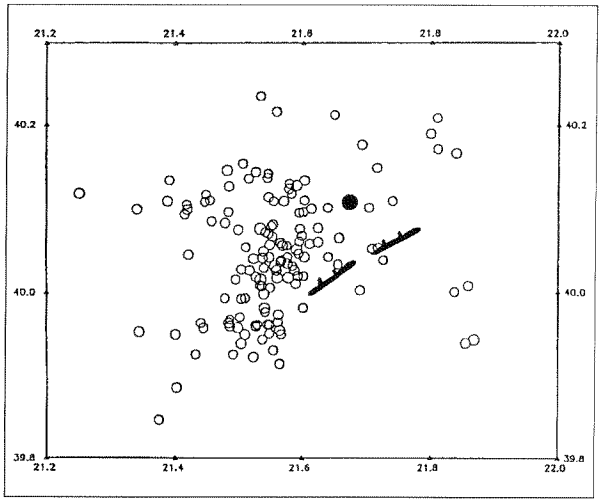

Fig. 3. Map view of the 150 best located aftershocks. Heavy line is the observed surface purture. Solid circle gives the location of the main shock.

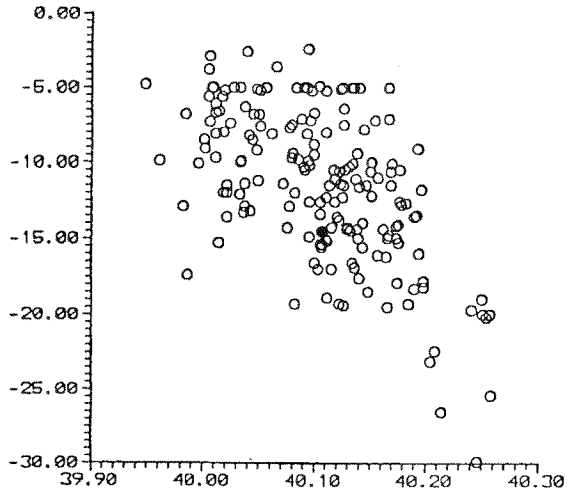

Fig. 4. Cross section perpedicular to the surface break. Solid circle gives the location of the main shock.

order to get an aftershock catalogue with precise locations and homogeneous distribution, 140 events were selected that had at least six (6) P and two (2) S readings and standard errors RMS < 0.2 sec, ERH <1.5 km and ERH < 2.0 km. This set of aftershocks is plotted in Fig. 3. The aftershocks cover an area of about 40 km by 20 km.

The majority of the events is located south east of the position of the main shock and north of the observed surface breaks. Thereis also a smaller cluster southeast of the termination of the surface rupture. Between the two clusters there is a gap which is not very clear defined.

On a cross section (Fig. 4) perpendicular to the fault trace, themain cluster appear as a clear northwestward dipping zone, while the majority of the aftershocks are located in the depth range of 20-20 km.

Focal mechanisms

By using P wave polarities from the permanent network of I.G. and those provided by the International Agencies, the fault plane solution for the main shock was determined. The solution (Fig. 5) is related with pure normal faulting on planes having directions N 240^{o} and N 72^{o}, dipping 35^{o} to the NW and 56^{o} to the SE respectively. The first plane coincides with the geometry of the surface faulting.

The CMT solution determined by Harvard suggests also a pure normal faulting. One plane is trending N240^{o} and dipping 31^{o} to the NW and the other one is trending N70^{o} and dipping 59^{o} to the SE almost identical like the mechanism determined in this study.

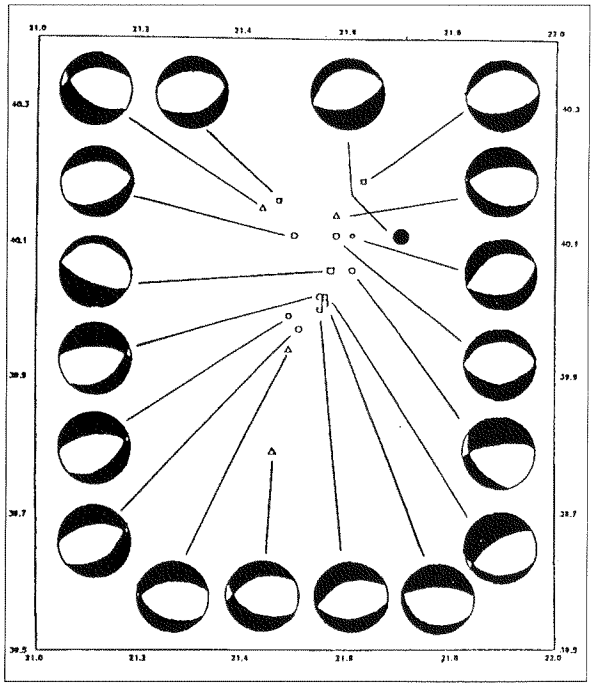

Fig. 5. Determined fault plane solutions. Solid circle gives the location of the main shock.

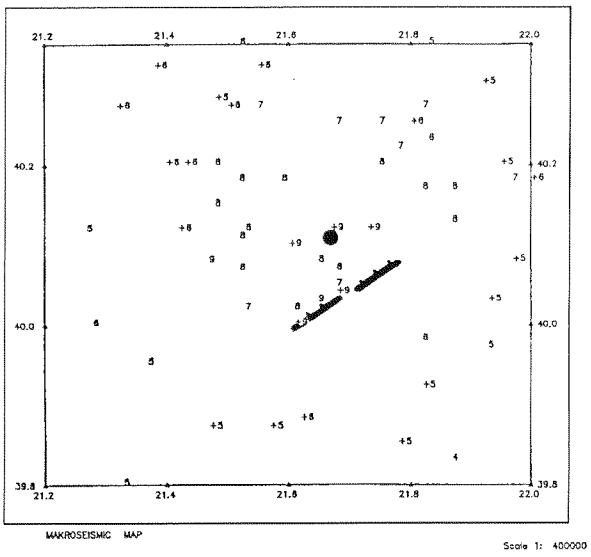

Fig. 6. Map showing the distribution of the makroseismic intesities. Heavy line is the observed surface rupture. Solid circle gives the location of the main shock.

For the determination of the focal mechanisms of the afterschocks the polarities of the local stations were used, while for some strong aftershocks polarities from the nearby permanent stations were additionally used. The solutions of 17 (Fig. 5) well constrained mechanisms are presented. All the solutions show normal faulting and one of the fault planes has a NE-SW direction and dips towards the NW.

Macroseismic information

Macroseismic information was selected from a questionnaire which sent to the villages of the affected area. The results are given on the Modified Mercalli (MM) scale (Fig. 6). The maximum intensity (IX+) was observed in the southern and southwestern part of the epicentral zone where the most of the damages were observed and some of the villages were completely or partly destroyed.

The distribution of the damages is very heterogeneous not only in the same village but also at different villages located very close and their macroseismic intensities differs considerably. This probably is due to site effect as the region is not homogeneous and appears strong vertical and lateral variations.

Conclusions

The purpose of this paper is the study of Kozani-Grevena earthquake sequence, on May 13, 1995, using local instrumental data and field observations. Although the study is still in progress some preliminary results are presented here.

The distribution of the aftershocks, not only on the surface but also in depth and the determined focal mechanisms of the main shock as well as of some aftershocks are in good correlation with the observed surface rupture.

These observations confirm that the earthquake caused by the reactivation of an existing fault, located at the southwestern extremity of the Servia fault zone. The reactivated fault has a N 70^{o} direction, dipping about 60^{o} to the NW.

The majority of the aftershocks are located at the north of the fault, on the hanging wall between 10 and 20 km in depth. The foreshocks and the main shock occurred at the northern extremity of the aftershock zone, indicating that the rupture initialized at that part and propagated southwest afterwards.

The observed length of the rupture and the vertical displacement as well as the calculated by Harvard seismic moment ($7.6*10^{18}$ Nm) are smaller than those expected for an earthquake of this magnitude. Probably, these are evidence that the rupture did not reach the surface.

Unclear also is the relation of the small aftershock group located south of the observed rupture with the main aftershock distribution. Is this caused by another fault which is not expressed at the surface or it is stress variation at the termination of the main rupture?

All these are starting points for further studies.

Acknowledgments:

We acknowledge Greek Public Power Corporation for providing us with data from the Polyphyto Dam local seismic network.

References

Brunn J.H., 1956. Contribution a l' etude geologique de Pinde septentrional et de la Macedoine occidentale. Ann. Geol. Pays Hellen. 7 1-358.

Jackson J.A. and MacKenzie D.P., 1988. The relationship between plate motions and seismic tensors, and the rate of active deformation in the Mediterranean and Middle East. Geophys. J. Int. 93, 45-73.

Johnes G. and Robertson A.H.F. 1991. Tectonostratigraphy and evolution of the Mesozoic Pindos ophiolite and related units, northwestern Greece, J. Geol. Soc, Lond. 148, 288.

Lee W.H.K. and Lahr J.C., 1975. HYPO71. A computer programme for determining hypocenter, magnitude and first motion pattern of local earthquakes. U.S. Geol. Surv., Open fild rep., 75-311.

Lekidis B. and Theodoulidis N., 1995. The earthquakes in Kozani-Grevena, May 1995: Preliminary report about the strong ground motion and the behaviour of the structures. Geotechnical review, 73, 73-78.

Makropoulos C., Drakopoulos J. and Latoussakis J., 1989. A revised and extended earthquake catalogue for Greece since 1900. Geophys. J. Int., 99, 305-306.

Papazachos B.C. and Papazachou C.B., 1989. Earthquakes in Greece Zitti Publ. Thessaloniki.

Pavlides S., and Mountrakis D., 1987. Extensional tectonics of northwestern Macedonia Greedce, since the late Miocene. J. Struct. Geol. 9, 4, 385-392.

PRELIMINARY RESULTS OF THE CATASTROPHIC EARTHQUAKE OF THE JUNE 15, 1995 AT AIGIO (N. PELOPONNESUS)

D. Papanastassiou, J. Baskoutas, D. Makaris, G. Panopoulou and G. Stavrakakis

Institute of Geodynamics, National Observatory of Athens, 11810 Athens, Greece

Abstract

At 00:15 GMT, on June 15 1995, a catastrophic earthquake of Ms=6.1 struck the area of Aigio. Twenty-six persons have been killed and serious damages have been also caused in the broader area of the Aigio city, in its environs, as well as at the northern coast of western Corintiakos Gulf. The aftershock activity continued for several weeks.

Following the main shock, the Institute of Geodynamics of the National Observatory of Athens (I.G.) installed a portable seismic network in order to monitor the aftershock activity. The spatial distribution of the aftershocks and the obtained focal mechanism of the main shock were in accordance to the seismotectonic observations, which have been performed in the field.

All the seismological data and the seismotectonic observation are discussed in order to understand the physical and tectonic properties of this earthquake sequence.

Introduction

The Gulf of Corinth has a form of an asymmetric half graben with an uplifted souther footwall and downward flexed northern hangingwall with minor antithetic faults. This is very clear when looking at the shape of the coastline which is sharp and linear in the south and sinuous with many peninsulas in the north. A series of normal faults (Psathopyrgos, aigion, Helice and Hylokastro) bound the high relief along the southern coast and enter eastward into the sea.

Several large earthquakes have destroyed the area of Aigion in the past, like the earthquakes of: 373 BC, 23 AD, 1403, 1748, 1817, 1861 and 1888 (Galanopoulos, 1960; Papazachos and Papazachou, 1989). It is difficult to assign which fault was ruptured during every earthquake. Those of 373 BC (Marinatos, 1960; Mouyaris et al., 1992) and 1861 accompannied by significant vertical displacement, while those of 1748, 1817 and 1888 caused severe damages mainly in the area of Aigion exactly like the studied earthquake. The epicenters of those historical earthquakes are plotted in Figure 1. In the same figure the instrumentally recorded earthquakes during this century (Makropoulos et al., 1989) are also given.

On June 15, 1995 an earthquake, Ms=6.1, occurred in the area of Aigion, at 00:15 GMT. Twenty-six people have been killed because of the collapse of two buildings in the Aigion area while extensive damage have been observed at Aigion and Eratini (northern coast of Corintiakos Gulf).

Following the main shock, I.G. deployed a temporary seismic network of 4 stations which operated for 15 days, in order to monitor the aftershock activity. In this study the results of the spatial distribution of the recorded aftershock by the portable network as well as tectonic observations collected in the field are presented. Finally the seismological and tectonic observations and the rupture process is discussed.

Special Publications of the Geological Society of Greece, No 6.

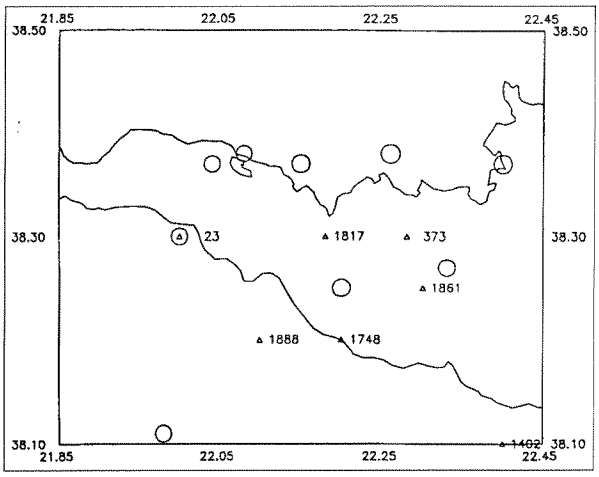

Fig. 1. Seismicity map of the western Gulf of Corinth. The historical earthquakes are denoted by triangles with the corresponding year of occurrence, while circles represent the instrumentally recorded earthquakes during this century.

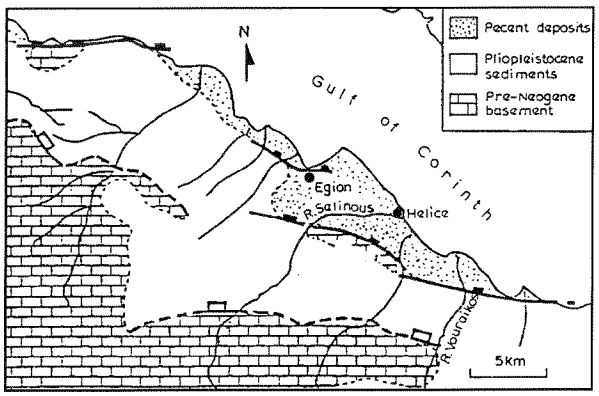

Fig. 2. Simplified geological map of the area of Aigio. The active faults of Psathopyrgos, Aigion and Helice, are given by continuous thick line. The less active faults located at the south are shown by broken line.

Geology - Tectonics of the area

The geology and the neotectonic of this area has been studied by several researchers, among them Dufaure (1975) and Poulimenos (1993). The southern coast of the western part of Gulf of Corinth is controlled by a number of right stepping, fault segments. These faults (Psathopyrgos, Aigion, Helice and Xylokastron) have onshore lengths between 10-25 km, strike of N90°-100°E on the average and dip towards the north of about 50°-60° near the surface. To the south, older and apparently inactive faults are mapped (Fig. 2) with similar trend.

Two limestone basement ridges occur in the footwalls of the coastal faults, while between the faults exist thick Plio-Pleistocen sediments mostly of fluvial - lacustrine and fan-delta deposits, alluvial conglomerates, consolidated marls and sandstones.

Just after the main shock the epicentral region has been examined for surface rupture. Although non tectonic slumps, fissures and landslides were abundant along the northern and southern coasts of this part of the Gulf, tectonic rupture on faults appears to have been limited to a fairly continuous break along the N 100°E striking, north dipping Aigion normal fault. The break consisted of open fissures and small scarp with normal slip up to 4cm. A total rupture of a length of at least 3 km observed between the villages of Agios Konstintinos on the west and the city of Aigion on the west.

Main shock on June 15, 1995

The main shock of Ms=6.1 occurred at 00:15 GMT (02:15 local time) without foreshock activity, while the largest aftershock, Ms=5.7, occurred just 15 minutes later. I.G. located the main shock at the northern coast of the Gulf of Corinth (38.37°N-22.15°E) at a depth of 26 km. This location gives a distance about 30 km from the city of Aigion.

For this shock the record from a three-component stro g motion instrument (SMA-1), belonging tc .G. and operated at the town of Aigion, sh. vs a time difference of 2.7 sec. between the S arrival and the triggering time. Assuming a mean P velocity larger than 5.5. km/sec. and a V_p/V_s ratio of 1.78, this time difference imply that the hypocentre must located at a minimum distance of 20 km from the city of Aigio and the depth of the earthquake should be shallower that 26 km.

The location given by NEIC (38.40°N-22.27°E) is moved about 12 km to the east, while Harvard's CMT location (38.17°N-22.36°E, with a depth of 17 km) 40 km SE of I.G.'s location. Harvard gave for the shock the seismic moment of 5.7 * 10^{18}Nm.

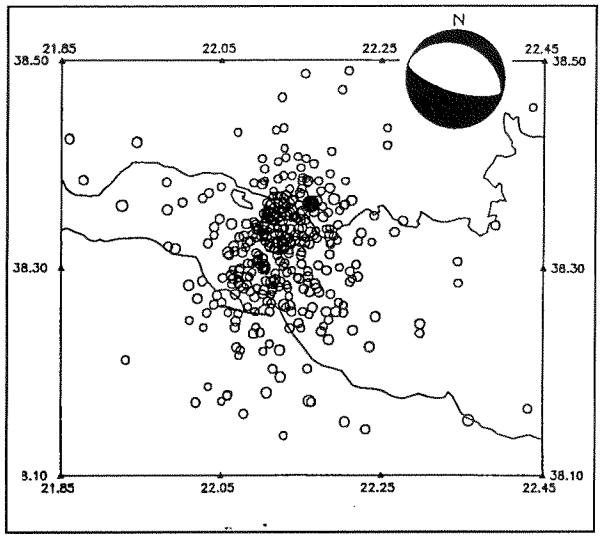

Fig. 3. Map view of the 359 selected aftershocks. Heavy line is the observed surface rupture. Solid circle gives the location of the main shock. The fault plane solution for the main event is also shown.

Analysis - location and distribution of the aftershocks

I.G., in order to monitor the evolution of the aftershock activity, operated in the epicentral region a temporary network of four (4) station from the 16th of June through the end of the month. The instruments were Sprengnether, MEQ-800 equipped with 1 Hz vertical seismometers. The network was complemented by four (4) more stations located around the Gulf of Corinth, from the permanent national network.

For the velocity structure a model consisting of seven layers proposed for this region by Rigo (1994) was adopted and the value 1.78 for the ratio V_p/V_s was used. The events were located by using the Hypo71 computer program (Lee and Lahr 1975).

The network during the operation recorded more than 1.000 events with Ml≥1.5 and 359 of them, recorded at all the local stations, were selected and located. This set of aftershocks is plotted in Fig. 3. The min bulk of the aftershocks is located north of the observed rupture and west of the location of the main shock. Their spatial distribution covers an area of 25 km by 20 km. The majority of the aftershocks is located at depths shallower than 20 km. On a cross section, of a group of 150 well located aftershocks with Ml>2.5 (Fig. 4) perpendicular to the fault trace, the aftershocks till the depth of 10 km appears as a zone dipping streply to the north, while for the rest 15 km the zone is less steep showing a dip of about 60°.

Fault plane solutions

By using P-wave polarities from the permanent network of I.G. and those provided by the International agencies the fault plane solution for the main shock was determined (Fig. 3). The solution is related to normal faulting. The planes have directions N104° and N290°, dipping 56° to the SW and 35° to the NE respectively. The second plane has the same direction with the surface faulting observed at the field. There is only a difference between the dip observed on the onshore faults (about 50°) and that one 35° calculated from the focal mechanism.

The CMT solution determined by Harvard is also of normal faulting. One plane is trending N88° and dipping 57° to the SW and the other one is trending 283° and dipping 34° to the NE. This solution is very similar with the obtained in this study.

The limited number of the temporary stations did not allow the plotting of fault plane solutions for the aftershocks. Nevertheless the majority of the existing polarities occypy positions around the center of the focal sphere. This means that the aftershocks may have focal mechanisms showing also normal faulting.

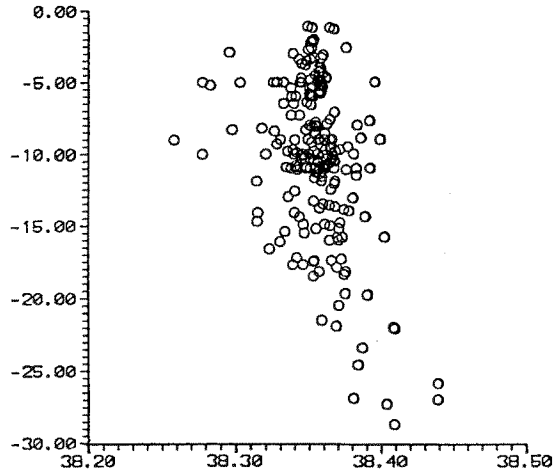

Fig. 4. Cross section of 150 well located aftershocks perpendicular to the fault trace.

Conclusions

The earthquake of June 15, 1995, took place in the western part of the Gulf of Corinth, a seismicaly active area where known large active faults are clearly expressed in the topography.

The main shock located at the eastern extremity of the aftershock zone, at a depth shallower than 20 km, indicating that the rupture initialized at this part and then it propagated westwards. The observed small length of the rupture as well as the small vertical displacement are also facts that the focus of the earthquake could not be located very deep because, at a different case the rupture, couldn't reach easily the surface.

The observed bend in the vertical cross section of the aftershocks and the steeper distribution of them with depths shallower than 10 km, it is possible to result from the network geometry as the majority of the local stations were installed at the area of north Peloponnesus. The bending of the aftershock distribution in depth, is also an evidence that the fault is flatten in depth. This is in accordance with the small dip obtained from the focal mechanism of the main shock, as well as with the results from other studies performed in this area (Rigo, 1994).

The presented results concerning the spatial distribution of the aftershocks, the focal mechanism of the main event are in good correlation with the seismotectonic observations performed in the field. All these evedence strongly support the aspect that this earthquake caused by the reactivation of Aigion fault.

References

Dufaure J.J., 1975. La relief du Peloponnese. These d'etat, Paris.

Galanopoulos A., 1960. A catalogue of shocks with $I_o \geq VI$ or $M \geq 5$ for the years 1801-1958. Seismological Laboratory, University of Athens.

Galanopoulos A., 1961. A catalogue of shocks with $I_o \geq VII$ for the years prior to 1800. Seismological laboratory, University of Athens.

Lee W.H.K. and Lahr J.C., 1975. Hypo-71, a computer program for determing hypocenter, magnitude and first motion pattern of local earthquakes. U.S. Geol. Surv., Open file rep., 75-311.

Makropoulos C., Drakopoulos J. and Latoussakis J., 1989. A revised and extended earthquake catalogue for Greece since 1900. Geophys. J. Int., 99, 305-306.

Marinatos S. 1960. A submerged town of classical Greece. Archaeology, 133, 186-193.

Mouyaris N., Papastamatiou D. and Vita-Finzi C., 1992. The Helice fault. Terra Nova, 4, 124-129.

Papazachos B.C. and Papazachou C.B., 1989. Earthquakes in Greece Zitti Publ. Thessaloniki.

Poulimenos G., 1993. Tectonics and sedimantation in the western Corinth graben. N. Jb. Geol. Palaeont. Mh. 10, 607-630.

Rigo A., 1994. Etude sismotectonique et geodesique du Golfe de Corinthe (Grece). These de Doctorat de l' Universite Paris VII.

Schmidt J., 1879. Studien uber erdbeben, Leipzig, 68-93.

SEISMICITY, SEISMOTECTONICS AND ACTIVE FAULTING

SOME ASPECTS OF SEISMICITY OF ALBANIA

Sulstarova Eduard

Intistute of Seismology, Tirana, Albania

Abstract

Data from the revised and complete Albanian Catalog for period 1901-1993 and atlas of 200 isoseismal maps of earthquakes occurred in our territory for the period 1800-1990 were used for the study of some characteristics of seismicity of Albania: macroseismic field effects, macroseismic field parameters, relation between macroseismic and instrumental parameters and distribution of seismicity in space and time.

I. Macroseismic field and relation between macroseismic and instrumental parameters

Studies of macroseismic field parameters and seismic active zones have been undertaken in Albania using different approaches (Sulstrarova E., 1974; Sulstrarova E., Koçiaj S., 1975; Sulstarova E., 1986, Sulstarova E., 1993 and Sulstarova E., Pitarka A., 1993). The recent establishment of data bank of the digitized isoseismal maps of earthquakes made possible a new study of macroseismic field effects, definition of the hazard ones by using the isoseismal maps, study of intensity attenuation for our territory in different directions of propagation; relation between macroseismic and instrumental parameters, etc.

From 200 isoseismal maps in our data bank there were selected 150 maps with epicentral intensity $I_0 \geq$ V degree MSK-1964 scale. The V degree has been chosen as the lower limit as it corresponds to the lowest intensity which can be evaluated with a certain degree of confidence from the damage caused to the building. Based on the methodology described in our last publication (Sulstarova E., Pitarka A., 1993), we compiled some maps of macroseismic field effects for intensity V, VI, VII and the map of cumulative of macroseismic effect **(Fig. 1).**

In the map of cumulative of macroseismic effects (Fig. 1) can be distinguished five dangerous zones, where index c is greater than zero or intensity VIII degree is felt, as the coastal area (in the region of Vlora, Saranda, Tepelena, Durresi and Shkodra) and the zone of Korça, Pogradeci (Ohrid Lake) and Peshkopia (Dibra zone). The use of the digitised isoseismal maps of large earthquakes occurred in the territory of Albania and this method will be very useful for the new seismic zonation of our territory which has already begun.

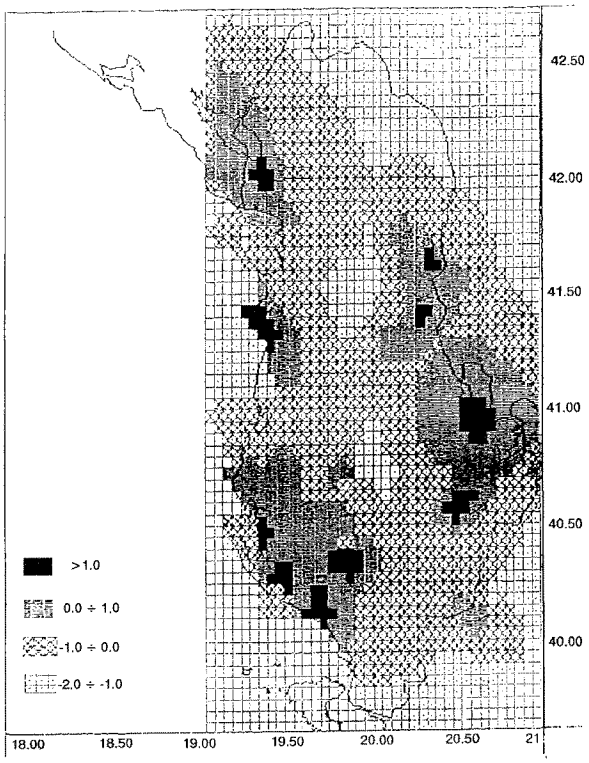

Fig. 1. The map of cumulative of macroseismic effect of intensity VII degree MSK-196.

MAP OF EARTHQUAKE OF ALBANIA
FOR THE PERIOD 1901-1987
For the Period 1901-1970 M>=5.0, and
1971-1987 M>=4.0

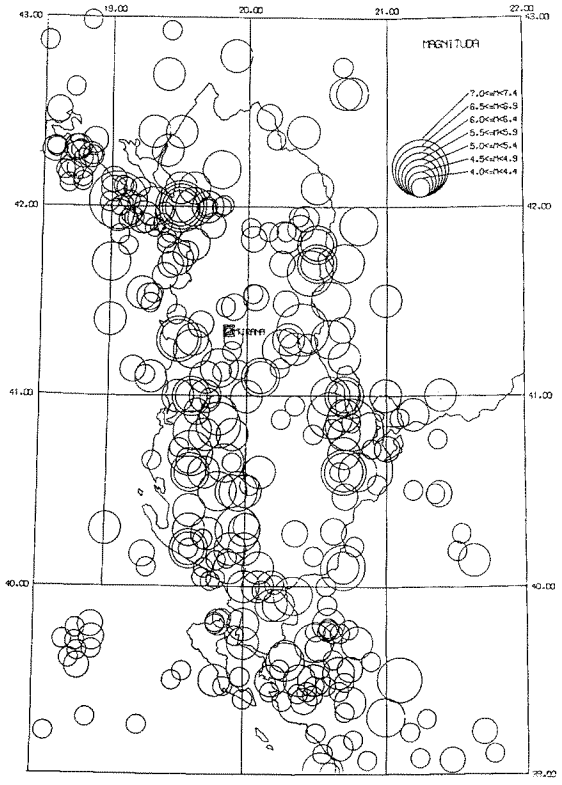

Based on the Blake model (1941) for macroseismic field and on statistical analysis the following relations between macroseismic and instrumental parameters are found:

$$M_s = 0{,}53\ (\pm 0{,}01) I_0 + 1{,}46\ (\pm 0{,}12) \quad (1)$$

$$I_0 = 1{,}97\ M_s - 3{,}06 \log h - 0{,}61 \quad (2)$$
for $h < 10$ km; $4{,}0 \le M \le 7{,}5$;

$$I_0 = 1{,}75\ M_s - 4{,}55 \log h + 3{,}45 \quad (3)$$
for $h < 10$ km; $4{,}0 \le M \le 7{,}5$;

As average:

$$I_0 = 2{,}1\ M_s - 4 \log h + 0{,}44 \quad (4)$$

In the cases of historical earthquakes where macroseismic data exists, the following formula is adopted for the calculation of macroseismic magnitudes:

$$M_{mac} = \frac{1}{b}(I_i + \gamma \log D_i + c); \quad (5)$$

where: D - hypocentral distance; I_i - seismic intensity; γ - coefficient of seismic intensity attenuation (average for our country $\gamma = 4$) b and c - coefficients (average b = 2,1; c = 0,44; see formula 5).

When $D_i >> h$ and the seismic intensity of the corresponding isoseist is 2 degree and smaller that epicentral intensity, $D_i \approx \Delta_i$, is a good approximation. It is observed that in the cases when accurate values of γ, b and c coefficients are obtained, the magnitude (M_{mac}) is equal to instrumental one (M_s), calculated according to formula (5). Considering these relations we come to the conclusion that in Albania and in the surrounding area, shaking of 6, 7, 8 and 9 degree of MSK-1964 scale are caused respectively by earthquakes of magnitude $M \ge 4{,}9$; $M \ge 5{,}2$; $M \ge 5{,}8$ and $M \ge 6{,}4$. For our territory and surrounding we found the relation between the length of an earthquake source (length L), magnitude M_S, seismic moment (M_0) and magnitude of surface waves (M_s):

$$\log L(km) = (0{,}46 \pm 0{,}05) M_S - (1{,}59 \pm 0{,}34) \quad (6)$$

Based on the relation (6) for the range of magnitude M=6, 0-7, 0, the lenght of earthquake generation fault should be between 16 km and 45 km. For the earthquake of April 15, 1979, with magnitude $M_s = 7{,}2$ relation (6) gives a length 60 km, while from distribution of aftershocks area within first hours the lenght of generation fault was 70 km.

Based on 85 earthquakes occurred in Albania and surrounding area for the period 1963-1991, we found the relation between seismic moment M_0 (in dyn. cm determined by spectral analysis) with magnitude M_S:

$$\log M_0 = 1{,}191 M_0 + 17{,}898 \quad (7)$$

This relation is in quite good agreement with the determination by Kiratzi A.A., et al (1985) and Papazachos B., Papazachos C., (1989) for the earthquakes in Greece.

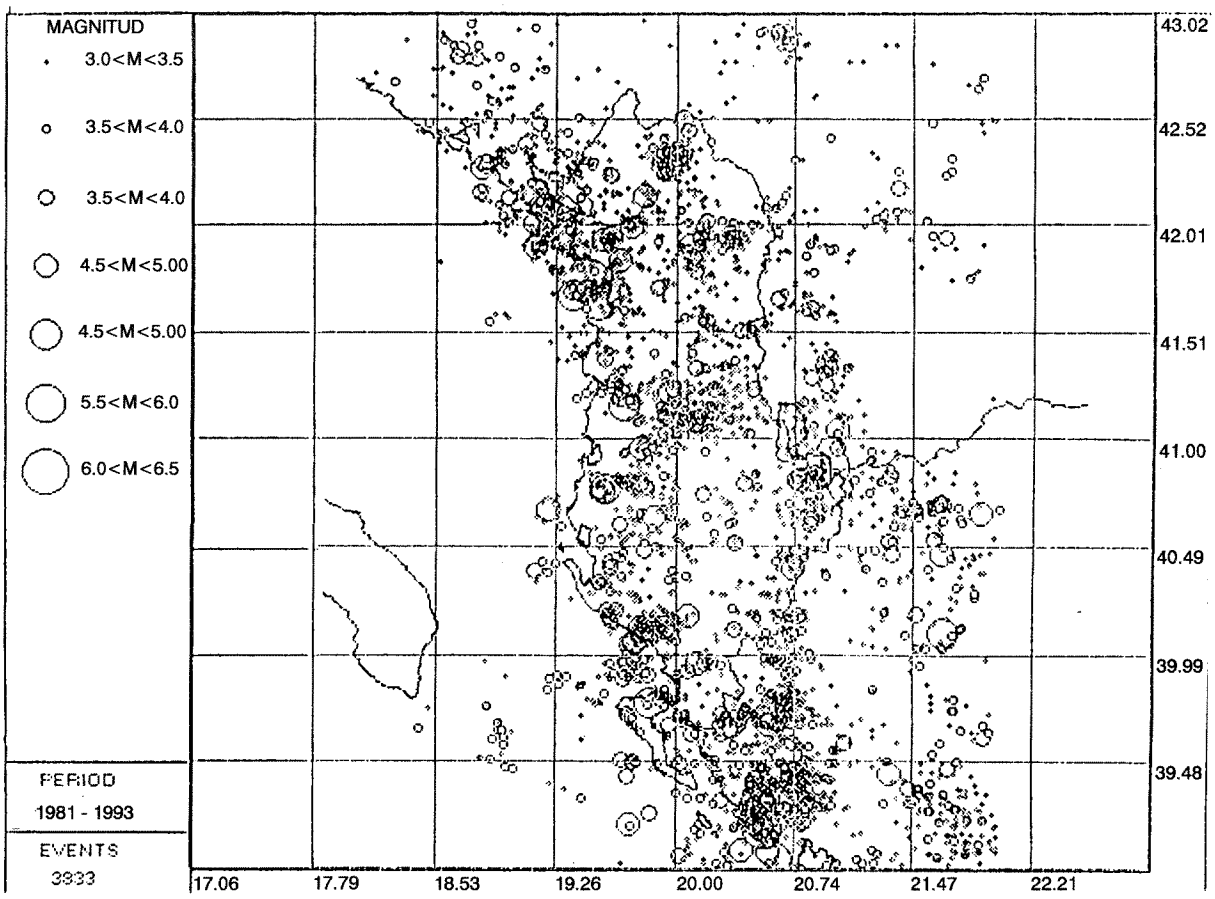

Fig. 3. Map of Earthquake epicentres of Albania for period 1981-1993.

II. Distribution in space and time of seismic activity and some pecularities

For the study of the distribution of seismic activity in space a series of maps of earthquake epicenters have been compiled (Sulstarova E., 1986, 1990, 1991). In this paper are presented two of them: The map of earthquake epicenters for the period 1901-1987 **(Fig. 2)** with two threshold magnitudes - $M_S \geq 5,0$ for period 1901-1970 and $M_L \geq 4,0$ for period 1971-1987, as well as the map of earthquake epicenters for period 1981-1993, $M_L \geq 3,0$ **(Fig. 3).**

From these maps it is clearly seen that earthquake foci are concentrated in the **Ionian - Adriatic** zone, along the Ionian and Adriatic coast, mainly in the external area of the Albanids and the vicinity where the "promontory" of Adriatic plate comes into collision with Albanids orogene; in **Korça - Ohri - Peshkopi (Diber)** along the **Drini fault zone** at the Eastern part of Albania (the internal area). These two seismic zones of NW-SE and N-S direction are intersected by Vlora - Elbasan - Dibra transversal belt are extended out of Albanian territory including the large part of Balcan region. Thus, the **Ionian - Adriatic seismogenetic zone** is extended along all the Adriatic and coast line and joins the Aegean are southward, while **Vlora - Elbasan - Diber** transversal belt continues tward Skopje up to Bulgaria.

Considering the epicenter map for the earthquakes of $M_L \geq 3,0$ for the period 1981 - 1993 (Fig. 3), it is obvious that in the zones where the strong earthquakes have occurred (in the two zones and belt mentioned above) weak earthquakes occur continuously, but in a greater number and frequency. This map also determines some other transversal lines, the most important of which is the transform fault of Shkodra - Peja in North Albania. By the focal mechanism solution of earthquakes occurred in Albania, two systems of seismic fault are distringuished: NW-

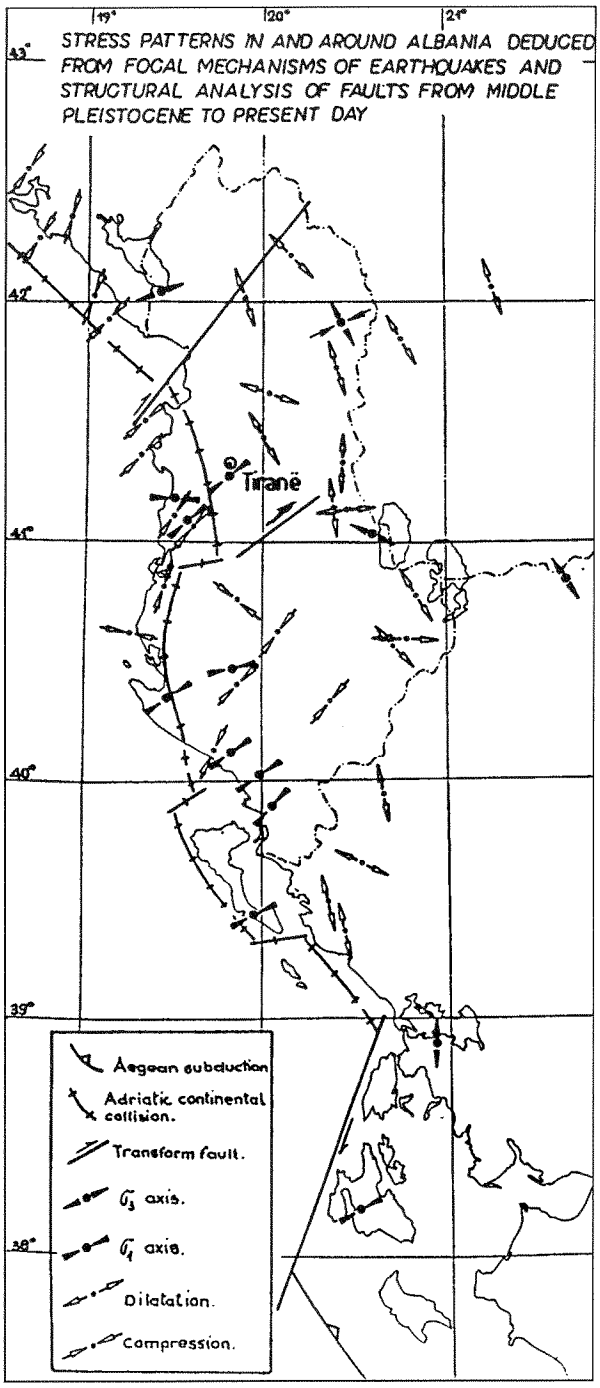

Fig. 4. Stress patterns in and around Albania deduced from focal mechanisms of earthquakes and structural analysis of faults from middle pleistocene to present day.

SE system, characteristic for external domain and NE-SW one (in eastern Albania NEN-SWS), characteristic for external domain and NE-SW one (in eastern Albania NEN-SWS), characteristic for external domain and transversal fault system. The focal mechanism solution (Sultarova E., 1974, 1980, 1986, 1987, 1988, 1991; and Muço B., 1992, 1994) and structural analysis of the faults from Middle Pleistocene up to our time (Aliaj sh., 1988, Tagari Dh., 1994) pointed out a compressional regime - compressional stresses axis SW-NE 225°, generally with reverse up to thrust type of the faults in the Western part of Albania (external domain) and a tensional one - tensional stresses axis are nearly N-S (~20° NWN) with normal and strike-slip type fault in the inner and Eastern part of Albania. The stress field, the fault system and spatial distribution of seismic activity show that the Albanian territory and surrounding area are constructed by many blocks which move relatively to each-other due to collision of the Adria plate (or the Adriatic [promontory] of African plate) with orogene of Dinarides and Albanides - Eurasiatic plate. In the seismogenetic zones and lines of Albania and in the surrounding area, as in Balcan in general, the epicenter of the earthquakes occur in narrow belts which satisfactorily follow the zones of active tectonic fault and generally appear distinctly in the morfology of the continent. The concentration of the epicenters in narrow belts leads to the conclusion that the earthquake foci in Albania and nearby are generally located in the granitic layer, therefore they are shallow up to 10-20 Km; few earthquakes have depth exceeding 50 km.

After the establishment of the Albanian Seismological Network in 1975 which consists of 13 stations (one central station and 12 - three components short period seismographs), in some seismic zones of our territory we have observed microearthquake activity - type swarm; the period of swarm activity is generally one month. We have observed swarm on September 1975 in Kepi i Rodonit, north of Durres city, in Puka region on November 1994, etc. Most important event was the swarm of Nikaj - Merturi in north Albania, near the high dam of Fierza H/P Reservoir and Reservoir of Komani H/P. this swarm has been the subject of several studies (Herak & Herak, 1986; Sultarova and Muço 1990, 1991). The swarm of Nikaj - Merturi started abruptly on November 10, 1995, reached its

peak by the end of November - beginning of December 1995 and then continued at a much lower level of activity for some months. A total of more than 17.000 microearthquakes with local magnitude $M_L \geq 1,0$ were recorded by Bajram Curri Seismological Station - the nearest station with the swarm zone; the hypocentral coordinates for 1800 of these events were determined. About 300 of them were felt and caused slight damages in the epicentral zone; the cumulative intensity was VI-VII degree of MSK scale. The maximum magnitude of earthquake in this swarm was $M_L = 4,6$ and the cumulative magnitude $M_L = 4,9$. the depth of microearthquake in this swarm was shallow up to 10-15 km. It is worth stressing here that in the end of October 1985, the reservoir of Koman H/C for the first time was full; the water reached its maximum; in this time the reservoir of Fierza H/C has reached a high water level, too. This swarm shows a clear relationship between seismic activity and maximum level of water in reservoirs of Koman and Fierza H/C.

It is asserted that the well known relation:

$$\log N = a - bM \tag{8}$$

of Gutenberg - Richter (1954) expressing the magnitude-frequency distribution accurately describes the seismicity of the region. Making use of the least square method and the maximum likelihood method (Utsu 1965, Aki, 1965) as well as data of our catalog for period 1901-1985 it is found the relation:

$$\log N = 5,74 - 1,10\ M \tag{9}$$

It is well known that coefficient b is a very important indicator of the seismic activity of a region. According to Kaila and Nari (1971) the value of $b \approx 1,10$ is characteristic for the region of ***high seismicity*** and correspondingly regions with a large number of small earthquakes and limited number of earthquakes with high magnitude. Our country for the period 1901-1994 was hit by 14 earthquakes with magnitude $M \geq 6,0$, which caused human losses and considerable damages; the strongest one was that of April 15, 1979, $M_S = 7,2$; its epicenter was situated between Albania and Montenegro in Adriatic sea, in a focus zone that had remained inactive for a long time. For the period 1981-1993 we had observed more than 7500 earthquakes $M \geq 2,4$ in out territory and surrounding. These data mean that our country and surrounding area are regions with ***high seismic activity.***

It is calculated the possible maximal magnitude for Albania using the third Gumbel asymptotic distribution:

$$\Phi_{III}\, f(x) = \exp\left[-\left(\frac{\omega - x}{\omega - u}\right)^k\right] \tag{10}$$

where $k \geq 0$; $x < \omega$; $n < \omega$; ω - is the upper limit; $k=1/\lambda$ is the shape parameter, u - is the characteristic largest value. The three parameters were calculated by the least square method making use of the data of 1901-1985 (Sulstarova, 1987), annual intervals were used, too, the curve of third asymtotic distribution defined by $\omega = 7,46$; $\lambda = 0,26$; $k = 3,83$ and $u = 4,99$ fits the observed data quite well. The value $M_S = 7,46$ can be considered as the magnitude of a largest possible event in Albania and surrounding area.

Conclusions

The above analysis leads to the conclusion that the territory of Albania and the surrounding area are regions with high seismic activity and correspondingly regions with a large number of small earthquakes and limited number of earthquakes with high magnitude. The value $Ms \approx 7,5$ can be considered as the magnitude of a largest possible event in Albania and surrounding area. The territory of our country and the surrounding area are divided into some blocks relatively large traced by some transversal faults most important of which are the faults of Shkodra - Peja and Vlora - Elbasan - Dibra. These blocks are interesected by longitudional faults of NW-SE trend, giving to the territory the view of a mosaic of blocks. The seams outlining these blocks are seismogeneous structural elements along which the earthquakes are generated from the motion of the blocks due to collision of Adria (or Adriatic) plate with continental plate (the orogene of Albanides and Dinarides) - Euroasiatic plate.

References

Aki K., 1965: "Maximum likelihood estimate of b in formula log N=a-bM and its confidence limits" Bull. Earth. Res. Inst. Tokyo Univ 43, 237-239.

Aliaj Sh., 1979: "Seismotectonic and geological criteria of the seismicity of Albania" Thesis, Seismological Center, Tirana, Albanai (in albanian).

Epstein B., C. Lomnitz, 1966: "A model for occurrence of large earthquakes" Nature, 211, 5052, pp 954-956.

Gumbel E.J., 1962 "Statistics of extremes" New York Columbia University press. Herak M., and Herak D., (1986) "Premonitory changes in the slope of frequency-magnitude relation before a swarm in Northern Albania, 1985-1986; Geophysical Institute, Faculty of Sciences and Mathematics, University of Zagreb.

Kaila K.L., and Narian H., (1971) "A new approach for preparation of quantitative seismicity maps as applied to Alpide Belt-Sunda Arc and Adjoining Areas; BSSA, 61, 1275-1921.

Kiratzi A.A et al. (1985) Seismic Source-parameter relations for earthquakes in Greece. Pageoph., Vol. 123, pp 27-41.

Muço B., 1991: "The swarm Nikaj-Merturi, Albania", Short notes in BSSA, Vol. 81, Nr. 3, pp 1015-1021.

Muço B., (1994) "Focal Mechanism solutions for Albanian Earthquakes for the years 1964-1988", Techtonophysics 231 (1994), 311-323.

Papazachos B., Papazachos C., (1989) Seismicity of Greece, Thessaloniki

Sulstarova E., 1974 "Sizmiciteti i Shqiperise", Disertacion, Qendra Sizmologjike

Sulstarova E., Koçiaj S., 1975: "Catalogue of earthquakes of Albania", Seismological Center, Academy of Sciences, Tirana, p 297 (in Albanian and English)

Sulstarova E., Kçiaj S. Aliaj Sh., 1980: "Seismic regionalization of Albania" Seismological Center, Academy of Sciences, Tirana, p. 297 (in Albanian and English)

Sulstarova E., 1986: "The focal mechanism of earthquakes and tectonic stress field in Albania", Thesis for Dr. of Sci., Seism. Center, Acad. of Sci., Tirana, pp 228 (in Albanian).

Sulstarova E., 1990: Seismic hazard Assessment at national and local levelin Albania. Proceeding of the UNDRO/USSR/UNESCO/UNDP training seminar, Frunze, Alma-Ata, 9-19 October 1990, UNDRO, Geneva p. 54-72.

Sulstarova E., 1993: "Some methodological considerations on the determination of macroseismic parameters and their relations in the study of Earthquakes of Albania". Proceedings of the 2nd Congress of the Hellemic Geophysical Union, Florina 1993, Vol.I., pp 532-540.

Sulstarova E., Pitarka A., 1993: "Macroseismic felt effects and evaluation of seismically Hazard zones in Albania" presented in 2nd Workshops - Statistical Models and Methods in Seismology, held in Cephalonia 2-5 June, 1993.

Tagari Dh., (1993): "Etudes neotectoniques et sismotectoniques des Albanides: Analyse des deformations et geodynamique du Langhien a l'actuel". These Dr. Sc., Universite Paris XI, Orsay, France.

Utsu T., 1965: "A method for determining the value of b in formula log n=a-bM showing the magnitude frequence relation for earthquakes", Geophys., Bull Hokkaido Univ. 13, 89-103.

ROMANIA'S SEISMICITY FILE: 1. PRE-INSTRUMENTAL DATA

Vasile I. Marza

Seismological Laboratory, NIEP
Bucharest, Romania

Abstract

We address here some issues on Romania's pre-instrumental (984-1900) seismicity as: re-evaluation of the data base, quantification procedures and standardization in order to fulfill the current developments and gudelines toward a uniform, complete and standard data file as suggested by the recent GSHAP recommendations. The Romania (historical as well modern one) seismicity has two main components, e.e., Vrancea subcrustal seismicity (very confined and active) and the crustal seismicity mor diffused and less active following mainly the Carpathian Orogeny.

1. Introduction

We try to re-arrange the Romanian historical seismicity data base according to the recent systematization requirements advanced by the Global Seismic Hazard Assessment Program (GSHAP), e.g.: Basham & Giardini (1993), Johnson & Halchuk (1993) etc. According to GSHAP approach the seismicity data should be considered in three time-period categories: (i) Pre-1990, pre-instrumental; (ii) 1900-1963, early instrumental: and (iii) 1964-present, modern instrumental. Here we will take on with the first period, the main efforts will be towards systematization, uniformity, consistency and completeness through re-avaluation, proper quantification and standardization. In re-assessing the Romanian historical data base we strive to adhere as much as possible to the technical guidelines and methodology recommended under the GSHAP umbrella. The main issues addressed bellow are as follows: correction and completion of the former compilations, extending as much as possible the data set by making use of all existing information, utilization of a unique and proper earthquake size descriptor by using some regression relationships between primary size descriptors and the adopted descriptor "that is, the moment magnitude scales (**M** for crustal sources and **m** for subcrustal/intermediate depth events"), adoption of a standard record format, i.e. the GSHAP primary seismicity data file format.

2. Data Sources and Seismotectonic Setting

The information on historical seismicity compilations of Romania is pretty rich and comes either from local or regional gatherings: Hepites (1893; 1894-1916), Stefanescu (1901), Montessus de Ballore (1906), Anestin (1916), Popescu (1937, 1938, 1939), Réthly (1952), Florinesco (1958), Atanasiu (1961), Evseev (1961), Petrescu & Radu (1963), Radu (1974), Kárnik (1968), Sagalova (1969), Shebalin et al. (1974), Kondorskaya & Shebalin (1977), Purcaru (1979), Constantinescu & Marza (1980; 1984), Radu & Polonic (1982), Zsiros et al. (1988), Cornovodeanu & Binder (1993), Chiper (1993), Toró & Nitoiu (1995, personal communication) etc.

Romania's seismicity has two components: (1) a major one, i.e., the subcrustal depth from 60 to roughly 200 km) seismicity of the Vrancea Seismogenic Zone (VSZ), with features which make it particular and unique not only for Europe, but also World-wide, and (2) the usual crustal seismicity, less active and spread more of less over the entire territory of the country and adjacent areas.

Special Publications of the Geological Society of Greece, No 6.

From texonomical point of view the Romanian seismic sources are hard to be assigned to the three main accepted seismotectonic origins [i.e., (i) stable continental regions (SCRs); (ii) active intraplate zones (AlZs); and (iii) plate boundary regions (PBRs)], however the first component (i.e., the subcrustal) one is mor close to AlZs and the second component (i.e., the crustal one) to SCRs.

VSZ (a compact foci nest placed under Carpathian arc bend, around the average epicenter 45.7N and 26.6E) puts its signature on the seismicity of Romania and even on its neighbouring areas (*N.B.* The large VSZ events have a perceptibility area more than half of Europe). The salient features of VSZ are: (1) subcrustal confined distribution on a very steep Wadati-Benioff zone (depth from 60 to cca 200 km); (2) outstanding persistence and high rate of activity with heave hazard impact; (4) stable faulting mechanism with predominant reverse faulting with both nodal planes striking NE-SW; (5) conspicuous recurrence regularities of major events etc. Due to its features VSZ's seismicity is most prominent studied, understood and considered for its hazard potential.

Accordingly, we will deal separately with the two components of Romania's seismicity.

3. Analysis' Principles and Techniques. Methodology and Philosophy

The main attempts of the analysis are directed toward:

(a) use of all available existent data;
(b) compilation of an as much as comprehensive list of events;
(c) a uniform size estimate, with uncertainty bounds, for a consistent data set;
(d) adhering to a standardized format and homogeneous tratment.

To build up a consistent data set the most important aspect it is the size descriptor. In this line Johnson & Halchuk (1993) have devised earthquake size descriptor is the moment magnitude scale M_w, originally developed by Kanamori (1977, 1978) and formally defined and designated through bold **M** by Hanks & Kanamori (1979).

For crustal events and instrumental type data the most logical size estimator it is indeed the M_w/**M** moment magnitude scale, but for deeper, that is subcrustal events we believe that M_w/**M** it is not particularly a meaningful physical descriptor because it is not appropriate to apply it to deeper sources that is, depths in excess of 50 km or 60 km (cf. NEIS and ISC practice, respectively) and indeed the common (international and traditional) practice it is not to compute a surface wave type magnitude for subcrustal origins. Here we come across an almost philosophical problem, i.e., generally it is accepted (e.g., Dziewonski & Woodhouse, 1983) that M_s (hence **M**) magnitude it is more reliable than mb as a means of yielding the relative "size" of a shallow - focus earthquake and as a consequence the current general practice it is to use M_s/M_w/**M** scale(s), moreover it is tacitly assumed that this apply (only) to shalloww/crustal events, as they are the largest fraction of the events accounted for (Abe & Kanamori, 1979).

However, as regard the deeper (subcrustal) sources the situation is left open. We suggest, based on the owrks of Abe & Kanamori (1980), Abe (1981, 1982) on mB scale (body wave magnitude based on broad-band or medium period recordings), that *the natural magnitude scale of choice for subcrustal sources it should be* m_w *(Kanamori, 1983).* In analogy with M_w/**M** scale we propose to designate this (new) scale by bold **m.** The great advantage of the **m** scale it is that it has a phisical meaning, yet a wider application, being suitable/applicable to entire depth range (shallow and deeper cources) and to a couple a seismic body wave phases. [*N.B.* The above mentioned shortcomings of the m_b scale do not imply that the $m_B m_w$/m scale(s) bear(s) the same drawback(s) and they should be regarded as different scales]. So, we adhere to m_w/**m** scale as the most logical and meaningful size estimator for use, at least, in the case of subcrustal seismicity, but because of the wide use of the M_w/**M** scale we will develop and present parallelly regression relationships, as well. Beside this, there is not any discrepancy or inconsistency between the two scales, **M** and **m**, once one value is ascertained the corresponding one should be assessed via compatible seismic moment (M_o) size.

4. Regression analysis

Because very few events (and especially the historical ones) have a directly determined seis-

Table 1. Regression Analysis Synopsis

(I) SUBCRUSTAL VRANCEA SEISMICITY:			
Eq. (1)	$M_{GR} = 0.56 * I_{max} + 2.18$		(Radu, 1974)
Eq. (2)	$M_{GR} = 9.85 * log\ (I_{max}) - 2.13$		(Purcaru, 1975)
Eq. (3)	$\log (M_{GR}) = 0.611 * log\ (I_{max}) + 0.271$		(Marza et al. 1995)
Eq. (4)	$M_{GR} = 9.02 * log\ (I_{max}) - 1.37$	[RMS=0.05]	(This paper)
Eq. (5)	$M_{GR} = 1.40 * m_w - 2.84$	[RMS=0.05]	(Ditto)
Eq. (6)	$M_{GR} = 0.86 * M_w + 0.85$	[RMS=0.05]	(Ditto)
Eq. (7)	$\mathbf{m} = m_w = 6.44 * log\ (I_{max}) + 1.05$		(Ditto)
Eq. (8)	$\mathbf{M} = M_w = 10.49 * log\ (I_{max}) - 2.47$		(Ditto)
Eq. (9)	$log\ (M_o) - 0.88 * I_{max} + 19.5$	[RMS=0.1]	(Ditto)
(II) CRUSTAL SEISMICITY:			
(A) FAGARASH, MUNTENIA, VRANCEA (CRUSTAL, CENTRAL MOLDOVA:			
Eq. (10)	$\mathbf{M} = M_w = 0.66 * I_{max} + 1.23$		(Radu, 1974)
(B) BANAT, TRANSYLVANIA, BIHOR, MARAMURESH, BUKOVINA:			
Eq. (11)	$\mathbf{M} = M_w = 0.60 * I_{max} = 0.52$		(Radu, 1974)

Note: The applicability range of the above relations are as follows:
(I) VSZ subcrustal seismicity - the eqs hold for a depth from 60 to 200 km and maximum intensities from V to X (MSK degrees);
(II) crustal seismicity - the eqs hold for maximum intensities ranging from V ti VIII (MSK degrees).

mic moment, we have to develop regression equations on other size measures. For historical events such other size measures could be: isoseismal (including total felt) areas, (average) radii of isoseismals, epicentra/maximum (macrocentre) intensity (I_o/I_{max}) etc. Hereinafter analysis will be particularly devoted to the quantification issues of the pre-instumental seismicity, although the discussion applies equally to the modern data.

4.1. Relationships for VSZ subcrustal earthquakes

Traditionally, the quantification of the VSZ subcrustal earthquakes it is done through M_{GR} scale, and the main catalogues of VSZ seismicity are using explicitly or tacitly this scale. For the historical VSZ (subcrustal) events the main and practically the only macroseismic descriptor is I_o/I_{max} descriptor, although it is ranked by Johnston & Halchuk (1993) as a particularly poor designator. This could be especially the case of shallow events, as they deal with in their study only with shallow earthquakes, however, in the case of VSZ deeper focus indicator due to a conjecture of physical features involved in the physics of the seismotectonic - physiographic environment, as: stable focal mechanisms and radiation patterns, a wide pleistoseismal area etc, all these features providing an average maximum intensity (more stable and significant measure than a punctual one).

The macroseismic intensity assessment for VSZ is made in terms of MSK-64 scale (hence compatible with the forthcoming new European macroseismic scale - EMS). The most formerly used and common regression relationships (Radu 1974; Purcaru 1975, 1979 etc) are presented in Table 1 together with the adopted relationships, developed in this papers using a revised, updated and enlarged data set, i.e., the eqs (4) to (9).

4.2. Relationships for crustal earthquakes

The relationships adopted and used for crustal sources are also presented in the Table 1 ac-

cording to groups of seismogenic sources having similar features. These equations are using as the main size descriptor the M_w scale as recommended by GSHAP. Note that eqs (10 & 11) in Table 1, section II, were originally developed for M_s scale, so here in the light of similarity of the M_s and M_w scales, we replaced M_s with M_w as a natural overlapping of the scales.

5. Vrancea Seismogenic Zone (VSZ) Subcrustal Seismicity

The data regarding VSZ subcrustal (i.e., intermediate depth, that is 60 to 200 km) seismicity span a time period longer than a millennium (e.g., Constantinescu & Marza, 1984) with time varying completeness thresholds.

Table 2. Seismological - Physiographic Provinces and zones of Romanian Territory (See also Figure 1) [After Constantinescu & Marza, 1980]

Province	Code		Zone's Name
Vrancea	**1**	**11**	Intermediate depth (subcrustal) earthquakes
		12	Normal depth earthquakes
Banat	**2**	**21**	Sînnicolau Mare
		22	Arad
		23	Timisoara
		24	Moldova Noua
		20	Romania/Serbia Border
Crisana	**3**	**31**	Carei
		32	Bihor
		30	Romania/Hungary border
Maramuresh	**4**	**41**	Oas
		42	Viseu
		40	Northern Romania/Ukraine border
Moldova	**5**	**51**	Bukovina
		52	Central Moldova
Transylvania	**6**	**61**	Fagarash
		62	Tîrnaveni
		63	Salaj
		64	Deva
		65	Cluj-Napoca
		66	Bistritza
Western Wallacia (Muntenia)	**7**	**71**	Câmpulung
		72	Northern Oltenia
		73	Southern Oltenia
Eastern Wallachia (Muntenia)	**8**	**81**	Northern Romania Plain
		82	Southern Romania Plain
		83	Romania/Bulgaria border
Dobroudja	**9**	**91**	Norther Dobroudja
		92	Southern Dobroudja
		90	Black Sea/Shabla

By using the new occurred or by searching and re-interpreting the old compilations on VSZ earthquakes it has been possible to add new events into the file historical data file making it more valuable for a variety of investigations ranging from macroseismicity to earthquake predictions. The backbone of the file for VSZ subcrustal events is the master catalogue of VSZ earthquake of constantinescu & Marza (1984) continuously updated, extended and revised, the last addition being Marza et al. (1995) which by searching the new came contributions (e.g., Cernovodeanu & Binder, 1993; Chiper 1993 etc) added new events for the subcrustal data set, the most outstanding one being a major (I_{max} = $VIII_{1/2}$, M_{GR}=7.0) earthquake occurred on 1411.

Briefly we should mention the main features of this component of Romania's seismicity (i.e., subcrustal), that is, earliest event into file it happened in the year 984 A.D., i.e. more than a millennium ago, the largest event (namely the Vrancea event of 1802 October 26) had a maximum intensity I_{max}=X (MSK) or the corresponding magnitudes m_w=7.5, M_w=8.0 or M_{GR}=7.7, the completeness threshold is m_w=6.9 (or M_w=7.0) since the year 1411 and m_w=6.3 (or M_w=6.1) since around 1.800 on, the two threshold corresponding to levels of I_{max} of VIII and $VI_{1/2}$ respectively, that is heavy damage and widely felt with minor damage respectively.

6. Romanian Crustal Seismicity

Although less significant than the highly active and threatening VSZ subcrustal seismicity Romanian Territory shares some crustal source origins which locally dictate the seismic hazard. Figure 1 depicts the seismological-physiographic provinces of Romania (cf. Constantinescu & Marza 1980) and the Table 2 shows the name and associated numerical codes of seismic zones on different level of regionalization. The backbone for the file of crustal seismicity is the paper of Constantinescu & Marza (1980) which was continuously improved by cross checked against as many sources as possible for refinement and adding new events into file, the most recent compilation used for updating the crustal segment of the seismicity file being Toró & Nutoiu (1995).

It would be perhaps interesting to mention an event that could be one of earliest case of induced seismicity - and in Romania certainly the first one - namely the cavnic earthquake of 1791 January 09th, origin time 09h00m (GMT), epicenter 47.7N, 23.8E, shallow depth and I_o=VI (MSK), happened in an intensive mining area and even the original reporter of the event associated it with mining works in the area, which knows the mining since ancient times yet.

The highest maximum intensity for a historical crustal earthquake in Romania is I_{max}=IX (MSK), corresponding to M_w=7.2, for an event occurred on 1550 October 26 in Fagarash zone (area code 61).

7. Concluding Remarks: The Scope of the Paper

We have tried to get: (i) an as much as extended historical data base; (ii) an uniform set of data, especially as regard the size descriptor; (iii) a standardized file format etc. Figure 2 display an epicentral plot of historical seismicity of Romania, and the striking feature is that it has a large similarity with the instrumental distribution of seismicity.

It is worth to point out the ebident linear trend of crustal epicentres orientated SW to NE which very likely is associated with the Intra-Moesian major fault and this is a seismological proof that it cross the Carpathian and goes to the Pannonian Basin.

Note that the RMS values in Table 1 do not represent overall uncertainty bounds, but rather internal statistical uncertainties of the particular data set used in regressions. As a rule, based on former experience and investigations the estimated uncertainties of M or m are æ0.4 for subcrustal origins and æ0.6 for crustal sources.

8. Acknowledgement

I thank Professor Liviu Constantinescu for reviewing the manuscript, Professor Dan Balteanu for supplying clarifications concerning the physiographic terminology of Romania's provinces and Mr Valeriu Grecu and Mr Dan Stiopol for assisting in plotting data.

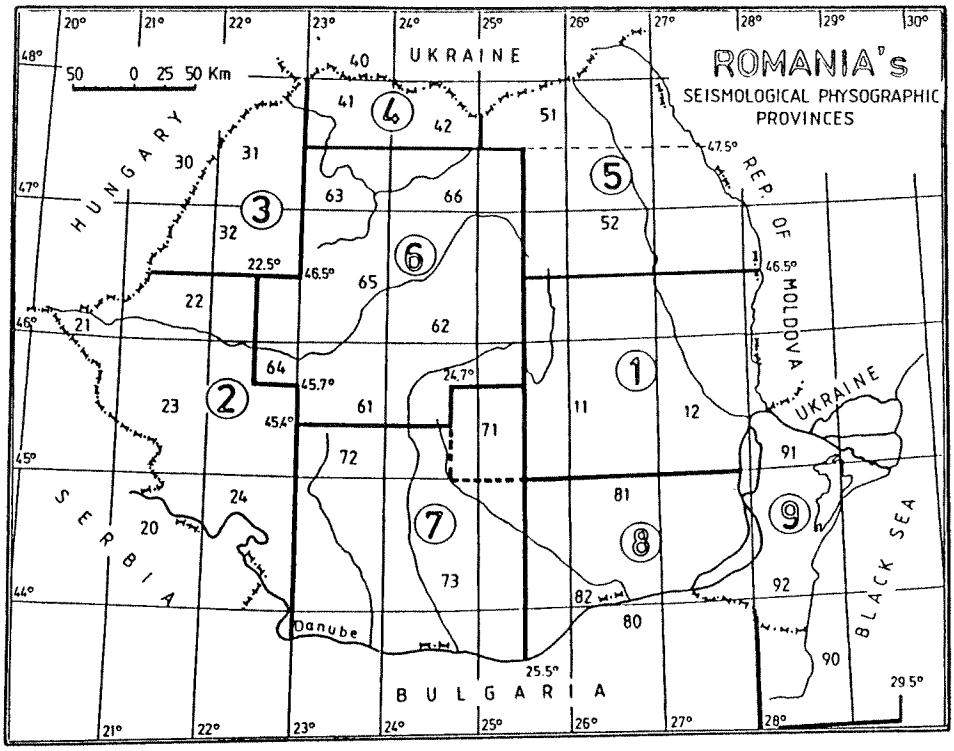

Fig. 1. Seismological - Physiographic Provinces and Zones of Romanian Territory.

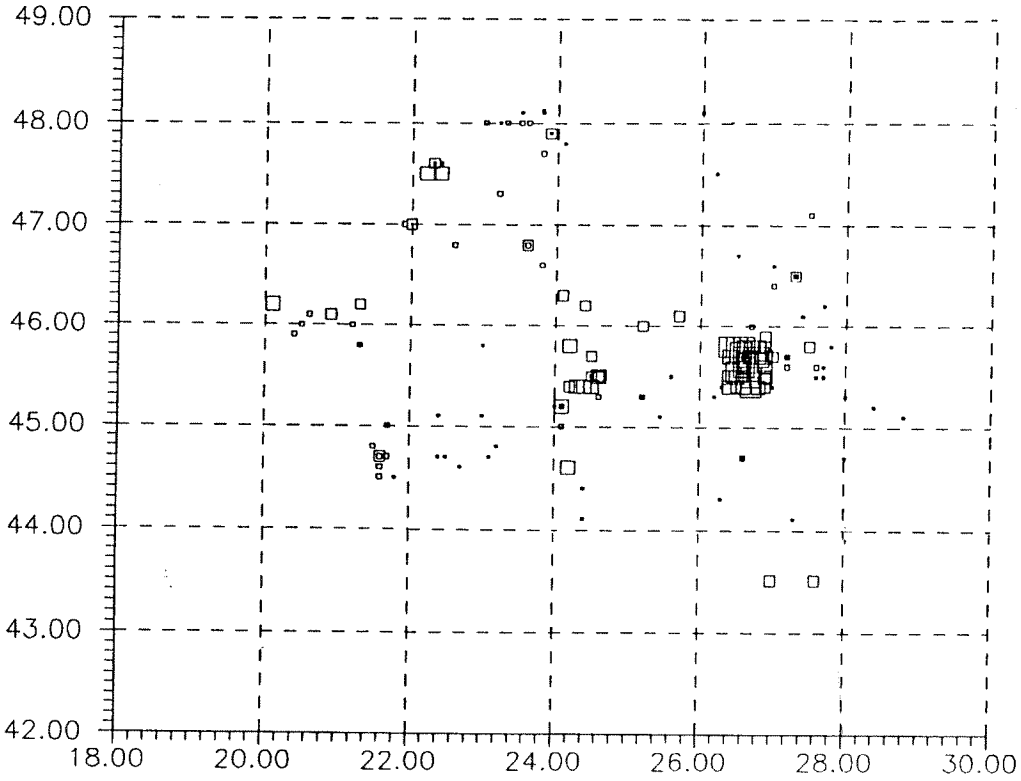

Fig. 2. Romanian Pre-Instrumental Seismicity (Prior 1900 AD).

9. Reference List

Abe K. (1981) Magnitudes of Large Shallow Earthquakes from 1904 to 1980, *Physics Earth planet. Interiors 27:* 72-92.

Abe K. (1982) Magnitude, Seismic Moment and Apparent Stress Drop for Major Deep Earthquakes, *J. Phys. Earth 30:* 321-330.

Abe K. & Kanamori H. (1979) Temporal Variation of the Activity of Intermediate and Deep Focus Earthquakes, *J. Geophys. Res. (B) 84:* 3589-3595.

Abe K. & Kanamori H. (1980) Magnitudes of Great Shallow Earthquakes from 1953 to 1977, *Tectonophysics 62:* 191-203.

Anestin V. (1916) *The Earthquakes. The Earthquakes in Romania,* Bucharest (in Romanian).

Atanasiu I. (1961) *Earthquakes in Romania,* Ed. Acad. RPR, Bucharest, 194 pp (in Romanian).

Cernovodeanu P. & Binder P. (1993) *Apocalypse's knoghts. Natural Calamities of Romania's Yesteryear (prior to 1800),* SILEX-Casa de Edit., Presa si Impres. SRL, Bucharest, 255 pp (in Romanian with a French Summary).

Chiper M. (1993) History of Seismic Activity in Romania, *in INCERC Report No. 135/1990* (in Romanian).

Constantinescu L. & Marza V.I. (1984) Master Catalogue of Vrancea Earthquakes (Romania) - Seismic Records over the Last Millennium (984-1984), *E.S.C. Abstracts, XIX Gen. Ass., Moscow, October 1-6, 1984,* p. 176-177.

Dziewonski A.M. & Woodhouse J.H. (1983) Studies of the Seismic Source Using Normal-Mode Theory, *in Kanamori H. & Boschi E. (Eds) Earthquakes: Observation, Theory and Interpretation,* North-Holland Publ. Co., Amsterdam, p. 45-137.

Evseev S.V. (1961) *Earthquakes of Ukraine,* Acad. Sci. Ukrainian SSR, Kiev, 120 pp (in Russian).

Florinesco A. (1958) Catalogue des Tremblements de Terre Resentis sur le Territoire de la R.P. Roumaine, (Le Résumé Français), Lit, Tip. Înv., Bucharest, 168 pp (in French).

Hanks T.G. & Kanamori H. (1979) A Moment Magnitude Scale, *J. Geophys. Res. (B) 84:* 2348-2350.

Hepites St. (1894-1916) The Register of Earthquakes in romania (1893-1916) *in anal. Inst. Meteor. Rom. VIII (1892) - XVIII (1902) & Bul. lunar Inst. Meteor. Rom. XVI (1907) - XXVI (1916),* Bucharest (in Romanian).

Johnston A.C. & Halchuk S. (1993) The Seismicity Data Base for the Global Seismic Hazard Assessment Program, *Annali di Geofisica* 36: 133-151.

Kanamori H. (1977) The Energy Release in Great Earthquakes, *J. Geophys. Res. (B) 82:* 2981-2987.

Kanamori H. (1978) Quantification of Earthquakes, *Nature 271:* 411-414.

Kanamori H. (1983) Magnitude Scale and Quantification of Earthquakes, *Tectonophysics 93:* 185-199.

Kárnik V. (1968) *Seismicity of the European Area, Part 1,* Academia, Praha.

Kondorskaya N.V. & Shebalin N.V. (Eds) (1977) *New catalogue of Strong Earthquakes on the USSR Territory from Oldest Time to 1975,* Izd. Nauka, Moscow, 536 pp. (in Russian).

Marza V.I., Pantea A. & Enescu D. (1995) Reappraisal of Historical Subcrustal Seismicity of the Vrancea (Romania) Seismogenic Region, *Proc. XXIV Gen. Ass. of the E.S.C., 19-24 September 1994, Athens, Greece* (submitted).

Montessus de Ballore F. (1906) La Roumanie Séismique, *in Anal. Inst. Meteor. Roum. XVII (1901):* 57-78.

Petrescu G. & Radu C. (1963) The Seismicity of the Romanian Territory prior to 1990, *Probl. Geofizica 2:* 79-85 (in Romanian).

Popescu G.I. (1937) Consideration sur les Tremblements de Terre de Roumanie, *C.R. Acad., Sci, Roum. 2:* 80 (in French).

Popescu G.I. (1938) Earthquakes in Dodroudja, *Analele Dobrogei XIX(1):* 22-46 (in Romanian).

Popescu G.I. (1939) Earthquakes in Bukovina, *Bul. Fac. St. Cernautzi 12* (in Romanian).

Rurcaru G. (1979) The Brancea, Romania, Earthquake of March 4, 1977 - A Quite Successful Prediction, *Physics Earth planet. Interiors 18:* 274-287.

Radu C. (1974) *These Dr. Sci.,* Univ. L. Pasteur, Strasbourg, France, 472 pp (in French).

Radu C & Polonic G. (1982) Seismicity of Romanian Territoty with special Reference to the Vrancea Region, *in Balan et all. (Eds) The 1977 March 4, Earthquake in Romania,* Edit. Academiei RSR, pp. 75-136 (in Ro-

manian).

Réthly A. (1952) *The Carpathian Basin Earthquakes,* Akad. Kiadó, Budapest (in Hungarian).

Sagalova E.A. (1969) On the Problem of the Seismic Zoning of Bukovina's Territory, *in Yurkevich O.I. (Ed.) Seismicity of Ukraine,* Vaukova Dumka, Kiev, pp. 70-80 (in Russian).

Shebalin N.V., Kárnik V. & Hadzievski D. (Eds) (1974) *Catalogue of Earthquakes: Part I - 1901-1970; Part II - Prior to 1901,* UNDP/UNESCO Survey of the seismicity of the Balkan Region, Skopje, pp. not numbered.

Stefanescu Gr. (1901) Earthquakes in Romania during 1391 Years, from 455 to 1846, i*n An Acad. Rom. s. II, t. XXIV,* 34 pp. (in Romanian).

Zsíros T., Mónus P. & Tóth L. (1988) Earthquake History of the Pannonian Basin and Adjacent Territories since 456 A.D., *Europ. Earthq. Eng 3:* 44-50.

AN EXAMPLE OF A GEOLOGICAL MULTIDISCIPLINARY RESEARCH AIMED AT SEISMOTECTONIC ZONATION OF SOUTHERN LATIUM (CENTRAL ITALY)

C. Carrara

ENEA Centro Ricerche Casaccia, C.P. n. 2400, 00100 Roma A.D.

Keywords: Quaternary Geology, Neotectonics, Seismotectonics, Seismic Zonation, Southern Latium, Central Italy.

Abstract

In the present paper the results of a geological multidisciplinary research aimed at defining a seismotectonic zonation of the sample area of Southern Latium (Central Italy) are summarized briefly. Studies, carried out since at least 15 years from many researchers of ENEA and other organizations and described in detail in a special volume in the print, allowed the division of the mentioned area into five sectors characterized by different geological and seismic behaviour.

In the present paper a multidisciplinary research on geological basis carried out in the Southern Latium (Central Italy) is briefly summarized. The complete description of the studies and their results is contained in a volume edited by C. Carrara, ENEA (in the press). This represents the first example, at least in Italy, of a long (about 15 years) and complex work on seismotectonics, carried out by a numerous staff of researchers of different subjects and organizations.

The research was aimed both at a better comprehension of the relationships between the tectonic activity and the seismic activity and to recognize the effects on the territory of morphogenetic processes inferred by climatic conditions. The area of the Southern Latium, including also the Fucino Basin and the Marsica Mounts (Fig. 1), has been chosen since it offers the possibility of studing recent geological events, being characterized by the occurrence of remarkable, both marine and continental, Quaternary deposits, of Pleistocene volcanic products, of a relatively uniform Meso-Cenozoic carbonatic substrate, able to preserve the forms cut in it, also related to seismic activity (faults, ruptures, scarps). The chosen area is also interesting because it can be divided into two parts: the Eastern part (Appenninic sector) showing middle to high seismicity, while the Western part (Tyrrhenian sector) is almost aseismic (Fig. 2).

The considered area is composed mainly of thick Meso-Cenozoic carbonatic formations organized into imbricate listric structures facing towards NE, separated by wedge-shaped masses of Miocene flysch and flysh-like sediments. The area is cut by normal and strike-slip faults, trending mainly NW-SE and NE-SW, subordinately N-S and W-E, which caused the formation of several intermontane basins, filled with Polo-Quaternary deposits.

Upper Pleistocene shore lines, notches and marine deposits occurring along the coast have been studied; they can be correlated to two phases of high sea level, the first represented by Strombus bubonius sediments and attributed to the Substage 5e (Eutyrrhenian, 125 ka), the second composed of marine sediments with Senegalese fauna devoid of Strombus, attributed to the Substages 5a/c (Neotyrrhenian, 90 ± 100 ka). Tectonic vertical movements have dislocated

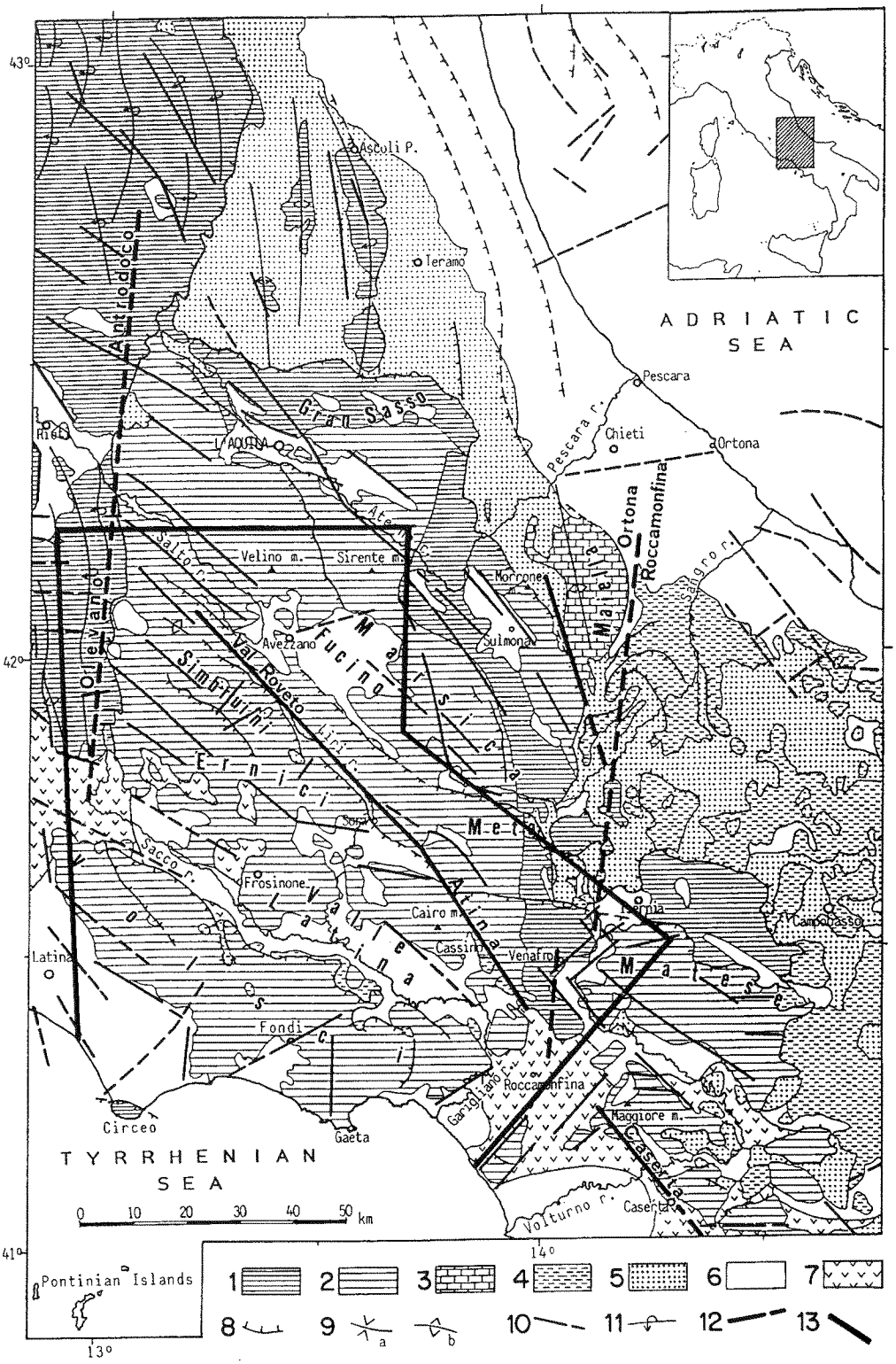

Fig. 1. Geological and structural scheme of the sample area of Southern Latium (from Funiciello et al., 1981, modified). Legend: 1. Umbromarchigiano pelagic basin and relative flysch; 2. Latium-Abruzzi carbonatic platform and relative flysch; 3. Adriatic platform (forebasin); 4. Allochthonous complex; 5. Late-orogenic formations; 6. Marine and continental Plio-Quaternary deposits; 7. Quaternary volcanic complex; 8. Thrusts; 9. a: Sincline axis, b: Anticline axis; 10. Normal faults; 11. Thrust faults; 12. Strike-slip faults; 13. Borders of the studied area.

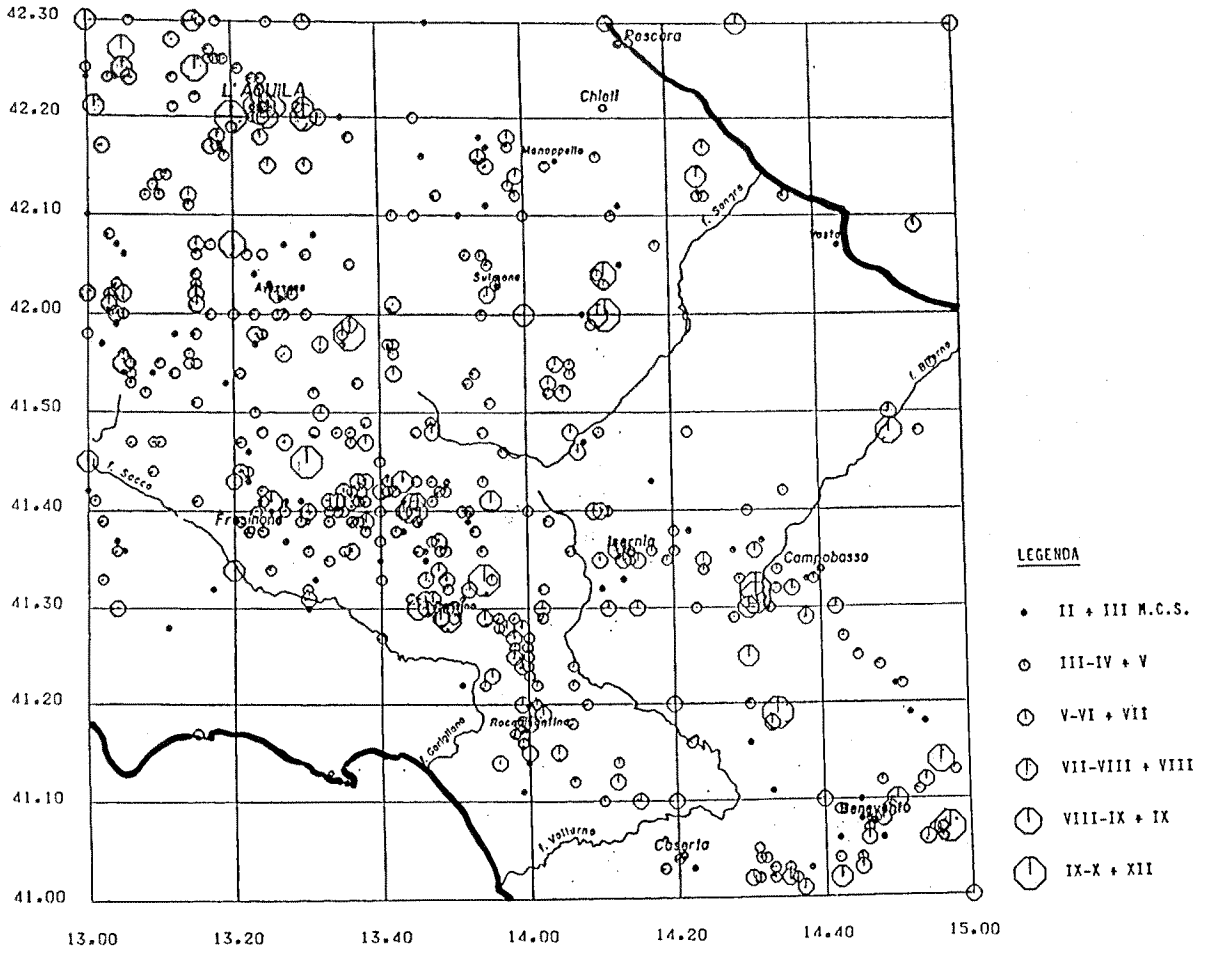

Fig. 2. Seismicity of the studied area.

by a few metres the Eutyrrhenian deposits, while the Neotyrrhenian ones show an undistrurbed attitude. The coast region, therefore, seems not to be affected by tectonic activity during the last 90 ± 100 ka.

A detailed survey of notches, terraces and submerged caves correlable to at least six sea levels lower than the present-day one (at -1,5, -7 ± 8, -10 ± 15, -17 ± 21, -24 ± 25 and -43 ± 47 m), preceding the Holocene rise, has been carried out. The research allowed to demonstrate that during a period comprised of between 8500 and 9000 years the sea level should have been 25 ± 30 m lower than the present-day one.

Also Quaternary forms and marine and continental deposits occurring in the Pontinian Islands at different altitudes have been mapped; they indicate that during the Quaternary the tectonic activity has been stronger than that of the previous area. Vertical tectonic movements of Late Holocene age and still active have been recognized not only in the islands, but also in the adjacent continental shelf. Holocene marine notches, uplifted by a few metres on the present-day sea level, have been observed.

The study of the Plio-Quaternary continental deposits occurring in the studied area allowed the reconstruction of a complete lithochronostratigraphic succession, based on several datings of different type (U/Th, ^{14}C, K/Ar, Aminostratigraphy), and the recognition of the most important tectonic structures. New and important data concerning the deposits of Late Pleistocene and Holocene age of the Fucino basin have been achieved. In the area comprised of between the Valle Latina and Val Roveto only the oldest Pliocene deposits have been dislocated by thrust and/or strike-slip compressional faults. Afterwards the tectonic style assumed an extensional character, connected to the uplift of the Apennine chain. Deep-slip faults trending mainly N40W and N70W, about N-S and E-W, have

dislocated the deposits, being active at least until the formation of several depressions filled with fluvio-lacustrine and pyroclastic sediments dated to Middle Pleistocene (600 ± 350 ka B.P.). A tectonic phase, occurred between the boundary Lower/Upper Pleistocene and the formation of the fluvio-lacustrine basins, has allowed for the rise of magmas along the faults and the formation of the great volcanic edifices of the area. Afterwards the intensity of the tectonic activity decreased quickly, even if it has continued to be active until at least the Upper Pleistocene. In the coastal area tectonic movements have mainly affected the Lower Pleistocene deposits; the tectonic dislocations observed in the Middle and Upper Pleistocene deposits are scarse and of little amplitude and seem to exhaust after the deposition of the Euthyrrenian sediments (125.000 years B.P.).

The Quaternary morphogenesis of the area has been determined on the basis of a morphostratigraphic study that allowed the reconstruction of the succession of the erosional phases which have conditioned the evolution of the relief. The work done indicates that the relief energy relative to Middle Pleistocene - Holocene period results higher and higher going from the aseismic Tyrrhenian sector to the seismic Apenninic one. The study has showed the occurrence of forms induced or controlled by instant energy release connected probably to seismic events.

Comparative pedogenetic investigation on the Plio-Quaternary deposits, particularly on the Late Quaternary ones, has been carried out. This provided a reliable succession of stable and unstable periods connected respectively to formation and degradation of soils. Six main Quaternary morphogenetic and pedogenetic cycles, characterized by different rates of pedoformation and different erosion/deposition ratios, have been determined. The first two cycles, attributed to Upper Pliocene-Lower Pleistocene and to Lower Pleistocene periods, are dislocated by extensional faults. The following two cycles, attributed to Middle Pleistocene, are made up of deposits containing volcanic products and are only partially affected by tectonics. The last two cycles are connected to Upper Pleistocene-Holocene alluvial terraced deposits and marine sediments, shore lines and notches, mainly interested by anthropic activity.

Investigation on speleothems of some caves of both the aseismic sector and the seismic one have showed that the first globally do not seem to have been affected by noticeable neotectonic events, while in the seismic sector two superimposed processes have taken place: a Northern tilting on E-W axis and dislocations and collapse of probable seismic origin during the last phase of concretion. In the aseismic sector the movement has been uniform slow and moderate; in the seismic sector, the movement has been instant and has had a clear polarity towards the North.

A mesostructural analysis of fault-slip and fracture structures in the area has been performed. Fault-slip data, collected with statistical criteria have been processed. The results confirm the well known, mainly compressional, Mio-Pliocene "apenninic phase" showing a mean N48E s_1 trend, related to the Pliocene tectonic phase responsible for the nearly North-South trending compressional structures. In the Plio-Quaternary deposits only extensional features have been recognized, which define a main about North-South extension (s_3 N10-20E); very weak or absent is the "apenninic" trend (NW-SE structures) that seems have be rotated to E-W direction. N-S and E-W structures are still active as suggested also by local seismicity.

The continental deposits of the Fucino basin have been mapped in detail. At least 6 depositional Plio-Quaternary cycles, made up mainly of breccia, alluvial and fluvio-lacustrine deposits, have been recognized. The deposits of Upper Pleistocene and Holocene age, composed mainly of fluvial sediments, often containing volcanic material and paleosols and affected by extensional tectonic movements, have been studied in more detail. The occurrence of faults, active in the last 30,000 years, mostly of which have been affected by movements also in historical epoch and have caused surficial faulting history consisting of a series of 5 great earthquakes that took place between 18 ± 20,000 and 13 ± 14,000 years ago, near 5 ± 5,500 years ago, around 3,100 years ago, in late-roman or already Medival epoch and in 1915 have been presumed.

Detailed volcanotectonic investigation on the Roccamonfina district has been carried out, in order to get a better understanding of the volcanic activity in the geodynamic evolution of the area. The results have shown that the volcanic activity has taken place in a relatively brief period comprised of between 600 and 160 ka B.P. The Roccamonfina volcano has been

subjected also to seismotectonic investigation, carried out on the basis of the comparison of the structural and morfologic data to those concerning the historical seismicity of the district. It has been shown that the seismic activity of the considered area can be connected to local unstable N-S tectonic structures.

Tephrostratigraphic studies on the Quaternary continental deposits occurring in the studied area have been carried out. The pyroclastic levels occurring within the studied deposits have been mapped, subjected to petrographic and chemical analyses and dated by means of K/Ar method. This allowed to recognize their provenance, to date and correlate different continental sequences.

Paleobotanical investigation has been carried out, aimed at the achievement of a climatic chronostratigraphy, useful to distinguish the effects of climatic variations from those of tectonics in the landform evolution. The analyses of both fossil pollen and macroremains have regarded the sediments occurring in different parts of the studied area; they allowed the recognition of sequences of steppic and forestal phases which took place under fresh and temperate climate respectively and could be correlated to different stages of the isotopic oxygen curve.

A geochemical study of the natural waters of the Southern Latium has been carried out. The chemistry of these waters has been controlled by the synergy of the following factors: the interaction between water and rocks; the mixing of different types of acquifers; the contribution of hydrothermal fluids, the circulation of which is influenced by the tectonic conditions and the local variations of the heath flow. In this case the most important process is represented by the rising of fluids of deep origin, mainly CO_2, both in volcanic and carbonatic complexes. CO_2 deriving from metamorphism of carbonatic paths and acts as carrier of other gases present in lower concentrations. This parameter influences not only the chemistry of water, but gives important information on the geodynamic evolution and for the study of the geochemical precursors of volcanic and seismic events.

The studied area has been subjected to a great amount of investigations of historical seismicity, associated with the analysis of the seismometric and accelerometric records, obtained from the ENEA networks. On the basis of this research the area can be subdivided into several sectors, characterized by different seismic activity (Fig. 2).

The Pontinian Islands area and the adjacent continental shelf, shows a certain seismicity characterized by remarkable frequency and intensity not higher than VII MCS degree. Tyrrhenian sector comprised of between the coast and the Valle Latina, results almost aseismic on the basis of historical seismology, while the seismometric records indicate the occurrence of a very weak activity (very few events with very low magnitude). The sector corresponding to the Valle Latina shows a seismic activity similar to that observed in the preceding Tyrrhenian sector, but with a higher frequency of events. The sector comprised of between the Valle Latina and the Marsica Mounts, particularly the belt coinciding with the regional tectonic structure known as Val Roveto-Atina line, is characterized by high seismic activity with remarkable frequency. Along this sector three main groups of epicenters, aligning in E-W (Sora centre) and N-S (Cassino and Roccamonfina centres) directions have been recognized. The Apenninic sector, comprehending the Fucino basin and the upper valley of the Salto river, represents a centre characterized by high seismic activity for intesity (XI MCS degree), but rather low for frequency. Paleoseismic investigation, furthermore, indicates that the return period of the high magnitude events (> 6.5) is very long. The Apennine sector comprehending the Marsica Mounts to SE of the Fucino basin and the Meta Mounts, shows a seismic activity similar to that of the Fucino basin.

Geodetic measurements, aimed at the recognition of still active deformation, connected to the seismogenetic potential of the area, have been done. The geodetic network has been realized in such a way as to determine eventual horizontal movements along the tectonic structures of the Valle Latina and the Val Roveto-Atina line. In the period 1984-85 three measurement campaigns on the network vertices have been carried out; the eleboration of the obtained data (not founded on a sufficiently long statistical base) seems to suggest that no horizontal deformation higher than the ellipsoid error occurs.

A detailed geomagnetic survey of the considered area allowed for the recognition not only

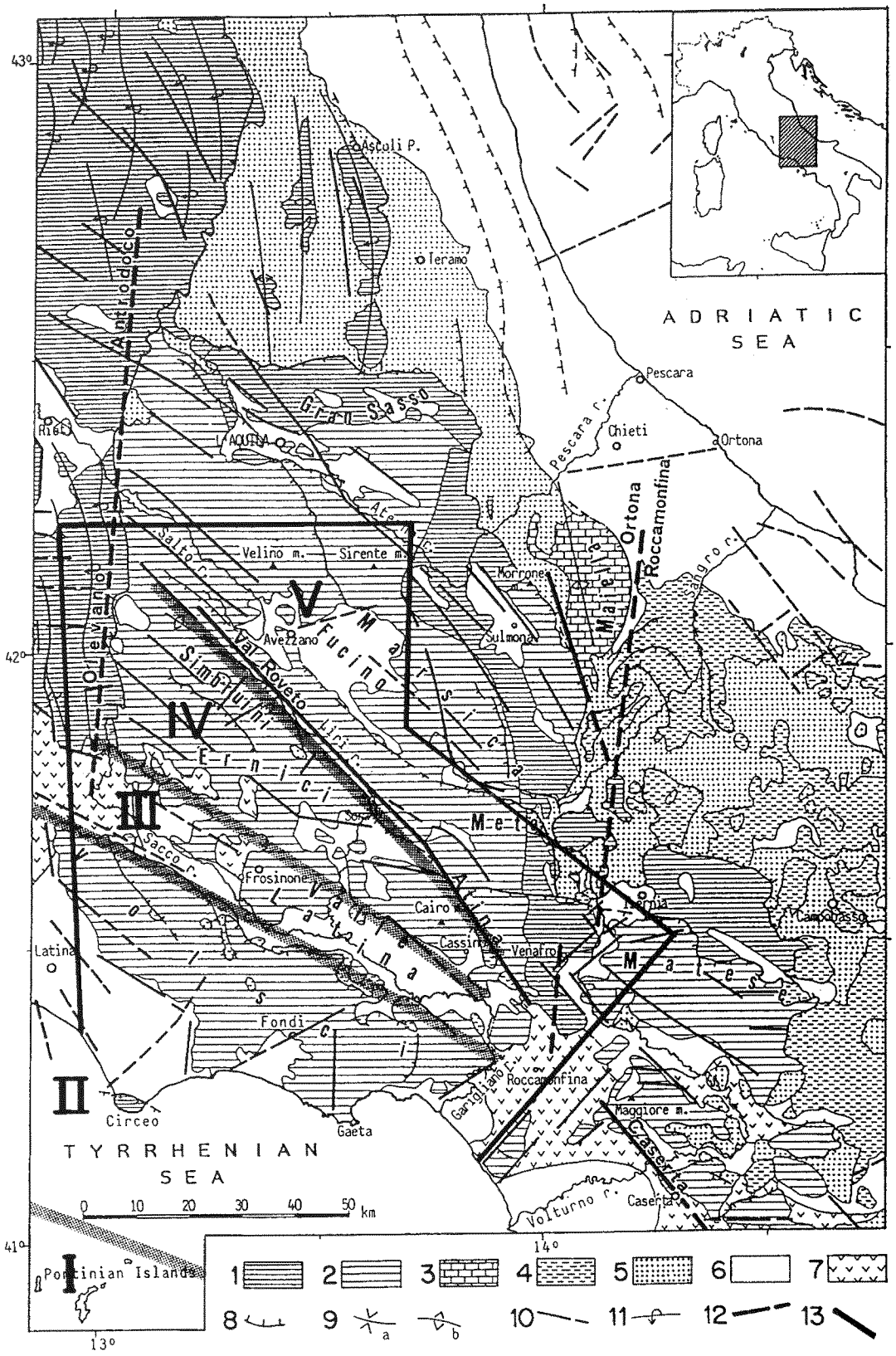

Fig. 3. Seismotectonic zonation of Southern Latium. Legend as in Fig. 1; I: Pontinian Islands sector; II: Tyrrhenian sector; III: Valle Latina sector; IV: Western Appenninic sector; V: Eastern Appenninic sector.

of deep and "permanent" tectonic structures such as the Latina and Val Roveto valleys, with magnetic markers becoming more and more surficial from the Tyrrhenian margin to the Apenninic chain, but also of structures trending N-S and E-W, already pointed out by means of geological mapping and mesostructural analysis.

Two seismic refraction profils have been realized: the first from Circeo Promontory (Tyrrhenian Sea) to the mouth of the Sangro river (Adriatic Sea), the second with Apenninic direction from Latina to Caserta-Avellino area. The interpretation of the obtained occurring in the area and the structural and geodynamic relationships between the crust and the mantle, has allowed for the recognition of a more complex geodynamic condition and a higher mobility of the Apennine sector. This sector has been affected by deep tectonic structures (i.e. Val Roveto-Atina line) that dislocate the Moho by some kilometres, while the Tyrrhenian sector shows a Moho with a rather horizontal, regular and uniform attitude.

The Apennine sector is characterized globally by a complex Quaternary geological, morphogenetic and dynamic evolution, connected to the still active uplifting of the chain. It is affected by deep structures that dislocate the Moho and by seismogenetic structures that have often been active repeatedly during prehistoric and historic times. On the contrary, the Tyrrhenian sector, except the area of Pontinian Islands, is characterized by a higher morphogenetic and dynamic stability, from at least late-Quaternary.

The seismic events occuring in the Apennine sector with hypocenters localized as far as 10 km are presumed to be originated in the sedimentary portion of the crust and to be caused by the condition of unstable equilibrium of the Meso-Cenozoic carbonatic, tilted blocks, resting on the basement throught detachment planes. The earthquakes with deeper hypocentres (as far as 25 km) could be due to implication of the basement and of the deepest parts of the crust in the geodynamic processes active in the region.

To conclude, the following schematic seismotectonic zonation of the studied area, based on the results of the multidisciplinary research, is reported (Fig. 3):

I) The **Pontinian Islands area** is characterized by a complex Plio-Quaternary morphogenesis, conditioned by tectonics and climatic variations; moreover, it is affected by Holocene, still active tectonic movements and by frequent seismic activity, with earthquakes of moderate maximum intensity ($\leq$ VII MCS).

II) **The Tyrrhenian sector,** including the coastal plains of Latina and Fondi and the Volsci chain, is characterized by a relative tectonic stability since at least the Upper Pleistocene. The deposits occurring in the area are related to eustatic movements, in turn due to climatic variations, and are affected by small vertical displacements (varying from a few decimetres to some metres) of Upper vertical displacements (varying from a few decimetres to some metres) of Upper Pleistocene age. Seismicity is lacking, apart a very low activity, instrumentally recorded, in the Gaeta and Garigliano zones.

III) **The Valle Latina.** Remarkable volcanic manifestations, which took place owing to an extensional tectonic phase comprised of between Lower and Middle Pleistocene, have conditioned the geomorphologic evolution of the valley. Subsequently the area has not been affected by important tectonic movements, but the formation of forms and deposits connected to climatic variations. A very low seismic activity has been recorded.

IV) **The Western Appenninic sector,** comprised of between the Valle Latina and the Liri Valley (Val Roveto-Atina line), is characterized by a great tectonic mobility, supported by extensional tectonic phases that took place during the Plio-Quaternary period. The Plio-Quaternary morphogenetic evolution of this sector is proved by the occurrence of several lithostratigraphic and pedogenetic sequences, encased the ones into the others and separated by tectonic and/or erosional phases due to climatic variations. This sector is limited towards NE by the main Val Roveto-Atina line that represents a deep regional polygenetic structure. Geophysical data demonstrate that the mentioned structure displaces the Moho by some kilometres and plays a great geodynamic importance; geological evidences demonstrate that the structure played a role of left strike-slip fault since the Upper Pliocene, while subsequently it transfomed into a dip-slip fault.

This sector is characterized by a seismic activity much higher than that of the previous areas and is affected by faults that, on the basis of geomorphologic evidences, have been active in recent times and, on the basis of historical and instrumental seismology, are still active.

V) **The Eastern Appenninic sector,** extending from the Liri Valley (Val Roveto-Atina line) to Fucino basin, is characterized by a complex geological and tectonic evolution during the Plio-Quaternary period and it is affected by recent and still active extensional tectonics. The seismicity is very high and includes strong events, characterized by long return times, which have caused surface faulting in prehistoric and historic times.

References

C. Carrara - ENEA (Eds.) - Southern Latium (Central Italy) - Synthesis of a Geological Multidisciplinary Research (in print).

THE MAIN RESULTS OF THE SEISMOLOGICAL OBSERVATIONS IN THE AEGEAN SEA

S. A. Kovacheva[a], I.P. Kuzin[a], L. I. Lobkovsky[a], A. V. Sonkin[a]

[a] *Shirshov Institute of Oceanology, Moscow, Russia*

Abstract

The detailed seismological observations with OBS were carried out in the region of the Hellenic Arc in 1987-1989. During 3 seismological experiments with total duration of 1 month about 3900 microearthquakes were recorded, and among them 400 hypocenters were located. Among new results, obtained in these experiments, the most interesting are: the revealing of the two-layer structure of the Benioff zone with outer subzone coupled with the Strabo trench and the inner one coupled with the Pliny trench; the continuity of the recurrence curve for the broad range of earthquake magnitudes from M_1 = 0.8 through M_1 = 6.7; the influence of the forthcoming strong earthquake with M=6 on the microseismic regime of the region, and the revealing of the new precursors as well.

1. Introduction

The Aegean Sea is characterized by the very complicated tectonics, which is not well understood by now. Besides, this region, especially the Hellenic Arc, is the most seismoactive region in the entire Europe, where, according to data by Greek seismologists (Calanopoulos, 1963), up to 2% of the Earth's seismic energy is released. The historical observations give numerous examples of the destructive earthquakes, when towns and villages were destroyed at one moment. One can also point to the volcanic activity in that region (e.g., the eruption of the Santorin Volcano, 1400 BC); usually the volcanic eruptions are accompanied by the weak shallow-focus earthquakes (Papadopoulos, 1984). All that leads us to conclude, that the study of the seismicity of the Aegean region is very important and interesting problem in both theoretical and engineering aspects.

Taking into account all mentioned above, academician Sergei Soloviev, the founder of the marine seismological investigations in Russia, decided to start the study of the seismicity of the Aegean region. During 1987-1989 the Laboratory of Marine Seismology of the Shirshov Institute of Oceanology carried out several successful seismological experiments in that region with ocean bottom seismographs (OBS), developed in the Laboratory. The recordings of seismic signals were mostly made in the high-frequency range (4-16 Hz), to take the advantage of the low seismic noise level at these frequencies (about 1 nm/Hz$^{1/2}$.

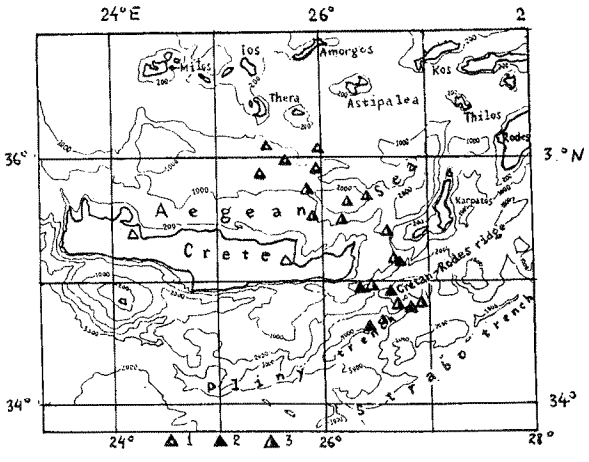

Fig. 1. Map of the region under study 1, 2, 3 - OBS networks in 1987, 1988, and 1989 accordingly.

The scheme of the deployment of the OBS during that experiments is given in Fig. 1. During the first and second experiments, carried out in 1987 and in 1988, 5 OBS's were installed in the Cretan Sea and near the eastern flank of Crete respectively. In 1987 400 microearthquakes were recorded during 10 days of observations, and among them 130 hypocenters were located. The 1988 experiment lasted 8 days, 468 microearthquakes were recorded and 120 hypocenters were located.

In 1989 special seismological expedition took place aboard RV "Dmitry Mendeleev". The expedition started with the deployment of 7 OBS's in the region of the North Aegean Trough; 180 earthquakes were recorded during 7 days of operation and 31 hypocenters were located. Next experiment was carried out near the eastern flank of Crete; totally 11 OBS's were deployed, and among them 5 in the frontal part of the Hellenic Arc, 5 in the Cretan Sea, and one OBS, that linked two groups, in the Strait of Kasos. During 9 days of operation, more than 3000 earthquakes were recorded, but because of the unfortunate loss of the "Linking" OBS, only 130 hypocenters were located [Soloviev et el., 1993].

Thus, as a result of 3 short-term marine experiments carried out in 1987-1989 in the Aegean Sea, totally 410 hypocenters were located, and among them 380 in the region of the Hellenic Arc. In spite of the episodic manner of the observations and their short duration, they allowed to reveal some principally new features of the seismicity of the Aegean Sea.

2. Instrumentation

For the purpose of the study of the regional seismicity of oceans and seas, two types of OBS's pop-up and tethered, were constructed in the Laboratory of Marine Seismology of the Shirshov Institute of Oceanology. They were described in our earlier publications [Kovachev et el., 1991; Soloviev et el., 1993, and others].

3. On some results of the bottom seismological observations in the Aegean Sea

The characteristic feature of seismological observations carried out with OBS in the area of the active continental margins, is the very high sensitivity of seismographs; in the case of the deployment of the OBS in the epicentral zone, the energy threshold of recorded events is 10^4-10^6 Joules. For the observations, carried out in the Aegean Sea, this threshold was 3 units of magnitude lower, than for the land-based observations carried out in the continental Greece (M_l=1 in the sea against M_l=4 in the continent) [Kovachev, Kuzin, in press].

One more advantage of OBS observations is the possibility of the deployment of the seismographs in the vicinity of the epicenters and, hence, very accurate location of the foci: 1-3 km for the epicenter and 1-5 km by depth [Soloviev et el., 1993]. This allows to study the space distribution of foci in comparison with the geological structure, to establish the activity of faults and their segments and even to reveal unknown bottom tectonic structures.

The set of new results was obtained during the detailed seismological observations with OBS's in the central Hellenic Arc. Among already published materials are the following: a) high microseismic activity within the crust of the back arc basin of the Hellenic Arc (it was revealed, that 75% microearthquakes occurred within the earth's crust) [Kovachev et el., 1992]; b) the Q-factor for S waves was determined for the lithosphere of the Cretan Sea (Q=200-300 at depths of 0-100 km) on the basis of instrumental data [Kovachev et el., 1991]; c) the

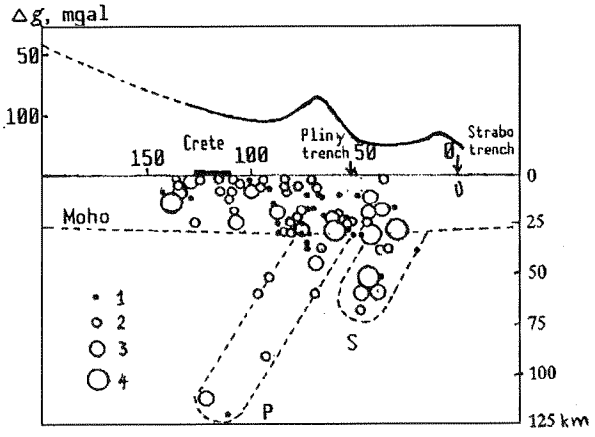

Fig. 2. Corssection of foci area of Strait Kasos from SE to NW
Microearthquake magnitudes, ML: 1. 0-0.5; 2. 0.6-1.0; 3. 1.1-1.5; 4. 1.5-2.0.

two-layer structure of the Benioff zone was revealed [Kovachev et el., 1992], the outer subzone being coupled with the Strabo trench and the inner one coupled with the Pliny trench. The maximum of the Bouguer anomaly corresponds to each subzone at the gravimetric profile across the Strait of Kasos; d) the low seismic activity of the Saros and Sporades depressions was established; the existence of the wedge-shape area in the upper mantle beneath the North-Aegean Trough was confirmed, which is similar to such area below the Wranch Mountains [Soloviev et el., 1992].

In the next sections some results of the detailed seismological investigation in the central Hellenic Arc, obtained recently, are considered.

4. On some characteristic features of the seismic regime of the low-energy earthquakes in the central part of the Hellenic Sea

The recurrence curve for the shallow earthquakes (h=0-60 km) with M > 4.5 in the entire Aegean region during 1901-1985 is given by the formula lg (N_i) = 5.1 - 0.71 (M_i) [Voidomatis, 1989]. It suggests, that about 80 earthquakes with M=4.5 can occur during this period, i.e. approximately 1 earthquake per year. The recurrence curve has the sharp slope **b**=-1.03 ± 0.11 in the region of the Hellenic Arc, including its outer part with the nonvolcanic islands and the volcanic belt (islands Milos, Nisiros, Tira and others) [Hatzidimitriou et el., 1985]; the value of **b** for the local region of the Crete island and its vicinity is **b** = -1.23.

For the recurrence curve, based on the OBS observations, chosen were the earthquakes, occurred in the region with coordinates 34-37° N, 24-28° E, and with focal depth less than 60 km (for better comparison with the above mentioned 85-years recurrence curve).

It appeared, that during the entire period of observations, the slope of the recurrence curve **b** have increased: in the 1987 experiment **b**=-1.25 ± 0.12 (69 earthquakes with magnitudes M_l=1.5-4.4) in 1988 **b**=-1.34 ± 0.27 (66 earthquakes with M_l=1.0-2.0), and in 1989 **b**=-1.43 (54 eartqhuakes with M_l=1.0-2.0). The total number of earthquakes, corresponding to the overlapping part of the energy range M_l=1.5-2.0, decreased in time. In 1987, 59 seismic events were recorded in this range of energies, in 1988 - 24 events (2.5 times less), and in 1989 - 17 events (3.5 times less). This phenomenon can be caused by the decrease of the microseismic activity in this range of magnitudes. It is known, that the two-time variations of the occurrence of weak earthquakes (M_l=3.3) and, consequently, microearthquakes (as the recurrence curve is continuous and monotonous) can be regarded as a natural fluctuation of the seismic activity [Fedotov, 1968]. Therefore, the above mentioned effect is not stochastic and it characterizes the properties of the seismic regime of the region during 1987-1989.

It is pertinent to note, that the slope of the recurrence curve, determined on the basis of the short-term observations (7-10 days) in 1987, **b**=-1.25 ± 0.12, coincides with its long-term value for M>4.5, only for the local region of the Crete Island and its vicinity: **b**=-1.23 [Hatzidimitriou et el., 1985]. The general drift of the coefficient **b** with time during 1987-1989 doesn't exceed it's RMS value.

The slope **b** of the recurrence curve for 1987-1989 observations (with the total duration of 1 month) for the Crete region (34-37° N, 24-28° E) for shallow microearthquakes (foci depth less than 60 km) is **b**=-1.06 ± 0.06. This value almost coincides with the average value, given by the Greek seismologists [Hatzidimitriou et el., 1985], for the entire region of the Hellenic Arc: **b**=-1.03±0.11. Therefore, the recurrence curve obtained during one-month OBS observations truly reflects the features of the seismic regime of the entire region. Thus, one can conclude, that there exists the minimal duration of OBS observations, when seismic regime at low energies becomes similar to the seismic regime at larger energies. In our case for the microearthquakes with M_l>0.8 this duration was 1 month. Consequently, the parameters of the seismic regime, derived from the observation of weak earthquakes, can be extended to stronger, even destructive earthquakes (M=6-7), while it usually takes ten years to obtain these parameters on the basis of observation of strong and moderate earthquakes [Kovachev, Kuzin, in press]. Thus, detailed seismological observations of the bottom seismicity of the Hellenic Arc confirm the conclusion about the continuous character of the recurrence curve in the broad range of

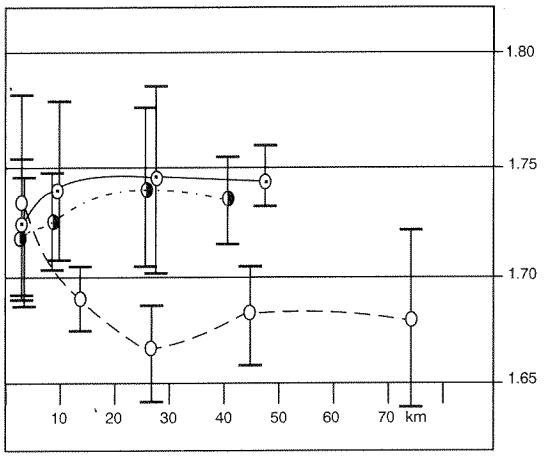

Fig. 3. Variation of V_p/V_s vrsus depth for different experiments: 1. 1987; 2. 1988; 3. 1989. Bars correspond to RMS for V_p/V_s ratio.

energies (M=0.6-4.5), obtained earlier during the land experiment in the Middle Asia [Vesson et el., 1976]. In this experiment data on M=0.6-1.1 were collected during 3 months, and for M=1.8-4.5 - during 15 years.

5. On the effect of the forthcoming strong earthquake on the microseismic activity

During 1985-1987 a strong earthquake with M>7 was expected on the South-East flank of the Hellenic Arc according to the prognosis by V. Papazachos and E. Papadimitriou [1987]. According to the approach developed by G. Papadopoulos [1988], such earthquake had to occur at the end of 1987. Nevertheless, this earthquake hasn't occurred yet, but weaker seismic event with M=6 took place on April 30 1992 in the Strait of Kasos. The preliminary analysis of the microseismicity of the central part of the Hellenic Arc, obtaind during the short-term observation of 1987-1989, i.e. 2.5-5.0 years before the earthquake, led us conclude about the forthcoming strong earthquake in the Strait of Kasos. The assumed magnitude for this earthquake was given as M>6.5, and the predicted time was the second half of 1991 [Kovachev, 1990; Soloviev et el., 1992]. This conclusion was based on the revealing of the anomalous seismoactive region at depths 0-100 km, oriented across the Hellenic Arc. Later the detailed study of the effect of the development of the strong earthquake on the microseismic activity was conducted with the use of contemporary methods [Kovachev, Kuzin, in press].

Among the precursors, usually utilized for the earthquake prediction, treated in the analysis of the microseismisity of the central Hellenic Arc were the time variations of **b** value of the recurrence curve for microearthquakes with M=0.8-2.5, and the V_p/V_s ratio. The concept of the usefulness of these factors for the earthquake prediction was formulated for the first time on the basis of the detailed study of the seismic activity in Middle Asia [Mamadaliev, 1964;

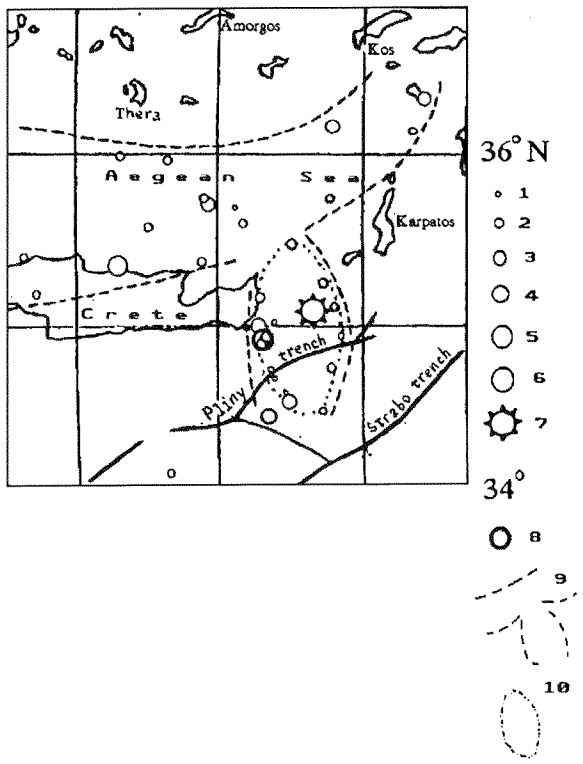

Fig. 4. Anomalous area of microearthquake foci at the depths 0-100 km beneath the Strait of Kasos
Magnitudes, ML: 1. 0-0.5; 2. 0.6-1.0; 3. 1.1-1.5; 4. 1.6-2.0; 5. 2.1-2.5; 6. 2.6-3.0; 7. Main shock on April 30, 1992 (M=6.0); 8. Its foreshock on April 21, 1992 (M=4.8); 9 - boundaries of seismic active areas; 10 - the supposed seismic gap of the second kind.

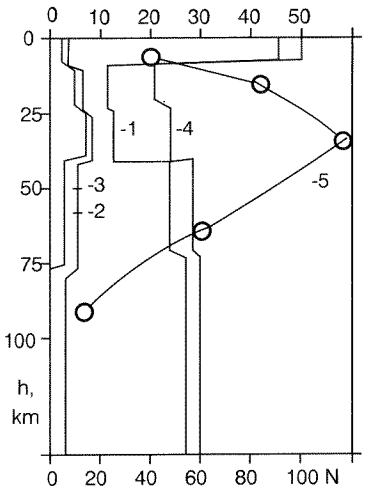

Fig. 5. Distribution of the microearthquakes number (5) and seismic energy in 1987-1989 (1-3 - annual energy for 1987, 1988 and 1989 accordingly); 4 - total energy for the whole period of observations.

Keilis-Borok, Malinovskaya, 1966; Semenov, 1969; Nereesov et al., 1971; Kulagina et el., 1982]. It was stated, that the variations of the slope of the recurrence curve for microearthquakes can be used for earthquake prediction. In our case this slope has increased by 15% from b=1.25 ± 0.12 in 1987 through **b**=-1.43 ± 0.18 in 1989, what points to the domination of the weak earthquakes and corresponds to the known data [Mamadaliev, 1964]. In addition, this result is also confirmed by the large (4 times) decrease of the daily average number of relatively strong microearthquakes (M_l>2.0) in 1988-1989 in comparison with 1987 [Soloviev et el., 1993].

The V_p/V_s ratio appeared to be less useful for the prediction of the strong earthquake, as microseismic observations within the central Hellenic Arc took place long before the strong eartqhuake (2.5-5 years); according to the available data, the significant change of the V_p/V_s ratio usually takes place 2-3 years before the earthquake with M=6 [Kulagina et el., 1982]. Nevertheless, in 1989, i.e. 2.5 years before the strong earthquake, a tendency of the of the dcerease of the V_p/V_s ratio was observed (Fig. 3).

The analysis of the microseismisity of the Hellenic Arc allowed to reveal new, non-traditional precursors of the strong earthquakes [Kovachev, Kuzin, in press]. The first of them is the above mentioned peculiarity of the space distribution of the microearthquake foci, that formed the seismoactive area at depth's of up to 100 km across the Hellenic Arc (Fig. 4). It was possible due to high accuracy of the hypocenter locations.

The other revealed factor is the peculiarity of the depth distribution of the microearthquakes. The minimum of the released seismic energy was observed in the depth interval 5-30 km along with the maximum of the microearthquake occurrence at the depth of 25 km (Fig. 5). This is in a good agreement with known seismological data [Keilis-Borok, Malinovskaya, 1966] and is very similar to the phenomenon of the generation of the acoustical emission before the collapse of the rock specimens in laboratory experiments (e.g., [Brace et el., 1976].

Thus, the results of the detailed study of the microseismic process in the region of the central Hellenic Arc allowed to reveal the effect of the forthcoming strong earthquake on the microseismisity 2.5-5.0 years before the earthquake.

Conclusion

The detailed seismological observation, carried out in 1987-1989 with the high-sensitive OBS in the central Hellenic Arc, have given some new unusual results; some of them are:

1. the high microseismic activity of the back arc area of the Hellenic Arc with 75% of the microearthquakes in the Earth's crust;
2. the revealing of the fine structure of the Benioff zone of the Hellenic Arc;
3. the revealing of the seismoactive area at the depth of 100 km below the Strait of Kasos, oriented across the Hellenic Arc, as the some kind of precursor for strong earthquake (M=6);
4. the determination of the continuity of the recurrence curve in the broad range of magnitudes (M=1-7) for the region of the Central Hellenic Arc;
5. the revealing of the influence of the forthcoming strong earthquake on the parameters of the microseismic activity.

All that led us to conclude, that marine seismic observations with OBS's, also known as "marine seismology", allow to solve the broad range of geotectonic problems in the regions of active continental margins.

References

Brace V.F., Miachkin V.I., Ditrich D.H., Sbolev G.A. 1976. Two models to explain the earthquake precursors. In: Soviet-American collected papers about earthquake prediction. V.1, N 2., Dushanbe=Moscow. P. 9-12. (in Russian).

Comninakis P.E., Papazachos B.C. 1982. A catalogue of earthquakes in Greece and in the surrounding area for the period 1901-1980. Geophys. Lab. Univ. Thessaloniki. Publ. 5. 146 p.

Fedotov S.A. 1968. On the seismic cycle, the possibility of the seismic zoning and the long-term earthquake prediction. Seismic zoning of the USSR. Moscow: Nauka. P. 121-150 (in Russian).

Galanopoulos A.G. 1963. On mapping of seismic activity in Greece. Ann Geofis. V. 16. P. 37-100.

Hatzidimitriou P.M., Papadimitriou E.E., Mountrakis D.M., Papazachos B.S. 1985. The seismic parameter b of the frequency-magnitude relation and its association with the geological zones of the area of Greece. Tectonophys. V. 120. P. 141-151.

Keilis-Borok V.I., Malinovskaya L.N. 1966. About regularity in the occurrence of strong earthquakes. The seismic methods of the research. Moscow: Nauka. P. 99-97 (in Russian).

Kovachev S.A., Kuzin I.P. (in press). On the features of the seismic regime for the small energy earthquakes in the Central Hellenic Arc. Fizika Zemli (in Russian).

Kovachev S.A., Kuzin I.P. (in press). On the seismological method of prediction of the strong earthquake in the region of the Hellenic Arc and the effect of the forthcoming strong earthquake on the parameters of the microseismisity. Fizika Zemli (in Russian).

Kovachev S.A., Kuzin I.P., Shoda O. Yu., Soloviev S.L. 1991. Attenuation of S-waves in the lithosphere of the Sea of the Crete according to OBS observations. Phys. Earth. Planet. Inter., V. 69. P. 101-111.

Kovachev S.A., Kuzin I.P., Soloviev S.L. 1992. Microseismicity of the frontal Hellenic Arc according to OBS observations. Tectonophysics. V. 201. P. 317-327.

Kovachev S.A. 1990. Microseismicity and properties of the lithosphere in the central part of Hellenic Arc and in the Cretean Sea according to be bottom seismological observations. Ph. D. Thesis. Moscow. Institute of the Physics of the Earth. 125 p. (in Russian).

Kulagina M.B., Kulagin V.K., Nikolaev A.V. 1982. The variations of the V_p/V_S ratio and the possibility of the earthquake energy prediction. Earthquake prediction. N1. Dushanbe: Donish. P. 135-158. (in Russian).

Mamadeliev Yu. A. 1964. On the research of the time and space parameters of the seismic regime. The problems of the regional seismicity in the Central Asia. Frunze: Ilim. P. 93-104. (in Russian).

Nersesov I.L., Semenov A.N., Simbireva I.G. 1971. Space-time distribution of the V_p/V_S ratio in the Harm region. Experimental seismology. Moscow: Nauka. P. 334-345. (in Russian).

Papadopoulos G.A. 1984. Seismic properties in the eastern part of the Southern Aegean volcanic Arc. Bull. Volcanol. V. 47. P. 143-152.

Papadopoulos G.A. 1988. Synchronized earthquake occurrence in the Hellenic Arc and implications for the earthquake predictions in the Dodecanese Islands (Greece). Tectonophysics. V. 145. P. 343-347.

Papazachos B.C., Comninakis P.E. 1971. Geophysical and tectonic features of the Aegean arc. J. Geophys. Res., V. 76. P. 8517-8533.

Papazachos B.C., Papadimitriou E.E. 1987. Probabilities of occurrence of large earthquake in the Aegean and surrounding area during the period 1986-2006. PAGEOPH. V. 125. N4. P. 587-612.

Semenov A.N. 1969 the variations V_p/V_S ratio before strong earthquakes. Izv. AN SSSR. Fizika Zemli. N4. P. 72-74 (in Russian).

Soloviev S.L., Kovachev S.A., Shoda O.Yu. 1992. Microseismicity of the North-Aegean Trough according to short-period OBS observations. Izv. AN SSSR. Fizika Zemli. N. 11. P. 25-37. (in Russian).

Soloviev S.L., Kovachev S.A., Kuzin I.P., Voronina E.V. 1993. Microseismicity of Aegean

and Tyrrhenian Seas according to OBS observations. Moscow: Nauka. 160 p. (in Russian).

Soloviev S.L., Kovachev S.A., Kuzin I.P. 1992. Some evidence of forthcoming strong earthquake in eastern Crete from observations with OBS. International Conference on Earthquake Prediction: State-of-the-Art. Strasbourg, France, 15-18 October, 1991, (Scientific-Technical Contributions): Preprints, Paris, P. 124-128.

Vesson R.L., Maksimov A.B., Nersesov I.L., Rulev B.G. 1976. Results of joint earthquake prediction. V.1. N. 1. Dushanbe-Moscow. P. 28-42. (in Russian).

Voidomatis P. 1989. Some aspects of seismotectonic synthesis in the North Aegean Sea and surrounding area. Boll. geofis. teor. appl. V. 31. P. 49-61.

FAULTS OF BIG EARTHQUAKES ($M_S \geq 8.0$) IN THE HELLENIC ARC

B.C. Papazachos

Laboratory of Geophysics, University of Thessaloniki, Thessaloniki GR 5400

Abstract

The faults of the two largest known shallow earthquakes in the contex side of the Hellenic arc (Hellenic trench) and of the two largest known intermediate depth earthquakes in the shallow part of the Benioff zone of this arc (concave part of the arc) are located and investigated, on the basis of clustering and delineation of recent strong ($M_S \geq 6.0$) earthquakes, reliable fault plane solutions and deep sea and coastal topography.

The first of the big shallow earthquakes (21 July 365, M_S=8.3) was generated in the western part of the Hellenic trench (southwest of Crete island) on a 300 km long thrust fault which strikes in a WNW-ESE direction and dips to NNE. Such an orientation of these two big faults and of other smaller thrust faults all along the Hellenic trench can be interpreted by an overthrust of the Aegean and south western Anatolia lithospheres on the eastern Mediterranean lithosphere in a southwest direction. Additional evidence is presented to support this kind of crustal deformation in the Hellenic trench.

The two big intermediate depth earthquakes (12 Oktober 1856, M=8.2 26 June 1926, M=8.0) were generated in the central part (north of Crete) and eastern part (west of Rhodos) of the arc on 220 km and 160 km long strike slip faults, respectivelly. The generation of these earthquakes is attribited to subduction of the remnants of an old oceanic lithospheric slab slab which is coupled is these depths (40-100 km) with the Aegean lithosphere.

Introduction

The Hellenic arc is one of the most important features of tectonic origin in the eastern Mediterranean area, with characteristics similar to other island arcs (Papazachos and Comninakis, 1969, 1971). Big shallow earthquakes along the convex side of the arc (Hellenic trench) and big intermediate depth earthquakes (h=40-100 km) along the concave part of the arc constitute a major threat for the whole south Aegean area as well as for other eastern Mediterranean countries, because the magnitude of such earthquakes can reach up to 8 or so. Four such earthquakes are known, the two are shallow and occured in the Hellenic trench (365 AD, M_S-8,3; 1303, M_S=8.0) and the other two are of intermediate focal depth and occured in the concave part of the arc (1856, M_S=8.2; 1926, M_S=8.0).

The main purpose of the present work is to locate the faults of these four earthquakes and investigate their properties (dimensions, orientation, type of faulting). For this purpose, information concerning distribution of epicenters of well located recent strong ($M_S \geq 6.0$) earthquakes (Papazachos and Papazachou, 1989) reliable fault plane solutions (Papazachos and Kiratzi, 1995) as well as deep sea and coastal topography is used.

Big Shallow Earthquakes in the Hellenic Trench

On the basis of the distribution of the epicenters of two samples of relatively recent strong shallow earthquakes (1801-1995, $M_S \geq$

Special Publications of the Geological Society of Greece, No 6.

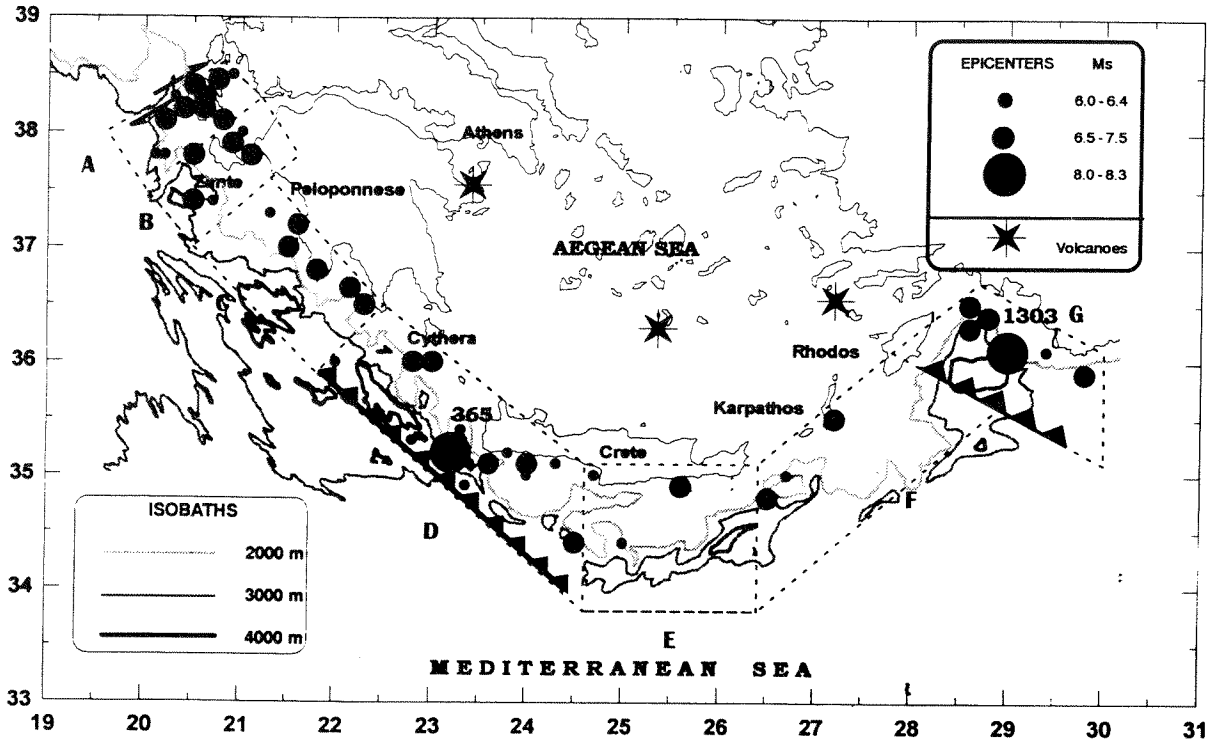

Fig. 1. The thrust faults of the two largest known shallow earthquakes in the western (365 AD, M_S=8.3) and eastern (1303, M_S=8.0) part of the Hellenic trench.

6.5; 1911-1995, $M_S \geq 6.0$) and on the most reliable fault plane solusions as well as on deep sea and coastal topography, the Hellenic trench is separated in seven seismogenic regions (fig. 1).

Region A is dominated by the Cephalonia strike slip dextral fault (with a thrust component) which has a length L=100 km with a maximum expected surface wave magnitude equal to 7.5. On the basis of four reliable fault plane solutions and the application of a method suggested by C. Papazachos and Kiratzi (1992), the following parameters were calculated (Papazachos et al., 1994) for the typical fault of this region

strike=42°, dip=44°, rake=167° (1)

This is the region with the highest crustal seismic deformation in the whole Aegean area (3 cm/yr).

For regions B, C, D, twelve very similar fault plane solutions are available (Papazachos and Kiratzi, 1995) from which the following typical fault parameters were calculated:

strike=312°, dip=19°, rake=96° (2)

It indicates that in the western part of the Hellenic trench low angle thrust faults occur and these faults strike in a NW-SE direction and dip to NE.

Region B (Zante) is very active but earthquakes with magnitudes no more than 7.2 occur there.

Region C (SW of Peloponnese) has a length L=170 km parallel to the fault strike, which, according to the following relation

$$\log L = 0.51\ M_S - 1.85 \quad (3)$$

that holds for the area of Greece (Papazachos and Papazachou, 1989), corresponds to a maximum earthquake with M_S=8.0. The largest earthquake which occurred in this region during the last two centuries had a magnitude equal to 7.5 (28.8.1886). There is, however, archeaological evidence which show that an earthquake with magnitude 8.0 or more occurred there in about 1.200 BC (Galanopoulos and Xanthakis, 1988). A deep depression of the sea bottom in this region (see fig. 1) supports the generation of so big earthquakes there and the occurrence of such an earthquake in the future will cause a

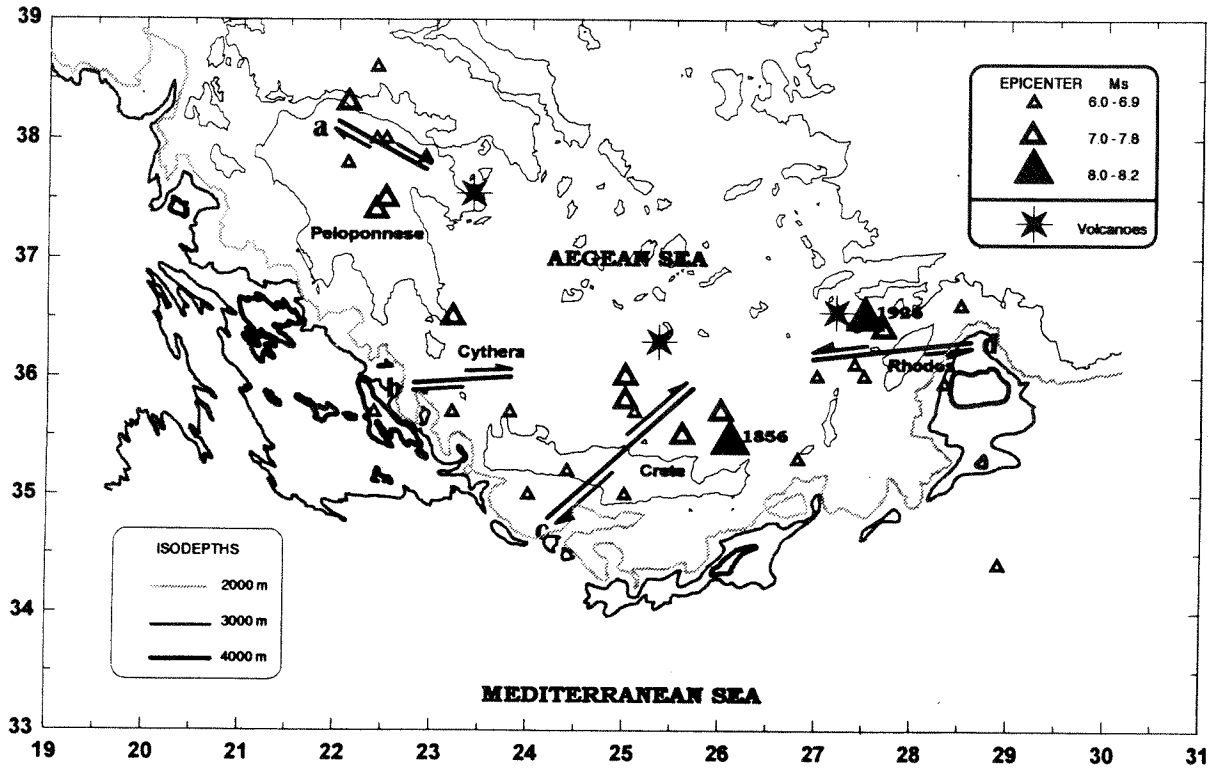

Fig. 2. The four strike-slip, with an inverse component, faults of the intermediate depth earthquakes in the Benioff zone (40-100 km) of the southern Aegean.

gigantic tsunami.

Region D (west of Crete) is that where the big earthquake of 21 July 365 occurred. This is the largest known shallow earthquake equal to 8.3, as it comes out from: the distribution of its macroseismic intensities (Papazachos and Papazachou, 1989), its coseismic elevation of 9 m in western Crete (Thommerete et al., 1981) and the length of its fault which is about 300 km (fig. 1). This earthquake has been associated with a gigantic tsunami which caused extensive destructions in several eastern Mediterranean countries. This is a natural thrust faulting in the rupture zone which includes a deep sea depression with maximum water depth of about 5 km (see fig. 1).

For regions E, F, G in the eastern part of the Hellenic trench, six reliable and very similar fault plane solutions are available (Papazachos and Kiratzi, 1995) from which the following typical fault parameters were calculated:

strike=290°, dip=27°, rake=97° (4)

It means that low angle thrust faults which strike in an ESE-WNW direction and dip NNE occur in the eastern part of the Hellenic trench.

In **regions E** (southeast of Crete) **and F** (southeast of Karpathos) no known earthquake with magnitude more than 7.2 occurred. It is probable that several parallel relatively small faults of the type (4) occur in these two regions.

In **region G** a big earthquake occurred in December 1303. Both the distribution of macroseismic intensities (Papazachos and Papazachou, 1989) and its fault length (L=170 km, see fig. 1) indicate a surface wave magnitude equal to 8.0. This earthquake also produced a gigantic tsunami which caused extensive damage in several eastern Mediterranean countries (Evagelatou - Notara, 1993).

The generation of this big earthquake by a thrust faulting in an area which includes a deep sea bottom depression (see fig. 1) explains the occurrence of this gigantic tsunami.

Big Intermediate Depth Earthquakes in the Hellenic Arc

On the map of figure (2) the epicenters of three samples of relatively recent intermediate depth (h=40-100 km) earthquakes (1801-1995, Ms ≥ 7.5; 1889-1995, Ms ≥ 6.5; 1911-1995, Ms ≥ 6.0) are shown. It is seen that almost all these epicenters are clustered in four regions (a, b, c, d) of the concave part of the arc. The typical fault of each of these four regions as derived by the available fault plane solutions, are also shown in figure (2). These faults are in accordance with a stress field which varies along the arc with the maximum tension being everywhere parallel to the downgoing lithospheric slab and the maximum compression being horizontal and everywhere parallel to the arc (Kiratzi and Papazachos, 1995).

For **region a** (northeast Peloponnese), three reliable fault plane solutions are available (Papazachos and Kiratzi, 1995) from which the following typical for this region fault parameters were calculated:

strike=124°, dip=58°, rake=132° (5)

This is a strike-slip dextral fault with an inverse component and strikes in a SE direction. The length of the seismogenic region parallel to this strike is about 100 km (fig. 2) which corresponds well with the magnitude of the largest earthquake observed in this region (28.5.1897, M_S=7.5).

For **region b** (Cythera) there are two reliable fault plane solutions (Papazachos and Kiratzi, 1995) from which the following typing fault parameters were calculated:

strike=85°, dip=72°, rake=140° (6)

This is a dextral fault with an inverse component and strikes in an about east direction. There are not enough data to estimate the length of the fault.

Region c (Crete) is that where the largest known intermediate depth earthquake in the Mediterranean area (12.10.1856, M=8.2) occurred. It caused extensive damage in Greece and other counties but was not followed by any important tsunami. Three reliable fault plane solutions are available from which the following typical fault parameters were calculated

strike=48°, dip=51°, rake=150° (7)

It is a dextral fault with an inverse component and strikes in a NE direction. This direction is in good agreement with the trend of this seismogenic region (fig. 2) and the length of the region parallel to this direction is 220 km which corresponds well with the magnitude (M=8.2) which has been determined by macroseismic data (Papazachos and Papazachou, 1989).

Region d (Rhodos) is that where the largest earthquake of the present century occurred in Greece for which instrumental information are available (26.6.1926, M=8.0). This big earthquake caused also destructions in Greece and other countries and was not associated with any tsunami. Four reliable fault plane solutions are available for this region from which the following typical fault parameters were calculated:

strike=86°, dip=62°, rake=54° (8)

This is a sinistral fault with an inverse component and strikes in an almost west direction. This strike is in good agreement with the trend of this seismogenic region (fig. 2) and the length of the region parallel to this direction is 160 km which corresponds well with its magnitude (M=8.00) as this magnitude was determined instrumentally.

Discussion

A result of the present paper, probably of general importance, is that by the use of reliable fault plane solutions and spatial clustering of epicenters of strong earthquakes (M_S ≥ 6.0), the orientation, the length and the type of faulting of big earthquakes M_s~8) in the Hellenic arc can be determined. Sea bottom and coastal topography also help for such determinations. The observed delineation of the epicenters of smaller earthquakes parallel to the fault of a big earthquake indicates that these smaller earthquakes (M_s ≥ 6.0) are generated by breaking parts of the big fault or of smaller parallel faults.

The NW-SE strike of the low angle thrust

fault in the western part of the Hellenic trench and the WNW-ESE low angle thrust faults in the eastern part of the trench can be attributed to an overthrust of the SSW direction, respectively. Such a movement is supported by the occurrence of the striking NE-SW dextral fault in the northwesternmost part of the trench (Cephalonia island) as well as by the observed large elevation of western Crete, which is part of the Aegean lithosphere, during the big 365 AD earthquake.

The variation of the stress field which produce the intermediate depth earthquakes in the shallow part (40-100 km) of the Benioff zone, so that the direction of the maximum tension to remain normal to the trend of the Hellenic arc and to dip to its concave part (Aegean), indicates that these earthquakes are due to the subduction of the remnants of an old lithospheric slab which is still in coupling with the Aegean lithosphere in these depths.

References

Galanopoulos, A.G. & Xanthakis, J., 1988. The Halley's comet a decisive agent for the Mycenean decadence, *Academy of Athens Public.,* **60,** 411-428.

Evagelatou - Notara, F., 1993. Earthquake in Byzantium, *"Parousia",* **24,** 1-184.

Kiratzi, A.A. & Papazachos, C.B., 1995. Active deformation of the shallow part of the subducting lithospheric slab in the southern Aegean, *Journal of Geodynamics,* **19,** 65-78.

Papazachos, B.C. & Comninakis, P.E., 1969/1970. Geophysical features of the Greek island arc and the eastern Mediterranean ridge, *C.R. Seance de la Conference Reunie a Madrid,* **16,** 74-75.

Papazachos, B.C., & Comninakis, P.E., 1971. Geophysical and tectonic features of the Aegean arec, *J. Geophys. Res.,* **76,** 8517-8533.

Papazachos, B.C., & Papazachou, C.B., 1989. The earthquakes of Greece, *Ziti Publ. Co., Thessaloniki,* 356 pp (in Greek).

Papazachos, B.C., Karakaisis, G.F., & Hatzidimitriou, P.M., 1994. Further information on the transform fault of the Ionian Sea. *proc. XXIV Gen. Assebl. Europ. Seismol. Commission, Athens 19-24 Sept. 1994* (in press).

Papazachos, B.C., & Kiratzi, A.A., 1995. Type of faulting and seismic deformation in the Hellenic arc. *Proc. XV congress of Carpatho-Balcan Geological Association, Athens, 17-20 Sept.,* 1995 (in press).

Papazachos, C.B., & Kiratzi, A.A., 1992. A formulation for reliable estimation of active crustal deformation and its application to central Greece. *Geophys. J. Int.* **111,** 424-432.

Thommerete, Y., Thommerete, J., Laborel, J., Montaggioni, L.F. & Pirazzoli, P.A., 1981. Late Hollocene shoreline changes and seismotectonic displacements in western Crete, *Geomorphol. Suppl.,* **40,** 127-149.

NEOTECTONIC FAULT SEGMENTS AND FOOTWALL GEOMORPHOLOGY IN EASTERN CENTRAL GREECE FROM LANDSAT TM DATA.

Athanassios Ganas[1], Kevin White[1,2]

[1] *Department of Geography, University of Reading, Whiteknights, Reading, RG6 2AB, UK. e-mail:sgrganas@reading.ac.uk*
[2] *Department of Geography, University of Canterbury, P.B 4800, Christchurch, New Zealand.*

Abstract

Spaceborne structural mapping provides a potential tool to improve our understanding of continental deformation. Using Landsat Thematic Mapper data, fault segmentation and footwall geomorphology for selected fault systems in Eastern Central Greece, were investigated. Fundamental seismic- related landforms, such as "wine-glass valleys" in the footwall of Atalanti fault, and fault bends, can be identified, measured and used to infer fault segmentation and seismogenic potential. These results may contribute towards calculating recurrence intervals of "characteristic" earthquakes and to drive probabilistic models of the regional seismic hazard.

Introduction

Central Greece is an actively deforming continental province undergoing lithospheric extension. The cause of extension is the southward migration of the Hellenic Trench, with a complementary horizontal compression induced by the westward escape of the Anatolian block (Taymaz et al., 1991). Extensional strains have been accommodated mostly by slip along sets of major normal faults of planar geometry and moderate to high-angle inclinations (Roberts and Jackson, 1991). These large normal faults are easily recognisable in satellite images and they mark the boundaries of several "rigid" structural domains, that are arranged at a high-angle to the regional orogenic trend (Figure 1). Fault-accommodated strain has given rise to rapid footwall uplift, and thus, to multiple small continental basins filled with Plio-Quaternary continental deposits.

A recent dense geodetic survey (Biliris et al., 1991) showed that most of fault slip occurs seismically. Indeed, the region has suffered major loss of life and property in the past. Two devastating earthquakes, in 1894, generated by the Atalanti-Martinon extensional fault system (Figure 2) killed more than 250 people and destroyed totally the surrounding villages (Ambraseys and Jackson, 1990). Five other large historic earthquakes are known to have occurred in the area north and east of mountain Kallidromon (Figure 1; Ambraseys and Jackson, 1990), though with great uncertainties regarding their epicentre location and focal depth.

The advent of helio-synchronous, near-polar orbit satellite imagery has provided new, advanced methods for landform reconnaissance and mapping (e.g., Marino and Tibaldi, 1988; Crosta and McMoore, 1989; White, 1993; Murphy, 1993; Deffontaines et al., 1994). This is primarily due to two reasons: first, a synoptic view of the landscape is offered to the researcher at regular time intervals, and secondly, the data are provided in digital form, that enables their subsequent manipulation with image processing techniques. This work is about using optical satellite data in order to distinguish characteristic

Special Publications of the Geological Society of Greece, No 6.

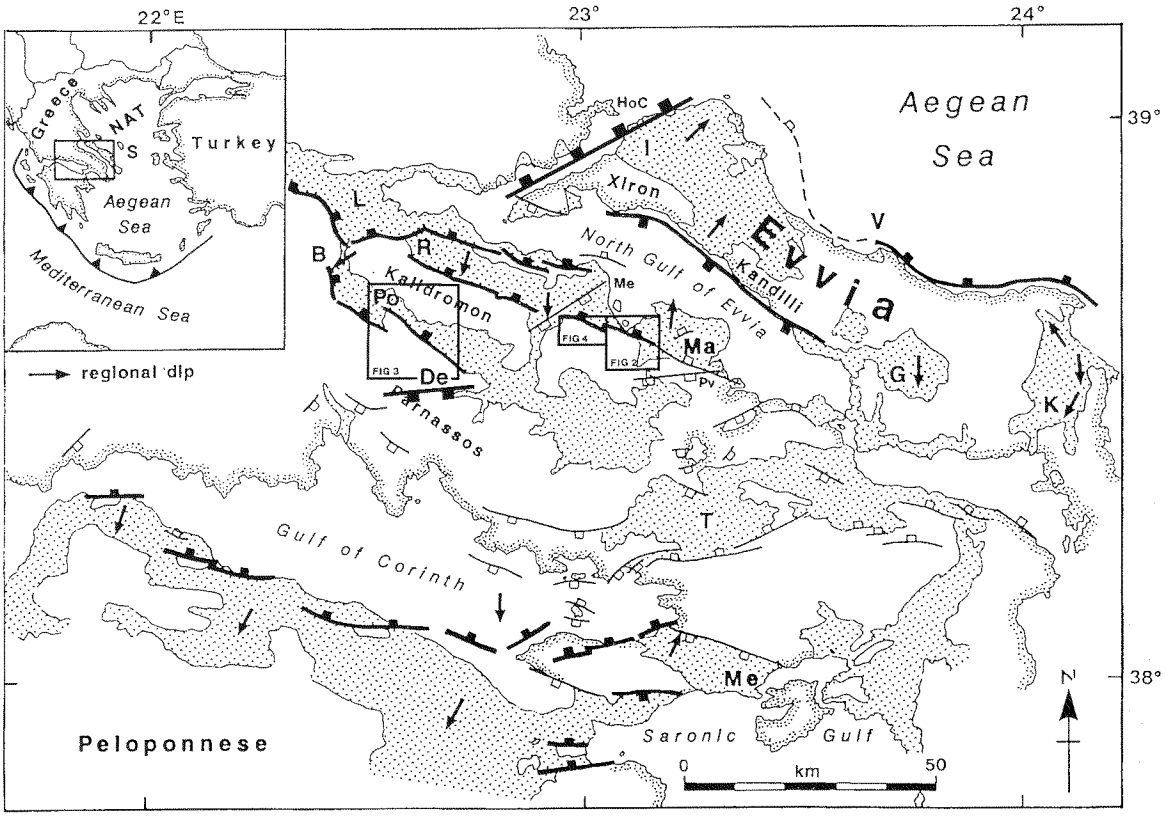

Fig. 1. Fault map of Eastern Central Greece showing major physiographic units and the basins (stippled) where Miocene-Recent sedimentary rocks are preserved. The structural province is identified in the inset map, where NAT is the North Aegean Trough. Several range-bounding faults are shown in bold lines with filled blocks on their downthrown side. Other large faults include De=Delfoi Fault, HoC=Horeoi Channel Fault, Me=Megaplatanos Fault, Pv=Pavlos Fault. Po=Polydroson step-over. Continental basins are : Lamia (L), Bralos (B), Renginion (R), Istiaia (I), and Malesina (M). Arrows show approximate regional dip directions within the basins. Modified after Roberts and Jackson, 1991.

footwall structures along major normal fault systems, and to extract quantitative data at regional scale on the geometry of neotectonic faults.

Geology and Neotectonics

The geology of Central Greece, in the region north of the Gulf of Corinth (Figure 1), is dominated by a series of "alpidic" rock units (Papanikolaou, 1986), that is rocks that have been involved in the Alpine orogenesis (mainly during the Paleocene), aligned in a N-S to NW-SE direction. The main lithology is Mesozoic limestone and dolomite, belonging to *Parnassos and Sub-Pelagonian* zones, accompanied by extensive ophiolitic outcrops and a significant "melange" formation of Upper Jurassic-Lower Cretaceous age. The contacts between the ophiolites and carbonate rocks are extensively tectonised, forming thick cataclastic and mylonitic belts ranging from hundreds of metres to several kilometres in length. A Triassic (Sideris, 1988) volcaniclastic formation also outcrops south of the town of Atalanti.

The regional neotectonic structure is dominated by a set of large normal faults with an WNW-ESE to NW-SE strike and northward dips (Figure 1). These faults control present-day topography, being responsible for the development of marine basins such as the Gulfs of Corinth and of Northern Evia. On several of these faults surface slip is thought to have occurred during recent or historic earthquakes (Ambraseys and

Fig. 2. The Polydroson step-over along the Parnassos fault system, as seen from space. This is a digital snapshot at the shortwave infrared part of the electromagnetic spectrum acquired on 28/1/88 by Thematic Mapper, on board the satellite Landsat 4. The NW striking Parnassos fault consists of two en-echelon geometric and possibly earthquake segments. The Viotikos Kifisos river can be also seen flowing parallel to the mountain-range. Scale 1:100000. The image is property of IGME (Athens, Greece).

Jackson, 1990), although detailed palaeoseismological studies have not been conducted in the region. Fault slip vector azimuths, are generally N-S (±20°; Pegoraro, 1972), similar to those derived from the 1981 earthquake focal mechanisms further south (Dziewonski and Woodhouse, 1983), but different from the NE-SW plate motion across the whole region (McKenzie, 1978). In addition, other faults striking NE-SW also occur and the relative importance of several prominent faults of this set may have not been appreciated so far (see discussion below).

Image processing of landsat data

A Thematic Mapper (TM) winter scene (system-corrected) with path/row coordinates 183/33 for 28 January 1988 was analyzed in detail. TM is an electromechanical scanner on board the Landsat-4 and -5 satellites. These satellites have the same orbital characteristics: altitude 705Km, inclination 98.2°, repeat cycle 16 days and a resultant swath width of 185Km. TM records Earth-leaving radiance at 6 spectral bands in the visible, near infrared and shortwave infrared part of the electromagnetic spectrum (0.45μm-2.35μm) and emitted radiation with a thermal infrared band (10.4μm- 12.5μm). The spatial resolution of the sensor is 28.5m for the reflective bands and 120m for the thermal band.

A series of standard image processing techniques were applied to allow spectral and textural discrimination of lithology and structural mapping. Techniques for lithological mapping included false colour imagery composition (especially, 431 and 754 band combinations), principal component analysis of the reflective bands and IHS transformations of various RGB combinations, however, with limited success, because of extensive vegetation and soil cover, high relief shadowing, agricultural overprint and snow.

To map the neotectonic fabric, visual inspection of the linear/non-linear contrast-stretched, near-infrared bands, was a major source of data. These spectral bands are practically free from atmospheric effects, plus, the low sun angle (25°) accentuates topography. Thus, structural and landform boundaries (such as fault scarps and alluvial fans, respectively), can be determined immediately. In areas of high relief, any FCC combination including bands 4 and 5, had to be displayed first, in order to discriminate snow cover from sun-facing scarps.

Several directional, high-pass filters, were also tested with a tetra- directional Sobel filter giving the best results. Textural segmentation by calculating pixel variances within a moving window, is another necessary technique, mainly to identify relatively undeformed, "homogeneous" domains at large scales (equal to/less than 1:50000). This technique is extremely useful in detecting carbonate versus other bedrock footwalls along large faults.

Interpretation

All neotectonic faults striking NW-SE, and dipping towards NE are easily mapped. Several of these faults comprise abrupt and imposing linear fronts (Parnassos, Kallidromon), and their lengths and azimuths can be accurately measured. The *Kallidromon fault* (Figure 1) is a major crustal-block defining structure, striking N290°, extending more than 38km in length and terminating near the village of Zelion, against a transverse 6.3km long ridge. The *Parnassos fault* comprises two "geometric" (dePolo et al., 1991) segments, with a 5.7km step-over in *Polydroson* area (Figure 2). This en- echelon arrangement with decreasing deformation tipwards, has been also mapped elsewhere (e.g Roberts and Gawthorpe, 1995), and may indicate earthquake segmentation. Within the stepover area, deformation becomes complex, and possibly three-dimensional with the development of orthorhombic fractures. The *Parnassos south* segment is 19km long, terminating right after the Tithorea gorge.

In above cases, typical footwall structures, such as triangular facets and "wine-glass" valleys can be studied quantitatively (Figure 3). These structures are characteristic features of mountain-range fronts in the western USA (e.g Hamblin, 1976), and form because of stream dissection that divides the active range front into alternating transverse spurs and valleys. In the case of the prominent Atalanti fault it was found that three generations of facets have developed in the *Chlomon segment,* at the western part of the fault (Figure 4). Two generations are seen in the Central *Kyparissi-Tragana-Pro-*

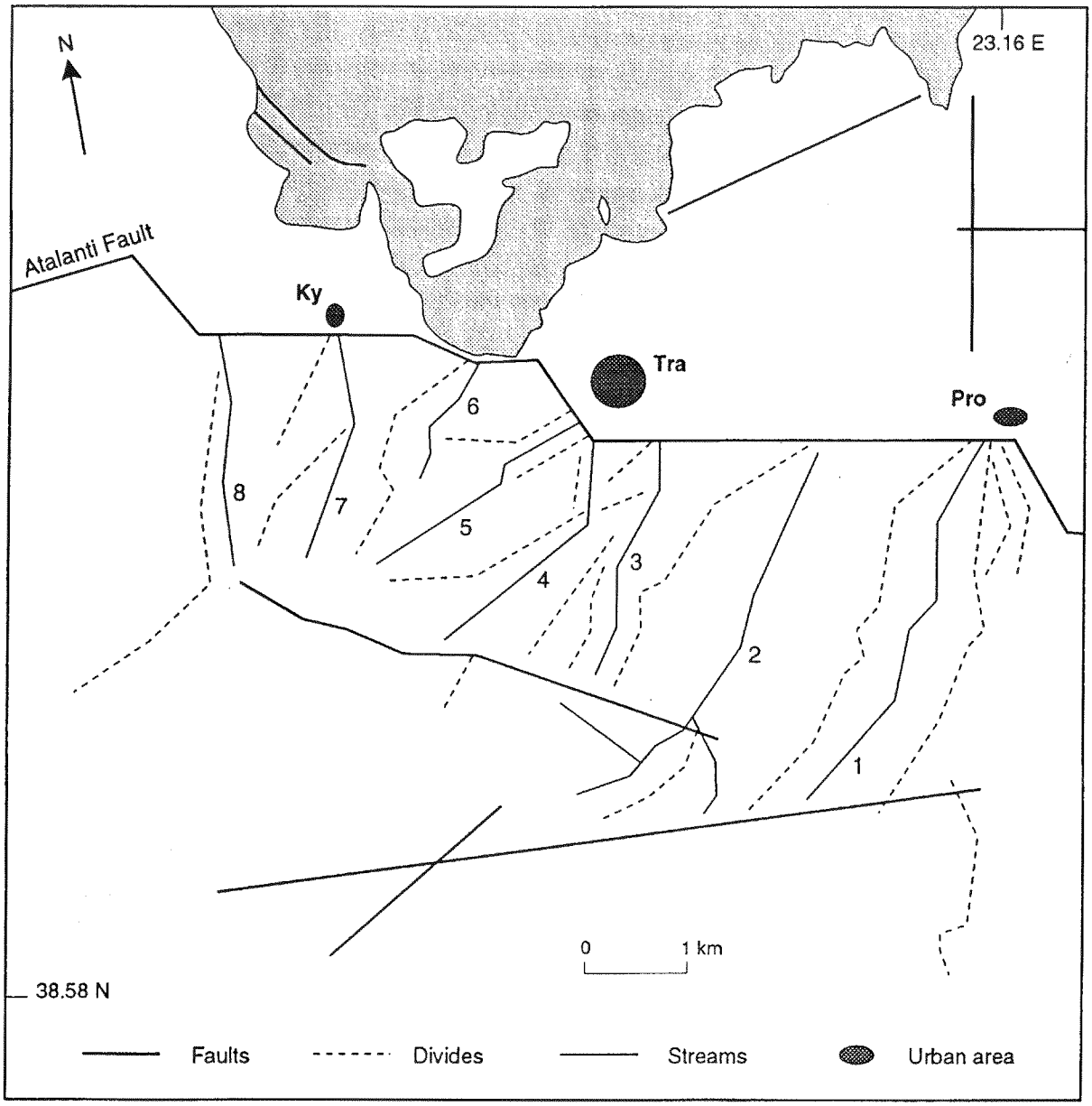

Fig. 3. Spaceborne tectono-geomorphological mapping along the Atalanti normal fault, Central Greece. The fault dips roughly northwards, except along the three bends where the dip direction is modified to NE. "Wine- glass" valleys developed on the footwall are numbered 1 to 8, westwards. Pro=Proskynas, Tra=Tragana, Ky=Kyparissi. Other significant and previously undetected normal faults are also shown.

skynas segment, whereas no facets have developed towards the eastern part of the fault. In the Central segment landform geometry is perturbed due to cross faults at Tragana bend. However, footwall "width" is maintained almost constant along strike and ranges between 3.5-4km for most of the fault extent, while six out of eight "wine-glass" valleys developed, have average lengths of 2.5km and intra-wall average distances of 700m.

We examined the western Malesina peninsula and surrounding areas to the south (N38,600-E23,200) in greater detail (Figure 3). Several previously unmapped fault scarps (IGME, 1989) are visible, and their lengths and azimuths were readily determined. The Atalanti fault itself strikes approximately ESE-WNW in this area, and is found to step to the right at three regions

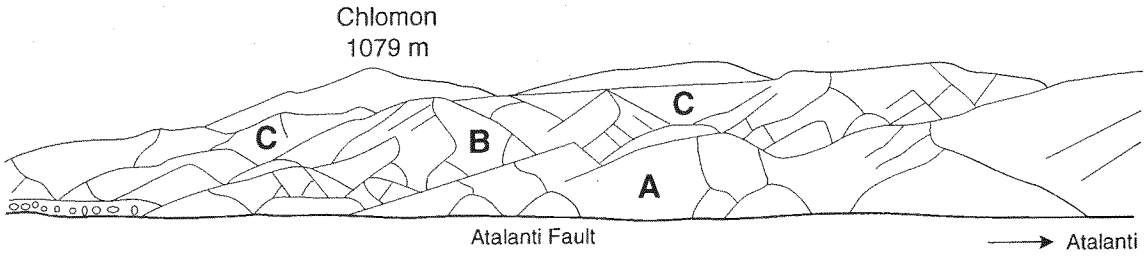

Fig. 4. Line-Drawing from a field photograph of triangular facets developed along the Chlomon range-front in the Lokris area, Central Greece. Three-generations of facets (A=youngest) can be seen. The rocks on the foreground are basic volcanics. The highest peak in the background consists of Mesozoic limestones. The city of Atalanti is located to the right of the photograph, along the range-front. The photo is towards the southwest.

along its trace, however, without losing its continuity. The three bends, namely the *Proskynas, Tragana and Kyparissi* bend, measure approximately the same length (1080m, 970m, and 1090m respectively), and they are parallel in strike (roughly NW-SE). In addition, they are spaced quite regularly along the fault strike: the end-to-end distance of Proskynas-Tragana bends is 4850m, while the distance Tragana-Kyparissi is 4200m. The *Tragana bend* has an orthogonal "wine-glass" valley developed in its footwall implying rupture continuity during large earthquakes, thus, confirming theoretical considerations predicting dip slip down the axis of the bend (Wheeler, 1987). The Kyparissi bend is also the present active fault because it has uplifted Neogene sedimentary rocks on its footwall (e.g Asprorema area). Therefore, on the basis of footwall geomorphology, bend geometry and growth we suggest that this central part of the fault constitutes a coherent earthquake segment, although range-front scarps are no longer visible due to extensive reworking of the land by humans. The 1894 earthquakes may have ruptured two distinct segments of the Atalanti fault zone, since instrumental and macroseismic info (Ambraseys and Jackson, 1990) shows a NW migration of epicentres. Towards the *Proskynas* bend to the East, the fault acquires a sharp trace, and a smooth topography, all the way up to the gulf of *Larymna,* where it terminates.

Other, regionally significant transverse structures, facing away from the sun, can be also mapped using their shadows. Several of the shadows are hemispherical in shape, implying a symmetric slip distribution and elliptical fault growth. Moreover, a set of large, sun-facing fault scarps was also identified, as well as evidence for strike-slip displacements (ridge offsets). Two of the sun-facing scarps are quite important neotectonic structures (Figure 1), as they both bound and predate the Atalanti fault. The first is the *Megaplatanos* fault, a 21km long, probably inactive structure, striking N60o, that is associated with a minor topography (another large sun-facing scarp, namely the Delfoi Fault, could be its westward continuation). The other structure is located 20km to the southeast, namely the *Pavlos* fault, that is almost parallel (N80°) to the former, measures 20.4km, and exhibiting an impressive linear trace, cutting through carbonate bedrock. In addition, very small faults along the Lokrs coastline, striking E-W have been also picked up by TM. Field mapping revealed that these are young, fresh fault scarps probably of Holocene age.

Finally, the azimuth (N312°), length (27km), relief (1200m) and dip direction (SW) of the Kandíllion fault (Figure 1), suggest that the latter is the conjugate structure of Atalnti fault (N295°, 34km, 1079m, NE, respectively), and that the Northern Evia gulf is a symmetrical rift, in direct contrast with the Parnassos half-graben structure.

Satellite structural mapping provides new research capabilities towards understanding continental deformation in this region. Further research efforts are needed on earthquake segmentation and on transfer zone growth and kinematics in Central Greece, so that the size of "characteristic" earthquakes (Schwartz and Coppersmith, 1984) may be calculated. This methodology, in combination with available catalogues of seismic events, may provide results that can be used to model the behaviour of the various seismic sources in the area, and to derive realistic seismic hazard maps.

Acknowledgements

We thank Geoff Wadge for a helpful review, Gerald Roberts and Richard Pope for useful discussions on Greek neotectonics and Yiannis Bacopoulos for assistance in the field. This research is funded by an IKY studentship to A. Ganas, and the University of Reading. A British Council travel grant to K. White is gratefully acknowledged. Satellite imagery was kindly provided by IGME (Institute of Geological and Mineral Exploration, Athens).

References

Ambraseys, N. N., and Jackson, J. A., 1990. Seismicity and associated strain of Central Greece between 1890 and 1988. *Geophys. J. Int.,* **101,** 663-708.

Biliris, H., Paradissis, D., Veis, G., England, P., Featherstone, W., PARSONS, B., Cross, P., Rands, P., Rayson, M., Sellers, P., Ashkenazi, V., Davison, M., Jackson, J., and Ambraseys, N., 1991. Geodetic determination of tectonic deformation in Central Greece from 1900 to 1988. *Nature,* **350,** 124- 129.

Crosta, A., and McM.Moore, J., 1989. Geological mapping using Landsat Thematic Mapper in Almeria Province, SE Spain. *Int. J. Rem. Sensing,* **10,** 505-514.

Deffontaines, B., Lee, J.-C., Angelier, J., Carvalho, J., and Rudant, J.-P., 1994. New geomorphic data on the active Taiwan orogen: A multisource approach. *J. Geophys. Res.,* **99,** 20243-20266.

dePolo, C. M., Clark, D. G., Slemmons, D. B., and Ramelli, A. R., 1991. Historical surface faulting in the Basin and Range province, western North America: implications for fault segmentation. *J. Struct. Geology,* **13,** 123-136.

Dziewonski, A. M., and Woodhouse, J. H., 1983. An experiment in systematic study of global seismicity: centroid-moment tensor solutions for 201 moderate and large earthquakes in 1981. *J. Geophys. Res.,* **88,** 3247-3271.

Hamblin, W. K., 1976. Patterns of displacement along the Wasatch fault. *Geology,* **4,** 619-622.

IGME, 1989. *Seismotectonic map of Greece, 1:500000.* (Athens:IGME Publication).

Marino, C. M., and Tibaldi, A., 1988. Use of Landsat and Seasat data as a tool in kinematic analysis: the Tunisian Atlas. Int. *J. Rem. Sensing,* **9,** 1659-1673.

McKenzie, D. P., 1978. Active tectonics of the Alpine-Himalayan Belt : the Aegean Sea and surrounding areas. *Geophys. J. Royal Astron. Soc.,* **55,** 217- 254.

Murphy, W., 1993. Remote Sensing of active faults : case studies from southern Italy. *Z. Geomorph. N. E., suppl. -Bd.* **94,** 1-23.

Papanikolaou, D., 1986. *Geology of Greece.* (Athens: Eptalofos Publications).

Pegoraro, O., 1972. Application de la Micro-Tectonique à une étude de NéoTectonique : Le Golfe Maliaque (Grèce Centrale), *Thèse (3ème cycle), Universitè des Sciences et Techniques du Languedoc,* 39p.

Roberts, G. P., and Gawthorpe, R. L., 1995. Strike variation in deformation and diagenesis along segmented normal faults: an example from the eastern Gulf of Corinth, Greece. *Geol. Soc. London Special Publicat- ion 80,* 57-74.

Roberts, S., and Jackson, J., 1991. Active normal faulting in Central Greece: an overview. *Geol. Soc. London Special Publication 56,* 125-142.

Schwartz, D., and Coppersmith, K., 1984. Fault behaviour and characteristic earthquakes: examples from the Wasatch and San Andreas fault zones. *J. Geophys. Res.,* **89,** 5681-5698.

Sideris, C., 1988. La sequence volcanosdiment-aire Triassique d' Atalanti (Locride, Grèce). *Ann. Geol. Pays Hellen.,* **33,** 353-369.

Taymaz, T., Jackson, J., McKenzie, D., 1991. Active Tectonics of the north and central Aegean Sea. *Geophys. J. Int.,* **106,** 433-490.

Wheeler, R.L., 1987. Boundaries between segments of normal faults-Criteria for recognition and interpretation. *U.S. Geol. Survey, Open-File 87-673,* 385-398.

White, K., 1993. Image Processing of Thematic Mapper data for discriminating piedmont surficial materials in the Tunisian Southern Atlas. *Int. J. Rem. Sensing,* **14,** 961-977.

SEISMIC HAZARD AND RISK ASSESSMENT
ENGINEERING SEISMOLOGY

INPUT DATA FOR THE SEISMIC HAZARD ASSESSMENT OF THE ADRIATIC REGION

Dario Slejko

Osservatorio Geofisico Sperimentale, Trieste, Italy

Abstract

The Adriatic region has been chosen as a test area in the framework of the GSHAP project. A complete seismotectonic study is under way to derive the correct input parameters for seismic hazard assessment. The guidelines for this study are the same as for a similar almost finished study devoted to a seismic hazard assessment of Italian territory for updating the national seismic zonation.

Introduction

The Adriatic region (Adria) has been chosen as one of the test areas in the Global Seismic Hazard Assessment Project (GSHAP, Giardini and Basham, 1992). A global seismic hazard assessment (SHA) is expected for areas on both sides of the Adriatic sea as result of this project (Slejko, 1994). In addition, two further seismotectonic results are expected as well: the definion, or at least some progress towards it, of the southern margin of the Adria microplate, and an understanding of the earthquake lineament from the Gargano Peninsula to the Croatian coast. The international scientific importance of this project is evident since it is an example of a hazard study involving many different European countries (Italy, Slovenia, Croatia, Albania, Greece). The milestones in the realisation of this project are three: 1) the definition of a global seismotectonic model, with identification of the main seismogenic zones (SZ): 2) the preparation of a common seismicity data for SHA purposes: and 3) an accurate SHA in a region containing high and low seismicity zones.

The basic information for SHA is not currently available for the study region in a satisfactory way because it has never been studied from a global point of view. A Balkan project devoted to SHA has been proceeding since the early Seventies, but the only seismic hazard estimates were performed at an early stage of the project (Algermissen et al., 1976) and never repeated since. No Italian territories and no marine sectors have ever been considered in the Balkan Project. A global seismotectonic model which considers the coastal areas along both sides of the Adriatic sea is, therefore, needed; and for achieving this a precise reconstruction of the kinematic evolution of the Adria microplate is needed as well. The seismicity data base involves many different countries, and the most innovative aspect to tackle, by common effort, regards the border earthquakes, which are all the events for which information is found in different countries. A trivial example is all the events in the Adriatic sea, which is considered almost aseismic, since a deep investigation has never been attempted.

A previous preliminary test

As a preliminary trial run for the Adria project, a hazard assessment of the Macedonia region was recently performed (Papoulia and Slejko, 1994). A correct seismogenic zonation, and the preparation of the accurate earthquake catalogue was far from the scope of that work, and, thus, only a quick revision of the data available in the literature was made. The Cornell (1968) approach was used for SHA, and the results obtained showed the importance of the

Special Publications of the Geological Society of Greece, No 6.

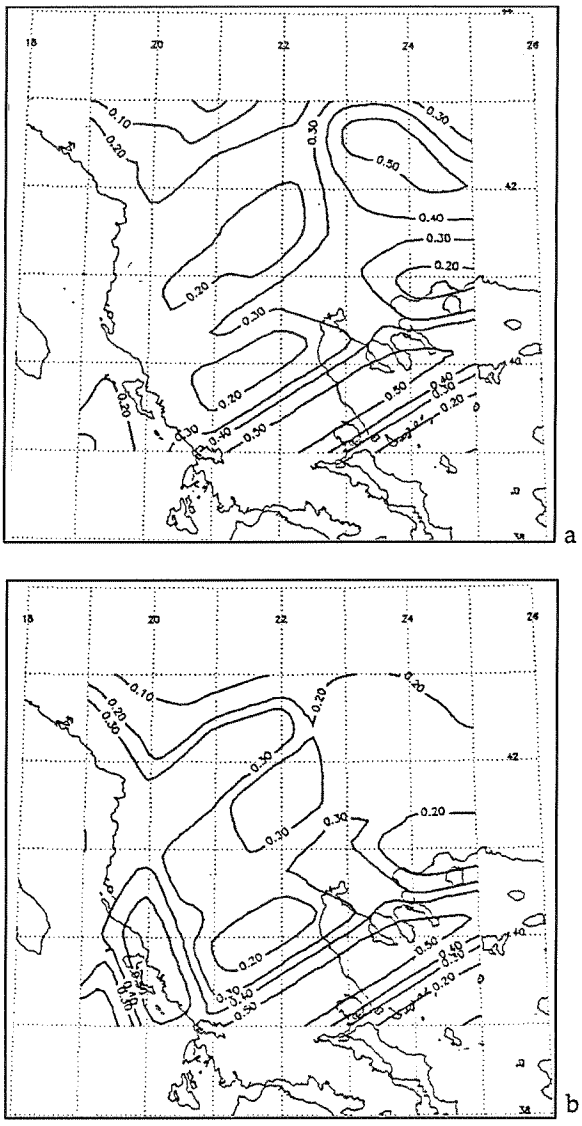

Fig. 1. Hazard maps for Macedonia where PGA with a 475-year return period is shown (from Papoulia and Slejko, 1994): a) using only the ISC data; b) using the complete catalogue.

earthquake catalogue considered. In fact, the seismicity rates used as input for the SHA code (Bender and Perkins, 1987) were computed in two different ways: 1) using the ISC catalogue data of this century (assuming, therefore, the data set to be complete), and 2) using different time windows of the ISC catalogue integrated with national catalogues which cover Macedonia in a broader way. The results obtained show relevant differences in proximity to the SZ's with notable historical seismicity (see Fig. 1).

This preliminary test has clearly shown the importance of properly defining the characteristic seismicity of the SZ'S. The two aspects, SZ definition and related seismicity computation, are linked together. In fact, a correct seismogenic zonation derives from a regional seismotectonic model, calibrated with allthe geological and geophysical data available (among which the seismological data are of primary interest), which explains the kinematic evolution of the area.

The Italian seismic hazard project

A SHA project was recentrly undertaken in Italy (see Slejko, 1995) for the revision of the national seismic zonation. A complete seismogenic zonation was defined for the Italian territory and neighbouring regions (see Fig. 2) and a hazard oriented earthquake catalogue was prepared for the same areas as well. Most of the territories of interest to the Adria project were of interest to the Italian project as well and, consequently, the seismogenic zonation and its related seismicity have already been studied and used as input to the SHA. In the Adria project a further refinement of this input is expected for the Balkan regions, and thus the seismotectonic model has to be derived from the kinematic evolution of Adria in a broader context. In addition, the preparation of a European earth-

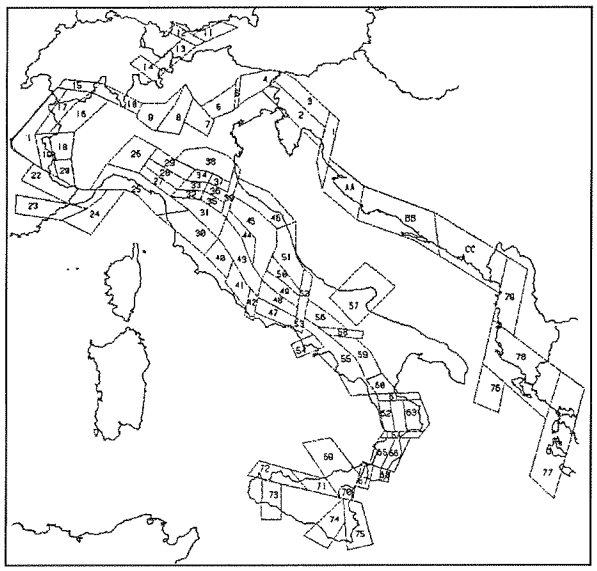

Fig. 2. Seismogenic zonation for Italy and surrounding regions (prepared by Meletti and Scandone for the Adria project).

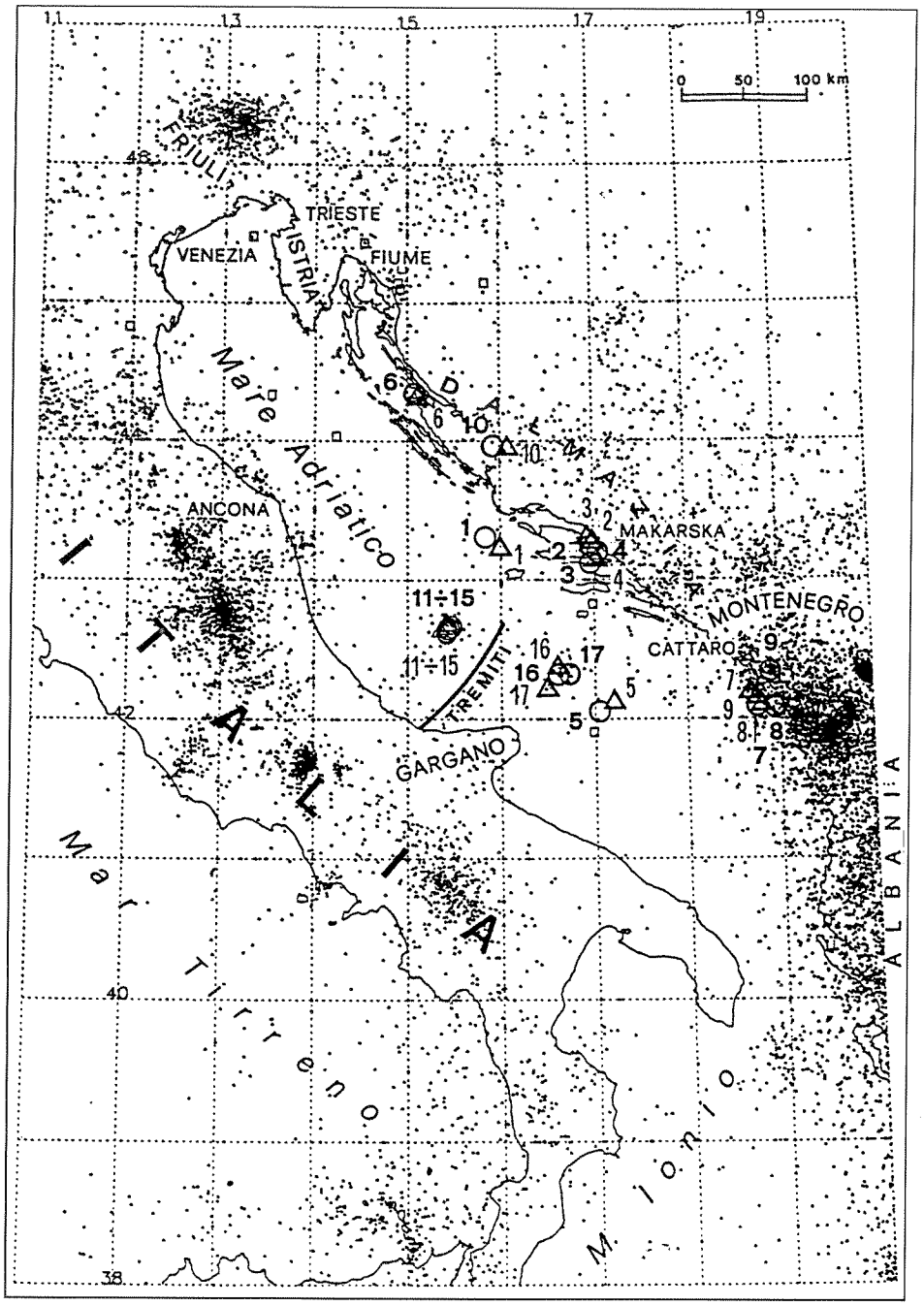

Fig 3. Epicentre map (ISC, 1989) of the earthquakes in Adria and adjacent regions between 1916 and 1989, and relocations (sympol with number) of some principal events (from Renner and Slejko, 1994).

quake catalogue is the theme of a CEC project (Stucchi, 1993); its first stage consists in producing a preliminary working file, obtained from an accurate merging of the existing national earthquake catalogues. The Adria project will benefit from the work of this CEC project, and the European preliminary earthquake work file will be used as the seismicity data base for SZ refinement and SHA.

New research for Adria

As said before, various seismotectonic aspects will be studied during the Adria project: the most important are a definition of the southern margin of the Adriatic microplate, and an explanation of the seismicity in the central Adriatic sea. These are not just interesting scientific

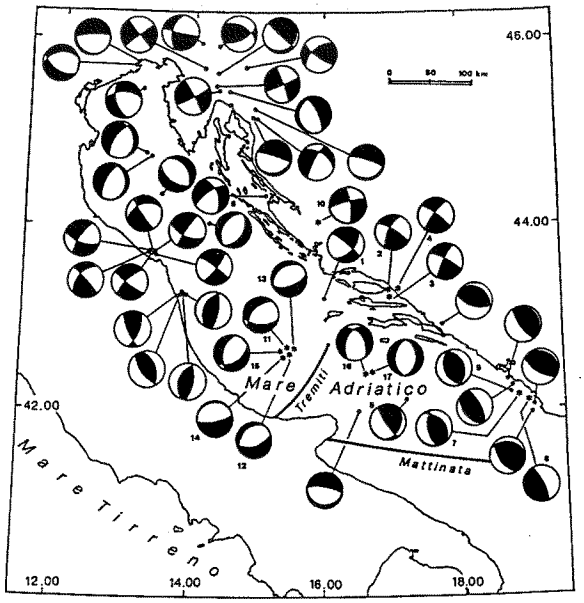

Fig. 4. Fault plane solutions of the principal earthquakes of Adria (from Renner and Slejko, 1994).

problems; they also condition the seismogenic zonation to be used for SHA. For this, an investigation is underway on the instrumental seismicity in the Adriatic sea. All events with enough recorded data have been considered, and hypocentral locations and fault plane solutions have been computed (Renner and Slejko, 1994a, 1994b). Fig. 3 shows the seismicity located for this century in and around Adria. Larger symbols with numbers indicate the relocated events: most of them affected a strip of sea from the Gargano promontory to Montenegro. Different interpretations have been proposed for this seismicity: minor events related to intraplate activity, or seismicity characterizing an active margin separating the northern sector of Adria from the southern; the two sectors would move with opposite rotational directions. Fig. 4 represents the fault plane solutions available for the region: those related to the offshore Gargano earthquakes are mainly of tensile character, and thus they do not support the presence of an active margin of the kind cited before.

References

Algermissen, S.T., Perkins, D.M., Isherwood, W., Gordon, D., Reagor, G. and Howard, C., 1976. Seismic risk evaluation of the Balkan region. In: Proceedings of the Seminar on seismic zoning maps, Unesco, Skopje, pp. 172-240.

Bender B. and Perkins D.M.; 1987: Seisrisk III: a computer program for seismic hazard estimation. U.S. Geological Survey Bulletin 1972, 48 pp.

Cornell, C.A., 1968. Engineering seismic risk analysis. Bull. Seism. Soc. Am., 58, 1583-1606.

Giardini D. and Basham P. (eds); 1993: Global Seismic Hazard Assessment Program. Annali di Geofisica, 33, n. 3-4.

Papoulia J., Slejko D. and Stanishkova I.; 1994: Seismicity and seismic hazard analysis in southern central Balkan region.. In: Abstract ESC XXIV General Assembly, 1994 September 19-24, Athens, Greece, pp. 108.

Renner G. e Slejko D.; 1994a: Sismicità della regione adriatica. In: 13° Convegno Nazionale G.N.G.T.S. Riassunti delle comunicazioni, Esagrafica, Roma, pp. 60.

Renner G. and Slejko D.; 1994b: Some considerations on the seismicity of the Adriatic region. Boll. Geof. Teor. Appl., 36, 381-398.

Slejko D.; 1995: Seismicity, tectonics and seismic hazard in Italy. In: Proceedings of the 5th international conference on Seismic Zonation, Quest Editions Presses Academiques, Nantes, pp. 493-500.

Slejko D.; 1994: The GSHAP Adria project. In: Abstacts ESC XXIV General Assembly, 1994 September 19-24, Athens, Greece, pp. 118.

Stucchi M.; 1993: A basic European earthquake catalogue and a database for the evaluation of long-term seismicity and seismic hazard. A proposal to CEC "Environment" / II. IRRS - CNR, Milano, 53 pp.

DETERMINISTIC ESTIMATES OF THE SEISMIC HAZARD IN BULGARIA

I. M. Orozova-Stanishkova[1], Giovanni Costa[2], Franco Vaccari[2], Peter Suhadolc[2] (1)

1 Institute of Geodesy and Geophysics, University of Trieste, via dell' Universita' N.7, 34100 Trieste, Italy
International Centre for Theoretical Physics, B.O. Box 586, 34100 Trieste, Italy
2 Institute of Geodesy and Geophysics, University of Trieste, via dell "Universita" N. 7, 34100 Trieste, Italy
International Centre for Theoretical Physics, B.O. Box 586, 34100 Trieste, Italy

An estimation of the Peak Ground Acceleration (AMAX) over the Bulgarian territory is performed by a deterministic approach (Costa et al., 1993), computing complete synthetic seismograms (Panza and Suhadolc, 1987).

The input data set consists of structural models (which determine the propagation effects) and seismic sources. The results consist in the deterministic computation of acceleration time series distributed on a regular grid over the studied territory.

The structural models reflect the lithospheric properties of the studied area. They are defined within several regional polygons and consist of a number of flat layers, each characterized by a thickness, density, P-and S-waves velocity and Q. Six regional polygons have been delineated on the territory of Bulgaria, mainly using the information of the crustal structure within each of the polygons. The parameters of the layers describing the structure below the Moho boundary were taken from Costa et al. (1993).

To define the seicmic sources it is necessary to use the information on the seismogenic zoning, the available focal mechanisms and the earthquake catalogue. Recently, Stanishkova and Slejko (1991) and Orozova-Stanishkova and Slejko (1994) proposed a seismic zoning of Bulgaria consisting of 16 seismogenic zones. These 16 seismogenic areas, slightly revised, have been used in the present study. The revision consisted in spatial reduction of some of the zones in order to limit the spatial distribution of sources, and to reduce the amount of computations.

A detailed description of the seismogenic zones is given in Stanishkova and Slejko (1991). Here only the most hazardous zones are noted in brief.

Gorna Oryakhovitza zone: This zone is situated in Central North Bulgaria. Two important earthquakes have affected the zone in the past: one with magnitude 7.2 in 536, and one with magnitude 5.0 in 1660. At the beginning of the 20th century, a magnitude 7.0 eartquake occurred in 1913 followed by a quiescence till 1986, when two relatively strong earthquakes damaged the town of Strazhitza: the first one with Ms-5.5 on February 21, and the second one with Ms=5.7 on December 7 (see e.g. Stanishkova and Slejko, 1990). The seismicity in the zone is shallow, concentrated mainly in the surficial 8-9 km, but with some sporadic events down to 30-32 km depth; the seismicity, tehrefore, occurs in the whole crust.

Varna zone: The zone is placed in the northeastern Bulgaria, arround Varna, one of the biggest cities in the country. Large earthquakes

Special Publications of the Geological Society of Greece, No 6.

occurred here mainly in the past: in 542 (Ms=7.5), and 1444 (Ms=7.5), but only medium/low seismicity is reported at present. The strongest events during this century are those of 1901 (Ms=5.2) and 1911 (Ms=4.7). The seismicity generally involves the surficial 10-15 km with very rare events down to 32 km.

Shabla zone: This zone is placed to the northeast of the previous one. The strongest earthquakes of the past are the 1832 magnitude 6.5, and the 1901 magnitude 7.2 earthquakes. The strongest event in the recent years is the 1956 magnitude 5.5, earthquake. The foci are located mainly in the upper 10-20 km, with few events down to 30-32 km.

Sofia zone: This zone comprises the area around the city of Sofia. Several strong earthquakes affected this zone, starting with the large magnitude 6.0 Sofia earthquakes ini 1818. The strongest event in the zone occurred in 1858 with magnitude 6.5. During the present century, the principal quakes were those in 1904 (Ms=5.0) and 1917 (Ms=5.2). The seismicity involves the surficial 32 km with highest density of hypocentres between 2 and 10 km depth. Of interest is an "inactive layer" located between 10 and 20 km, beneath the Vitodha fault, and a second smaller concentration of foci between 20 and 32 km of depth (Stanishkova and Slejko, 1991).

Maritza zone: The zone is placed in the central part of the country. This is the largest zone, defined following the extension of the Maritza fault. Furtherly, the zone could be divided into smaller zones, according to the different seismic activity along the fault. The strongest earthquakes are the 1750 magnitude 7.4, and the 1982 magnitude 7.2 events. The hypocentre distribution involves the surficial 25 km with very few deeper events (maximum focal depth around 40 km) involving, therefore, almost exclusively the upper crust.

Struma zone: This zone is situated in the southwestern part of Bulgaria. The strongest events affected the zone in 1641 (Ms=7.3), in 1886 (Ms=7.1), and in 1904 (Ms=7.8). The deepest earthquakes in Bulgaria occurred in the Struma zone (maximum focal depth down to 50 km), where the crustal thickness is also big (under the Rila-Rhodopa block it reaches 45-50 km). The hypocentres of the earthquakes are mainly distrubuted in the surficial 35 km, thus the seismicity involves the upper crust (the granite layer thickness is about 24-26 km in the west Rhodopian massif). The lower crust is only partly active.

Mesta zone: The zone is placed just to the east of the Struma zone. The strongest event here occurred in 1759 (Ms=7.5), followed by seismic quiescence until 1870 when a phase of seismic activity began in the zone. The hypocentral distribution involves mainly the depth interval between 2 and 35 km, few events reaching 40 km of depth.

To define the source mechanisms, a number of published fault-plane solutiions over the territory of Bulgaria (Stanishkova and Slejko, 1991; Shanov and Georgiev, 1992; Shanov et al., 1992, Solakov and Simeonova, 1993) were used. One single double-couple (DC) point source located in the center of each cell replaces all the events falling within the cell. The orientation of the double couple point source is obtained from the available focal-plane solutions. The depth derived from the focal-plane solution has been assigned to each source. The earthquake catalogue, used in the present study, is described in details in Stanishkova and Slejko (1991) and Orozova-Stanishkova and Slejko (1994).

When the structures and the srouces are defined, synthetic accelerations are computed using the modal summation technique (Panza, 1985; Panza and Suhadolc, 1987; Florsch et al., 1991) at receivers placed on the grid covering the whole territory under investigation.

The maximum ground acceleration (AMAX) has been chosen as the parameter representing the strong ground motion and consequently the seismic hazard. Only the maximum value of the AMAX at each receiver is considered in this study.

The highest values of AMAX are obtained in southwestern Bulgaria, Struma zone (0.2-0.3 g). High AMAX values (0.1-0.2 g) are calculated in SW and NE Bulgaria (Mesta, westernmost Maritza, Shabla and Varna zones). The Gorna Oryakhovitza, Trun, Sofia, the central and eastern parts of Maritza zone are characterized by 0.05-0.1 g AMAX. The same results are obtained also in the Ardino and Devin zones. The northwestern and southeastern parts of Bulgaria are the less dangerous zones. It should be mentioned that the biggest Bulgarian cities, with relevant economical cultural importance, such as Sofia, Plovdiv and Varna are situated in the zones with high seismic hazard.

The estimation of AMAX obtained in the present study takes into account only the Bulgarian seismicity. The influence of the seismicity of the surrounding countries, such as Greece, Turkey, former Yogoslavia and Romania was not investigated here.

The deterministic approach for assessing the seismic hazard in Bulgaria led to results, similar to those obtained using probabilistic approaches (Orozova-Stanishkova and Slejko, 1994).

References

Costa, G., G.F. Panza, P. Suhadolc and F. Vaccari, 1993. Zoning of the Italian territory in terms of expected peak ground acceleration derived from complete synthetic seismograms. Proc. School on Geophysical Exploration in areas of Complex Geology, Erice 1992, Journal of Applied Geophysics, 30, 149-160.

Florsh, N., D. Faeh, P. Suhadolc and G.F. Panza, 1991. Complete synthetic seismograms for high-frequency multimode SH waves. In: El Escorial workshop proceedintgs. Udias, A. and E. Buforn, Editors, Pageoph 136, 529-560.

Orozova-Stanishkova, I. and D. Slejko, 1994. Seismic hazard of Bulgaria. Natural Hazards, 9, 247-271.

Panza, G. F., 1985. Synthetic seismograms: The Rayleigh waves model summation. J. Geophysics, 58, 125-145.

Panza, G. F. and P. Suhadolc, 1987. Complete strong motion synthetics. In: Seismic Strong Motion Synthetics. B. A. Bolg, Editor, Computational Techniques 4, Academic Press, Orlando, 153-204.

Shanov, S. and Tz. Georgiev, 1992. The Jenuary 23, 1984 Pavlikeni earthquake and its seismotectonic interpretation. Journal of the Bulgarian Geological Society, 53.1, 85-90. (in Bulgarian).

Shanov, S., E. Spassov and Tz. Georgiev, 1992. Evidence for the existence of a paleosubduction beneath the Rhodopean massif (Central Balkans). Tectonophysics, 206, 307-314.

Solakov, D. E. and S. D. Simeonova, Editors, 1993. Bulgaria Catalogue of Earthquakes 1981-1990. Bulgarian Academy of Sciences, Sofia, 40 pp.

Stanishkova, I. D. and Slejko, 1991. Some seismotectonic characteritics of Bulgaria. Boll. Geof. Teor. Appl., 33, 187-210. Voutkov, V., St. Chanov, and A. Demirev, 1986. Evaluation de l' intensite et de l' accelaration maximale en zones seismiques. Geologia Applicata ed Idrogeologia 21.1, 13-22.

A LINEAR AND BAYESIAN SOURCE MODEL FOR SEISMIC HAZARD ESTIMATION ALONG SUBDUCTION ZONES

J. Papoulia[1], G. Stavrakakis[2] and S. Kavadas[1]

[1] *National Center for Marine Research, 16604 Athens, Greece*
[2] *National Observatory of Athens, 11810 Athens, Greece*

Abstract

A Linear and Bayesian source model is proposed to estimate the seismic hazard in Crete and surrounding area (southern Hellenic arc). The seismic sources are identified on the basis of the main seismotectonic characteristics of the region and the seismic epicenter distribution. According to both models, higher hazard values are expected south of Crete, close to the subduction zone of the Eastern Mediterranean. However, the attenuation of expected peak ground acceleration with distance from the causative fault is significanty higher in the linear model, emphasizing the sensitivity of the model to source geometry and the need of the existence of a clear relationship between geotectonics and earthquake occurrences. On the other hand, hazard is more homogeneously distributed in the Bayesian approach, whereas the introduction of dipping sources seems to be more realistic in the case of subduction zones.

Seismic Hazard Assessment

The classical models developed fot the probabilistic assessment of seismic hazard (Cornell, 1968; McGuire, 1974) are based on the assumption that the total energy released during an earthquake is radiated from the focus of the earthquake (point source models). While this assumption is acceptable for small magnitude events, it is not valid for major earthquakes in which the total energy released is distributed along the rupture zone that could exceed several kilometers (Kanamori and Stewart, 1978). In this respect, the calculated hazard for sites equally distant from the focus would be the same irrespective of the distance from the causative fault; it is obvious that such a process leads to an underestimation of the seismic hazard of those sites that the closer to the fault.

In the fault rupture models, the rupture length is the most significant parameter in seismic hazard estimation. According to these models (Aki, 1979; Kikuchi and Kanamori, 1982; Kikuchi and Sudo, 1984; Stavrakakis, 1985), an earthquake propagates as a discrete series of slips along the fault and the maximum expected ground motion is determined by the rupture segment that is closest to the site. The length of rupture is dependent of the energy released, type of fault and other seismological and geological factors.

The Frisk Model

The procedures used to calculate seismic hazard for the case where faults are identified as the potential sources of earthquakes are documented in detail (i.e. Der Kiureghian and Ang, 1977; McGuire, 1978). Under the assumption that the occurrence of earthquakes is a Poissonian process, the probability of exceedence of an

Special Publications of the Geological Society of Greece, No 6.

amplitude z of ground motion, given one event of random size, *M,* rupture length, *Lr,* and location, *X,* on a fault is given by

$$P[Z>z] = \iiint p[Z>z/M, L(M), X]fM(m)fL(l)fX(x)dmdldx \quad (1)$$

In the evaluation of (1) the following assumptions are made:

a. The length of active fault is related to the magnitude.

b. The intensity of the ground motion parameter at a site is a function of magnitude and distance to the closest slip.

c. The log-frequency vs. magnitude relationship for earthquakes is shown through truncated Richter-Gutenberg's formula.

d. The average focal depth of earthquakes is constant.

To calculate the expected number of exceedences, the probability *P[Z>z]* is multiplied by the mean activity rate for the time of interest and the total number of exceedences is calculated as the sum of expected numbers from each fault.

The Bayes Model

The crucial problem in seismic hazard estimation is the time span and the completeness of the sesimological data. Bayesian statistics enables the user to incorporate subjective information for a reliable estimation of the seismicity of a region with limited historical data. Emphasis is given to the representation of seismic sources, as areas of potential future seismic activity, whereas in classical statistics, a minimum earthquake data in each source is necessary.

Furthermore, Bayesian approach combines the statistical uncertainty in error estimations with the inherent uncertainty of random variables. In the parameters estimation, classical statistics treats the seismicity parameter as constant, whereas in Bayes statistics, it is considered a random variable. In this respect, the statistical uncertainty of the parameters of seismicity is incorporated in the model with the probabilistic uncertainty of earthquake occurrences.

According to Mortgat and Shah (1979) and Guidi (1979), the Bayesian seismic hazard model is consisted of three steps:

a. The location of seismic sources is identified on the basis of the seismotectonic characteristics of the region. Various geometrical representations, such as dipping fault planes, horizontal area sources, as well as line sources at constant depth can be used in the model.

b. The seismicity of each source is obtained assuming that earthquakes follow a Poisson process where the mean rate of occurrence, λ, is treated as a random variable. The sample likelihood function on λ is obtained using historical information, while the posterior distribution on λ is obtained combining prior and historical information by means of the Bayes Theorem (Benjamin and Cornell, 1970). Then, distribution of magnitudes is developed using a Bernoulli process. The probability of occurrence of n events of Magnitude M_i, given that n' is the total number of earthquakes in the area, is obtained using the binomial distribution.

c. The Bayesian model uses the type of attenuation associated with the log-normal distribution, in order to incorporate the uncertainty inherent in the use of such relationships. Furthermore, it allows the introduction of two attenuation relationships valid for different focal depths. The rupture length and the shortest distance from the ruptured length to the site is also used in this model.

Application

The area of Crete and surrounding region is characterized by intense seismicity, most of which occurs in its southern part, following the bathymetric expression of the Hellenic Trench (McKenzie, 1978). The majority of earthquakes in this region have focal depths varying between 20 and 60 km, whereas deeper events (h>100 km) occur mainly north of Crete.

The delineation of seismic sources was based on the geographical distribution of epicenters and the main tectonic features of the region (Angelier et al., 1982) (Fig. 1).

Figure (2) illustrates the seismic source model proposed for the application of the FRISK haz-

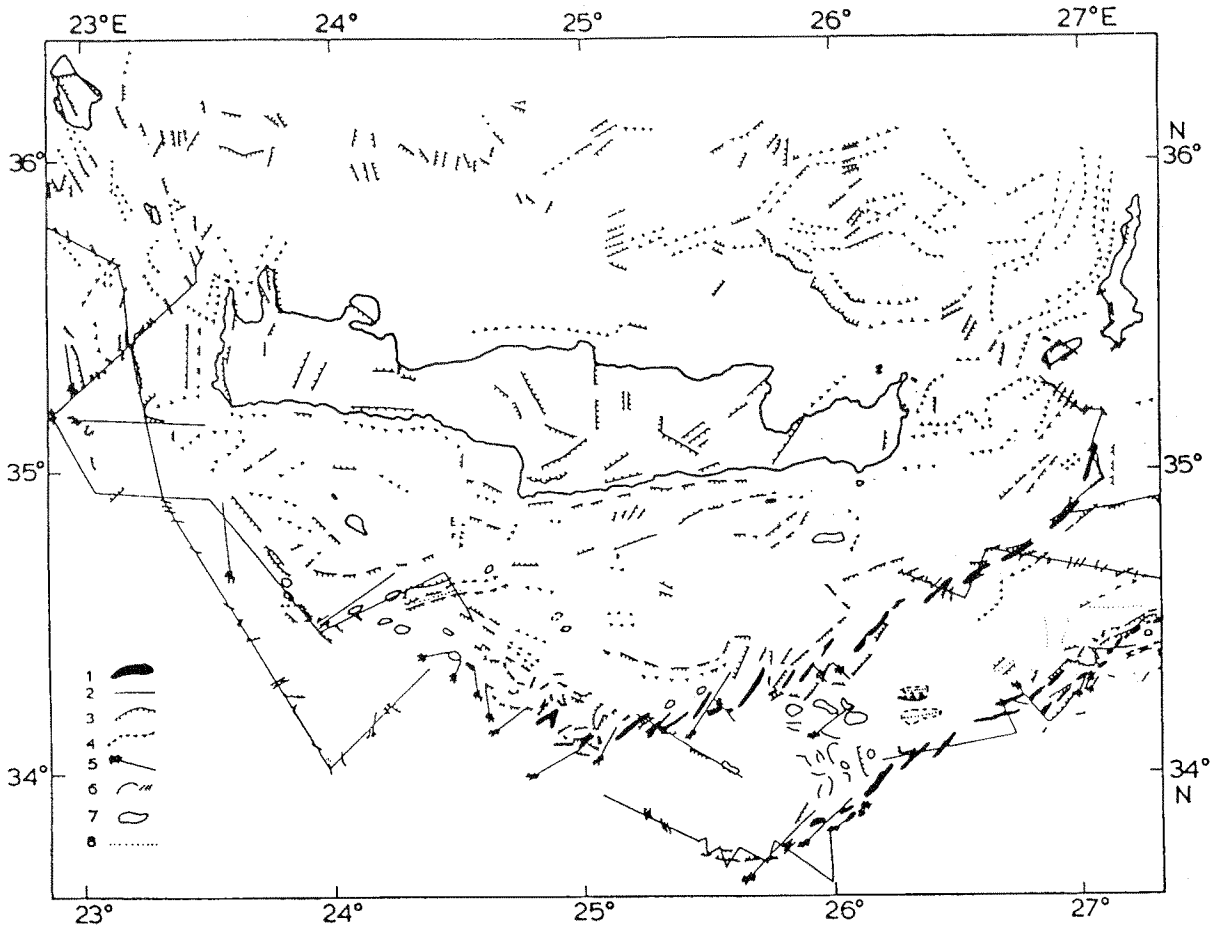

Fig. 1. Main tectonic characteristics in and arround Crete island (Angelier et al., 1982). 1 = en echelon troughs; 2=deepest portion of trench; 3=normal fault scarp; 4=probable normal fault scarp; 5=strike slip fault; 6=topographic ridge interpeted as anticline; 7=diapiric structure; 8=axes of topographic highly.

ard model. The code considers seismogenic lines, at constant depth, recognizing the rupture length as the most important parameter in seismic hazard assessment.

Special attention was given in the Bayesian representation of seismic sources, presented in figure (3). Bayes code considers two kinds of seismogenic sources, line sources of type I and areal sources of types II and III. Type I seismic sources are those for which the length, direction and location of potential fault are known. When the exact location of the fault - or system of faults - is not known, seismic source is characterized as areal of type II. When neither the location nor the direction of the fault is known, seismic source is areal of type III.

The most important feature of the Bayesian model is the introduction of the dipping areal sources, providing the advantage of the representation of dipping fault planes. The analysis of big earthquakes (Kanamori and Cipar, 1974; Stewart et al., 1980, King and Nebelek, 1985) has shown that the dipping plane is the most realistic representation of seismic sources. In figure (3), line sources L4 and L5, correlated with the lerapetra trench, are assigned as type I. Sources L7 and L9-L10 are correlated with the Messara trench and Western Crete trench, respectively, whereas the remaining seismic sources are considered of type II.

The main characteristics of the proposed seismic source models are given in Tables I and II.

Results

The output of the present analysis, in terms of maximum horizontal peak ground acceleration expected not to be exceeded at 90% probability,

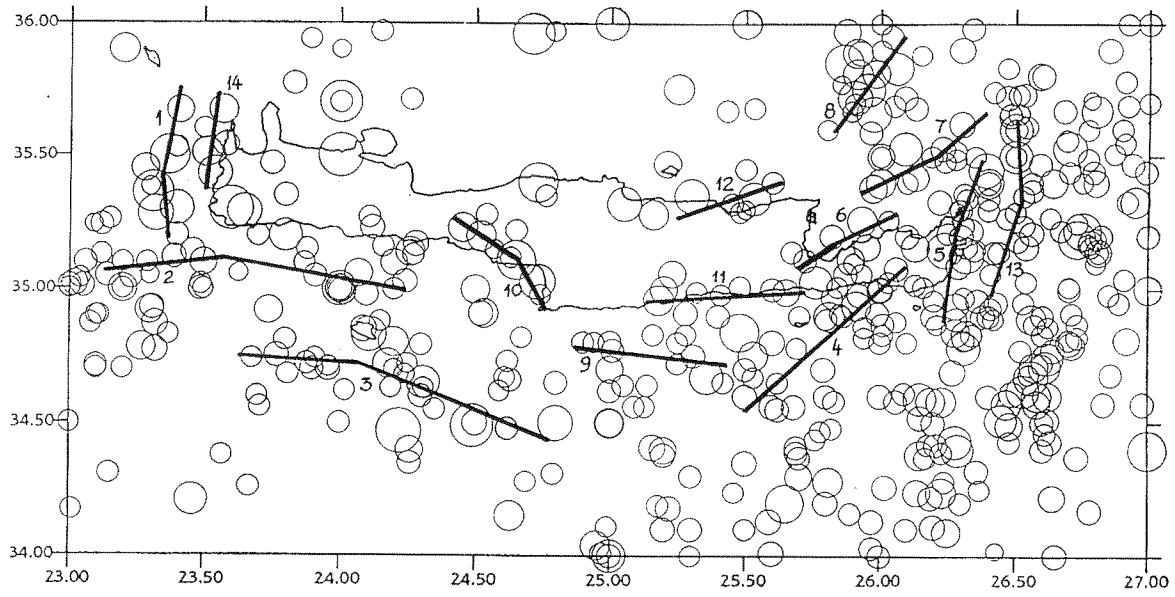

Fig. 2: Proposed seismic source model for the FRISK code (McGuire's approach).

in 100 years, is presented in Figures (4) and (5).

For both codes, maximum hazard values are expected from the south of Crete. This is in accordance with the high magnitude earthquakes originating from this area, due to the subsidence of the African plate under the Eastern Mediterranean plate, taking place south of Crete. However, the overall picture of isoacceleration curves differs significantly in the two maps, emphasizing the differences of the models.

The most spectaculous feature to notice in fig (4) (McGuire's approach) is the extremely high peak ground acceleration close to the seismogenic fault, exceeding 0.7 g. These values are rapidly attenuated with distance from the causative fault. Different values can be reached however according to the attenuation relation considered and the seismicity rates chosen. Nevertheless, the overall picture would be

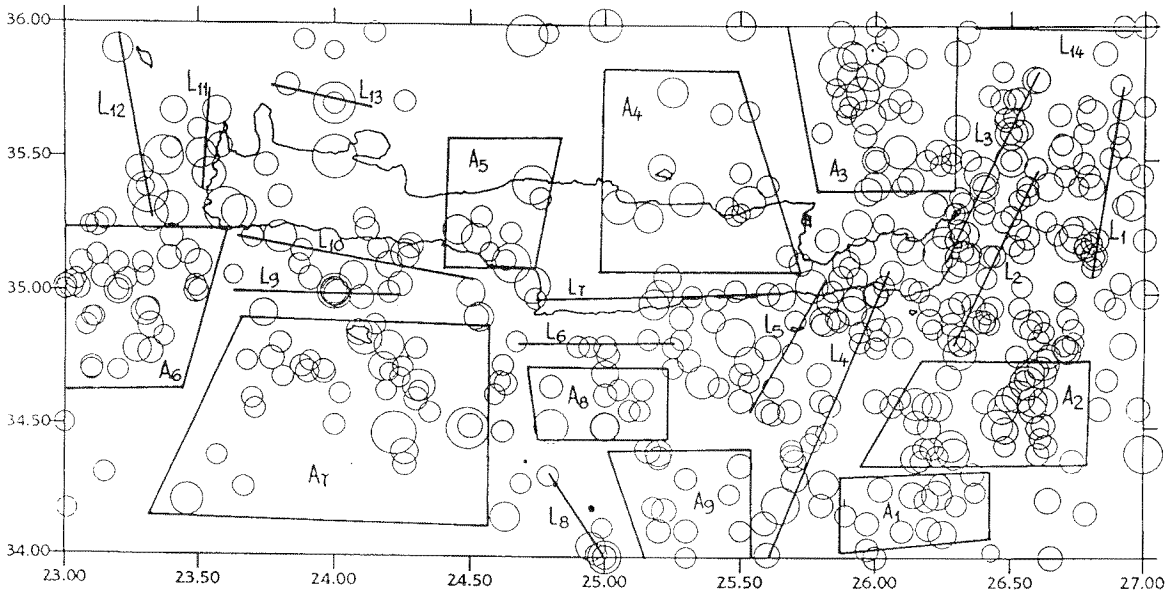

Fig. 3: Proposed seismic source model for the BAYES approach.

Table I. Characteristic seismicity parameters of the seismic faults for the FRISK model. M_1 is the maximum observed magnitude, M_2 is the maximum expected; λ is the annual rate of earthquakes exceeding M_3; β is the parameter of the magnitude exponential distribution.

Line source	M_1	M_2	M_3	λ	β
1	4.4	6.5	7.0	0.148	0.810
2	4.4	6.0	6.5	0.159	1.065
3	4.4	6.7	7.2	0.161	1.412
4	4.4	6.0	6.5	0.165	0.883
5	4.4	5.9	6.4	0.176	1.074
6	4.4	5.3	5.8	0.090	0.655
7	4.4	5.6	6.1	0.054	2.064
8	4.4	6.2	6.7	0.221	1.637
9	4.4	6.2	6.7	0.059	0.898
10	4.4	6.2	6.7	0.072	1.103
11	4.4	5.4	5.9	0.092	0.654
12	4.4	5.6	6.1	0.028	1.150
13	4.4	5.2	5.7	0.177	1.713
14	4.4	5.7	6.2	0.087	0.365

Table II. Characteristic seismicity parameters of the seismic sources (linear and area) of the proposed model for the Bayesian approach. M_1 is the maximum observed magnitude, M_2 is the maximum expected magnitude, N is the total number of earthquakes, h is the mean depth of source.

Seismic Source	M_1	M_2	N	h (km)
A_1	5.2	5.75	15	23
A_2	5.9	6.25	15	22
A_3	6.1	6.50	22	19
A_4	5.0	5.90	11	17
A_5	6.1	6.50	9	20
A_6	6.4	7.00	53	20
A_7	6.6	7.00	27	20
A_8	6.2	6.75	22	20
A_9	5.5	6.10	16	24
L_1	6.0	6.25	18	20
L_2	5.0	5.25	10	20
L_3	5.8	6.25	18	20
L_4	6.0	7.00	20	17
L_5	5.3	6.10	10	23
L_6	5.7	6.25	6	24
L_7	5.3	6.00	17	20
L_8	6.4	7.00	10	25
L_9	5.9	6.25	11	26
L_{10}	6.1	6.50	4	28
L_{11}	5.5	6.00	6	33
L_{12}	6.2	6.25	12	21
L_{13}	4.9	5.25	3	13
L_{14}	4.5	5.25	6	15

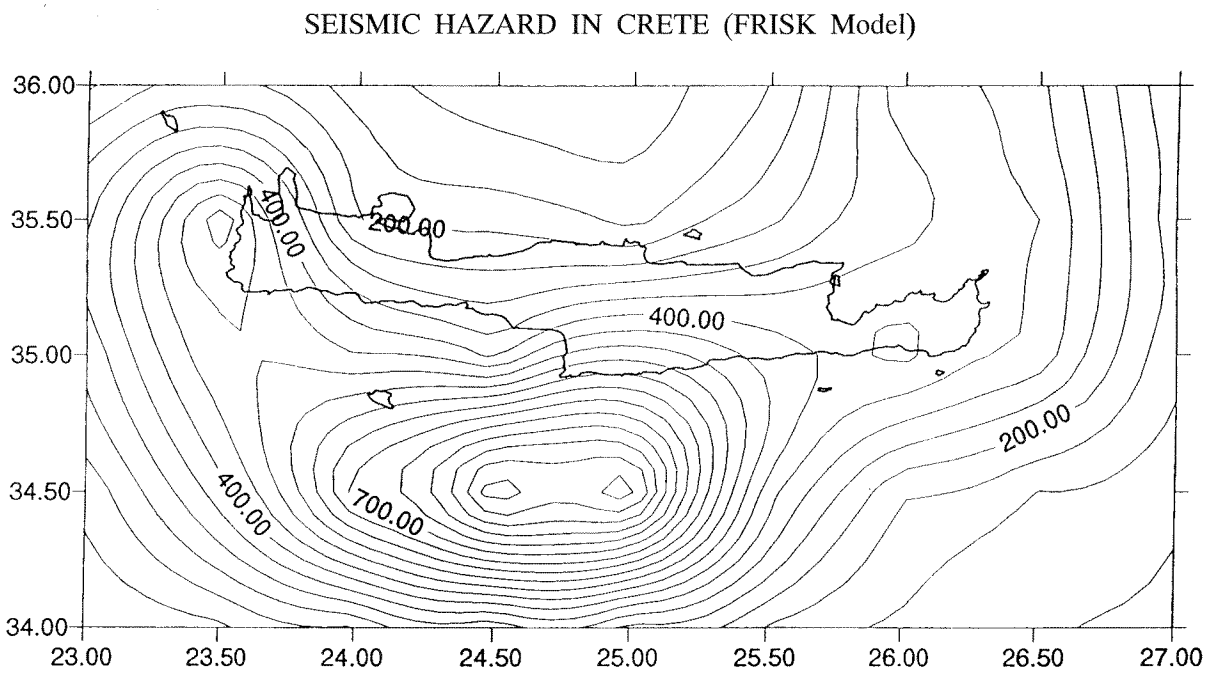

Fig. 4: Peak Ground Acceleration with 90% Probability not to be exceeded in 100 years (RP=475 yrs).

slightly different, emphasizing the need of a good knowledge of the seismotectonic model of the area (sensitivity of the code to the delineation of seismogenic faults). In fact, the model is valid in areas where there is a clear correlation between geotectonics and earthquake occurrence, being more reliable when it comes to the estimation of hazard from a individual fault of well defined characteristics.

On the other hand, in the Bayesian approach

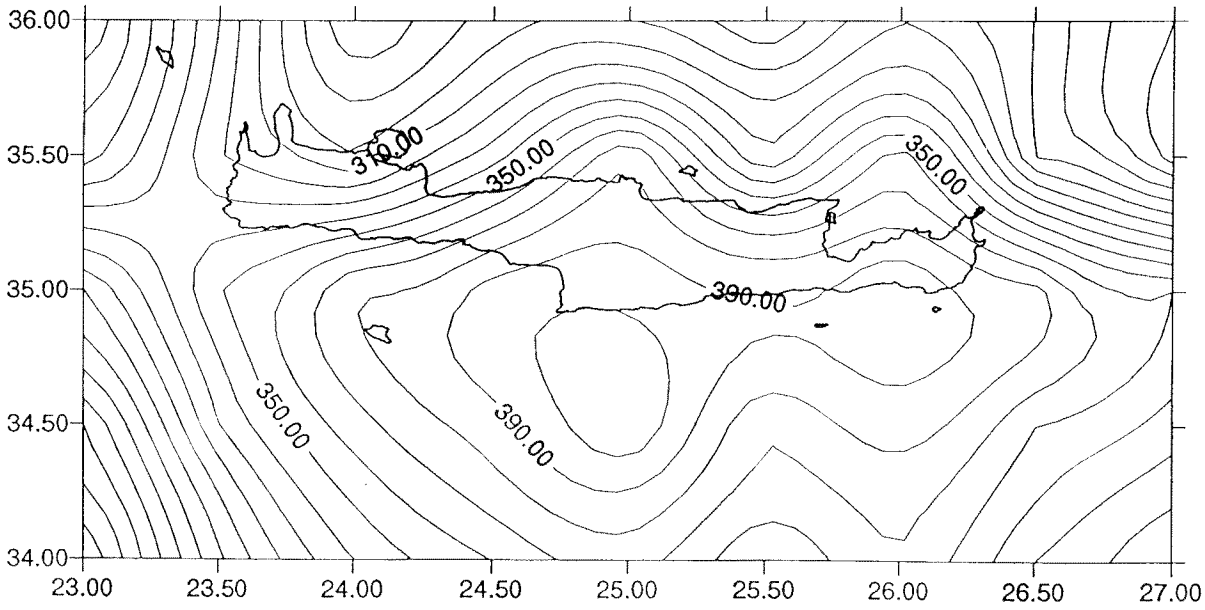

Fig. 5: Peak Ground Acceleration with 90% probability not to be exceeded in 100 years (RP=475 yrs).

there is a more homogeneous distribution of hazard values and the results are considered more reliable, closer to maximum actual observed values in the region. Maximum expected values are significantly lower, while the attenuation rate is low, as well.

It seems that the Bayesian representation of seismic sources is better compared to the classical fault ruprure model. Moreover, the introduction of dipping sources seems to be more realistic in the case of subduction zones, like that of the southern part of the Hellenic arc, in the present study.

References

Aki, K., 1979. Characterization of barriers on earthquake fault. *J. Geophys. Res.,* 84, 6140-6147.

Angelier, J., Lyberis, N., Le Pichon, X., Barrier E., 1982. The tectonic development of the hellenic arc and the sea of Crete: A synthesis. *Tectonophysics,* 86, 159-196.

Benjamin, J. and Cornell, C.A., 1970. Probability statistcs and decision for civil engineers. *McGraw-Hill Book Company,* New York.

Cornell, C.A., 1968. Engineering seismic risk analysis. *Bull. Seism. Soc. Am.,* 58, 1583-1606.

Der Kiureghian, A. and Ang, A.H-S., 1977. A fault rupture model for seismic risk analysis. *Bull. Seism. Soc. A.,* 67, 1173-1194.

Guidi, G.A., 1979. Computer programs for seismic hazard analysis - a user manual. *The John A. Blume Earthquake Engineering Center, Dept. of Civil Engineering,* Stanford University, Rept. N^{0}36.

Kanamori, H. and Cipar, J.J., 1974. Focal process of the great Chilean earthquake May 22, 1960. *Physics of the Earth and Planetary Interiors,* 9, 128-136.

Kanamori, H. and Stewart, G.S., 1978. Seismological aspects of the Guatemala earthquake of February 21, 1977. *J. Geophys. Res.,* 83, 3427-3434.

Kikuchi, M. and Kanamori, H., 1982. Inversion of complex waves. *Bull Seism. Soc. Am.,* 72, 491-506.

Kikuchi, M. and Sudo, K., 1984. Inversion of teleseismic P-waves of Inzu-Oshima, Japan earthquake of January 14, 1978. *Journal Phys. of the Earth,* 23, 161-171.

King, G. and Nabelek J., 1985. Role of fault bends in the intiation and termination of earthquake rupture. *Science,* 228, 984-987.

McGuire, R.K., 1974. Seismic structural response analysis incorporating peak response regressions on earthquake magnitude and distance. *M.I.T. Department of Civil Engineering Research,* Report R74-51.

McGuire, R.K., 1978a. FRISK-computer program for seismic risk analysis using faults as earthquake sources. *U.S. Geol. Surv. Open-File Report,* 78-1007, 71 pp.

Mckenzie, D., 1978. Active tectonics of the Alpine-Himalayan belt: the Aegean sea and surrounding regions, *Geophys. J. R. astr. Soc., 55, 217-254.*

Mortgat, C.P. and Shah, H.C., 1979. A Bayesian model for seismic hazard mapping. *Bull. Seism. Soc. Am.,* 69, 1237-1251.

Stavrakakis, G., 1985. Strong ground motion assessment due to strong earthquakes in Greece. *Individual Studies of I.I.S.E.E.,* Vol. 21, Tsukuba, Japan.

Stewart, G.S., Chael, E.P. and McNally, KC., 1980. The November 29, 1978, Oaxaca, Mexico earthquake: A large simple event. *J. Geophys. Res.,* 86, 5053-5060.

ON THE VALIDITY OF THE REGIONAL TIME AND MAGNITUDE PREDICTABLE MODEL IN GREECE AND ITALY

B.C. Papazachos, G.F. Karakaisis and E. E. Papadimitriou

Laboratory of Geophysics, University of Thessaloniki, Thessaloniki GR54006

Abstract

The regional time and magnitude predictable model' is expressed by the relations:

$$LogT = McM_p + a \quad M_f = CM_p + A$$

where T is the interevent time between two mainshocks in a seismogenic region, M_p the magnitude of the proceding mainshock and M_f the magnitude of the following mainshock in the region. The parameters **c** *and* **C** *are assumed to be the same for all regions of an area, with a positive value for* **c** *and negative value for* **C**, *while the parameters* **a** *and* **A** *depend on the minimum magnitude of the mainshocks considered as well as on the seismicity level of the region. Reliable instrumental data for ten seismogenic regions of Greece and Italy have been used to examine the validity of these two relations by a* **t** *test statistical procedure. It is found that both relations are valid at a very high confidence level (> 0.99) and a large percentage of the data are explained by the first of these relations (R^2=0.89) as well as by the second one (R^2 = 0.88).*

Introduction

Much work has been carried out recently on the time dependent seismicity models. Two kinds of such models have been proposed, the time predictable model' and the "slip predictable model". According to the first of these models the time between two large shocks in a single fault or in a simple plate boundary is proportional to the coseismic slip of the first shock, while according to the second model the coseismic slip of the second shock is proportional to the time elapsed since the previous shock (Bufe et al., 1977; Shimazaki and Nakata, 1980).

Papazachos (1989) used instrumental data for the area of Greece to show that the intervent time, T, for seven seismogenic regions (or sources), which include the main fault where the largest mainshocks occur and other smaller faults where smaller mainshocks in the region according to the relation:

$$\log T = cM_p + a \qquad (1)$$

where the parameter [a] depends on the seismicity of each region and on the minimum (cutoff) magnitude, M_{min}, of the mainshocks considered. A representative of all sources positive value equal to 0.3 was found for parameter **c,** when M_p is the surface wave magnitude and **T** is measured in years. The methodology was further developed by adding another relation which gives the magnitude, M_f, of the expected mainshock in a region by the relation:

$$M_f = CM_p + A \qquad (2)$$

where C has a negative value the same for all seismogenic regions and A depends on the seismicity level of each region and on the minimum magnitude of the mainshocks considered (Papazachos, 1992). The parameters a and A can be expressed as linear functions of M_{min}

Special Publications of the Geological Society of Greece, No 6.

and of the rate of seismic moment released, $\mathbf{m}_o$ (Papazachos and Papaioannou, 1993).

The model expressed by the relations (1) and (2) is called **"regional time and magnitude predictable model"** because it can be applied to predict both the time (relation 1) and the magnitude (relation 2) in a seismogenic region which may include more than one fault.

Very recently, Mulargia and Gasperini (1995) have also shown that time dependent seismicity models are compatible also with a three dimension geometry (seismogenic regions) and proposed a method for defining seismogenic regions by two independent regionalization criteria based on neotectonics and clustering of epicenters. Furthermore, they applied a statistical procedure (t-test) to test the validity of time and slip predictable model in each one of several seismogenic regions in Italy, Greece and elsewhere but arrived at negative conclusion for these models. However, in each of their samples, where this test was applied, the uncertainties of the earthquake size (errors in the magnitude, seismic moment, coseismic slip) are comparable with the range of this size (difference between maximum and minimum size).

The purpose of the present paper is to use instrumental data concerning earthquakes in Greece and Italy to test the validity of the regional time and magnitude predictable model, as this model is expressed by the relations (1) and (2) (with positive and C negative). Parameters for historical earthquakes are not included in the data used in the present study because historic information is sometimes very uncertain especially with respect to the magnitude of these earthquakes.

Data used

Two sets of instrumental data are used in the present study. The first set concerns earthquakes which occurred in Greece and the other earthquakes which occurred in Italy.

The data for Greece concern strong earthquakes which occurred in seven seismogenic regions (sources) and are already published (Papazachos, 1989). These earthquakes occurred after 1911 since when modern seismographs are in continuous operation in Greece. These data are homogeneous, that is, the magnitudes of the earthquakes were calculated in the same way and are also complete, that is, no earthquake with $M_S \geq 5.8$ is missed during this time period. The error in the magnitudes are within the interval ±0.3 (Comninakis and Papazachos, 1986). The values of the magnitudes range between 5.8 and 7.4.

The data for Italy concern earthquakes which occurred in four seismogenic regions in each one of which three or more mainshocks occurred during the present century. These data are also published (Mulargia and Gasperini, 1995). The regions are: Irpinia - Basilicata (with five shocks with M_L = 5.6 - 6.5 since 1910), Region 20 (with fourty one shocks of M_L = 3.6 - 4.8 since 1968), Region 31 (with twenty four shocks of M_L = 3.0 - 3.9 since 1970) and Region 37 (with nine shocks of M_L = 4.5 - 5.4 since 1908).

The declustering of the data, that is, the procedure to exclude preshocks and postshocks, is that one described by Papazachos and his colleagues (1995). In this procedure, the preshock time is considered constant (equal to three years) and the postshock time is increasing with the magnitude of the preceding mainshock.

Method Applied

The validation of the relation (1), which expresses the regional time predictable model, can be made by the t-test in two ways. The first way is to apply this relation to the data of each seismogenic region and to test the goodness of fit (Mulargia and Gasperini, 1995) and the second way is to apply this relation to the whole set of data in an area, which includes several seismogenic regions, and to test the goodness to fit.

The application of relation (1) to the data of a seismogenic region (seismogenic source) and its goodness of fit can be tested only if the range of variation, M, of the magnitude, M_p, in each region is large enough. Unfortunatelly, the available data do not satisfy this conditions, since is not much larger than the uncertainties in the determination of the magnitudes. For this reason, the application of relation (1) to the data of each region is not a proper way neither to test the validation of this relation nor to reliably determine the value of the parameter c for predictive purposes.

On the contrary, the application of relation (1) to all data concerning all seismogenic regions of the area is a proper way to test the validity of this relation because the magnitude range is large enough. This is also a proper way to reliably determine the value of the parameter c

because this parameter does not vary much from region to region (Papazachos et al., 1995). As to the dependence of the parameter a on the seismicity level of each seismogenic region and on the magnitude of the smallest mainshock considered it can be easily taken care by reducing the value of a to the same level by the following method (Papazachos, 1989):

By using an arbitrary initial value for the parameter c (e.g. c=0) in equation (1), values of the parameter a were determined for all available interevent times, T, in an area (e.g. Greece) and the average, $\overline{a}$, of all these values is calcuted. In the same way, the average value, $\overline{a}_{ij}$, which corresponds to each group of interevent times with the same minimum magnitude of each group of interevent times with the same minimum magnitude of each seismogenic region is determined. Then, the quantities $\log T^* = \log T + \overline{a} - \overline{a}_{ij}$ are calculated for all available repeat times and a new value of the parameter c is determined by a least - squares fit to the data ($LogT^*$, M_p). The new value of c is used as initial one and the procedure is repeated until a convergence to certain final values of c and "a" are obtained. Then, this test is applied for both parameters and the t(c), t(a) values, as well as the corresponding confidence intervals, P(c), P(a), are calculeted. Then, the value of R^2 which indicates the percentage of the data interpreted by the model, is also calculated.

The same procedure was followed to calculate the values C and A of the relation (2) and to test the validity of this relation.

Validation Tests for the Regional Time and Magnitude Predictable Model

The method described above was first applied to test the validity of relation (1) by using separately the data for Greece and the data for Italy. High values for the confidence intervals (P>0.99) for all four parameters in both areas were found, while the value of R^2 was found equal to 0.76 for Greece and 0.68 for Italy. In other words, the data for seismogenic regions of both Greece and Italy fit the regional time predictable model to a very satisfactory degree.

However, the results are better when all data, for the seven seismogenic regions of Greece and for the four seismogenic regions of Italy, are used together, because for this case the following values were calculated:

$$t(c) = 22, \quad t(a) = -7, \quad P(c)>0.99, \ P(a)>0.99, \ R^2 = 0.89 \tag{3}$$

which means that the model is valid at a very high significance level and that the fraction of data explained by the model is 89 per cent. Figure (1) shows a plot of the reduced data ($LogT^*$, M_p) which have been fitted, in the least squares sense, by the relation:

$$LogT^* = 0.29 \ M_p - 0.55 \tag{4}$$

The value of the parameter c (=0.29) is very close to the value of this parameter (c=0.33) determined by a huge sample of data concerning 274 seismogenic regions in the whole continental fracture system (Papazachos et al., 1995).

The same procedure was followed to test the validity of the regional magnitude predictable model expressed by relation (2). By using the data (M_f, M_p) for the seven seismogenic regions in Greece together with the corresponding data for the four seismogenic regions in Italy the following values were calculated:

$$t(C) = 57, \ t(A) = -21, \quad P(C)>0.99, \ P(A) = 0.99, \ R^2 = 0.88 \tag{5}$$

which means that the model is valid at a very high significance level and that the fraction of the data explained by the model is 88 per cent. Figure (2) shows a plot of the reduced data (M_f^*, M_p), fitted in the least squares sense by the relation:

$$M_f^* = -0.55 \ M_p + 8.87 \tag{6}$$

with a negative slope, as it is expected by the model (Papazachos, 1992).

The relations (4) and (6) indicate a negative correlation between the interevent time and the size of the following shock. Indeed, a test of a linear relation between logT and M_f, by the use of these instrumental data for Greece and Italy, gave a negative slope for this line with a high degree of confidence ($R^2 = 0.82$). This contradicts the "slip predictable model" because, according to this model, the size of the following shock increases with increasing interevent time. Therefore, the slip predictable model does not fit these data.

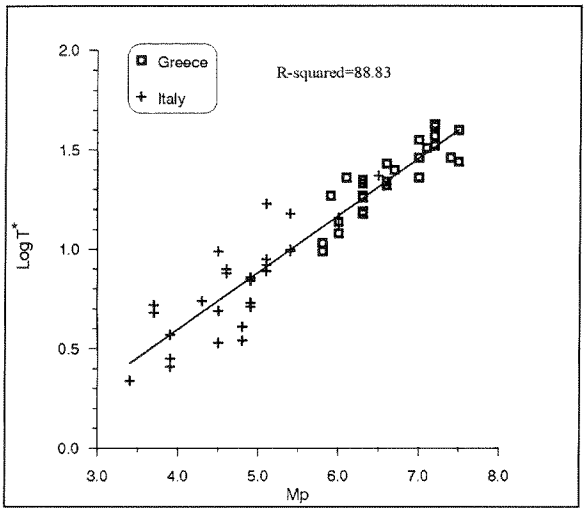

Fig. 1. Dependence of the repeat time, T^*, on the magnitude, M_p, of the preceding main shock.

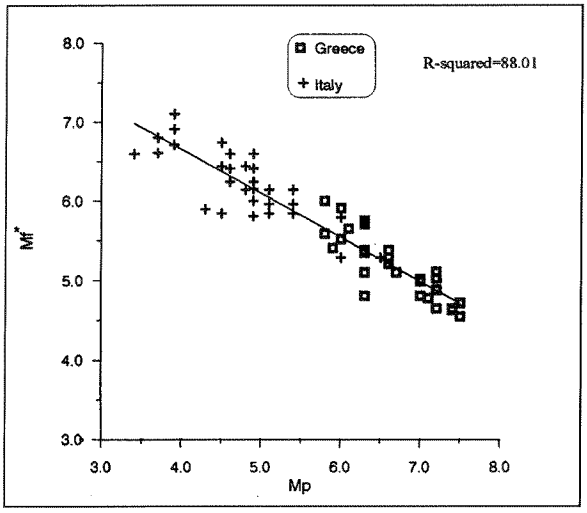

Fig. 2. Dependence of the magnitude of the following main shock, M_f^*, on the magnitude, M_p, of the preceding main shock.

Discussion

The statistical procedure applied in the present paper to reliable instrumental data, for mainshocks in seismogenic regions of Greece and Italy, has shown that these data fit the **[regional time and magnitude predictable model]** with a high degree of confidence. This model has been already tested by data in several seismogenic regions of the continental fracture system and has been proved superior to classical seismicity models (Papazachos et al., 1995).

However, Figures (1) and (2) show a still considerable scatter of the data in respect to this model. This scatter is due to a systematic (intrinsic) deviation, which reflects variation of the process from the model and also to uncertainties in the input data especially in the magnitude of the earthquakes. For this reason, only long term earthquake prediction and an estimation of the size of the expected earthquake is possible by this model at the moment.

The deviation of the observed magnitudes from the expected by the model magnitudes is considerable (see Fig. 1, 2) and when historical data are included in the data sample this deviation can reach up to one magnitude unit or more. For this reason, validation tests cannot be effectively applied to samples with small magnitude ranges (difference between maximum and minimum magnitude). This explains the negative results of Mulargia and Gasperini (1995) for the applicability of the time predictable model in Italy and Greece, because they applied this validation test in samples with magnitude ranges comparable to the uncertainties in the magnitudes. On the contrary, the sample of data which was used in the present paper and tested successfully to follow the regional time and magnitude predictable model includes earthquakes with a magnitude interval of the order of four magnitude units, that is, much larger than the uncertainties in the magnitude.

Acknowledgements

This research work has been partially supported by the EEC Environment Research Projects EV5V-CT94-0513.

References

Bufe, C. G., Harsch, P. W. and Burford, R. O., 1977. Steady - state seismic slip: A precise recurrence model, *Geophys. Res. Lett.,* **4,** 91-94.

Comninakis, P. E. & Papazachos, B. C., 1986. A catalogue of earthquakes in Greece and surrounding area for the period 1901-1985, *Publ. Geophys. Lab., Univ. Thessaloniki,* **1,** 167 pp.

Mulargia, F. & Gasperini, P., 1995. Evaluation of the applicability of the - time - and slip-predictable earthquake recurrence models to Italian seismicity, *Geophys. J. Int.,* **120,** 453-473.

Papazachos, B. C., 1989. A time - predictable model for earthquakes in Greece, *Bull. Seism. Soc. Am.,* **79,** 77-84.

Papazachos, B. C., 1992. A time and magnitude predictable model for generation of shallow earthquakes in the Aegean area, *Pure Appl. Geophys.,* **138,** 287-308.

Papazachos, B. C. & Papaioannou, Ch. A., 1993. Long - term earthquake prediction in the Aegean area based on a time and magnitude predictable model, *Pure Appl. Gophys.,* **140,** 593-612.

Papazachos, B. C., Papadimitriou, E. E., Karakaisis, G. F. and Panagiotopoulos, D. G., 1995. Long term earthquake prediction in the circum - Pacific convergent belt, *Pure Appl. Geophys.,* (in press).

Shimazaki, K. & Nakata, T., 1980. Time predictable recurrence model for large earthquakes, *Geophys. Res. Lett.,* **7,** 279-282.

RELATIONSHIPS BETWEEN SOME SEISMICITY PARAMETERS OBTAINED BY DIFFERENT METHODS IN THE EURASIAN SEISMIC BELT

Theodoros M. Tsapanos

Aristotle University of Thessaloniki, Geophysical Laboratory, 54006 Thessaloniki, Macedonia, GREECE.

Abstract

Relationships between seismicity parameters obtained from the "whole process" and the "part process" methods, and by the application on the strain energy release technique are derived in the present work. The Eurasian seismic belt is chosen for this purpose and the forecasts of earthquake magnitudes with an average return period of 88 years, obtained by the prereferred methods, are presented. Relationships between the parameters of the Gumbel III distribution (part process) and the quantities M1 (the most probable annual maximum magnitude, obtained from the whole process), M2 and M3 (magnitudes which are equivalent to the mean annual rate and the maximum possible energy release in one earthquake of the strain energy respectively), reveal slight differences between the methods. Similar relationships with those established by Burton and Makropoulos (1985), between the Gumbel III parameters and the quantities m1(1), X2 and ϖ, which are notionally similar to M1, M2 and M3 are found through the examined seismic belt. This belt is of different tectonic environment from the circum-Pacific, with which the previous authors are involved. This lead to the conclusion that these relationships are globally valid.

1. Introduction

Various statistical models have been applied to the analysis of earthquake occurrence with differing degrees of success. The commonest description of earthquake occurrence is provided by Gutenberg and Richter (1994) cumulative frequency-magnitude law. In a given region and during a given time span this is given by:

$$\log N = a_k - bM \qquad (1)$$

where a_k and be are parameters and N is the number of the earthquakes. The index k denotes the time period for which data are available for analysis and this is usually normalised to a period of 1 year for which a_k=a. This is based on the knowledge of the occurrence of all earthquakes in a region, the "whole process".

A commonly used method, which analyses the "part process" of seismicity occurrence by considering only the largest or annual extreme earthquakes, is the theory of extreme values (Gumbel 1958). Gumbel's third (GIII) asymptotic distribution takes the form:

$$G^{III}(m) = \exp\left[-\left(\frac{\omega - m}{\omega - u}\right)^{k}\right], \quad k>0, \qquad (2)$$

with three parameters: the upper bound magnitude, ϖ the characteristic extreme magnitude value u (not the modal value) and k(=1/λ) which relates to curvature of the distribution. G(m) is the probability that magnitude m is an annual extreme. The finite amount of strain energy storable in a given volume determines the upper bound of earthquake magnitude in that volume (Esteva 1976).

Earthquake magnitude and strain energy re-

lease, E (ergs), can be related through Bath's (1958) equation:

$$\log E = 12.24 + 1.44\ M \quad (3)$$

This approach is useful to describe earthquake occurrence because it allows for cycles of strain energy input and release with notionally upper bounded earthquakes occurring with finite return period.

The Eurasian seismic belt has the second highest seismicity in the world after the circum-Pacific belt. Seismicity parameters of the Eurasian belt have been investigated by several authors (Galanopoulos 1968, Karnik 1968, 1971, Kaila and Narain 1971, Kaila and Rao 1975, Makropoulos 1978, Burton 1978, 1979, Burton et al. 1984, Nowrooozi and Ahmadi 1986, Papazachos et al. 1994). The aim of the present work is to demostrate the usefulness of the extreme value theory when applied to the estimation of earthquake occurrence and to compare with results obtained using other methods. Burton and Makropoulos (1985) demostrated that the three parameters of the GIII distribution are related to physical release of the strain energy through the quantities M1 (of the whole process), M2 and M3 obtained from the strain energy release process, and these relationships will be applied here.

2. Data and Method

A global complete and homogeneous catalogue (Tsapanos et al. 1990) for $M \geq 5.5$ has been revised by considering the magnitudes given in a published catalogue (Pacheco and Sykes 1992) and is used in the present work. The data set used is extracted from this catalogue and covered the time period 1897-1985. The method used to assess the completeness of the data has been described elsewhere (Tsapanos 1990).

Individual cells of 15°latitude X 15°longitude have been selected moving eastwards along the Eurasian belt and starting at 30°N and 15°E (the first cell is 30°-45°N and 15°-30°E). The exception is the Burmese arc (cell 8) which is bounded between 15°-30°N and 90°-105°E (**Fig. 1**). For each cell the annual mode M1 is calculated using equation (1) and the least squares method. The mean annual energy release expressed as the equivalent magnitude M2 and the quantity M3 representing the notional maximum strain energy that can be accumulated and released in a maximum possible earthquake in a region are also computed.

For the present work the parameters ϖ, u and λ of Gumbel's third asymptotic distribution are also estimated for each of the cells. For each cell values of the largest earthquake magnitude expected over an interval of 88 years are forecast using the Gumbel III distribution (m88), as well as the 88 years mode obtained using the "whole process" method (RM88). Relationships are derived finally between parameters and the significance of any similarities and differences discussed.

3. Theoretical considerations of the applied methods

The methods applied here in order to estimate the seismicity parameters are outlined briefly below.

3.1. Evaluation of the parameter M1

The distribution of earthquake magnitudes in time and in size is usually studied, using the whole available data set of magnitudes (whole process) and can be expressed by equation (1). The weaknesses of this process are that it does not include information in the upper bound magnitude, as well as the lack of accuracy, homogeneity and completeness inherent in the data sets analysed, especially in the lower magnitude ranges. From equation (1) and for N/year = 1, the most probable annual maximum magnitude (mode) is:

$$M1 = a/b \quad (4)$$

and the the T-year mode is given by:

$$M = \frac{a + \log T}{T} \quad (5)$$

The T-year modal magnitude for T=88 yr will be reported to as RM88.

3.2. Gumbel III parameters

Gumbel's theory of extreme values has the

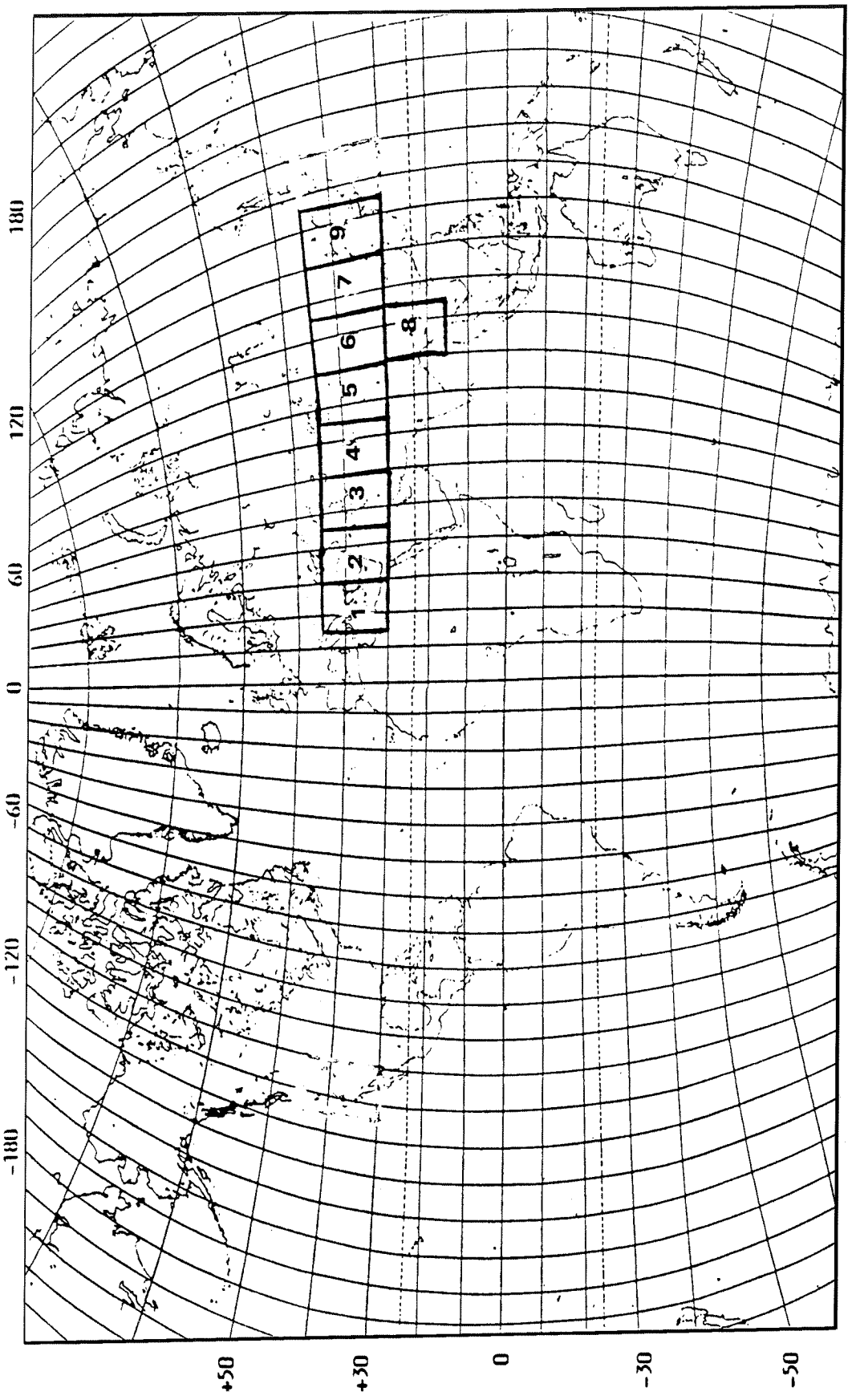

Fig. The nine (9) cells of the investigated area.

advantage that the entire history of earthquake occurrence need not be analysed, it requires only the extreme value magnitudes (part process). Gumbel's third asymptotic distribution can be expressed through equation (2) or rearranging for the next T-years the modal extreme magnitude m1(T) is given by:

$$m1\,(T) = \omega - (\omega - u)\left[\frac{(1-\lambda}{T}\right]\lambda \qquad (6)$$

setting T=1 the modal extreme magnitude takes the form:

$$m1\,(1) = \omega - (\omega - u)\,(1-\lambda)^{\lambda} \qquad (7)$$

The forecast largest earthquake magnitude expected over a time interval T=88 years will be referred to as m88, replacing the magnitude m(T) of equation (6).

3.3. The strain energy parameters

In general the energy-magnitude formula can be written as:

$$\log E = A + Bm \qquad (8)$$

A combination between equations (1 and 8) provides the parameters of the strain energy release model (Makropoulos and Burton 1983).

These are the magnitudes equivalent to the mean annual rate of energy release and the maximum possible energy release from a notional maximum credible earthquake referred hereafter as M2 and M3, respectively. These parameters can be obtained from both analytical and graphical methods. If M2 and M3 are obtained through the analytical method then the formulae derived by (Makropoulos and Burton 1983) are:

$$M2 = \frac{1}{B}\left[bM1 + (B-b)\,M3 + \log\left(\frac{b}{B-b}\right)\right] \qquad (9)$$

and

$$M3 = \frac{1}{B-b}\left[BM2 - bM1 - \log\left(\frac{b}{B-b}\right)\right] \qquad (10)$$

can be used to calculate the quantities M2 and M3, B=1.44 from equation (3), b and M1 are identified in equations (1) and (4), respectively.

4. RESULTS OF THE ANALYSIS

The whole process annual mode M1 obtained from equation (4) should be an approximately equivalent quantity to m1 of Gumbel III, such that:

$$M1 = \frac{a}{b} \approx m1\,(1) = \omega - (\omega - u)\,(1-\lambda)^{\lambda} \qquad (11)$$

and the T-year mode RM88 can be compared similarly with m88:

$$RM88 = \frac{a + \log T}{b} \approx m88 = \omega - (\omega - u)\left[\frac{(1-\lambda)}{R}\right]^{\lambda} \qquad (12)$$

The mean annual rate of energy release M2, can also be expressed as an equivalent magnitude X2 which is derived from (Burton and Makropoulos 1985) and is given by:

$$M2 \approx X2 = \omega + \frac{1}{B}\ln\left(\frac{C\Gamma\,(k)}{B^{k}}\right) \qquad (13)$$

where ϖ is the upper bound magnitude of Gumbel III, B=1.44, and (k) is the Gamma function.

The upper bound earthquake ϖ of GIII is similar to M3 although there is a conceptual difference. The latter corresponds to a statistical upper limit to the variate and a theoretical infinite return period whereas M3 corresponds fo finite, rather than infinite, waiting time between notionally maximum possible occurrences (Burton and Makropoulos 1985). The conceptual difference between and M3 suggests that:

$$\varpi - M3 \geq 0 \qquad (14)$$

irrespective of whether M3 is estimated through analytical or graphical method (Burton and Makropoulos 1985).

We can see that it is easy to examine the seismic hazard in the Eurasian seismic belt using the Gumbel III distribution with careful assessment of all three of its parameters and to relate

Table 1. Numerical cell values of the Gumbel III parameters: ϖ, u and λ, the ensuing forecast magnitude m88 (part process) and the quantity M3 (strain energy release method).

CELL	LAT. (^{0}N)	LONG. (^{0}E)	ϖ	u	λ	m88	M3
1	30 - 45	15 - 30	8.76	6.00	0.28	7.95	8.30
2	30 - 45	30 - 45	9.22	6.25	0.21	8.06	8.29
3	30 - 45	45 - 60	8.03	5.72	0.43	7.70	8.01
4	30 - 45	60 - 75	8.19	6.27	0.60	7.91	8.11
5	30 - 45	75 - 90	9.59	6.58	0.20	8.38	8.60
6	30 - 45	90 - 105	8.80	6.42	0.43	8.45	8.70
7	30 - 45	105 - 120	8.82	5.94	0.55	8.29	8.74
8	15 - 30	90 - 105	8.70	5.90	0.43	8.28	8.66
9	30 - 45	120 - 135	8.68	6.86	0.39	8.23	8.63

Table 2. Numerical cell values of M1 and M2 and the corresponding quantities m1 and X2. The 88-years mode referred as RM88 (whole process) is also tabulated. Cell coordinates are as in Table 1.

CELL	M1	m1	M2	X2	RM88
1	6.18	6.24	7.18	7.11	8.21
2	6.28	6.39	7.24	7.46	8.31
3	6.00	6.21	6.95	7.28	8.25
4	6.42	7.00	7.26	7.54	8.61
5	6.52	6.71	7.52	7.81	8.94
6	6.54	6.93	7.65	7.52	9.07
7	6.38	6.84	7.61	7.39	8.91
8	6.43	6.49	7.51	7.15	8.69
9	6.70	7.13	7.62	7.84	8.75

these through M1 (of the whole process) and M2 and M3 of the physical release of strain energy. In this way we give a physical link through strain energy release to seismic hazard statistics.

The values of the Gumbel III parameters (ϖ, u, λ), the forecasting magnitude m88 and the quantity M3 are listed in Table (1) for each cell. Values for the GIII parameters have been estimated by Burton (1979) for the same regions using smaller cells and for this reason they are not directly comparable. Table (2) presents the numerical cell values of M1 and M2 and the corresponding equivalent quantities m1 and m2. The value of the T-year modal magnitude RM88 of the whole process is also tabulated in this Table.

It is easy therefore to derive relationships, to make comparisons between the seismicity parameters and relationships amongst them may now be sought, using the whole and the part process, as well as the strain energy release method. Thus the m1 magnitude appear to be slightly greater than M1 and is given by:

$$m1 - M1 = 0.28 \pm 0.18 \qquad (15)$$

The quantities X2 and M2 are very nearly equal:

$$X2 - M2 = 0.6 \pm 0.24 \quad (16)$$

and are certainly to within the uncertainty limits. The upper bound magnitude ϖ is systematically greater by 0.30 magnitude units than M3 throughout the Eurasian seismic belt.

The relations between the quantities RM88, m88 and M3 are:

$$RM88 - M3 = 0.20 \pm 0.18 \quad (17)$$

$$RM88 - m88 = 0.50 \pm 0.15 \quad (18)$$

$$M3 - m88 = 0.31 \pm 0.08 \quad (19)$$

From the relations derived above we can conclude that it is easy to estimate any of the involved parameters if the other one is known. These relationships show that RM88 magnitude is greater than the two others (M3 and m88) and M3 is greater than m88. It appears that m1 is slightly greater than M1 while X2 is found to be almost equal to M2 within the uncertainties limits.

5. Conclusions

From the remarkably similar results for M2 and X2, as well as for M1 and m1 we can make some conclusions. The relationships obtained between the parameters of the two different processes used to describe the same phenomenon, are almost valid over the different seismotectonic regimes from which Eurasian seismic belt is consisted. The frequency-magnitude law (Gutenberg and Richter 1944) and Gumbel's III distribution are simply expressed through equation (11), which records the annual determined from both methods. Similarly equation (13) provides a direct link between the physical process of the strain energy release and the parameters of Gumbel III, expressed through the mean annual energy release in the investigated seismic belt. In all regions M3 is less than ϖ and this is compatible with the physical interpretation of ϖ and M3. In accord to that corresponds to a magnitude with a theoretically infinite return period, whereas M3 is seen to have a finite "waiting time" between expected occurrences.

This is a remarkable simple demonstration that the quantities M1 (obtained from the whole process) and M2 (strain energy release process) can be expressed in terms of Gumbel's III parameters (part process) and the results be compatible. In general the method of Gumbel's third asymptotic distribution and the strain energy release technique, provide a mutually compatible description of the seimic features of a region.

Aknowledgements

The author carried out this work, while he was a research fellow in the University of East Anglia, School of Environmental Sciences. He would like to express his sincere thanks to Dr. P.W. Burton who reviewed the paper and made useful suggestions in order to improve it.

References

Bath, M., 1958. The energies of seismic body waves and surface waves. (In H. Benioff, M. Ewing, B. F. Howell, Jr and F. Press, eds Contribution in Geophysics) London: Pergamon, 1-16.

Bath, M. and Duda, S.J., 1963. Strain energy release in relation to focal depth. Geofis. Pura and Appl., 56, 93-100.

Burton, P.W., 1978. The application of extreme value statistics to seismic hazard assessment in the European area. Proc. Symp. Anal. Seismicity and Seismic Risk, Liblice, 1977 Oct. 17-22, Academia, Prague, 323-334.

Burton, P.W., 1979. Seismic risk in southern Europe through to India examined using Gumbel's third distribution of extreme values. Geoph. J.R. astr. Soc., 59, 249-280.

Burton, P.W. and Makropoulos, K.C., 1985. Seismic risk of circum-Pacific earthquakes: II. Extreme values using Gumbel's third asymptotic distribution and the relationship with strain energy release. Pageoph, 123, 849-869.

Esteva, L., 1976. Seismicity. In: Seismic Risk and Engineering Decisions. (eds. Lomnitz, C. and Rosenblueth E.), Elsevier Scient. Publ. Comp., Amsterdam, 425 pp.

Galanopoulos, A.G., 1968. On quantitative determination of earthquake risk. Annali Geofis., 21, 193-206.

Gumbel, B. and Richter, C.F., 1944. Frequency of earthquakes in California. Bull. Seismol. Soc. Am., 34, 185-188.

Kaila, K.L. and Narain, H.A., 1971. A new approach for preparation of quantitative seismicity maps as applied to Alpide belt-Sunda arc and adjoining areas. Bull. Seism. Soc. Am., 61, 1275-1291.

Kaila, K.L. and Madhava Rao, N., 1975. Seismotectonic maps of European area. Bull. Seismol. Soc. Am., 65, 1721-1732.

Karnik, V., 1968. Seismicity of the European area. Parti I. D. Reidel Publishing Company, Dordrecth Holland, 364 pp.

Karnik, V., 1971. Seismicity of the European area. Part II. D. Reidel Publishing Company, Dordrecth Holland, 218 pp.

Makropoulos, K.C., 1978. The statistics of large earthquake magnitude and an evaluation of Greek seismicity. Ph. D. thesis, University of Edinburgh, 193 pp.

Makropoulos, K.C. and Burton, P.W., 1983. Seismicity risk of circum-Pacific earthquakes: I. Strain energy release. Pageoph., 121, 247-267.

Nowroozi, A.A. and Ahmadi, G., 1986. Analysis of earthquake risk in Iran based on seismotectonic provinces. Tectonophysics, 122, 89-144.

Tsapanos, T.M., 1990. b-values of two tectonic parts in the circum-Pacific belt. Pageoph, 134, 229-242.

Tsapanos, T.M., Scordilis, E.M. and Papazachos, B.C., 1990. A global catalogue of strong ($M_S \geq 5.5$) earthquakes during the time period 1897-1985. Publ. of Geophysical Lab., University of Thessaloniki, 10, 90 pp.

TIME DEPENDENT SEISMICITY ALONG THE HELLENIC ARC

B. C. Papazachos, Ch. A. Papaioannou and G. F. Karakaisis

Geophysical Laboratory, University of Thessaloniki, Thessaloniki 540 06, Greece

Abstract

Both shallow and intermediate depth earthquakes consitute a major threat to urban areas located in the southern Aegean region, thus making necessary the estimation of probabilities of occurrence of strong earthquakes in this region for seismic hazard assessment purposes. For this reason, reliable instrumental data along with well-documented historical information have been used as a data base. By the use of the known relations which govern the recently proposed regional time and magnitude predictable model, probabilites for the occurrence of large shallow and intermediate depth earthquakes during the next years have been determined for the seismogenic regions of this area. The magnitudes of the future earthquakes have also been determined.

1. Introduction

Historical information and instrumental data suggest that earthquakes constitute a major threat for the urbanized areas of the southern Aegean sea. Historical reports concerning the extent of damage caused by the larger earthquakes which occurred in this area, being both of shallow and intermediate depth origin, allow a fairly reliable estimation of their magnitudes, which reach up to $M_s \approx 8.3$.

It is, thus, of much importance to define those parts of the southern Aegean sea where large shallow and intermediate depth earthquakes occur and, on the other hand, to calculate probabilties for the generation of large earthquakes (Ms ≥ 37.0) during the next years.

2. Method and data

Among the numerous probabilistic and deterministic models which have been developed over the last 30 years to depict various aspects of seismic occurrence patterns for long-term earthquake prediction purposes two alternative representations for seismic recurrence patterns, consistent with the geophysical description of the earthquake generating process, have been proposed; the slip predictable model and the time predictable model (Bufe et al., 1977; Shimazaki and Nakata, 1980).

Recently Papazachos (1989, 1992) presented the results of an investigation aiming to identify time-dependent relationships between main shocks which occurred in Greece. He proposed a model in which the interevent time and the magnitude of the following main shock were quantitatively expressed in terms of the magnitude of the smallest main shock considered and the magnitude of the preceding main shock in a given source area. This model was subsequently improved by taking into account the annual seismic moment release in the source area (Papazachos and Papaioannou, 1993). The *regional time- and magnitude predictable model* has been applied in almost all areas where strong shallow earthquakes occur (Panagiotopoulos, 1995; Papadimitriou, 1993, 1994; Karakaisis, 1994a, b; Papazachos et al., 1994, 1995a), while its validity has statistically been tested against time independent models (Papazachos *et al.*, 1995a, b).

This model is expressed by two relations which give the repeat time, T_t, and the surface wave magnitude, M_F, of the following main

Special Publications of the Geological Society of Greece, No 6.

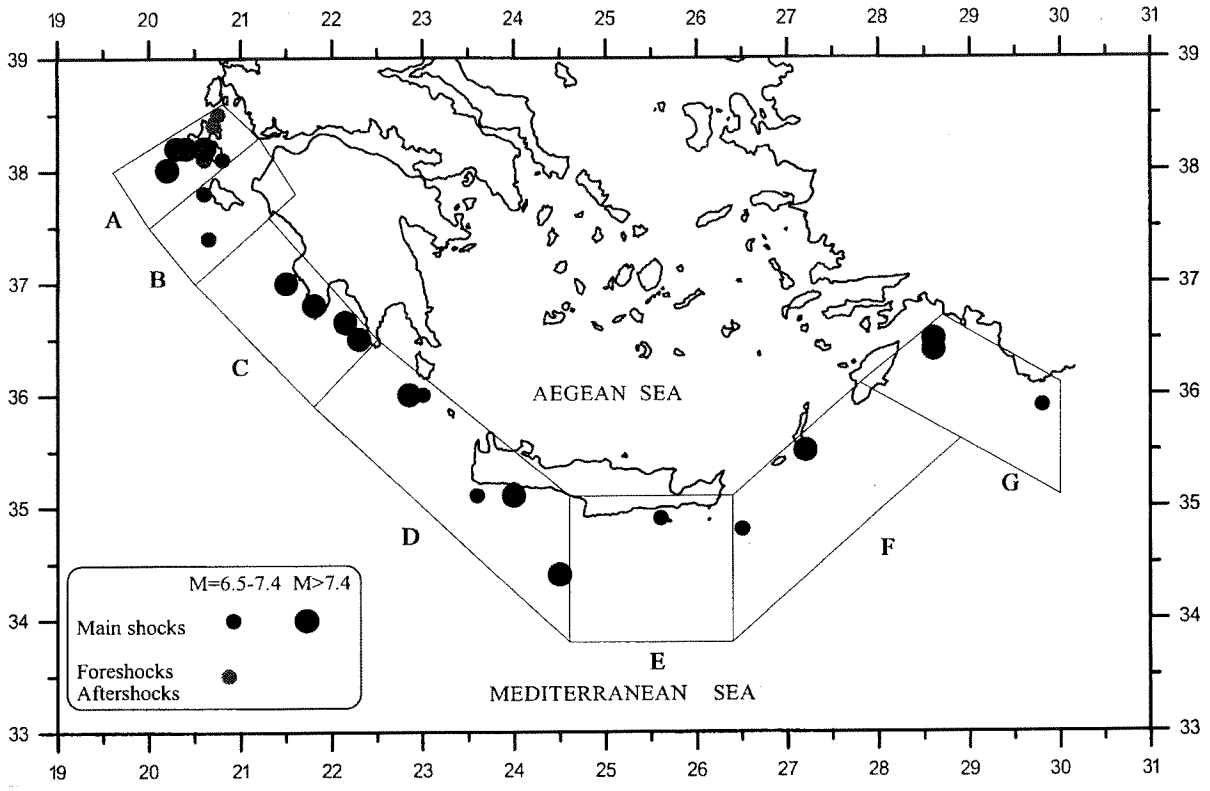

Fig. 1. The seismogenic regions of shallow earthquakes in the Hellenic arc.

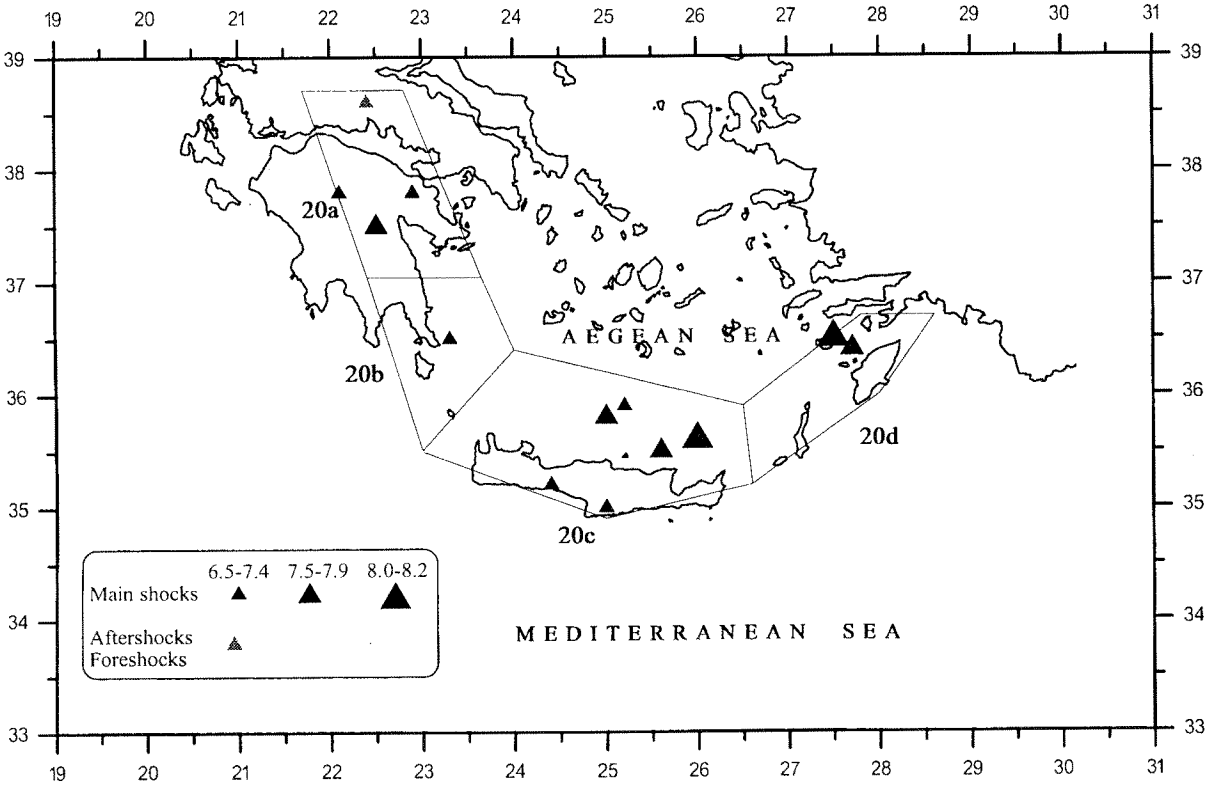

Fig. 2. The seismogenic regions of intermediate depth earthquakes in the southern Aegean area.

Table 1. Information on the earthquakes considered in this study.

Source	Completeness		Date	Epicenter		M_S	M
A	1911	6.5	22.07.1767	38.2	20.3	7.2	7.2
Cephalonia	1767	7.2	04.02.1867	38.2	20.4	7.2	7.2
			24.01.1912	38.1	20.8	6.8	7.0
			27.01.1915	38.4	20.7	6.6	a
			07.08.1915	38.5	20.7	6.7	a
			11.08.1953	38.1	20.6	6.8	f
			12.08.1953	38.2	20.6	7.2	7.3
			17.01.1983	38.0	20.2	7.0	7.0
B	1911	6.5	15.11.1959	37.8	20.6	6.8	6.8
Zakynthos			11.05.1976	37.4	20.6	6.5	6.5
C	1867	7.0	20.09.1867	36.5	22.3	7.1	7.1
SW. of Peloponnese			27.08.1886	37.0	21.5	7.5	7.5
			01.07.1927	36.6	22.1	7.1	7.1
			06.10.1947	36.8	21.8	7.0	7.0
D	1911	6.5	03.07.1805	35.1	24.0	7.2	7.2
W. of Crete	1805		06.02.1866	36.0	23.0	6.8	6.8
			11.08.1903	36.0	22.8	7.5	7.5
			17.12.1952	34.4	24.5	7.0	7.0
			04.05.1972	35.1	23.6	6.5	6.5
E	1815	6.5	00.12.1815	34.9	25.6	6.7	6.7
SE.of Crete							
F	1911	6.5	13.08.1922	34.8	26.5	6.8	6.8
SE. of Carpathos			09.02.1948	35.5	27.2	7.1	7.1
G	1911	6.5	28.02.1851	36.4	28.6	7.2	7.2
E. of Rhodos Isl.	1851	7.2	18.03.1926	35.9	29.8	6.9	6.9
			24.04.1957	36.4	28.6	6.8	f
			25.04.1957	36.5	28.6	7.2	7.3
20a	1911	6.5	28.05.1897	37.5	22.5	7.5	7.5
NE Peloponnese	1897	7.5	06.07.1925	37.8	22.1	6.6	6.6
			28.08.1962	37.8	22.9	6.8	7.0
			31.03.1965	38.6	22.4	6.8	a
20b	1911	6.5	30.08.1926	36.5	23.3	7.2	7.2
CyThera							
20c	1911	6.5	16.02.1810	35.5	25.6	7.8	7.8
Crete	1810	7.6	28.03.1846	35.8	25.0	7.7	7.7
			12.10.1856	35.6	26.0	8.2	8.2
			01.08.1923	35.0	25.0	6.8	6.8
			25.02.1935	35.9	25.2	7.0	7.0
			24.07.1948	35.2	24.4	6.6	6.6
20d	1911	6.5	22.04.1863	36.4	27.7	7.8	7.8
Rhodos	1863	7.6	26.06.1926	36.5	27.5	8.0	8.0

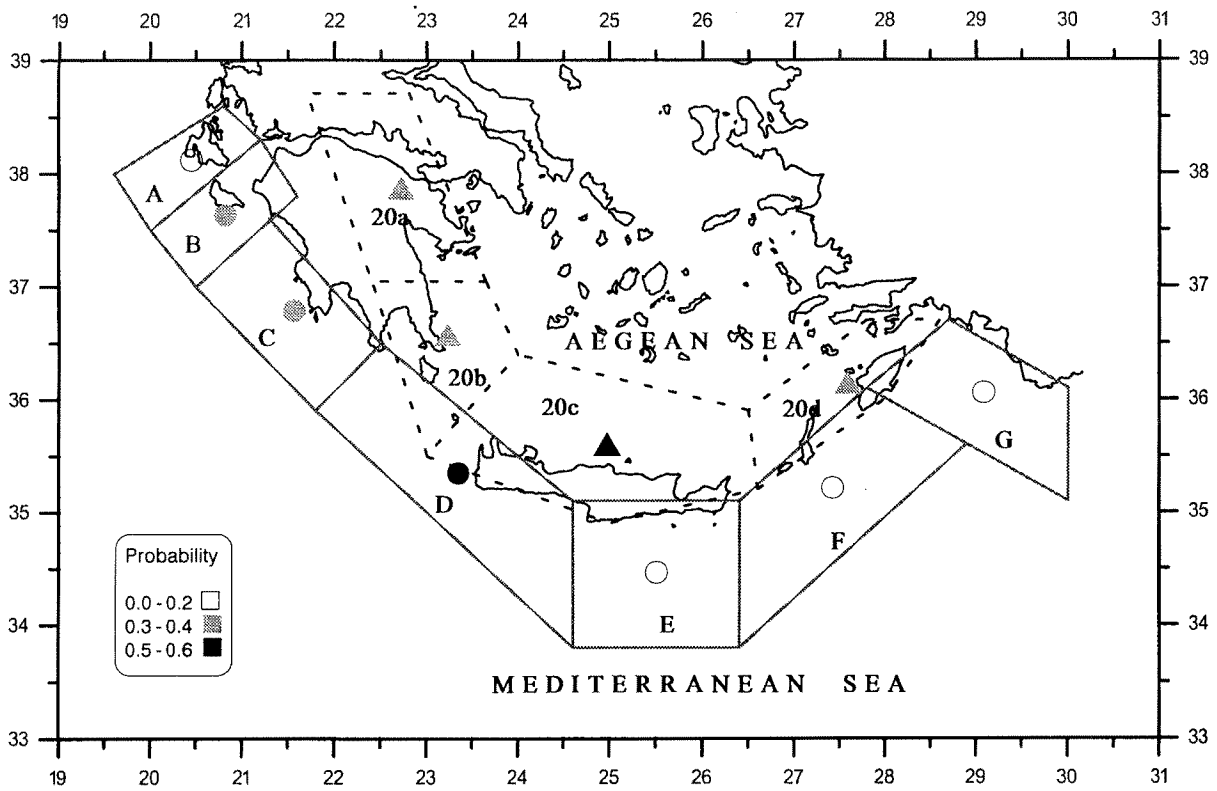

Fig. 3. Centers of the seismogenic sources and probabilities of occurrence of large ($M_S \geq 37.0$) shallow (circles) and intermediate depth earthquakes (triangles) in the southern Aegean area.

shock in a certain seismogenic region as a function of the magnitude, M_{min}, of the smallest main shock considered, the magnitude of the preceeding main shock, M_P, and the moment release rate, m_o, (dyn.cm.yr^{-1}). These two relations have the form:

$$\log T_t = bM_{min} + cM_P + d\log m_o + q \quad (1)$$

$$M_F = BM_{min} + CM_P + D\log m_o + m \quad (2)$$

where b, c, d, q, B, C, D and m are parameters which have to be determined.

The method applied in the present paper is based on regionalization, determination of the annual seismic moment release and declustering of the data and is described in detail by Papazachos *et al.* (1995a).

On the basis of new historical evidence, the seismogenic regions along the Hellenic trench-arc system have been defined (Papazachos, 1995) and are shown in Fig. 1, along with the earthquake epicenters of the complete data used in the present study. Black circles show epicenters of main shocks and grey circles show epicenters of foreshocks and aftershocks. Figure 2 shows the seismogenic regions where intermediate depth earthquakes occur (h=40-100 Km), as well as the earthquake epicenters of the complete data considered. Information on the surface wave magnitudes and on the epicenters of the earthquakes plotted in Figures 1 and 2 were taken from the catalogue of Comninakis and Papazachos (1986) for the period 1901-1986 and from the monthly bulletins of the National Observatory of Athens and of the Geophysical Laboratory of the University of Thessaloniki for the period 1986-1992. For historical earthquakes such information was derived from the book of Papazachos and Papazachou (1989).

Table 1 lists the parameters of the earthquakes which are shown in Figs. 1 and 2. For each seismogenic region, the year since the data are complete above a certain cut-off magnitude is written. The third, fourth and fifth columns give the date, epicenter coordinates and the surface wave magnitude of the earthquakes that fulfil the completeness criteria given in the second column. The sixth column gives the cumulative

Table 2. Information on the data used for the detrmination of the parameters q and m of the relations (1) and (2).

Source	M_{min}	M_P	M_F	T (years)	t_P	t_F
A	7.0	7.0	7.3	41.55	1912	1953
		7.3	7.0	29.43	1953	1983
	7.2	7.2	7.2	99.53	1767	1867
		7.2	7.3	86.62	1867	1953
B	6.5	6.8	6.5	16.49	1959	1976
C	7.0	7.1	7.5	18.94	1867	1886
		7.5	7.1	40.84	1886	1927
		7.1	7.0	20.27	1927	1947
	7.1	7.1	7.5	18.94	1867	1886
		7.5	7.1	40.84	1886	1927
D	6.5	7.0	6.5	19.38	1952	1972
	6.8	7.2	6.8	60.59	1805	1866
		6.8	7.5	37.51	1866	1903
		7.5	7.0	49.35	1903	1952
	7.0	7.2	7.5	98.11	1805	1903
		7.5	7.0	49.35	1903	1952
	7.2	7.2	7.5	98.11	1805	1903
F	6.8	6.8	7.1	25.49	1922	1948
G	6.9	6.9	7.3	31.10	1926	1957
	7.2	7.2	7.3	106.16	1851	1957
20a	6.6	6.6	7.0	37.14	1925	1962
20c	6.6	6.8	7.0	11.57	1923	1935
		7.0	6.6	13.41	1935	1948
	6.8	6.8	7.0	11.57	1923	1935
	7.7	7.8	7.7	36.12	1810	1846
		7.7	8.2	10.54	1846	1856
	7.8	7.8	8.2	46.65	1810	1856
20d	7.8	7.8	8.0	63.18	1863	1926

Table 3. Information on the parameters b, a, Mmax and logmo calculated for each region. The last four columns give information on the expected magnitudes, MF, and the corresponding probabilites, P10, of strong ($M_s \geq 36.5$) and large earthquakes ($M_s \geq 37.0$) along the Hellenic trench-arc system for the time period 1993-2002.

Source	b´	a	M_{max}	$logm_o$	MF $M_{min} \geq 36.5$	P_{10}	M_F $M_{min} \geq 37.0$	P_{10}
A	1.10	5.82	7.5	25.44	6.9	0.22	7.2	0.13
B	1.10	5.48	7.2	24.98	6.8	0.29	7.2	0.21
C	1.10	5.51	8.0	25.33	6.8	0.35	7.2	0.29
D	1.10	5.66	8.3	25.60	7.1	0.55	7.4	0.47
E	1.10	5.37	7.2	24.87	6.7	0.23	7.1	0.21
F	1.10	5.49	7.2	24.83	6.6	0.24	7.0	0.18
G	1.10	5.32	8.0	24.98	6.6	0.22	7.0	0.16
20a	0.62	2.57	7.5	25.40	6.8	0.37	7.2	0.30
20b	0.62	2.25	7.5	25.08	6.7	0.27	7.0	0.22
20c	0.62	2.76	8.2	26.20	7.3	0.63	7.6	0.59
20d	0.62	2.71	8.0	25.98	6.8	0.31	7.2	0.26

magnitude, M, of each sequence, that is, the magnitude that corresponds to the total seismic moment released by the major shocks (the main shock and its largest foreshocks, "f", and aftershocks, "a") of the sequence according to the moment-magnitude relation of Kanamori (1977):

$$\text{Log } Mo = rM + k \quad (3)$$

where r and k are equal to 1.5 and 16.1, respectively, with M_o being given in *dyn.cm.*

Table 2 gives information for every seismogenic region, on the magnitude M_{min} of the smallest main shock considered, the magnitudes M_P and M_F of the preceeding and the following main shock and the observed interevent time T, which is the difference of the year of occurrence of the preceeding main shock, t_P, from the year of occurrence of the following main shock, t_F.

Table 3 lists the values of the parameters a, b, M_{max} and logmo for each seismogenic region. M_{max} is the magnitude of the largest known earthquake while the parameters a and b are calculated by complete samples of mainly instrumental data. The annual seismic moment release, mo, being a measure of seismicity level, varies between source regions and it can be reliably calculated if enough data are available for each region. Its determination is based on Molnars method (1979) and is described by Papazachos and Papaioannou (1993).

3. Results

Very recently, the first three parameters of both relations (1) and (2) have been determined by using a large data sample consisting of 1811 observations (T, Mmin, MP, MF) which come from the seismogenic regions of the continental fracture system (Papazachos et al., 1995a). It has been shown (Papazachos et al., 1995a) that these parameters (b, c, d, B, C, D) do not depend much on the seismotectonic environment and for this reason their values, calculated by the above mentioned data sample, have been adopted with relations (1) and (2) taking the form:

$$\log T_t = 0.19M_{min}+0.33M_P-0.39\log m_o+q \quad (4)$$

$$M_F = 0.73M_{min}-0.28M_P+0.40\log m_o+m \quad (5)$$

The parameters q and m are determined by the use of all available data and their mean values are equal to 7.89 and -6.10 with standard deviations equal to 0.26 and 0.26, respectively.

In order to proceed to the determination of probabilities for the generation of strong earthquakes by using relation (4), the probability density function of the observed interevent time, T, given in Table 2, to the calculated interevent time, Tt, must be defined. It has been shown (Papazachos and Papaioannou, 1993) that the quantity T/Tt follows a log- normal distribution.

The relation (5) is applied for estimating the magnitude of the expected main shock in each seismogenic source.

Table 3 gives, in its last four columns, information on the expected magnitudes, MF, and the corresponding probabilites, P_{10}, of strong ($M \geq 36.5$) and large earthquakes ($M_s \geq 37.0$) along the Hellenic trench-arc system for the time period 1993-2002.

Figure 3 shows a map of the centers of the seismogenic sources with proper symbols indicating the range of probabilities for the occurrence of large ($M_s \geq 37.0$) shallow (circles) and intermediate depth (triangles) earthquakes for the decade 1993-2002. It is observed that the seismogenic sources D (W. Crete) and 20c (Crete) exhibit the highest probabilities, with expected main shock magnitudes equal to 7.4 and 7.6, respectively.

Acknowledgements

This work has been partially supported by the EC Projects EV5V-CT94-0513 and EV5V-CT94-0443 (Climatology and Natural Hazards).

References

Bufe, C. G., Harsch, P. W. and Burford, R. O., 1977. Steady-state seismic slip: A precise recurrence model. Geophys. Res. Lett., 4: 91-94.

Comninakis, P. E. and Papazachos, B. C., 1986. A catalogue of earthquakes in Greece and the surrounding area for the period 1901-

1985.
Geophysical.Laboratory, University of Thessaloniki, No. 1, 167 pp.
Kanamori, H., 1977. The energy released in great earthquakes. J. Geophys. Res., 79: 2981-2987.
Karakaisis, G. F., 1994a. Long-term earthquake prediction along the North and East Anatolian Fault Zones based on the time and magnitude predictable model. Geophys. J. Int., 116: 198-204.
Karakaisis, G. F., 1994b. Long term earthquake prediction in Iran based on the time and magnitude predictable model. Phys. Earth Planet. Interiors, 83: 129-145.
Molnar, P., 1979. Earthquake recurrence intervals and plate tectonics. Bull. Seismol. Soc. Am., 69: 115-133.
Panagiotopoulos, D. G., 1995. Long term earthquake prediction in central America and Caribean sea based on the time and magnitude predictable model. Bull. Seismol. Soc. Am., (in press).
Papadimitriou, E. E., 1993. Long term earthquake prediction along the western coast of south and central America based on a time predictable model, Pure Appl. Geophys., 140: 301-316.
Papadimitriou, E. E., 1994. Long term prediction in North Pacific seismic zone based on the time and magnitude predictable model. Natural Hazards, 9: 303-321.
Papazachos, B. C., 1989. A time-predictable model for earthquakes in Greece. Bull. Seismol. Soc. Am., 79: 77-84.
Papazachos, B. C., 1992. A time and magnitude predictable model for generation of shallow earthquakes in the Aegean area. Pure Appl. Geophys., 138: 287-308.
Papazachos, B. C., 1995. Faults of big earthquakes ($M_S \geq 38.0$) in the Hellenic arc. Proc. XV Congress of the Carpatho-Balkan Geological Association, 17-20 September 1995, Athens (in press).
Papazachos, B. C. and Papazachou, C. B., 1989. The earthquakes of Greece. Ziti Publications, Thessaloniki, Greece, 365 pp.
Papazachos, B. C. and Papaioannou, CH. A., 1993. Long-term earthquake prediction in the Aegean area based on a time and magnitude predictable model. Pure Appl. Geophys., 140: 593-612.
Papazachos, B. C., Papadimitriou, E. E., Karakaisis, G. F., and Tsapanos, T. M., 1994. An application of the time and magnitude predictable model for the long term prediction of strong shallow earthquakes in the Japan area. Bull. Seismol. Soc. Am., 84: 426-437.
Papazachos, B. C., Papadimitriou, E. E., Karakaisis, G. F. and Panagiotopoulos, D. G., 1995a. Long-term earthquake prediction in the circum-Pacific convergent belt. Pure Appl. Geophys., (in press).
Papazachos, B. C., Karakaisis, G. F. and Papadimitriou, E. E., 1995b. On the validity of the regional time- and magnitude predictable model. Proc. XV Congress of the Carpatho-Balkan Geological Association, 17-20 September 1995, Athens (in press).
Shimazaki, K. and Nakata, T., 1980. Time-predictable recurrence model for large earthquakes. Geophys. Res. Lett., 7: 279-282.

SOME PROBLEMS OF THE SEISMIC STRUCTURAL DESIGN

L. Tzenov

Central Laboratory for Seismic Mechanics & Earthquake Engineering, Bulgarian Academy of Sciences, Acad. G. Bontchev str., bl. 3, Sofia 1113, Bulgaria

Abstract

The development of the construction, the creation of new engineering solutions, as well as the increased requirements concerning the reliability of the structures, naturally call for certain changes, supplements and / or improvements of the way of their seismic design and safety. In many cases it is necessary to take into account the nonuniform distribution of the ground accelerations at the different points of the structure's foundation and the most unfavorable or effective directions of the seismic excitation. These problems are of central importance for the seismic protection of the structural systems.

Introduction

The development of the construction, the creation of new engineering solutions, as well as the increased requirements concerning the reliability of the structures, naturally call for certain changes, supplements and/or improvements of the way of their seismic design and safety. In many cases it is necessary to take into account:

— the nonuniform distribution of the ground accelerations at the different points of the structure's foundation;
— the most unfavorable or effective directions of the seismic excitation.

Distribution of the ground acceleration along the structure

During an earthquake the ground motion is a complex process containing many components (seismic waves) with different characteristics. Their joint effect on a given structure is practically impossible to be envisaged and estimated. For this reason it is assumed that the seismic waves with frequencies coinciding or being nearest to the natural frequencies of the structure will be the effective ones. In such a case, if we know the velocity of the seismic waves propagation in the ground medium, for every period T_i, corresponding to the i-th mode of the natural vibration of the treated structure, the length λ_i of the effective seismic wave can be determined.

The "ground motion" of the structure is generally accepted to be treated as translation. This means that the ground acceleration in each point of the structure base in a given moment is the same. In reality only for a limited number of structures whose length L is much less than the length λ_i of the effective seismic wave, this assumption can be justified. When the lengths L and λ_i are commensurable, the ground accelerations are not uniformly distributed along the structure length.

The influence of the real distribution of the ground accelerations along the structure on its seismic design is illustrated by a case study of a 6 storey residential large panel building with dimensions in plan 10/54 m. The results are shown in fig. 1.

On the x-axis is plotted a ratio between λ_1 - the length of the effective seismic waves, corresponding to the fundamental mode of the natural vibrations of the structure - and its length in plan L. On the y-axis is plotted Δ - the ratio between the design seismic loading applied on

Special Publications of the Geological Society of Greece, No 6.

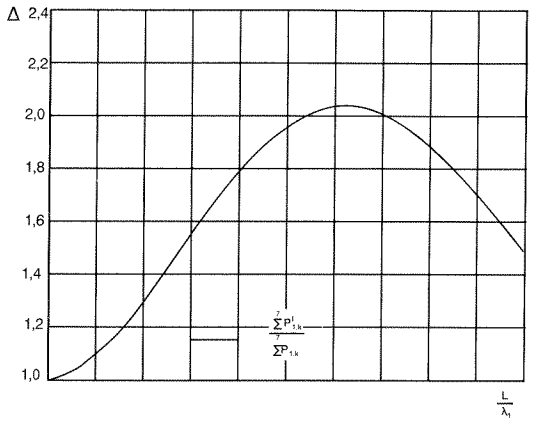

Fig. 1. Influence of the real distribution of the ground accelerations along the structure on its seismic design.

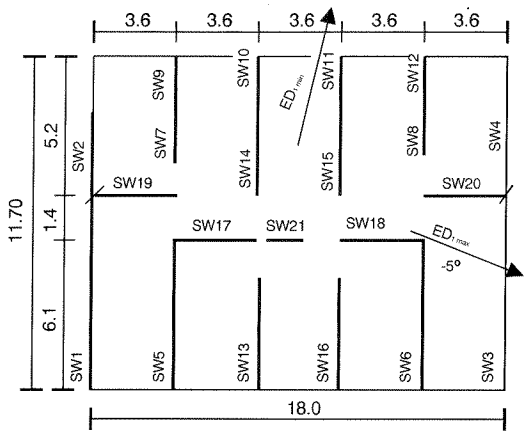

Fig. 2. Regular structural system.

the shear walls at the ends of the building, determined with the without taking into account the nonuniform distribution of the ground accelerations along the structure.

For certain values of the ratio L/λ_1 (depending on the velocity of the seismic waves propagation in the ground medium), the seismic loading applied on the shear walls at the ends of the treaded building can exceed two times the design seismic loading in case, when the nonuniform distribution of the ground acceleration along the structure is not taken into account. This fact could be fatal for the building as a whole.

Effective directions of the seismic excitation

The seismic excitation is identified with the ground accelerations direction. Hence, it is considered that the horizontal component of the seismic excitation is of interest before all. This assumption is motivated by the fact that the structures are designed for a vertical seismic loading and only the presence of additional seismic loading can change qualitatively their strain and stress state. It is important to note, that this assumption can be justified for the "ordinary" residential buildings, but not for a large number of industrial buildings, bridges, etc.

Following the seismic Codes, the design of the structure is carried out under the suggestion that the total energy of the seismic excitation is concentrated in a definite direction, namely one of the "main directions" of the treated structure. For a regular structural system the [main directions] in plan in fact coincide with its longitudinal and transversal axes. However, the existence of main directions suggests that the orthogonal coordinate system Oxyz can be oriented towards the studied structure in such a way that the modes of its natural vibrations can be divided into two groups. The first group will include those modes of natural vibrations at which the components on the axis Oy of the amplitudes of the all points of the structure are negligibly small in comparison with their respective components on the Ox axis. For the second group of natural modes the components on the Ox axis of the amplitudes of all the points of the structure can be neglected in comparison with the respective components in the axis Oy. Obviously, there is a number of structures for which such a grouping if the modes of their natural vibrations is not possible. These structural systems have to be considered as irregular. The investigations of the dynamic behaviour of the irregular structural systems proved the great importance of the taking into account the effective directions of the seismic excitations for the safety of these structures.

In order to illustrate the necessity of the determination of the effective directions of the seismic excitations a 6 story residential building is considered. Type "A" is a regular structural system with location of its shear walls, as shown in fig. 2.

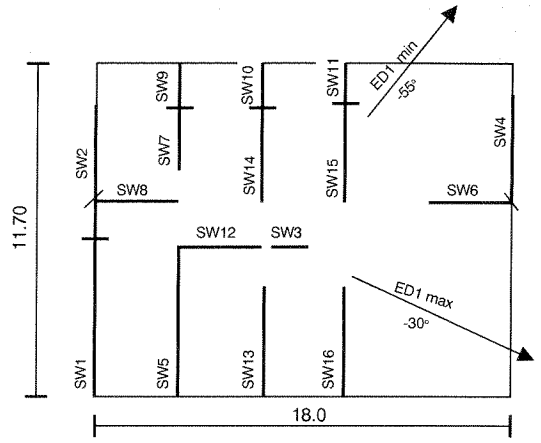

Fig. 3. Irregular structural system.

Type "B" is an irregular structural system because of the nonsymmetrical situation of its shear walls, as shown in fig. 3.

The obtained effective directions of the seismic excitation for the building of type "A" (regular structural system) are practically identical with its longitudinal and transversal aces. For example ED_1 at $\alpha = 0^0$ is only about 1% less than the ED_{1max} at $\alpha = -5^0$, where

— ED^1 is the energy of the deformation due to the design seismic loading, corresponding to the first natural mode of the structural system under investigation;
— α is the angle determining the seismic excitation direction towards the axis Ox.

For the type "B" bulding (irregular structural system) ED_1 at $\alpha = 0^0$ is 45% less than the ED_{1max} at $\alpha = -30^0$. This means that when cosidering the angle $\alpha = 0^0$, i.e. one of the "main directions" (in this case - the longitudinal axis), the structure is not seismically designed. This fact confirms the necessity of the determination of the effective directions of the seismic excitations for the seismic safety of the structural systems.

Conclusion

The treated in the paper problems are essential for the seismic safety of the structural systems. However, these problems are a part from the general problem - mitigation of the seismic vulnerability. The successive solution of this vitally important problem for every country with a high level of seismic risk supposes and imposes a permanent and operating international collaboration between the specialists on earthquake engineering and the specialists on the different fields of the earth sciences.

DUCTILITY DEMAND OF REINFORCED CONCRETE IRREGULAR FRAMES

Elena Vasseva

Ph. D. Chief research fellow at Central Lab for Seismic Mechanics and Earthquake Engineering, Bulgarian Academy of Sciences, Sofia 1113, Acad. "G. Bonchev", Bl. 3, Tel, Fax, 359 2 703107

Abstract

In the seismic design of earthquake-resistant buildings symmetry and regularity are commonly recommended. But in a lot of cases these two requirement cannot be met. In this paper such type of analysis is used to study the behavior of R/C frames with vertical irregularities.

On the problem of seismic behavior of buildings with irregularities in evelation a lot of research work. Syrmakezis (1994) try to give the definition of irregularity or regularity in a quantitative way. Bonelli and Cassis (1994) study the influence of wall discontinuities in evelation upon the earthquake response. They conclude the results from linear analysis should be corrected to obtain a satisfactory response, due to the development of important stress concentrations. Aranda (1984) made the inelastic analysis of R/C frames to vertical irregularities and receive the value of ductility demands. Similar results are found by Costa, Oliveria and Duarte (1988). The main objectives of whole these investigations are to identify the peculiarities of the response, and to evaluate the traditional code design methods in light of nonlinear dynamic response.

In this paper two frames with irregularities in evelation are considered.

2. Analysis method

The procedure of nonlinear analysis of R/C frame structure can be summarized as fellows:

- Formulation of the equation of motion on the basis of the equilibrium condition of all forces at each joint. Inertia forces, damping forces, resisting forces and external forces are set to be in equilibrium.

$$M\ddot{x} + C\dot{x} + k(x) = F(t) \qquad (1)$$

where: M is mass matrix; C is damping matrix; k(x) is internal resisting force vector and F(t) is external dynamic force vector.

The initial conditions are:

$$x_o = x_S \; ; \; \dot{x}_o = 0$$

$$\ddot{x}_o = - M^{-1}[F(t_o) + K_o x_S]$$

where x_s is the vector of static displacements present in the structure when the seismic action stars.

The equation of motion is nonlinear differential equation of second order and is not solvable in a closed form.

- Numerical integration of the differential equation. In this study the two-parameter method is used.

The unknown vector x, $\dot{x}$, $\ddot{x}$ at $t_1=t_o+h$, where h is the time step are determined by the modified equation according to (Simeonov, 1988).

$$M\ddot{X}_1 + C\dot{x}_1 + (1 - \alpha)k(x_1) = F_1(t) - \alpha k(x_o), \qquad (2)$$

Where $x_1, \dot{x}_1, \ddot{x}_1$ are approximate values of x (t_1), $\dot{x}(t_1)$ and $\ddot{x}(t_1)$
and α is a free parameter ($a \geq 1/3$) and the additional equations

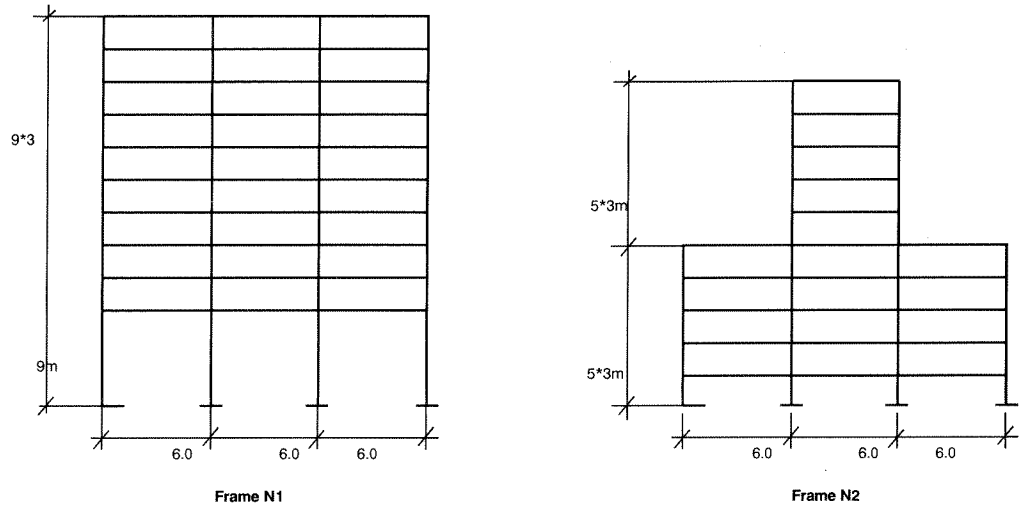

Fig. 1

$$x_1 - x_o = \frac{h}{2}\left[(1-\alpha)\,\dot{x}_o + (1+\alpha)\,\dot{x}_1\right]$$

$$\dot{x}_1 - \dot{x}_o = \frac{h}{2}\left[(1-\alpha)\,\ddot{x}_o + (1+\alpha)\,\ddot{x}_1\right] \qquad (3)$$

For each time step the solution of the discrete nonlinear equation is obtained by means of simple iterations. The following iteration process is used:

$$x_1^{(\nu+1)} = x_1^{(o)} + D^{-1}\,[Kx^{(nu)} - (1 - \text{alpha})$$

$$(1+\alpha+\zeta)^2\,h^2 k\,(x_1^{(nu)})]$$

$$x_1^{(o)} = D^{-1}\,P; \quad D = 4M + K \qquad (4)$$

$$P + (1+\alpha+\xi)^2 h^2\,[F_1 - \alpha k\,(x_o)] +$$

$$+ 4M\left\{x_o + hx_o + \frac{1}{4}\left[1 - (\alpha+\zeta)^2\right] h^2\,\ddot{x}\right\}$$

where ξ is the viscous damping ζ is the article viscous parameter

This method has the advantage to being stable for all periods and time steps. Another important feature is the overshooting truncating ability in the high frequency range.

- Linearization of a nonlinear member end force-displacement relation by an instantaneous stiffness matrix for a small increment of force and displacement.

- Formulation of an instantaneous structural stiffness matrix on the basis of the compatibility relation of displacements at a joint and the equilibrium of external forces at a joint with resisting structural forces.

Displacements at the joints of a frame in the global coordinates are computed by the above mentioned numerical techniques, including step-by-step and iteration schemes for the solution of the nonlinear equations, based on instantaneous stiffness. The member's instantaneous stiffness are determinated through the hysteresis model of Takeda (Takeda, 1970), (Vasseva, 1988).

3. Ductility demand

Using nonlinear dynamic analysis we have received information about the ductility demand. Ductility demand at a zone with plastic hinge in "yielding frame" can be expressed by the curvature ductility factor DFC = κ_u / κ_y, where κ_u is the maximum curvature at the section and κ_y is the curvature at the section at first yield. It should be emphasized that although ductility factor is not a unique measure of energy dissipation, it may be considered as a useful index that can measure the suitability of a structure in seismic regions.

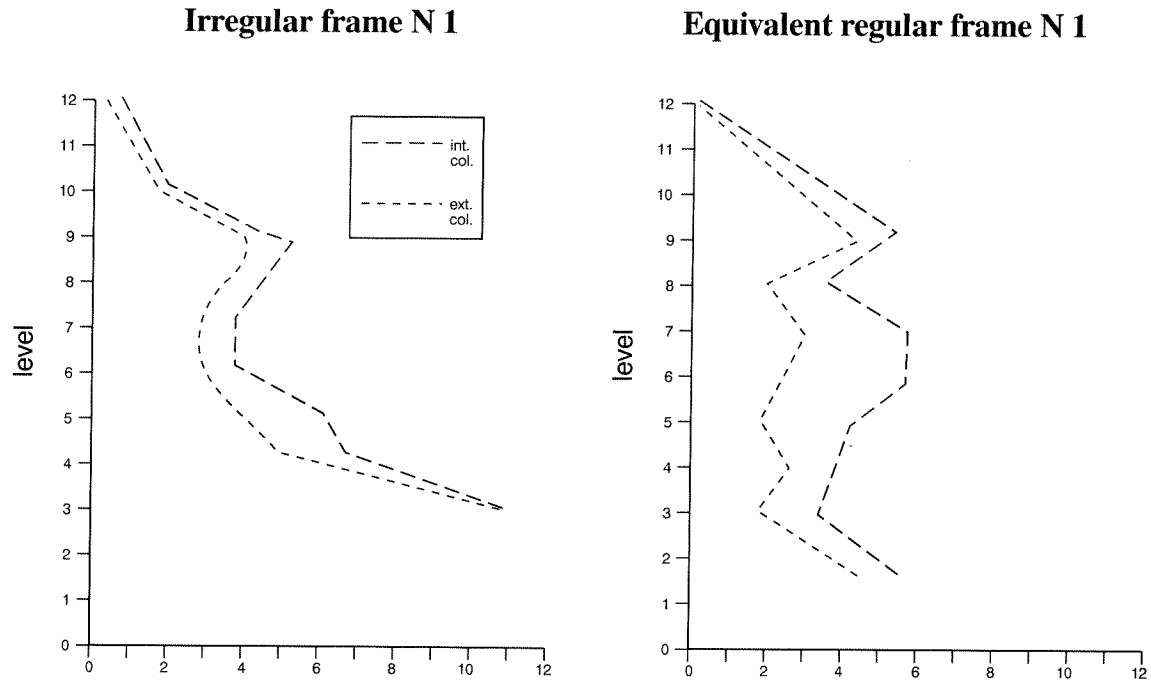
Irregular frame N 1
Equivalent regular frame N 1
int. col.
ext. col.
level
0
1
2
3
4
5
6
7
8
9
10
11
12

Fig. 2

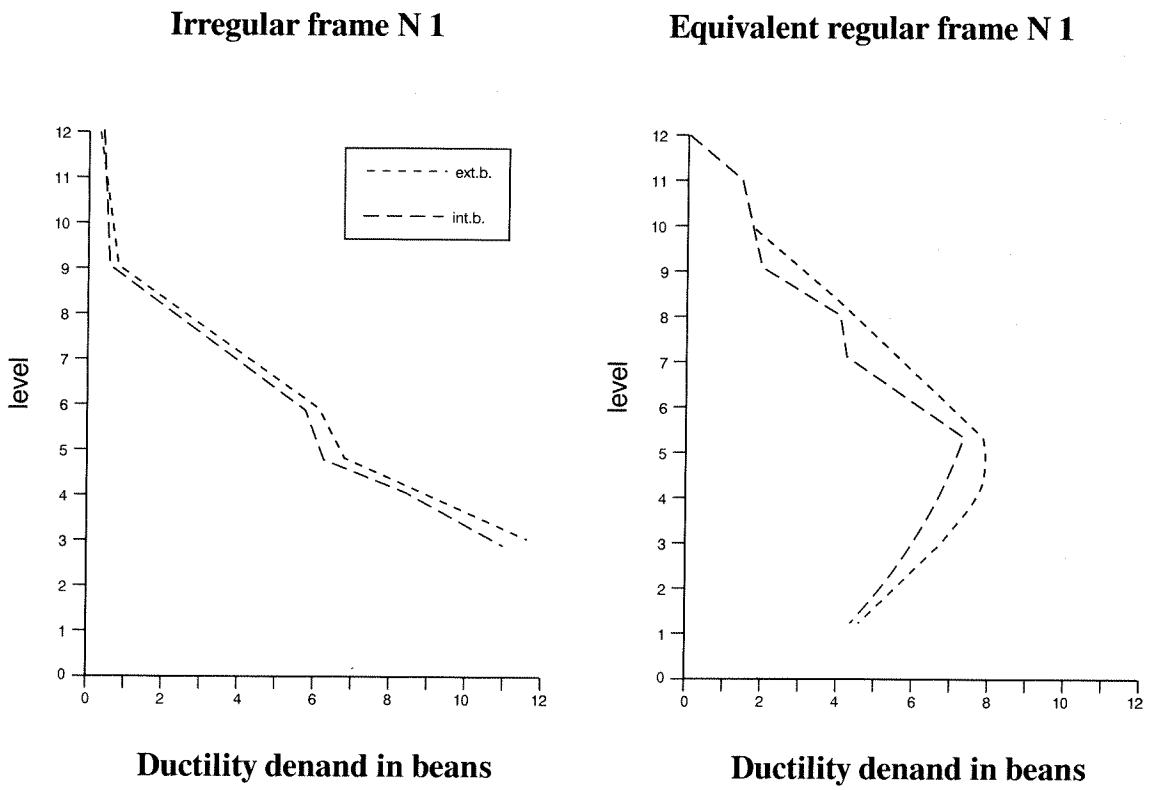
Irregular frame N 1
Equivalent regular frame N 1
ext.b.
int.b.
level
0
1
2
3
4
5
6
7
8
9
10
11
12
Ductility denand in beans
Ductility denand in beans

Fig. 2

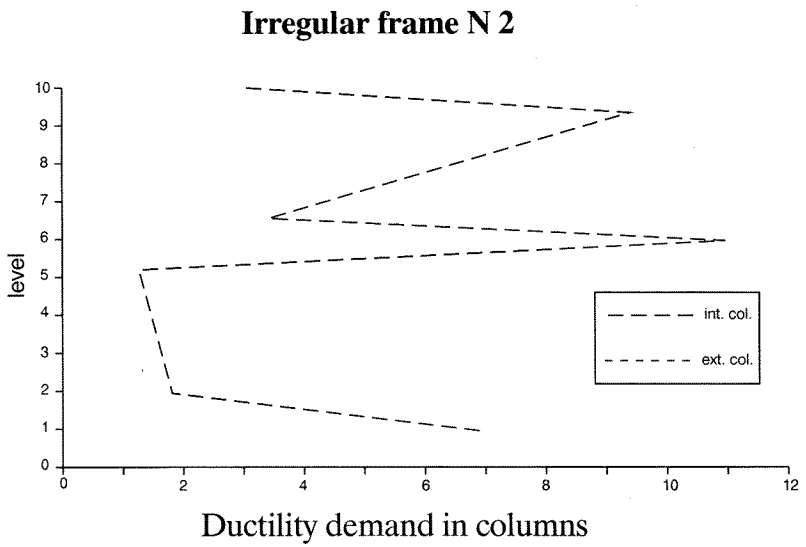
Irregular frame N 2
level
int. col.
ext. col.
Ductility demand in columns

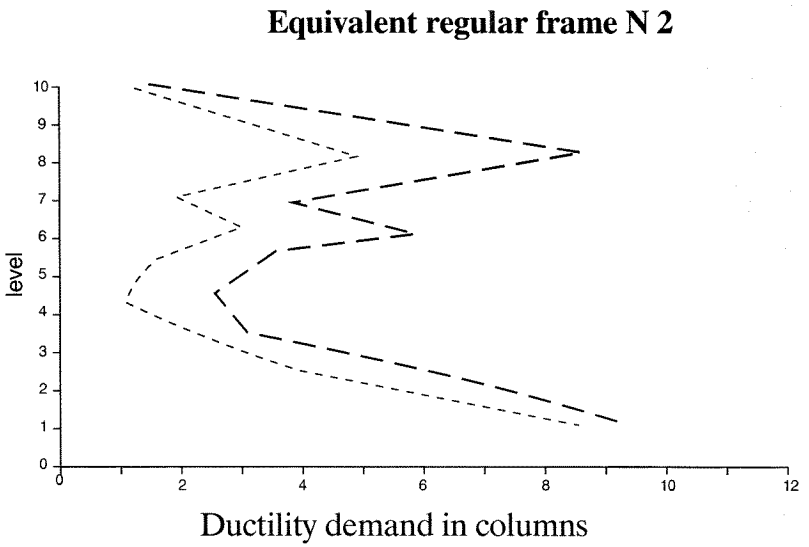
Equivalent regular frame N 2
level
Ductility demand in columns

Fig. 3

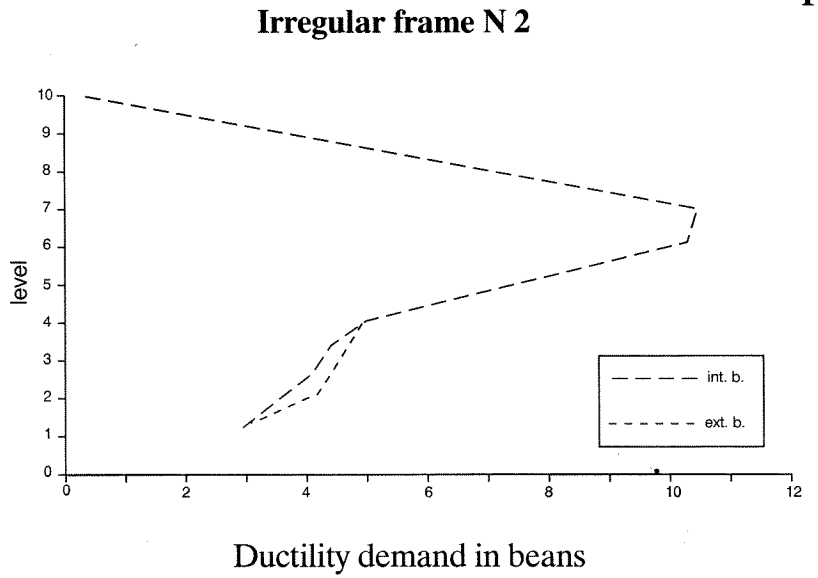
Irregular frame N 2
level
int. b.
ext. b.
Ductility demand in beans

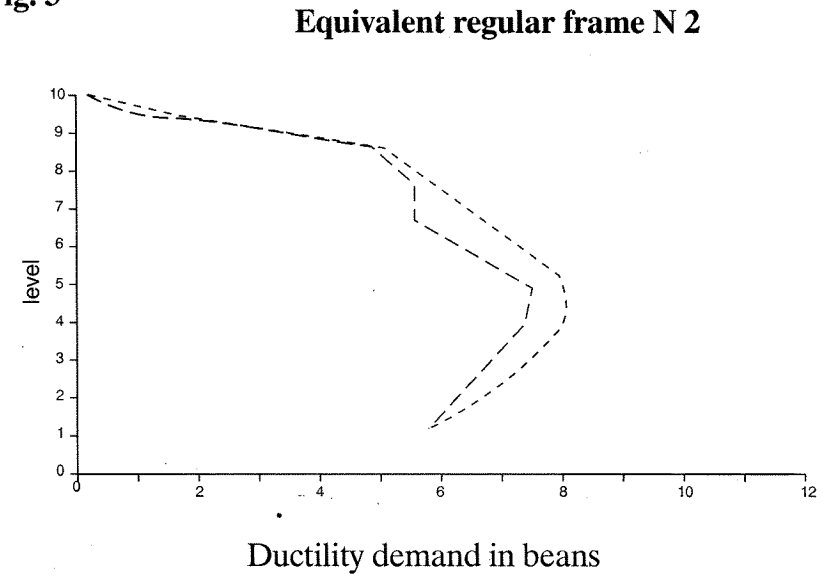
Equivalent regular frame N 2
level
Ductility demand in beans

Fig. 3

4. Numerical examples

Using program NLDRF (Vasseva, 1988) developed on the basis of the above mentioned step - by - step method, two frames, shown in Fig. 1 are studied. They are investigated as regular and as irregular frames. The frames are designed for seismic loads corresponding to seismicity of 8 degree, according to Bulgarian Code for seismic design (1987), design acceleration 0.15 g and medium ground conditions. The input ground motion is presented by accelerogram - NS component of the Bucharest record Vrancea 1977 earthquake. The maximum displacements, velocities and accelerations at floor levels are received in addition to the maximum base shear forces and moments are received with this program. Besides maximum response values are obtained for each frame member in term of moments, rotations and ductility of flexural elements. Figures 2 to 3 show the ductility demands in columns and beams for both frames irregular and equivalent regular. It is found that for both modes the demands in exterior beams are larger than in the interior ones. In columns of the irregular frame the demands in interior columns are greater than in the exterior ones. It is believed that this results is due to the included effect of second order. It is to be noted that the values of ductility demand in the zones of irregularities show large variation. For the irregular frame this factor increase about 2.

5. Conclusions

The importance of taking into account the nonlinear behavior in the seismic analysis of R/C frames irregular in elevation is shown. It is found that irregularities in elevation increase the ductility demand. This effect is significant when there is a sudden change in the siffness distribution of the frame. Besides the variation along the height of stiffness would be carefully controlled to avoid undesirable concentrations of the inelastic deformations. Only by means of nonlinear dynamic analysis could be investigated the behavior of structures with special feature in geometry and stiffness distribution. This analysis and specially the ductility demand gives a necessary information about the endangered sections of the structural system. The investigations in this field and the effort internationally have to continue with tool to define more precisely the concept of irregularities or regularity of a structural and to find some relationship between the behaviour factor and the degree of irregularity.

Acknowledgments

The results reported herein, form a part of a development research project, financed by Bulgarian Foundation Scientific Research, Earth Sciences, HZ418/94.

References

Aranda, R. 1984. Ductility demands for R/C frames irregular in evelation, *Proc. 8th World Conference on earthquake Eng.: 4/559-4/556 San Francisco.*

Bonelli P., Cassis J., 1994. Earthquake-resistant design of R/C buildings with irregularities in elevation, *Earthquake Resistant Construction and Design, ERCAD Berlin 94, 2/691-2/698*

Costa, A., C. Oliveria & R. Duarte 1988 Influence of vertical irregularities on the seismic response of buildings, *Proc. 9th World Conf. on Earthquake Eng.: 5/491-5/496, Tokio, Kioto.*

Norm for Design of Building and Structures in Seismic Regions, Sofia, 1987 (in Bulgarian)

Simeonov S. 1988. On one numerical method in dynamic of elastic system, *Theor. Appl. Mech., No 1, BAS, 1988 (in Bulgarian).*

Syrmakezis, C.A., I. Vayas & A. Sophocleous, 1994. An approach to the quantitative estimation of the degree of (ir) regularity in elastoplastic structures, *Earthquake Resistant Construction and Design, ERCAD Berlin 94, 2/653-2/660*

Takeda, T., Sozen, M. A., Nielsen, N.N., 1970. Reinforced concrete response to simulated earthquakes, *J. Strc. Division, ASCE, Vol. 96, No ST2, Proc. Paper 7759, Dec. 1970, pp. 2557-2573.*

Vasseva E., 1993. Nonlinear dynamic analysis of reinforced concrete frames, J. *Natural Hazards, pp. 279-290, No 3, volum 7 May 1993.*

EARTHQUAKE PREDICTION - INSTRUMENTATION OF SEISMIC NETWORKS AND EARTHQUAKE CATALOGUES

MONITORING OF THE PREPARATION OF STRONG INTERMEDIATE-DEPTH EARTHQUAKES IN VRANCEA, ROMANIA, USING THE CN ALGORITHM

O.V. Novikova[1], I. A. Vorobieva[1], D. Enescu[2], M. Radulian[2], I. Kuznetzov[1], C. Moldoveanu[2] and G. F. Panza[3,4]

[1] *International Institute of Earthquake Prediction Theory and Mathematical Geophysics, Academy of Sciences of Russia, Moscow*
[2] *National Institute for Earth Physics, Bucharest*
[3] *Istituto di Geodesia e Geofisica, Universita' di Trieste*
[4] *International Center for Theoretical Physics, Miramar*

Keywords: Earthquake prediction, CN algorithm, Vrancea

Abstract

The preparation of strong, intermediate-depth earthquakes in the Vrancea region is monitored with the application of the CN algorithm to a newly compiled earthquake catalogue, for the period from 1930 to 1994. The catalogue has been obtained by merging Romanian and U.S.S.R. data. Four out of the five strong earthquakes, with magnitude above 6.4, are preceded by a Time of Increased Probability of the occurrence of an earthquake (TIP alarm). The total TIP alarm occupies 21.7% of the time interval under consideration, i.e. about 2.5 years for each strong earthquake.

Introduction

Vrancea is characterized by relatively high-level seismicity: four catastrophic earthquakes, with magnitude equal or greater than 7.0 occurred during this century (Table 1). These earthquakes cause heavy destruction not only in Romania, but in other European countries, so the problem of prediction is extremely important, also considering the fact that, in the territory that can be shaken by one of such events, several nuclear power plants are presently operating.

Several attempts have been made for the long-term prediction of the strong earthquakes in Vrancea. Enescu et al. (1973, 1974) made the first attempt to predict Vrancea intermediate-depth earthquakes, based on observations of the periodicity of these earthquakes. In agreement with the hypothesis of periodicity, introduced on statistical grounds, the model predicts the occurrence of three different major earthquakes during the first fiftly years of the 21st century: the first in 2004 ± 4, the second in 2020 æ 5, and the third in 2040 ± 5. Another attempt to predict Vrancea earthquakes was made by Enescu and Ianas (1975) by using Wiener predictive filters. Based on a model of the time variation of the focal mechanism for Vrancea earthquakes, Enescu (1983) predicted that within four years from 1983, a major earthquake will occur in the Vrancea region. The prediction was confirmed by the occurrence of

the 1986 event.

For intermediate-term prediction of strong earthquakes the algorithm CN (Keilis-Borok) and Rotwain, 1990) can be used. The algorithm which has been applied on a global scale to shallow seismicity, is based on the quantitative analysis of premonitory phenomena, which can be detected in the seismic flow preceding the occurrence of strong earthquakes. Since the algorithm, originally developed for the California-Nevada region, uses normalized functions, it can be applied without any adjustment of the parameters, to the determination of the Time of Increased Probability (TIP) of strong earthquakes for any other seismic region (for a recent application see Costa et al., 1994). Details about the applicability of the CN algorithm to the data on intermediate-depth seismicity are given by Novikova et al. (1995). Here we briefly illustrate the results of the application of the CN algorithm, to Vrancea intermediate-depth earthquakes, that allow us to monitor, on the intermediate time scale, the preparation of strong intermediate-depth earthquakes in the Vrancea region.

Seismicity of Vrancea and Input Data

There are at least three catalogues of earthquakes for the Vrancea seismoactive region.

The first one it is Romanian local catalogue compiled after Redu (1979) and Constantinescu and Marza (1980). It covers the time interval from 1900.1.1 to 1979.12.31 and contains the earthquakes localized in the rectangle 41.2°N-48.4°N, 20.8°E-29.8°E (actually all intermediate-depth earthquakes are located in the region 45.°N-46.°N, 26.°E-27.°E). The second catalogue is Earthquakes in the USSR (1965-1992) which covers the period of time from 1962.1.1 to 1990.12.31, and contains the earthquakes localized in the rectangle 44.°N-46.° N, 24.°E-28.°E. The third one is the Romanian local catalogue. It covers the period of time from 1980.1.1 to 1994.12.31, and contains only intermediate-depth earthquakes (h > 60 km). The catalogue is compiled by Trifu and Radulian (1991) and extended here till the end of 1994.

Application of the Algorithm Cn to Vrancea

One of the basic problems in the application of the algorithm CN is the choice of the regionalization to be used, as indicated, for instance by Costa et al. (1994; 1995) for the Italian territory. In this respect Vrancea offers a special opportunity since a single zone can be considered, quite well defined by the seismic activity.

To apply the CN algorithm Novikova et al. (1995) compiled a catalogue composed of theree parts, choosing, for each period of time, the most representative data. For the last period, from 1980 to 1993, the best catalogue is the Romanian local catalogue, for the period from 1962 to 1979 the best is the catalogue Earthquakes in the USSR (1965-1992). The completeness level of the Romanian catalogue (Radu, 1979) for the period from 1900 to 1978 is much worse than that of the other two catalogues, and therefore the determination of reliable parameters of CN for the period of time before 1962 is not possible. The above-mentioned catalogue was updated to the end of 1994 by Moldoveanu et al. (1995) and used in the present paper for the application of the CN algorithm.

As result of the merging of the catalogues,

Table 1. Strong earthquakes in Vrancea from 1900 (Our Catalogue, see the text)

Date			Time		Hypocenter			
yy	mm	dd	hh	mm	Lat (o)	lon (o)	depth (km)	M
1940	11	10	1	39	45.80 N	26.70 E	133	7.2
1977	3	4	19	21	45.78 N	26.80 E	110	7.1
1986	8	30	21	28	45.51 N	26.47 E	138	7.0
1990	5	30	10	40	45.83 N	26.74 E	90	7.0

Table 2. Results of the CN algorithm for the period from 1966 to 1994 (1966-1993 retrospective, 1993-1994 forward monitoring), obtained merging the catalogue Earthquake in the USSR (1965-1992), from 1962 to 1979, with the Romanian Catalogue, from 1980 to 1994, M_0 = 6.4.

Start of TIP	Strong earthquakes Date	M	End of false alarm	Duration of TIP (months)
1.9.1974			1.7.1976	22.0
1.1.1977	4.3.1977	7.1		2.1
1.1.1981			1.9.1982	20.0
1.11.1982			1.7.1985	32.0
1.11.1985	30.8.1986	7.0		10.0
1.11.1989	30.5.1990	7.0		7.0

total number of strong earthquakes = 3

3 earthquakes have been predicted

total duration of TIPs = 93.0 months (27.9% of total time)

the largest schocks occurred in Vrancea in this century are listed in Table 1. Accordingly with the data in Table 1, during the period of time from 1962 to 1994, three such earthquakes occurred in 1977 (M = 7.1), in 1986 (M = 7.0) and in 1990 (M = 7.0). The result of TIP diagnosis is given in Table 2. All three strong earthquakes are preceded by TIPs, and the duration of TIPs occupies 27.9% of the total time interval considered. This result is quite close to the global values.

In the period of time from 1932 to 1962 the catalogue is not complete for magnitudes above M_0 = 2.5, and therefore the algorithm CN cannot use the possibility of self-adjustment to the data. Therefore, in analogy with what was done by Costa et al. (1994) in the Italian region, the 1932-1962 data are not used for the parameter

Table 3. Results of the CN algorithm for the period from 1936 to 1994, (1936-1993 retrospective, 1993-1994 forward monitoring) obtained using the complete catalogue from 1932 to 1994, compiled by us, M_0 = 6.4.

Start of TIP	Strong earthquakes Date	M	End of false alarm	Duration of TIP (months)
1.7.1940	10.11.1940	7.2		4.3
	7.9.1945	6.4		failure to predict
1.11.1945			1.11.1946	12.0
1.3.1948			1.1.1951	34.0
1.9.1974	4.3.1977	7.1		30.1
1.1.1981			1.9.1982	20.0
1.11.1982			1.7.1985	32.0
1.11.1985	30.8.1996	7.0		10.0
1.9.1989	30.5.1990	7.0		9.0

total number of strong earthquakes = 5

4 earthquakes have been predicted

total duration of TIPs = 151.3 months (21.7% of total time)

Table 4. Results of the CN algorithm for the period from 1936 to 1994, (1936-1993 retrospective, 1993-1994 forward monitoring) obtained using the complete catalogue from 1932 to 1994, compiled by us, M_0 = 6.5.

Start of TIP	Strong earthquakes Date	M	End of false alarm	Duration of TIP (months)
1.7.1940	10.11.1940	7.2	1.1.1951	4.3
1.11.1945				62.0
1.9.1974	4.3.1977	7.1		30.1
1.1.1981			1.9.1982	20.0
1.11.1982			1.7.1985	32.0
1.11.1985	30.8.1986	7.0		10.0
1.11.1989	30.5.1990	7.0		9.0

total number of strong earthquakes = 4
4 earthquakes have been predicted
total duration of TIPs = 167.3 months (24.0% of total time)

determination. The algorithm CN is applied, using the parameters determined for the period of time from 1962 to 1993, to the part of the Romanian catalogue (Radu, 1979) from 1932 to 1962. Only intermediate-depth (h > 60 km) main shocks, defined accordingly with Dmitrieva et al. (1987) are considered. We note that CN, is applied till the end of 1993 as retrospective analysis, while from the beginning of 1994 we start the forward monitoring.

There are two strong schocks, one with magnitude 7.2, in 1940 and the other with magnitude 6.4 in 1945. The TIP is diagnosed before the earthquake of 1940, while the earthquake of 1945 is a failure to predict.

Thus, for the period of time from 1932 to 1994 TIPs precede four out of the five strong earthquakes, and they occupy 21.7% of the total time considered (Table 3).

Analysis of the Results

Even if the total TIPs duration is not large, there are four false alarms (Table 3). The first one is associated with the earthquake in 1945 M = 6.4 (failure to predict), the second one lasts for three years from 1948 till 1951, and it is not associated with any strong earthquake, since there are no earthquakes with M>6 in this period. Two false alarms, in 1981 and 1982, are due to short interruptions of the long TIP preceding the strong earthquake in 1986. All false alarms are due to seismic activation, as indicated by the occurrence of several relatively strong main schocks, followed by a large number of aftershocks.

Since 1930 there are four earthquakes with magnitude in the range 7.0-7.2, and only one earthquake with magnitude 6.4. This last earthquake is a failure to predict. If M_0 is increased to 6.5, all four strong earthquakes are preceded by TIPs, and the total duration of TIPs slightly increases to 24% (Table 4). The increase of the total duration of TIPs is due the occurrence of a long false alarm, associated with the shock with M=6.4, occurred in 1945.

Let us now consider the actual patterns in the earthquakes flow that precede the occurrence of the events with $M > M_0$ (strong earthquakes). The analysis of the features of the seismic flow producing TIPs shows that three out of the four predicted strong earthquakes, namely those occurred in 1940, 1977 and 1986 are preceded by seismic activation, which is expressed by the occurrence of several main shocks of intermediate magnitude, and followed by aftershocks. The behaviour of seismicity before the last strong earthquake, occurred in 1990, is different. The precursory phenomenon of this earthquake is quiescence. Therefore, there is not a unique

scenario of the process of preparation of strong earthquakes in Vrancea region, and the use of a so complete prediction algorithm as CN is fully justified.

Conclusions

Vrancea is not a typical region for the application of the CN algorithm. Usually CN is used to predict shallow earthquakes on a territory with linear size of hundreds kilometers. In Vrancea the main seismicity occurs at intermediate depth and is concentrated in a very narrow zone.

CN algorithm can predict the intermediate-depth strong earthquakes, using only intermediate-depth seismicity. The results of the retrospective tests indicate the importance to continue regularly the monitoring of intermediate-depth seismicity in Vrancea; this is made possible by the use of the Romanian local seismic catalogue (Trifu and Redulian, 1991), which is continuously update (Moldoveanu et al., 1995).

Acknowledgements

The authors are grateful to I. M. Rotwain for very helpful discussion and to M. Popa for her assistance with the Romanian earthquake catalogues. This research has been made possible by the NATO Linkage Grants ENVIRLG. 931206, CN. SUPPL. 940880.453, and by ICTP-Trieste support and COPERNICUS contract (CIPA-CT94-0238).

References

Constantinescu, L. and Marza, V. (1980), A computer-compiled and computer-oriented catalogue of Romania's earthquakes during a millennium (984-1979), Rev. Roum. Geol. Geogr. Geophys., 24, 193-234.

Costa, G., Staniskova, I., Rotwain, I. and Panza G. F. (1995), Regionalization and Stability of CN algorithm: the case the Italy, in preparation.

Dmitrieva, O.E., Keilis-Borok, V. I., Kossobokov, V. G., Kuznetsov, I. V., Levshina, T. A., Mirzoev, K. M., Negmatullaev, S. Kh., Pisarenko, V. F., Rotwain, I. M., and Schreider, S. Yu. (1987), Identification of the periods of increased probability of strong earthquakes in seismoactive regions of USSR and other countries, Computational seismology, 20, Nauka, Moscow.

Earthquakes in the USSR. 1962-1990. Nauka, 1965-1992, Moscow.

Enescu, D. (1983), New data regarding the periodicity of Vrancea earthquakes and attempts to give a tectonophysical explanation of this periodicity (in Romanian), Studies and Researches in Geophys., 21, 24-30.

Enescu, D. and Ianas, M. (1975), Attempts at predicting earthquakes in Vrancea for the periods 1976-1980 and 1981-1990, Rev. Roum. Geophys., 19, 27-35.

Enescu, D., Marza, V. and Zamarca, I. (1974), Contributions to the statistical prediction of Vrancea earthquakes, Rev. Roum. Geophys., 18, 67-79.

Enescu, D. and Zamarca, I. (1973), A brief report concerning the Vrancea earthquake prediction, Report of the Institute for Geology and Geophysics, (IGG) 1973; paper presented to the Reports Session of IGG on May 17, 1973.

Keilis-Borok V. I. and Rotwain I. M. (1990), Diagnosis of Time of Increased Probability of strong earthquakes in different regions of thw World: Algorithm CN, Phys. Earth Planet. Int., 61, 57-72.

Moldoveanu, C., Novikova, O. V. and Vorobieva, A. (1995). Updating of the Vrancea intermediate-depth earthquakes catalogue. ICPT Int. Rep., in preparation.

Novikova O. V., Vorobieva I. A., Enescu D., Radulian M., Kuznetzov I. and Panza, G. F. (1994), Prediction of the strong earthquakes in Vrancea, Romania, using the CN algorithm, Regeoph, in press.

Radu, C. (1979), Catalogue of strong earthquakes originated on the Romanian territory, Part II: 1901-1979, in "Seismological Researches on The Earthquake of March 4, 1977" - Monograph (eds. I. Cornea and C. Radu, Central Institute of Physics, Bucharest).

Trifu, C.-I. and Redulian, M. (1991), A depth-magnitude catalog of Vrancea intermediate depth microearthquakes, Rev. Roum. Geophys., 35, 35-45.

USE OF STRONG MOTION DATA IN THE RELOCATION OF EARTHQUAKES OCCURRED IN THE AREA OF GREECE

Dimitris Papanastasiou

Geodynamic Institute, National Observatory of Athens, 118 10 Athens, GREECE

Abstract

It is accepted that the determination of the earthquake parameters is not accurate, as the solution is influenced by many factors like the distribution of the stations and their average spacing, the quality of the input data and the accuracy of the velocity model used. Many methods exist to relocate strong events which are widely and clearly recorded, but the problem remains for earthquakes with smaller magnitudes.

In this study, 34 earthquakes with magnitudes Ms ≥ 4.4, occurred mainly in western Greece during the period 1973-1993, were relocated by including in the data set information from good quality and uniformly processed strong motion records obtained from lose stations.

Introduction

The routine earthquake locations given by different agencies cannot generally be regarded as accurate. The main reasons are the inadequate azimuthal station coverage, the systematic and random reading errors and bias due to the difference between the real earth and the velocity model used in the location procedure. As strong earthquakes are usually clearly and widely recorded, reading errors as well as errors produced by the station distribution will be reduced. So the assumed earth model will be responsible for the larger part of the remaining errors.

In recent years, many studies have shown that the teleseismic locations of large earthquakes in the area of Greece may have errors by more than 10 Km (Soufleris and Stewart 1981; Jackson et al., 1982; Soufleris et al., 1982; Lyon-Caen et al., 1988). In order to improve these locations the relative relocation method of Jackson and Fitch (1979) was employed by Soufleris and Stewart (1981); Soufleris et al., (1982); Jackson et al., (1982) and Taymaz et al., (1991). In these works the best recorded event by a local portable seismic network also well recorded teleseismically was chosen as the master event and the other events relocated with respect to it. It is obvious that for smaller earthquakes not enough and accurate information could obtained from far away stations to relocate them, so the location errors will remain considerably larger, especially in focal depth (Jackson, 1980).

In this study we relocated 34 earthquakes occurred in western Greece and recorded by the permanent network of Geodynamic Institute of the National Observatory of Athens (GI-NOA) as well as by international agencies. The earthquakes have triggered strong motion accelerographs belonging to the same Institute. In an attempt to obtain more accurate solutions, we relocated the events by including in the data set the time difference between the S arrival and the triggering time from strong motion records. The final solutions have solved focal depths and are in better accordance with information obtained from differet sources.

Relocation of the earthquakes

GI-NOA besides the national seismological network, operates a permanent network of three-component strong motion instruments (SMA-1).

Special Publications of the Geological Society of Greece, No 6.

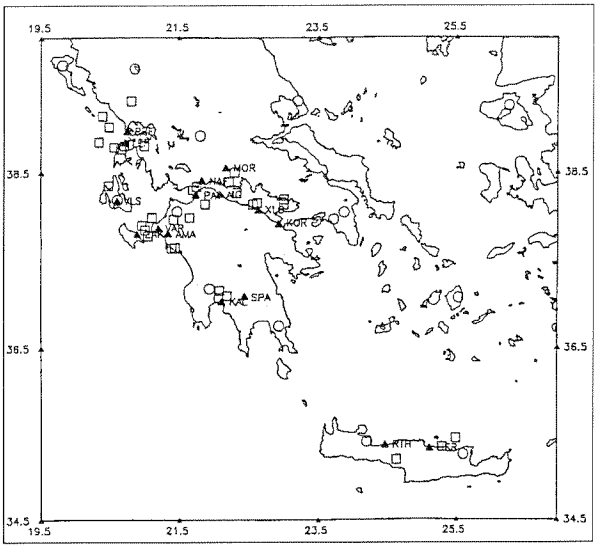

Fig. 1. Location of the seismological stations (circles), the strong motion stations (triangles) and the epicentres (squares) of the relocated 34 earthquakes.

Recently it completed the re-evaluation of the existing strong motion records which covered the period 1973-1994 (Stavrakakis et al., 1992; Kalogeras and Stravakakis, 1995).

For 34 earthquakes mostly of moderate to large magnitude, Ms ≥ 4.4, occurred mainly in western Greece during this period, good quality, uniformly processed strong motion records from very close stations were available (Fig. 1). The earthquakes were routinely located by GI-NOA and their locations are listed in the published monthly seismological bulletins. For every earthquake, from the nearest available strong motion record, the first clear time difference between the S arrival and the triggering time was recognized and finally measured. As the strong motion station located in very close distance to the epicentre of the examined shock, the triggering within the limits of the reading errors. The 34 events were relocated by applying two possibilities of the Hypo-71 (Lee and Lahr, 1975) computer program: to use the measured S-P time difference and to have after every solution updated station corrections. The other parameters like the arrival times of the different seismological stations, the velocity model used, the Vp/Vs ratio of 1.73 e.t.c. are listed in the published monthly seismological bulletins by GI-NOA. In order to improve the final solutions we performed iterations by using every time the previous obtained hypocentral solution and the updated stations corrections. After a few iterations we reached to converged solutions which had also the minimum standard errors and resolved focal depths.

The obtained relocated positions were listed in Table 1. For comparison the locations by GI-NOA as well as by the International Seismological Centre (ISC) are also given. The last column gives the time difference between the S arrival and the triggering time which was measured as well as the corresponding strong motion station. The epicentres of GI-NOA, ISC and the relocated ones are plotted for comparison in figures 2a - 2e. Every figure correspond to different area like the Ionian sea, the Gulf of Corinth, the area of Pirgos, the area of Kalamata and the Crete respectively.

Discussion and Conclusions

The obtained relocated positions and those given by the local determination and by the international centre are in a good agreement. Taking into account that there exist uncertainties in the velocity models and reading errors, differences in position of up to 10 Km so have no significance.

For the area of Greece ISC locations show shift mainly along a north-south axis. This shift is towards the north for the area of Ionian sea and Pirgos (Fig. 2a and 2c), for the area of Kalamata and Crete (Fig. 2d and 2e) it is to the south while for the area of the Gulf of Corinth (Fig. 2b) no systematic shift is observed. Our relocated positions didn't show any systematic shift, in many cases remain to the position given by GI-NOA.

What this study shows is that we can have resolved focal depths. Usually the depths determined my major agencies, using a greater number of distant stations, is deeper than that given by local agencies. The inability to constrain the focal depth derives mainly from the network geometry and the location of the earthquake in relation to the network. With this procedure we changed the array geometry and the location of the event in relation to the array as we improved the station coverage of the earthquake by including one more station, the strong motion

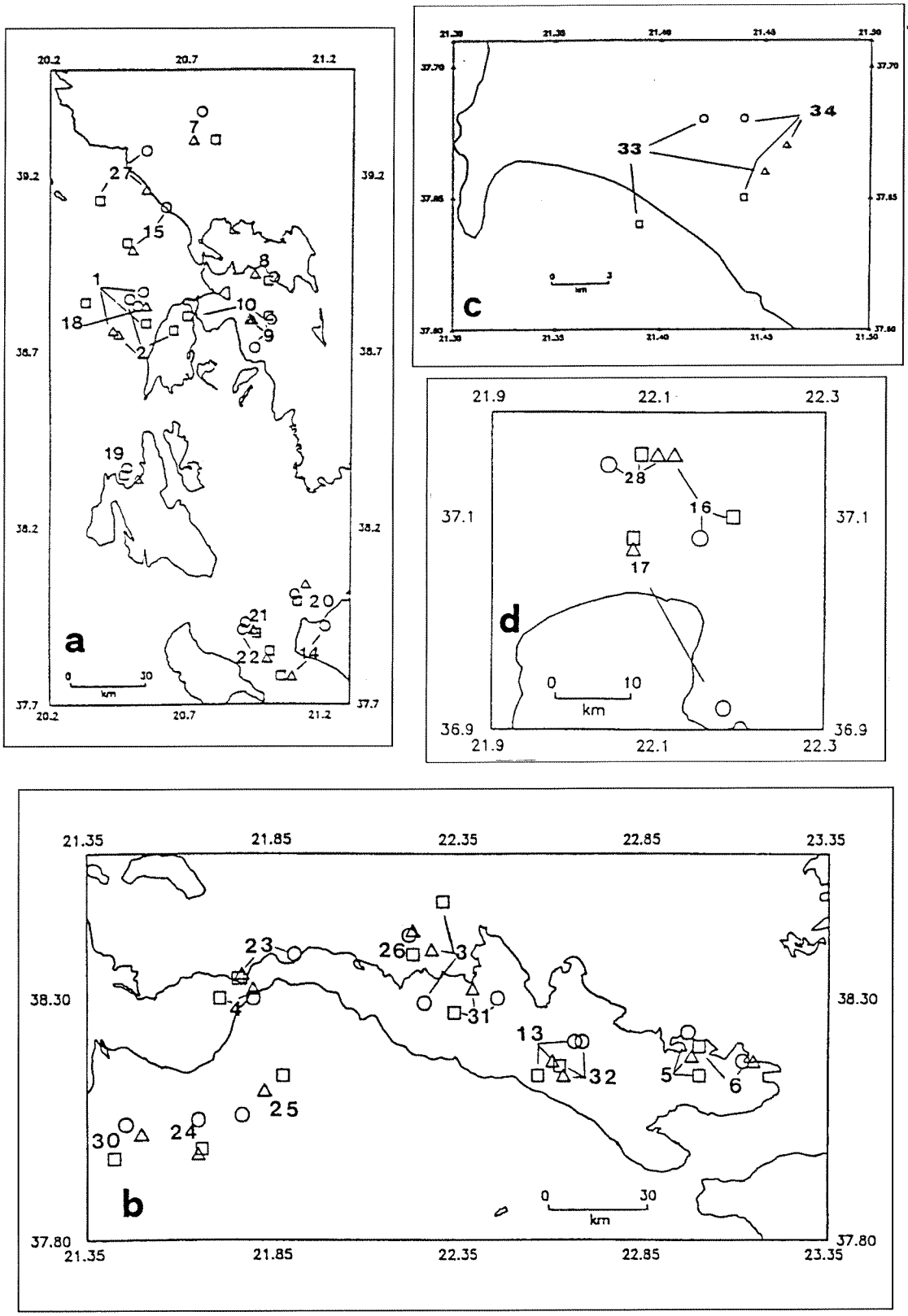

Fig. 2. Epicentres of the events located in (a) Ionian sea, (b) Gulf of Corinth, (c) the area of Pirgos and (d) the area of Kalamata. GI-NOA locations are given by squares, ISC by circles and relocated positions by triangles.

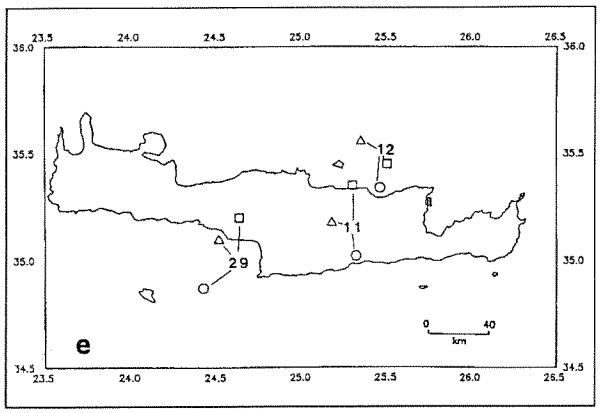

Fig. 2e. Epicentres of the events located in Crete. GI-NOA locations are given by squares, ISC by circles and relocated positions by triangles.

One, which was located close to the epicentre at distance, almost in all the cases, less than the focal depth. The estimated depths are shallower than those given by ISC in almost all the cases, while those given by GI-NOA are still shallower. The depths given by GI-ISC, which are greater than 30Km, are also deeper than the relocated.

For some cases ISC determinations are not in agreement with results obtained from temporary networks or from other relocation methods. For the earthquakes of February and March 1981, occurred at the eastern part of the Gulf of Corinth (Fig. 2b), ISC solutions have much greater depths (30 and 32 Km) from those (around 10 Km) obtained from an aftershock

Table 1

	DATE			Hr	G.I. Mn	N.O.A. MAG	LAT °N	LON°E	I.S.C. D	LAT °N	RELOCATION LON °E	D	LAT °N	LON °E	D	DIF (sec)
1	1973	NOV	4	15	52	5.9	38.78	20.55	5f	38.87	20.54	13	38.75	20.45	12	LEF: 3.5
2	1973	NOV	4	16	11	5.0	38.76	20.65	5f	38.85	20.49	36	38.76	20.43	25	LEF: 33.4
3	1977	DEC	29	16	52	5.2	38.50	22.30	5f	38.29	22.25	37	38.40	22.27	16	PAT: 32.6
4	1978	MAY	18	00	18	4.5	38.30	21.70	50	38.30	21.79	26	38.32	21.79	8	PAT: 30.7
5	1981	FEB	24	20	53	6.7	38.14	23.00	5f	38.23	22.97	18	38.18	22.98	10	KOR: 33.6
6	1981	FEB	25	02	35	6.3	38.20	23.00	5f	38.17	23.12	30	38.17	23.15	11	KOR: 32.3
7	1981	mar	10	15	16	5.8	39.30	20.80	5F	39.38	20.75	32	39.30	20.72	9	PRE: 32.3
8	1981	APR	10	08	33	4.7	38.90	21	5f	38.91	21.02	24	38.92	20.95	18	LEF: 32.3
9	1981	MAY	25	23	03	4.7	38.80	21.00	5f	38.71	20.95	30	38.79	20.94	11	LEF: 32.0
10	1981	MAY	27	15	04	5.5	38.80	20.70	5f	38.79	21.01	25	38.79	20.9 3	17	LEF: 32.4
11	1983	MAR	19	21	41	5.7	35.35	25.30	28	35.02	25.32	65*	35.18	25. 18	46	HER: 35.2
12	1984	MAR	1	09	08	4.7	35.45	25.50	61	35.34	25.46	84	35.56	25.35	35	HER: 31.0
13	1984	AUG	17	21	22	4.7	38.14	22.56	18	38.21	22.68	24	38.17	22.6 0	24	XLC: 32.6
14	1985	AUG	13	13	49	5.4	37.78	21.05	60	37.92	21.21	45*	37.78	21. 09	38	AMA: 33.0
15	1985	AUG	31	06	03	5.3	39.01	20.48	5f	39.11	20.62	33*	38.99	20. 50	11	PRE: 32.1
16	1986	SEP	13	17	24	6.0	37.10	22.19	5f	37.08	22.15	9*	37.16	22.1 2	10	KAL: 31.95
17	1986	SEP	15	11	41	5.3	37.08	22.07	5f	36.92	22.18	10f	37.07	22. 07	9	KAL: 31.5
18	1988	APR	24	10	10	5.0	38.84	20.33	5f	38.83	20.52	4	38.83	20.55	9	LEF: 31.5
19	1988	MAY	18	05	17	5.8	38.35	20.47	5f	38.37	20.48	17*	38.34	20. 52	9	VLS: 31.2
20	1988	SEP	22	12	05	5.5	37.99	21.11	5f	38.01	21.10	12*	38.04	21. 14	10	AMA: 32.9
21	1988	OCT	16	12	34	6.0	37.90	20.96	4	37.93	20.92	22*	37.91	20.9 5	14	VAR: 32.4
22	1988	OCT	31	02	59	4.8	37.85	21.01	5f	37.91	20.91	44	37.83	21.0 0	9	VAR: 32.8
23	1988	DEC	22	09	56	5.0	38.34	21.75	19	38.39	21.90	38	38.35	21.7 6	27	NAF: 31.3
24	1989	JUN	7	19	45	5.3	37.99	21.65	5f	38.05	21.64	25	37.98	21.64	9	PAT: 35.5
25	1989	AUG	31	21	29	4.8	38.14	21.87	5f	38.06	21.76	23*	38.11	21. 82	15	PAT: 33.8
26	1990	MAY	17	08	44	5.0	38.39	22.22	33	38.43	22.21	39	38.44	22.2 2	26	AIG: 33.0
27	1990	JUN	16	02	16	6.0	39.13	20.38	38	39.27	20.55	32	39.16	20.5 5	17	PRE: 34.1
28	1990	AUG	8	00	35	4.8	37.16	22.08	5f	37.15	22.04	10*	37.16	22.1 0	9	SPA: 31.8
29	1991	JUN	17	00	26	4.4	35.20	24.63	5f	34.87	24.42	21	35.10	24.5 1	9	RTH: 34.0
30	1992	MAY	30	18	55	5.1	37.97	21.42	12	38.04	21.45	26*	38.02	21. 49	15	AMA: 35.2
31	1992	NOV	18	21	10	5.7	38.27	22.33	23	38.30	22.45	12*	38.32	22. 38	16	MOR 34.5
32	1993	FEB	4	02	22	5.1	38.16	22.62	5	38.21	22.66	20	38.14	22.63	13	XLS: 32.1
33	1993	MAR	26	11	45	5.0	37.64	21.39	5f	37.68	21.42	32	37.66	21.4 5	8	AMA: 33.0
34	1993	MAR	26	11	58	5.5	37.64	21.44	5f	37.68	21.44	25	37.67	21.4 6	11	AMA: 33.8

f: fixed focal depth
*: focal depth obtained by the use of pP-P interval

study (King et al., 1985) or from relocation (Jackson et al., 1982; Taymaz et al., 1991). Our determinations are in better agreement not only in depth (11 and 9Km) but 1986, in aftershock study (Lyon-Caen et al., 1988), showed that the seismic discrepancy between the positions of the three determinations is that ISC locates the event of 15th of September 25 Km southward from the aftershock area. For the events of March 1993 occurred in the area of Pirgos (Fig. 2e) all the locations are almost the same with no significant difference. The study of this sequence (Papanastassiou et al., 1995) revealed that the aftershocks had depths shallower than 20 Km. Our relocation gave depths of 8 and 11 Km while ISC gave 32 and 25 Km respectively.

It is obvious that focal depths determined from teleseismic data are too inacaccurate to distinguish differences in focal depth in the range of 0 to 10 Km while for small and medium size earthquakes the depth estimated from local and temporary networks is quite adequate.

The use of the time difference between the triggering time and the S arrival time shows that is a useful and appropriate way to relocate events and resolve their depth for not very strong events. Attention must be given that this method mainly based on good quality uniformly processed records, supported by reliable seismological information.

References

Jackson J. and Fitch T.J., 1979. Seismotectonic implications of relocated aftershock sequences in Iran and Turkey. Geophys. J. R. Astron. Soc., 75, 209-229.

Jackson J., 1980. Errors in focal depth determination and the depth of seismicity in Iran and Turkey. Geophys. J. R. Astron. Soc., 61, 285-301.

Jackson J., Gagnepain J., Houseman G.,King G.C.P., Papadimitriou P., Soufleris C. and Virieux J. 1982. Seismicity normal faulting and the geomorphological development of the Gulf of Corinth (Greece): the Corinth earthquakes of February and March 1981. Earth and Planetary Science letters, 57, 377-397.

Kalogeras I. and Stavrakakis J., 1995. Analysis of Greek accelerograms recorded at stations of NOA's network. Time period 1990-1994. Publ. No 5 of the Geodynamic Institute, Athens, 404 p.

King G., Ouyang Z., Papadimitriou P., Deschamps A., Gagnepain J., Houseman G., Jackson J., Soufleris C. and Virieux J., 1985. The evolution of the gulf of Corinth (Greece): an aftershock study of the 1981 earthquakes, Geophys. J.R. Astron. Soc., 80, 677-693.

Lee W.H.K. and Lahr J.C., 1975. HYPO-71: A computer programm for determining hypore, magnitude and first motion pattern of local earthquake, U.S. Geol. Surv., Open File Rep., 75-311.

Lyon-Caen H., Armijo R., Drakopoulos J., Baskoutas J., Delibasis N., Gaulon R., Kouskouna V. Latoussakis J., Makropoulos K., Papadimitriou P., Papanastasiou D. and Pedotti G., 1988. The 1986 Kalamata (South Peloponnesus) earthquake: detailed study of a normal fault, evidences for east-west extension in the Hellenic Arc. J. Geophys. Res., 93, 14967-15000.

Papanastassiou D., Stavrakakis G. and Drakopoulos J., 1994. A study of the March 26, 1993 Pirgos (W. Peloponnesus, Greece) earthquake sequence. Proceedings of the XXIV General Assembly of the European Seismological Commission. 19-24 Sept. Athens. (Under publication).

Soufleris C., Jackson J.A., King G.C.P., Spencer C.P. and Scholz C.H., 1982. The 1978 earthquake sequence near Thessaloniki (northern Greece). Geophys. J. R. Astr. Soc. 68, 429-458.

Stavrakakis J., Kalogeras I. and Drakopoulos J., 1992. Analysis of Greek accelerograms recorded at stations of NOA's network. Time period 1973-1990. Publ. No 4 of the Geodynamic Institute, Athens, 431 p.

Taymaz T., Jackson J. and McKenzie D., 1991. Active tectonics of the north and ral Aegean Sea. Geophys. J. Int. 106, 433-490.

AN EARTHQUAKE CATALOGUE FOR THE CIRCUM-PANNONIAN BASIN

R.M.W. Musson

Global Seismology Group, British Geological Survey, Edinburgh, EH9 3LA.

Keywords: Seismicity, earthquake catalogues, Balkans, Pannocian Basin

Abstract

Earthquake catalogues are fundamental to seismic hazard research, since from them is derived the essential information about distribution of earthquakes in both space and time. Although the main innovative focus of the Copernicus project [Seismic hazard of the Circum-Pannonian Basin] is on the numerative synthesis of ground motion, an earthquake catalogue for the study area is still required. In the absence of a homogenised catalogue for the whole region, based on original data treated in a uniform way, it has been necessary to compile a working catalogue from readily available cources. For the modern period (ie post-1964) the database of the ISC provides a data set of high quality; for the earlier period a number of other sources are used, some of which need to be treated with caution. The regional limits of this catalogue are from 12-30 East and 42-50 North.

In this paper, the construction of the catalogue is described and some basic analyses of the seismicity of the region are presented.

Introduction

Earthquake catalogues are fundamental to seismic hazard research, since from them is derived the essential information about distribution of earthquakes in both space and time. Although the main innovative focus of the Copernicus project "Seismic hazard of the Circum-Pannonian Basin" is on the numerative synthesis of ground motion, an earthquake catalogue for the study area is still required. In the absence of a homogenised catalogue for the whole region, based on original data treated in a uniform way, it has been necessary to compile a working catalogue from readily available sources. The regional time of this catalogue are from 12-30 East and 42-50 North. The minimum magnitude is 4; three magnitude values are catered for in the data file (Ms, mb and ML) and an event accredited with a 4 magnitude in any of these three scales was included in the catalogue.

It should be stressed from the outset that the assembling of an earthquake catalogue for a large region such as this, which has both relatively high seismicity (at least in part) and a very long long recorded history, is not a task to be entered into lightly. It would be agreeable if there were a single recognised earthquake catalogue for the whole of Europe from which one could simply extract the data required, At present, such a resource does not exist. Taking current national catalogues and merging them is a poor substitute, which inevitably leads to many problems. In the first case, different catalogues are at quite different stages with regard to historical research. For example, recent studies (eg Hammerl 1993) have shown that the famous (and regionally important) Villach earthquake of 1348 has been misplaced by most previous researchers and is in fact a Friuli earthquake. Merging two catalogues, one of which contains this event as an Italian earthquake and the other as an Austrian one, will produce duplications which may not be immediately apparent.

Secondly, homogeneity is a problem which

cannot be adequately resolved. Different catalogues use different procedures to estimate parameters such as (critically) magnitude, and the results may not be really compatible. Often such estimated magnitudes are not properly defined, either. This easily leads to discrepancies in the final, merged catalogue.

Thirdly, when resolving conflicts between national catalogues, any mechanical approach is prone to errons which would be spotted by a historian - seismologist with local expertise in the area in question. Each case should really be treated on its merits, preferably with reference to primary data. Such attention to detail is usually not possible without major effort.

While an important initiative is underway to resolve these problems for the benefit of future studies (Stucchi 1993), the results from it are in no way imminent. Therefore, for the present study, it is necessary to accept the limitations outlined above and work within them.

Data sources

For convenience of discussion, the catalogue can be broken down into three sections by date: up to 1900, 1900-1963 and 1964-1992. These will be discussed in reverse order.

Modern data

Data for the most recent period was taken exclusively from the database of the ISC. This data source therefore defines the dates of this part of the catalogue - 1964 is the first year for which ISC data are available and 1992 the most recent complete year. (To be precise, the ISC data starts with April 1964.) Standardising on one agency for this period has the great advantage that determinations are homogeneous; and the overall quality of ISC data is believed to be high. The data obtained from ISC includes revision of many earlier earthquakes, therefore parameters in the catalogue may be different from those in the original ISC bulletins. Determinations for this period from other agencies, particularly local ones, may be superior for some minor events, but in the context of the present study it was decides that the benefits of pursuing such minor improvements were outweighed by the cost involved.

Early instrumental data

For the most part data for the period before 1964 were obtained in the same way, and much of the discussion in this section is pertinent to bothe the 1900-1963 period and to pre-20th century period.

In order to obtain computer-readable data rapidly, two existing resources were used. These were the BGS World File (Burton 1978), covering the post - 1900 period only, and the NEIS EPIC data file (Reagor 1994), which covers a wider time span. Both of these are compilations of other sources, including Karnik (1969) and Shebalin et al (1974).

Some further sources were accessed via the EPIC data files, as follows. The catalogue of Van Gils (1988) is known to have a number of problems due to faulty compilation (many fake quakes are included and about two-thirds of French earthquakes are missing altogether). However, it is the only publicly -available source for Austria. Van Gils's German catalogue, and the source in EPIC that comprises German catalogues by Grünthal and Leydecker, were both used. The Greek catalogue belonging to Istituto Nazionale di Geofisica. For Romania there is the catalogue of Constantinescu and Marza (1980). The northeastern part of the study area also receives events from the catalogue of Kondorskaya and Shebalin (1982) for the former USSR.

These are all the sources that were obtained from EPIC. In addition, a catalogue of Hungarian earthquakes (Zsiros et al 1988) was obtained for inclusion, as well as the Postpischl (1985) catalogue for Italy. Where times in some sources appear to be Central European Time, the hour values were corrected to UTC.

Pre-instrumental data

The sources for pre-1900 data were essentially the same as those in the previous section. The extra problem here relates to the absence of magnitude values in some sources; only maximum intensity being given. It is not appropriate to give here a long discussion about the problems of estimating magnitude from macroseismic data. It is sufficient to say that reasonable magnitude determinations can only be made from macroseismic data in cases where one has either (a) the focal depth of (b) the felt area. Working from maximum intensity alone gives a very high

unertainty in the estimates because of the big effect of depth; this is certainly true in this region, where considerable variations in focal depths are observed.

However, since the alternatives were either some form of gross simplification or the discarding of a large amount of data, the former option was chosen. The relationship

$$M=0.53\ lo + 0.96 \quad (1)$$

was taken from Karnik (1969) as the formula most appropriate for the then Yugoslavian territories, the Carpathians, and Italy, which is a reasonable approximation to the study area. Where intensities are given as ranges, the midpoint was chosen (eg 6-7 translates as 6.5), and an intensity given as >7 is translated as the next point on the scale, in this case, 8. It may be noted that the magnitude values derived from this formula appear to be on the low side, since it supposes that magnitude 7 is equivalent to an lo of 11.

Where possible, magnitude values were taken directly from catalogues that gave them (eg Zsiros et al 1988) on the assumption that these were likely to be better determined. This is not always the case; some sources seem to have determined magnitude from lo in the same way as outlined above.

It should be clear that one of the problems with a catalogue of this sort is that one has no guarantee that magnitudes are consistent of compatible. In fact, almost certainly they are not, since it appears from comparing different sources that there is some confusion about magnitude types. It is common to see a magnitude value listed by one author as Ms appearing, for the same earthquake, as ML in a different source. The only way to dispose of this problem is to redetermine all magnitude values in a consistent way.

Constructing the catalogue

As a first step all the sources were merged without duplicates being deleted. Then an attempt was made to group lines of the file so that records referring to the same earthquake were indicated as such. The first stage was handled automatically by computer, with the following criteria: records from different agencies with times differing by no more than an hour and epicentres differing by no more than 200 km, were assumed to refer to the same earthquake. These groups were then processed according to a priority order of sources, largely arranged so as to favour recent sources over earlier sources.

The resulting file was then processed by hand to check the computer associations. This revealed many instances where records that do not meet the above criteria still appear to be duplicates. In such cases, where there was doubt the general rule was to assume duplication.

Obviously the catalogue is only as good as the original sources used. However, where particularly obvious errors could be identified, records were deleted. This resulted in the removal of such notorious fake quakes as the 1000 Ljubljana earthquake. One earthquake that received special treatment was the large 1556 earthquake in the Austria/Slovenia area. None of the sources used give parameters for this event. Rather than leave it out, a very crude and approximate epicentre and magnitude were estimated.

Once all duplications had been resolved as well as possible, a short version of the catalogue was prepared by printing only the prime determinations. It is this short version on which the analyses in this paper are based.

The parameters listed in the atalogue are as follows: day, month, year, hours, minutes, seconds, latitude, longitude, depth, Ms, mb, ML, agency code. In the short version of the catalogue only the magnitude type reported by the prime agency is used (id secondary magnitudes are not carried over from other agencies).

To obtain a unified magnitude value it was necessary to convert mb and ML values to Ms where Ms is missing. To obtain conversion formulae, regressions were performed on the available records with more than one magnitude. The following (reduced mean axis) equations were obtained:

$$Ms = O.64\ mb + 1.82 \quad (2)$$

on the basis of 141 observations, and

$$Ms = 1.04\ ML - 0.21 \quad (3)$$

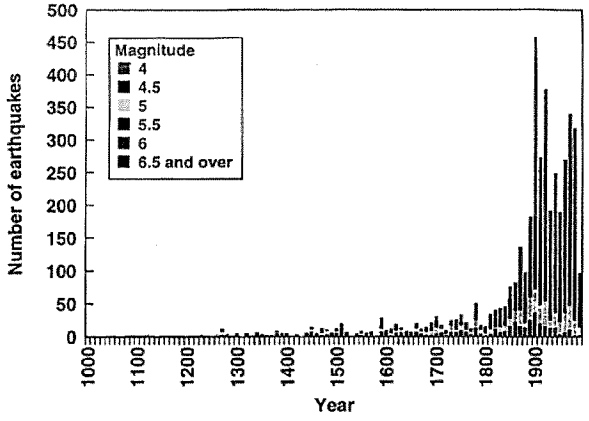

Fig. 1. Numbers of earthquakes per decade in the whole of the catalogue.

from 552 observations. The slope of the Ms/mb relationship in equation (2) is unconventional but not unprecedented = the formula is not too different from those derived by Passechnik et al (1970) for the USSR and Gupta et al (1972) for Asia. It is no doubt influenced by the presence in the catalogue of large deep Vrancea earthquakes with relatively high mb and the absence of large shallow earthquakes rich in surface waves.

Preliminary analyses of the seismicity

Time distrubution

Figure 1 shows the numbers of earthquakes per decade in the catalogue. It illustrates clearly how little information there is on early earthquakes. There is almost nothing before 1200, then a very slow increase in information until about 1800, when the increase becomes much more rapid. There seems to have been something of a crisis in seismicity around 1900, with more events recorded than during the mid 20th century.

One can get a rough idea of catalogue completeness from examination of this figure, but this subject is analysed in more detail in the next section.

Completeness

Common sense indicates that completeness for the catalogue will be variable over the area covered as well as varying by magnitude. From even slight knowledge of the history of the area one may deduce that completeness will be much better for Italy than for the areas formerly under Ottoman control. Nevertheless, it is a useful first exercise to subject the whole catalogue to a completeness analysis.

The method used involves calculating the average number of earthquakes per year exceeding a given magnitude value, for different subsets of the catalogue. Each subset has the same end date (the last complete year in the catalogue) but different start dates. Each value is calculated by taking the total number of events in a subset and dividing by the length of the subset; thus, for magnitude 4, the value plotted against the date 1800 will be the number of earthquakes ≥4 since 1800, divided by 192. Where the catalogue subset is short (only a few tens of years) then short-term fluctuations in seismicity have a disproportionate effect and the average is very unstable. As the subset lengthnes the average value stabilises. However, as one travels back in time to the period for which the catalogue is incomplete, the average drops as more and more earthquakes are missed out. The break in slope represents the date for which the catalogue is complete for the given magnitude. The results of this analysis for the catalogue are as follows:

Magnitude	Completeness date
4.0	1885
4.5	1885
5.0	1835
5.5	1780
6.0	1590

Spatial distribution

A map of all the earthquakes in the catalogue is shown in Figure 2. This shows a richly varied distribution of seismicity. The belt of high seismicity around the Adriatic is clear, although one notes something of a gap in the region of Croatia. The well-known concentration of seismicity in the Vrancea region of Romania stands out (not surprisingly). One also notes the areas where seismicity is particularly lacking: the Ukraine in the Northeast, the Bohemian Plain in the Northwest, and also the area of Southern Romania - Northern Bulgaria.

Some interesting apparent lineations are immediately apparent, notably a SW-NE feature running through Austria and into Slovakia, and

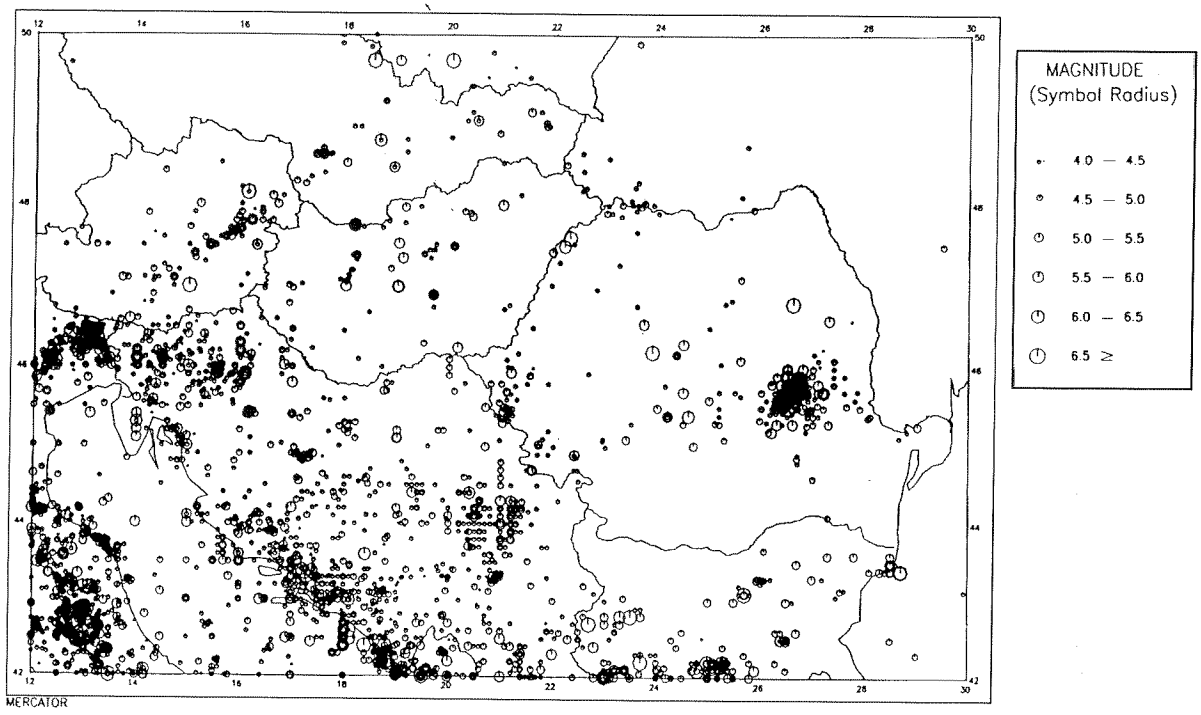

Fig. 2. Map of all the earthquakes in the catalogue. Symbol size is proportional to magnitude.

possibly a roughly parallel lineation in Hungary. Some apparent lineations running exactly N-S or E-W (for example, in Serbia) are obviously artificial and the result of giving very rounded epecentral co-ordinates to uncertainly located events.

Magnitude distribution

The data from the whole of the catalogue after 1885 (this date chosen as being the completeness date for the lowest magnitude, and thus, the whole catalogue) was analysed in terms of the Gutenberg - Richter magnitude / frequency distribution (Figure 3). As is well known, a plot of the logarithm of the cumulative number of events per year above a given magnitude, against magnitude, should give the relation.

$$\text{Log } N = a - b\ M \qquad (4)$$

where b is expected to have a value close to 1.0. The data are almost perfect; the regression line is

$$\text{Log } N = 5.59 - 1.00\ M \qquad (5)$$

giving exactly the theoretical value for b, and there is almost no roll-off at the top end of the graph, indicating that the 1885 completeness date for magnitude 4.0 is pretty close to correct and certainly correct for magnitude 4.5.

Conclusions

A new catalogue of earthquakes in the Danube Basin and surrounding area has been compiled from available sources, without revision of earthquake parameters. The catalogue has

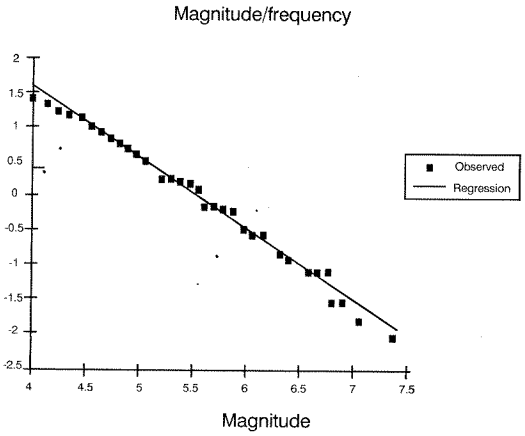

Fig. 3. Magnitude-frequency plot for the whole catalogue.

been kept in two version; the original file preserves all the data from different merged source catalogues in one large compendium. The working file has all duplicate entries removed so that each earthquake has one entry only, with a standardised magnitude value (Ms). The threshold magnitude for inclusion is magnitude 4.

The total number of earthquakes in the working file is 4345. This includes foreshocks and aftershocks. The start date for the catalogue is nominally 1000; in fact the first earthquake occurs in 1010. The last event in the catalogue is dated 9 March 1993.

The catalogue as a whole is believed to be complete since 1885. For events larger than 5.5 Ms it is complete for another hundred years before that, and for the largest events (≥6.0 Ms) it is complete since 1590.

Until revaluation of historical earthquakes in this area, from original source material, is complete, the catalogue described here provides the best available resource for the study of seismic hazard in the Circum-Pannonian Basin.

Acknowledgements

I would like to thank M Stucchi and T Zsiros for their help. This work was conducted as part of the Copernicus Programme project "Quantitative Seismic Zoning of the Circum Pannonian Region", and funded party by the Commission of the European Community and partly by the Natural Environment Research Council (NERC). This report is published with the permission of the Director of the British Geological Survey (NERC).

References

Burton, P.W., 1978. The IGS [now BGS] file of seismic activity and its use for hazard assessment, Inst. Geol. Sci. Seis Bull. No 6, HMSO, London.

Constantinescu, L. and Marza, V.I., 1980. A computer-compiled and computer-oriented catalogue of Romania's earthquakes during a millenium (984-1979), Rev. Roumanie de Géol., Géeophys. et Géog., Ser Géophys, vol 24, pp 171-191.

Gupta, H.K., Sitaram, N.V.D. and Narain, H., 1972, Surface-wave and body-wave magnitudes of som Sino-Soviet explosions and earthquakes, Bull. Seism. Soc. Am., vol 62, pp 509-517.

Karnik, V., 1969. Seismicity of the European Area, Reidel, Dordrecht.

Kondorskaya, N.V. and Shebalin, N.V., (eds) 1982. New catalogue of strong earthquakes in the USSR from ancient times through 1977, World Data Centre A for Solid Earth Geophisics Report No SE-31, Boulder Co.

Hammerl, C., 1993. The earthquake of January 25, 1348 - Reconstruction of a natural occurrence, PhD thesis, University of Vienna.

Papazachos, B.C. and Papazachos, C., 1986. Seismicity of Greece, Ziti, Thessaloniki.

Passechnik, I.P., Dashkov, G.G., Polikarpova, L.A. and Gamburtseva, N.G., 1970, The magnitude method for indentification of underground nuclear explosions, Izv. Acad., Sci. USSR Phys. Solid Earth, , vol 1, pp 19-4.

Postpischl, D., 1985, Catalogo dei terremoti Italiani dall' anno 1000 al 1980, Consig. Naz. delle Ricerche Prog. Fin. Geodin., Bologna.

Reagor, G., 1994. EPIC user's guide, USGS/NEIC, Denver Co.

Shebalin, N.V., Karnik, V. and Hadziewski, D., 1974. UNDP/UNESCO Survey of the Seismicity of the Balkan Region: Catalogue of earthquakes, UNESCO, Skopje.

Stucchi, M., 1993. Recommendations for the compilation of a European earthquake catalogue, with special reference to historical data prior to 1990, EC Project PHISE "Review of Historical Seismicity in Europe", unpublished draft.

Van Gils, J.M., 1988. Catalogue of European earthquakes and an atlas of European seismic maps, CEC Report No EUR 11344 EN.

Zsiros, T., Monus, P. and Toth, L., 1988. Hungarian earthquake catalogue (456-1986), Geod. and Geophys. Res. Inst., Budapest.

AUTHOR INDEX